

HIGHWAY RESEARCH RECORD

Number | Asphalt and
468 | Asphalt Mix Technology

10 reports
prepared for the
52nd Annual Meeting

Subject Areas

25	Pavement Design
31	Bituminous Materials and Mixes
33	Construction
34	General Materials

HIGHWAY RESEARCH BOARD

DIVISION OF ENGINEERING NATIONAL RESEARCH COUNCIL
NATIONAL ACADEMY OF SCIENCES—NATIONAL ACADEMY OF ENGINEERING

Washington, D.C.

1973

NOTICE

These papers report research work of the authors that was done at institutions named by the authors. The papers were offered to the Highway Research Board of the National Research Council for publication and are published here in the interest of the dissemination of information from research, one of the major functions of the Highway Research Board.

Before publication, each paper was reviewed by members of the HRB committee named as its sponsor and accepted as objective, useful, and suitable for publication by the National Research Council. The members of the review committee were chosen for recognized scholarly competence and with due consideration for the balance of disciplines appropriate to the subject concerned.

Responsibility for the publication of these reports rests with the sponsoring committee. However, the opinions and conclusions expressed in the reports are those of the individual authors and not necessarily those of the sponsoring committee, the Highway Research Board, or the National Research Council.

Each report is reviewed and processed according to the procedures established and monitored by the Report Review Committee of the National Academy of Sciences. Distribution of the report is approved by the President of the Academy upon satisfactory completion of the review process.

ISBN 0-309-02254-1

Library of Congress Catalog Card No. 73-21484

Price: \$4.00

Highway Research Board publications are available by ordering directly from the Board. They are also obtainable on a regular basis through organizational or individual supporting membership in the Board; members or library subscribers are eligible for substantial discounts. For further information write to the Highway Research Board, National Academy of Sciences, 2101 Constitution Avenue N. W., Washington, D. C. 20418.

CONTENTS

FOREWORD	v
ASPHALT RHEOLOGY IN THE NEAR-TRANSITION TEMPERATURE RANGE	
Herbert E. Schweyer	1
Discussion	
R. L. Davis	15
Author's Closure	15
CRACK DEVELOPMENT IN PAVEMENTS	
Joseph E. Soussou and Fred Moavenzadeh	16
PROPOSED METHOD OF PRODUCING ASPHALT CONCRETE BEAMS FOR LOW-TEMPERATURE TESTING	
L. F. Rader, R. T. Ochalek, and E. O. Busby	30
ASPHALT DURABILITY CORRELATION IN IOWA	
Dah-yinn Lee	43
STORAGE OF BITUMINOUS CONCRETE IN INERT GAS	
Prithvi S. Kandhal and Monroe E. Wenger	61
Discussion	
R. L. Davis	72
Authors' Closure	72
IRRECOVERABLE AND RECOVERABLE NONLINEAR VISCOELASTIC PROPERTIES OF ASPHALT CONCRETE	
James S. Lai and Douglas Anderson	73
RAPID DETERMINATION OF ASPHALT CONTENT USING PENNSYLVANIA PYCNOMETER	
Prithvi S. Kandhal, William C. Koehler, and Monroe E. Wenger	89
EVALUATION OF MINERAL FILLERS FOR ASPHALT PAVING MIXTURES	
S. K. Rao and B. R. Sen	100
STUDY OF MINERAL FILLERS FOR SHEET-ASPHALT MIXTURES	
V. Venkatasubramanian and T. S. Venkataraman	109
ASPHALT CONTENT DETERMINATION USING NUCLEAR TECHNIQUES	
Robert C. Klotz	115
SPONSORSHIP OF THIS RECORD	130

FOREWORD

Papers in this RECORD are of interest both to asphalt materials researchers and to practicing highway engineers concerned with asphalt pavements. Reflecting recent theoretical and applied research efforts, the reports cover a wide variety of subjects including (a) properties of asphalts and their relation to pavement performance, (b) determination of asphalt content of paving mixtures, (c) hot storage of asphalt paving, (d) failure mechanisms (and the elastic and viscoelastic behavior of asphalt paving), (e) mineral fillers for asphalt paving, and (f) laboratory preparation of asphalt paving specimens.

In the first paper, Schweyer presents viscosity, penetration, and ductility data for 35 asphalts. Rheology of asphalt cements in the temperature range from 5 C (41 F) to 60 C (140 F) is emphasized, and a major part of the work concerns temperature susceptibility of asphalt cements. A main conclusion is that the temperature susceptibility of asphalt cements is a most important material property that can be, and should be, evaluated by absolute viscosity measurements rather than by empirical tests.

Soussou and Moavenzadeh discuss methods for analyzing crack development in pavements, methods that consider variations in temperature, loading conditions, and materials properties. In the short range, an approach based on a modification of Miner's law is preferred because of its simplicity and availability of data, whereas approaches based on fracture mechanics concepts are preferred in the long range because of their completeness.

Rader, Ochalek, and Busby present laboratory procedures for fabricating asphalt-concrete beam specimens. The California kneading compactor, with a modified tamping foot and compaction mold, is used. They conclude that the method presented can consistently produce homogeneous beams of acceptable densities and aggregate arrangement.

In a paper by Lee, eight asphalt cements and paving projects using these asphalts are evaluated relative to their changes in rheological and chemical properties in pavement service. Lee concludes that 46 hours in the Iowa durability test will age asphalt to the equivalent of 60 months in Iowa pavements. A tentative specification for paving asphalt, including durability requirements based on the Iowa durability test, is recommended in lieu of the thin-film oven test.

Kandhal and Wenger present results of a laboratory and field study evaluating the effects of prolonged hot storage on properties of a bituminous paving mix. They found that, if maximum allowable storage time is determined from criteria of minimum percentage of retained penetration on thin-film oven test residue, it can vary depending on asphalt source, composition of the bituminous mix, and the temperature and time of mixing.

Results of uniaxial compression creep tests on asphalt concrete for a variety of loading conditions are presented by Lai and Anderson. They conclude that nonlinear viscoelastic behavior of asphalt concrete can be represented by a nonlinear Kelvin model that is made up of a nonlinear dashpot in series with a nonlinear Kelvin chain.

Kandhal, Koehler, and Wenger describe development and testing of a pycnometer proposed for rapid determinations of the asphalt content of paving mixtures. The method is based on procedures of ASTM D 2041.

Rao and Sen report on an evaluation of three mineral fillers based on their dry compacted void contents and their influence on the unconfined compression creep behavior of a fine sheet asphalt paving mixture. They found that a minimum rate of strain occurred at a particular filler-asphalt ratio for each of the fillers. The authors interpret differences in effectiveness of the fillers in terms of their dry compacted void contents.

The influence of mineral fillers on the rheological behavior of sheet asphalt is described in a paper by Venkatasubramanian and Venkataraman. Using simple beam de-

flection tests as a base, they describe effects of three different mineral fillers on resistance of sheet asphalt to deformation under steady creep conditions. For testing conditions used, they found that fillers could be rated from the standpoint of resistance to deformation under steady-state creep strain.

In the final paper, Klotz describes an evaluation of a nuclear asphalt content gauge. The accuracy of asphalt content determinations for the laboratory study phase is reported to be considerably better than that for a field study phase. The gauge did not yield the expected degree of accuracy, but the author concludes that it can be used for quick and accurate determinations of asphalt content in either field or laboratory situations.

—Bernard F. Kallas

ASPHALT RHEOLOGY IN THE NEAR-TRANSITION TEMPERATURE RANGE

Herbert E. Schweyer, University of Florida, Gainesville

This paper provides information on some 35 asphalts of various types and sources in the service temperature range from 5 C (40 F) to 60 C (140 F). Data were presented on the penetration, ductility, and viscosity for this temperature range in an effort to explain in depth certain peculiarities in asphalt behavior and the empirical tests. This was done through a study of the viscosity temperature susceptibility in which emphasis was placed on the lower temperature and on comparisons of the different hardening effects caused by lowering the temperature. This could be of significance in connection with cracking of pavements, for recent investigators have been emphasizing the variations in pavement performance as related to asphalt sources. Another study of this report relates to the proposed Carré and Laurent relation between penetration and viscosity at various temperature levels. It was shown that this relation has a limited usefulness with respect to sensitivity of viscosity measurements because the variability may be shown to exceed ± 25 percent. The analysis included comparative data with the sliding-plate, Florida capillary, and cone-plate methods. Further information in the paper reports on the empiricism of the ductility tests and its relation to absolute viscosity measurements. Comparisons with previous data of other investigators are shown. The growing trend in asphalt technology to recognize the inadequacies of the old empirical tests and to use new techniques is confirmed in this paper.

●THE acceptance of viscosity grading at 60 C of asphalt cements for specifications has been a major advance in asphalt technology. It recognizes the advantages of the use of a scientific test to replace the empiricism of archaic procedures.

An outgrowth of this development has been the recent interest in studies of viscosity in absolute units at temperatures as low as 0 C. This interest has been generated because of the cracking of asphalt pavements, which must be related in some way to the low-temperature rheology of asphalt cements. Unfortunately, there are many problems associated with such measurements because of the very high consistency level that is reached, which is of the order of 1,000 megapoises or higher.

In general, as the temperature is lowered, asphalts become more viscous and eventually exhibit glassiness where their coefficients of expansion change differently with temperature change, brittle fracture develops, and other elasticoviscous behavior is observed.

The glass-transition region is a gray area for research on the deformation properties of asphalt cements. These materials may exhibit all of the types of flow behavior shown in the following ranges:

1. High temperatures—In this region, higher than 60 C, the asphalt behaves as a fluid that may or may not be Newtonian. There appear to be no great rheological problems for measurements in this region other than to ensure proper temperature control.

2. Near-transition range—Temperature in this region is lower than 60 C and goes down to the range temperature at which the asphalt behaves as an elastic solid. This is

the region of interest in this paper. For most asphalt highway service, the pavement is exposed to temperatures higher than 0 C and lower than 60 C for the major portion of its daylight life (at least in the United States). Depending on the viscosity grade, viscosity measurements at 10 C (50 F) to 40 C (104 F) can be made readily by instruments such as the Florida capillary method, the cone and plate method, or the sliding-plate method. Viscoelastic behavior enters the rheological analysis at the lower temperatures and must be considered quantitatively.

3. Far-transition range—In the glass-transition region lower than 0 C, many non-crystalline materials exhibit definite volumetric changes, and asphalt behaves more and more as an elastic solid. The deformation mode must be changed to accommodate the high stresses required, and the elastic component of viscoelasticity predominates. It is this region where tensile strength techniques can be utilized when the asphalt is sufficiently rigid. The glass-transition temperature T_g procedures have been used here, but the question is raised as to what their significance is. Actually, measurement of T_g may be considered primarily as a temperature susceptibility parameter. Asphalt cements may become essentially elastic solids at temperatures somewhat above their T_g . It is believed future research will demonstrate the practical importance of glass-transition phenomena in explaining asphalt behavior.

From experience it is known that asphalt cements from different sources exhibit these behaviors at different temperatures because they vary in composition. Composition variations produce different internal phase changes that influence the temperature susceptibilities. Different methods of processing also affect the deformation behavior as do the pressure conditions existing during deformation.

It is the main objective of this paper to present quantitative data on a variety of quite different asphalts in the near-transition region. A second objective is to show briefly how absolute viscosity information relates to common empirical tests.

LITERATURE SURVEY

The high viscosities encountered in the glass-transition region present some difficulties in viscosity measurement as indicated by recent publications. Some investigators have employed the sliding-plate technique from 25 C to 4 C (and lower) without apparent difficulties (1-4).

Puzinauskas (5) in a comprehensive study pointed out the desirability of developing more knowledge concerning the low-temperature rheological behavior of asphalt bitumen. He reported on viscosity data obtained at 4 C (39.2 F) by using the cone-plate method and at 25 C (77 F) and 7.2 C (45 F) by using the sliding-plate method. Comparisons of these data with penetration ductility and tensile strength measurements at the lower temperatures were also given. In addition, data obtained by using the falling-plunger method were reported for a temperature of 15.5 C (60 F). A new modified sliding-plate rheometer was used with apparent success by Fenign and Kroosof (6) at temperatures as low as -10 C for 80 penetration asphalts.

Busby and Rader (7) have suggested modifications to the sliding-plate viscometer for use at 4 C (39.2 F). The Cannon cone-and-plate viscometer has been used at low ambient temperatures by Lefebvre and Robertson (8). Comparative data on different viscometers at 25 C (77 F) were given by Schweyer (9). Evans and Gorman (10) presented a rigorous comparative study on the ASTM methods (11) for two asphalts at 25 C (77 F).

Other investigators have considered tensile stress or similar measurements for low-temperature rheology of asphalts. Reiner (12) provides the background for this type of analysis. In general, although the techniques are acceptable for research purposes, they are not satisfactory for routine testing. Sisko (13) compared the tensile strength of aged and unaged asphalt films at temperatures from 0 to 25 C. Haas and Anderson (14) have shown tensile strength curves for asphalts at temperatures as low as -70 C. Williams, Grimmer, and McAdams (15) reported a tensile-strength technique as did Marek and Herrin (16). Heukelom (17) has discussed tensile-strength relations and a stiffness modulus for asphalt. Earlier, Lee and Rigden (18) reported on tensile-strength tests, and Reiner (19) made an in-depth review of the subject.

The glass-transition temperature technique has been proposed by numerous investigators for low-temperature studies, but it has not been generally accepted as a useful tool. Schmidt and Santucci (20) and Dobson (21) among others provide some recent information and references on this subject.

Schweyer and Busot (22) proposed a technique based on a confined compression mode for study of asphalt cements at the lower temperature regions (0 C) where an attempt was made to separate the elastic from the flow effects. Majidzadeh and Schweyer (23) and others (12, 24, 25) have reported on the complex modulus technique for study of elastic and viscous effects.

The WLF relation developed for polymers by Williams, Landel, and Ferry (26) has been employed by many asphalt technologists for glass-transition studies. It is essentially a temperature-viscosity correlation.

In the present paper, the material presented will concern the rheology of asphalt cements in the intermediate temperature region of 5 C (41 F) to 60 C (140 F). The results are based on viscosity measurements at a constant stress or constant rate of shear by the Florida capillary method (9) on a variety of asphalts given in Table 1. Comparable data for the common empirical tests of penetration, ductility, and ring-and-ball softening point are also given. There is no intent here to rationalize these empirical tests because they eventually will be replaced.

In general, references to other research will be limited to recent articles noted only where data on a large number of asphalts were reported. In addition, certain empirical test data (penetration and ductility) will be included where available for orientation purposes for the reader who is not familiar with thinking in terms of absolute viscosity units.

TEMPERATURE SUSCEPTIBILITY

ASTM Viscosity Relation

The temperature susceptibility of asphalt having a temperature of 60 C and higher has been reported by many investigators. Recently, the author demonstrated that asphalts of different types and consistencies all fit linearly on the ASTM viscosity chart from 60 to 195 C. It was shown that, although the slope is constant, the rate of change of viscosity with absolute temperature is a function of the temperature and the equation constants:

$$d\eta/dT = (2.303 BM)T^{M-1}e^{2.303 BT^M} \quad (1)$$

where η is viscosity in centipoises, T is absolute Rankine temperature (= 459.7 + temperature in deg F), and B and M are empirical constants. Numerical values of the slopes of the ASTM chart for different asphalts (Table 1) are discussed in a later section of this paper based on data given in Tables 2, 3, and 4.

The ASTM chart applies at the higher temperatures for asphalts and as low as 41 F for some asphalts, but there are many asphalts that show a change in slope in the region of 0 to 70 C (9). This has been indicated by numerous investigators, and Griffin, Izzat, and Lettier (3) demonstrated a very important point for asphalts that were studied through changes in the mixing plant and up to 5 years in the pavement. It was shown that the shear susceptibility affected the slope of viscosity temperature line. It was noted also that the slope could increase or decrease below 25 C. Similar effects have been noted by others and generally are explained by variations in composition differences and phase changes occurring in the transition regions. Some asphalts do not show (9) this change of slope where their degree of complex flow is essentially unity ($C = 1$ in the power-law equation).

Additional new data of this type are shown in Figures 1 and 2 for a broad variety of asphalts. These results confirm those of previous studies.

It is not the purpose of this paper to show a large number of plots but rather to demonstrate the type of plots that were found. Thus, the data in Figures 1 and 2 show the linear ASTM relation at temperatures higher and lower than 60 C. For some materials with an appreciable shear susceptibility ($C < 1$), asphalt 33 may show a lower slope at

Table 1. Base data on asphalts studied.

Asphalt		Viscosity at 60 C					Ductility at 25 C		Viscosity at 25 C	
		Penetration at 25 C	Vacuum Kp	Capillary		Ring and Ball (deg C)			Megapoises ^a	C
Number	Material			Kp	Kp		C			
BPR Asphalts (1971-72 data)										
1	S64-8	177	0.832	—	—	41.1	>150	0.265	0.71	
2	S64-9	49	1.38	—	—	47.8	106 ^b	4.46 ^b	0.76 ^b	
3	S64-20	101	1.74	—	—	51.1	117 ^b	0.49	0.74	
4	S64-22	21	2.81	—	—	53.3	42	19.5 ^b	0.69 ^b	
5	S64-42	65	2.75	—	—	48.9	>150	1.77 ^b	0.85 ^b	
6	S64-43	26	3.86	—	—	55.6	>150	13.3	0.85	
7	S64-46	43	6.82	—	—	53.3	>150	3.93	0.83	
8	S64-47	19	5.55	13.4	1.01	53.3	55	49.4	0.74	
Regular Asphalts										
9	S71-4	87	1.70	3.62	0.95	45.6	>150	0.910	0.69	
10	S71-8	62	3.04	4.80	0.89	53.3	>150	2.22	0.85	
11	S71-10	92	0.708	1.53	1.06	47.2	>150	0.912	0.99	
12	S71-13	27	5.09	—	—	61.1	>150	19.6	0.83	
13	8580	82	1.78 ^b	—	—	50.6	—	1.10	0.90	
14	8581	59	3.32	—	—	54.4	—	2.68	0.92	
15	8589	77	2.80	—	—	56.1	—	1.14	0.75	
16	8617	90	1.54	—	—	48.9	—	1.15	0.78	
17	8621	60	4.78	—	—	55.0	—	2.31	0.64	
18	R72-3	88	1.14 ^b	3.05	0.96	45.0	>150	1.43	0.97	
19	R72-4	54	6.00	5.71	1.06	54.4	>150	3.64	0.83	
Special Asphalts										
20	S71-10	94	21.8	—	—	63.9	49	9.28	0.74	
21	S71-19	46	7.44	—	—	53.3	>150	3.96	0.70	
22	R71-9	67	4.21	—	—	52.8	>150	2.72	0.73	
23	S71-20	86	1.82 ^b	—	—	49.4	>150	1.02	0.83	
24	S71-21	108	1.29	—	—	46.7	>150	0.590	0.92	
25	S71-22	158	0.737	—	—	—	—	—	—	
26	S71-23	294	0.317	—	—	40.0	>150	0.226	1.08	
27	R72-5	73	3.11	—	—	50.6	>150	1.08	0.68	
28	S63-2	Soft	—	—	—	—	Soft	0.285	0.96	
29	S63-3	Soft	—	—	—	43.3	132	0.258	0.98	
30	S66-2	79	1.84 ^b	3.72	1.09	46.1	>150	2.46	1.01	
31	S68-3	147	0.95 ^b	—	—	40.6	>150	0.339	1.04	
32	S68-5	93	0.426	—	—	45.6	122	0.568	1.12	
33	S71-28	33	40.4	44.5	0.69	68.4	24.5	9.64 ^b	0.58 ^b	
34	S71-29	22	2,500	453	0.48	92.1	4.0	21.9 ^b	0.44 ^b	
35	R71-8	23	—	—	—	90.6	3.8	25.6	0.41	

^aViscosity at a power input of 10⁵ ergs/(sec-cm²).
^bAverage of two or more tests.

Table 2. Rheological data, 5 C to 15.5 C.

Asphalt		5 C ^a				10 C				15.5 C			
		Penetration (dmm)	Ductility (cm)	Viscosity (megapoises)	C	Penetration (dmm)	Ductility (cm)	Viscosity (megapoises)	C	Penetration (dmm)	Ductility (cm)	Viscosity (megapoises)	C
1	S64-8	19	>150	16.7	1.13	28	>150	13.5	0.64	55	>150	0.858	1.02 ^b
2	S64-9	—	—	—	—	8	0.7	802	0.61	12	10 ^b	39.3	0.78 ^b
3	S64-20	14	8.8	60.0	1.03	18	19.4	12.8	0.76	41	>150	3.74	0.73
4	S64-22	—	—	—	—	5	—	—	—	7	5	247	0.82 ^b
5	S64-42	10	12.2	267	1.20	11	67 ^b	44.3	0.88	29	>150	10.9	0.89
6	S64-43	—	Broke	—	—	6	0.6 ^b	774	0.80	8	10	278	1.01 ^b
7	S64-46	7	1.0	944	0.95	12	11 ^b	582 ^b	0.68 ^b	16	>150	58.1 ^b	0.74 ^b
8	S64-47	—	Broke	—	—	3	—	1,910 ^b	0.56 ^b	6	3	784	0.77
9	S71-4	12	6.0	404	0.88	19	11	37.2	0.70	29	70	5.18 ^b	0.63 ^b
10	S71-8	—	—	—	—	—	—	—	—	—	—	—	—
11	S71-10	8	7.6	583	0.87	11	>150	110 ^b	0.78 ^b	24	>150	13.7	0.98
12	S71-13	5	Broke	—	—	4	0.5	3,193 ^b	0.74 ^b	12	14.5	256	1.14 ^b
18	R72-3	6 ^b	1.7	287 ^b	1.45 ^b	12	>150	132 ^b	1.03 ^b	24	>150	18.8	0.83
19	R72-4	8 ^b	6.0	1,874	1.31	12 ^b	14.5	186	0.97	20	>150	21.7	0.91
20	S71-18	—	—	—	—	9	2.3	463	0.70	14	6.0	118	0.92
21	S71-19	—	—	—	—	10 ^b	—	—	—	—	12.5	37.9	0.65
22	R71-9	—	—	—	—	13	0.6	119	0.83	21	>150	1.89	0.75
23	S71-20	10	8.0	210	0.98	15	20 ^b	24.8	0.69	26	—	—	—
24	S71-21	12	17.5	129	1.27	20	>150	17.2	0.70	34	—	—	—
25	S71-22	17	74	51.0	1.07	24	>150	7.11	0.77	41	—	—	—
26	S71-23	—	—	—	—	—	—	—	—	—	—	—	—
27	R72-5	18	6.3	116	0.87	20	13	43.6	0.81	31	>150	9.42	0.55
28	S63-2	52	>150	1.08	1.0	120	104 ^b	3.27	0.90	250 ^b	80	2.75	0.96 ^b
29	S63-3	13	77	1.05	1.24	26	>150	9.86	0.85	40	>150	—	—
30	S68-2	6	1.0	1,002	1.17	12	>150	184	1.17	21	>150	25.9	0.97
31	S68-3	12	>150	217	1.61	20	>150	32.4	1.13	40	>150	—	—
32	S68-5	8	0.1	740	1.24	10	>150	45.0	0.82	25 ^b	129	14.4	1.01
33	S71-26	10	0.5	1,157	0.59	11	4.0	230	0.58	15	5.5	47.9	0.73 ^b
34	S71-29	8	0.8	2,067	0.68	9	3.4	342	0.48	13	3.5	123	0.57 ^b
35	R71-8	—	—	—	—	—	—	—	—	—	—	—	—

^aAll data at constant shear rate except for the tests at 5 C and those indicated at 15.5 C, which were at constant stress [all at a power input of 10⁶ ergs/(sec-cm²)].
^bAverage of two or more tests.

Table 3. Rheological data, 25 C to 60 C.

Asphalt		25 C				40 C				60 C			
Number	Material	Penetration (dmm)	Ductility (cm)	Viscosity (megapoises)	C	Penetration (dmm)	Ductility (cm)	Viscosity (megapoises)	C	Penetration (dmm)	Ductility (cm)	Viscosity (megapoises)	C
1	S64-8	177	>150	0.265	0.71	—	—	—	—	—	—	—	—
2	S64-9	49	108 ^b	4.46 ^b	0.76 ^b	—	—	—	—	—	—	—	—
3	S64-20	101	117 ^b	0.49	0.74	—	—	—	—	—	—	—	—
4	S64-22	21	42 ^b	19.7 ^a	0.69 ^b	204	>150	0.143	—	0.79	—	—	—
5	S64-42	65	>150	1.77 ^b	0.85 ^b	—	—	—	—	—	—	—	—
6	S64-43	26	>150	13.3	0.85	168	—	—	—	—	—	—	—
7	S64-46	43	>150	3.93	0.83	206	—	—	—	—	—	—	—
8	S64-47	19	55	49.4 ^a	0.74 ^a	148	—	—	—	—	—	—	—
9	S71-4	87	>150	0.910	0.69	—	121	0.54	—	0.93	13.4	—	1.01
10	S71-8	62	>150	2.22	0.85	—	—	—	—	—	4.60	—	0.89
11	S71-10	92	>150	0.912	0.99	—	—	—	—	—	1.53	—	1.06
12	S71-13	27	>150	19.6	0.83	—	—	—	—	—	—	—	—
18	R72-3	88	>150	1.43	0.97	—	—	0.039 ^b	—	1.24 ^b	3.05	—	0.96
19	R72-4	54	>150	3.64	0.83	—	—	0.15	—	1.02	5.71	—	1.06
20	S71-16	34	49	9.28	0.74	98	129	0.601	—	0.73	—	—	—
21	S71-19	46	>150	3.98	0.70	—	—	—	—	—	—	—	—
22	R71-9	67	>150	2.72	0.73	—	—	—	—	—	—	—	—
23	S71-20	86	>150	1.02	0.83	—	—	—	—	—	—	—	—
24	S71-21	108	>150	0.590	0.92	—	—	—	—	—	—	—	—
25	S71-22	158	>150	0.226	1.08	—	—	—	—	—	—	—	—
26	S71-23	294	—	0.076	1.10	—	—	—	—	—	—	—	—
27	R72-5	73	>150	1.08	0.68	—	—	—	—	—	—	—	—
28	S63-2	Soft	Soft	0.285	0.96	—	—	—	—	—	—	—	—
29	S63-3	Soft	132	0.258	0.98	—	—	—	—	—	—	—	—
30	S68-2	79	>150	2.48	1.01	—	—	—	—	—	3.72	—	1.09
31	S68-3	147	>150	0.339	1.04	—	—	—	—	—	—	—	—
32	S68-5	93	122	0.568	1.12	—	—	—	—	—	—	—	—
33	S71-28	33	24.5	9.64 ^a	0.58 ^b	94	>150	0.832	—	0.65	44.5	—	0.69
34	S71-29	22	4.0	21.9	0.44	47	—	6.7	2.49	0.48	453	—	0.48
35	R71-8	23	3.8	25.6	0.41	—	—	—	—	—	—	—	—

^aAll data at constant shear rate [all at a power input of 10^5 ergs/(sec-cm²)].

^bAverage of two or more tests.

Table 4. Comparative temperature susceptibilities.

Asphalt		Penetration at 25 C	Ring and Ball (deg C)	TSI, Eq. 2		PI, Eq. 3
Number	Material			5 to 60 C	>60 C	
32	Special S	93	45.6	5.343 ^a	3.790	-0.82
12	Canadian	27	61.1	4.386	3.779	-0.13
8	K-40	19	53.3	4.180	3.528	-2.25 ^a
22	AB	67	52.8	3.811	3.462	0.21
27	AB	73	50.6	3.773	2.941 ^b	-0.10
30	Special A	79	46.1	3.754	3.574	-1.12
7	E-10	43	53.3	3.712	3.597	-0.75
23	AB	86	49.4	3.675	3.464	0.05
5	C-10	65	48.9	3.568	3.442	-0.88
3	E-5	101	51.1	3.505	3.418	0.99
19	Venezuelan B	54	54.4	3.466	3.412	0.03
21	AB	46	53.3	3.456	3.596	-0.60
9	Mid-continent	87	45.6	3.400	3.473	-1.02
11	Canadian	92	47.2	3.400	3.400	0.37
18	Callifornian	88	45.0	3.375	3.931 ^a	-1.17
20	AB	34	63.9	2.991	3.553	0.86
1	D-5	174	41.1	2.968	3.636	-0.12
31	Special A	147	40.6	2.825	—	-1.07
33	Rfg. - F	33	68.4	2.690	3.494	1.56
34	Rfg. - S	22	92.1	1.779 ^b	3.527	3.87 ^b

^aHighest temperature susceptibility.

^bLowest temperature susceptibility.

the lower temperatures, which confirms results by Sisko (27). Where $C > 1$, indications were that increased consistency with increasing shear stress may give higher slopes at low temperatures. Where the material demonstrates essentially Newtonian characteristics (S63-20), the ASTM slope was essentially constant throughout the entire temperature range studied (Fig. 1). However, the slope may also be offset but essentially parallel to the high-temperature plots as shown in Figure 2 for sample 11. Data in Figure 2 also show the effect of measuring viscosity at different shear rates.

Currently, with the test procedures available, there is considerable evidence of irregular variations in the complex flow index C with temperature change. This could affect viscosity values differently, depending on which rate of shear is selected for reporting tests. For example, one possible complication for some hard asphalts is that the 0.05-sec^{-1} data ($\eta_{0.05}$) may be so low in the shear range that the power law C approaches unity and Newtonian flow results. Accordingly, comparative data given in Tables 2 and 3 for typical asphalts of different types were evaluated at a constant power input of 10^5 ergs/(sec-cm³). The variation in the complex flow index C may approach unity as the materials are heated and become more fluid. As the temperature approaches the near-transition region, the index may go above unity, which probably characterizes the onset of glassiness.

The negative of the slopes of the plots may be considered as measures of a temperature susceptibility index (TSI) to give a quantitative value of the susceptibility. The log-log η coordinate does desensitize the data, and, accordingly, the last significant figure of the slope may be important (note that viscosity must be in centipoises):

$$\text{TSI} = \text{negative of the slope} = \log(\log \eta_1 / \log \eta_2) / \log(T_2 / T_1) \quad (2)$$

where η is viscosity in centipoises, and T is absolute temperature in degrees Rankine.

A comparison of these slopes of the ASTM chart is given in Table 4 at the high (above 60 C) and intermediate (5 to 60 C) temperature levels to give some indication of the numerical variations to be expected. The larger numbers reflect the greater change in viscosity with temperature. Where data are available, it also is possible to judge whether to expect the material to be less (or more) susceptible in the lower temperature ranges than at high temperatures. This can be valuable in predicting pavement performance.

The data also give a subjective evaluation of how the empirical penetration index compares with a more sophisticated mathematical expression of temperature susceptibility.

Penetration Index

There has been considerable interest generated recently in the use of a penetration index (PI) for measuring temperature susceptibility. This is another black-art empirical relation, based on a concept proposed by Holmes, Collins, and Child (28), that became somewhat more sophisticated (29). In its present form it appears as follows:

$$\text{PI} = \frac{20 - 500 \alpha}{1 + 50 \alpha} \quad (3)$$

$$\alpha = \frac{\log(800/\text{penetration})}{T_{R88} - 25 \text{ C}} \quad (4)$$

At best this parameter is a composite of eight empirical test procedures or empirical relations with the latter being somewhat controversial. For example, it is assumed that the penetration of all asphalts at their softening point is 800 and implied that their viscosity at that temperature is the same for most asphalts. Data in Figure 3 demonstrate that the first relation is questionable, and Griffith and Puzinauskas (30), as well as others, have shown that the viscosity at the softening point is definitely not a constant value.

Figure 1. Variation in susceptibility.

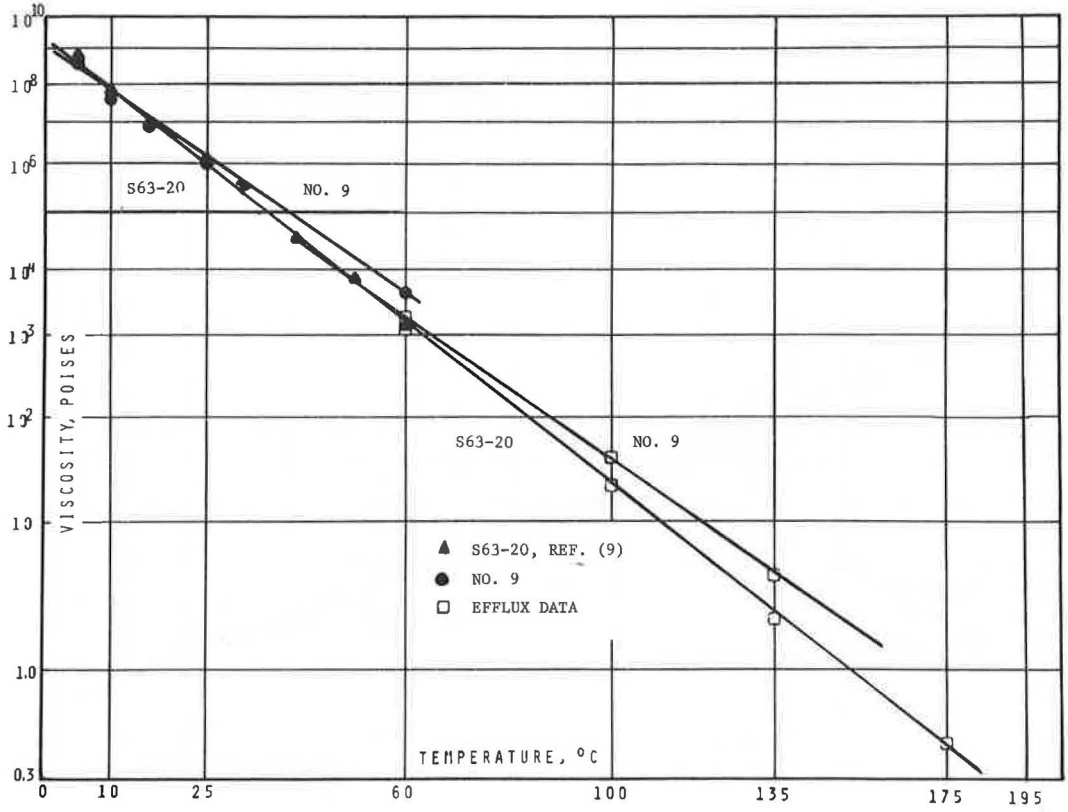


Figure 2. Asphalt viscosity in the near-transition range.

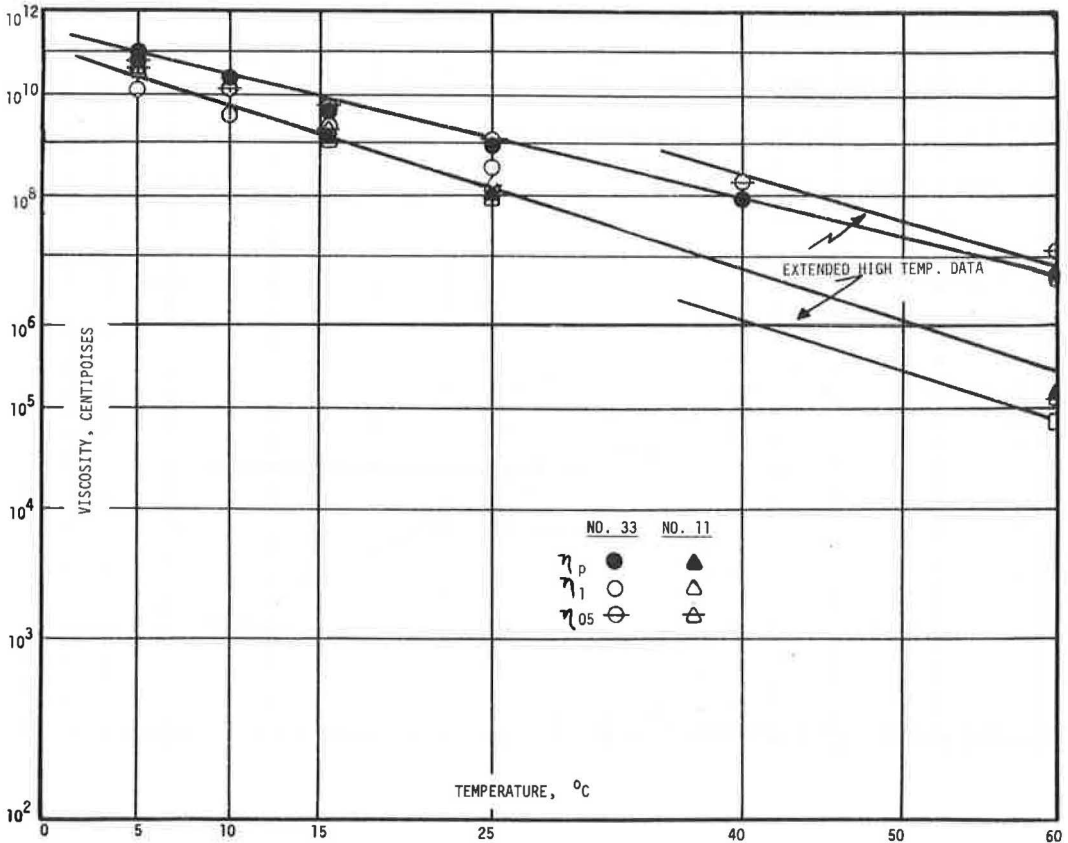


Figure 3. Analysis of penetration–viscosity at equishear rate.

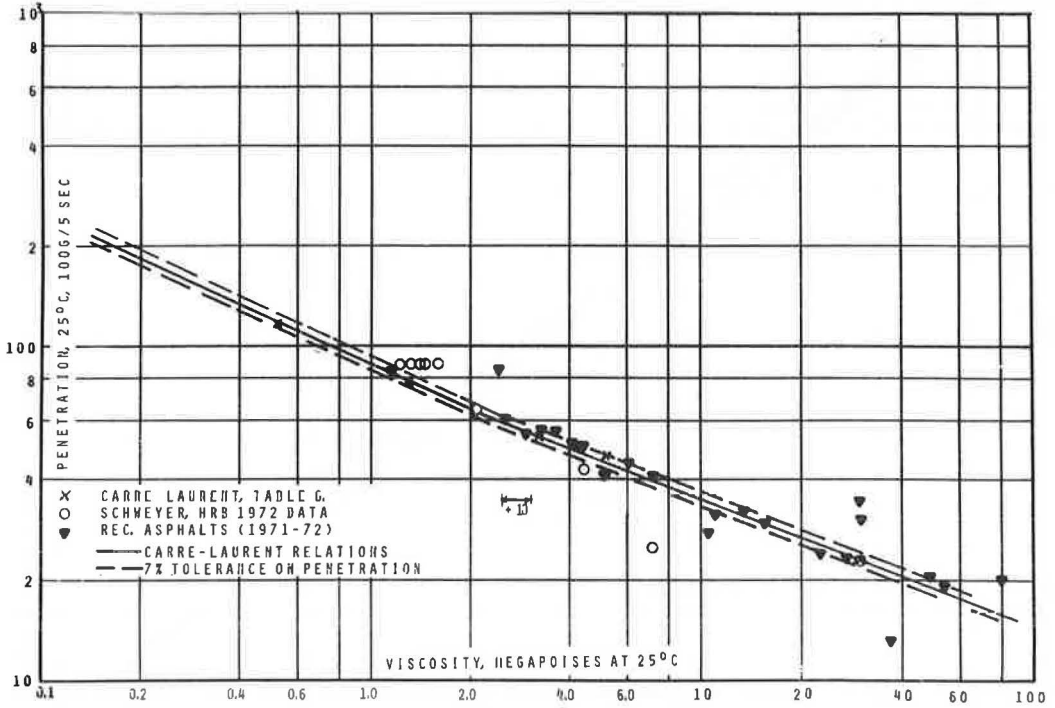
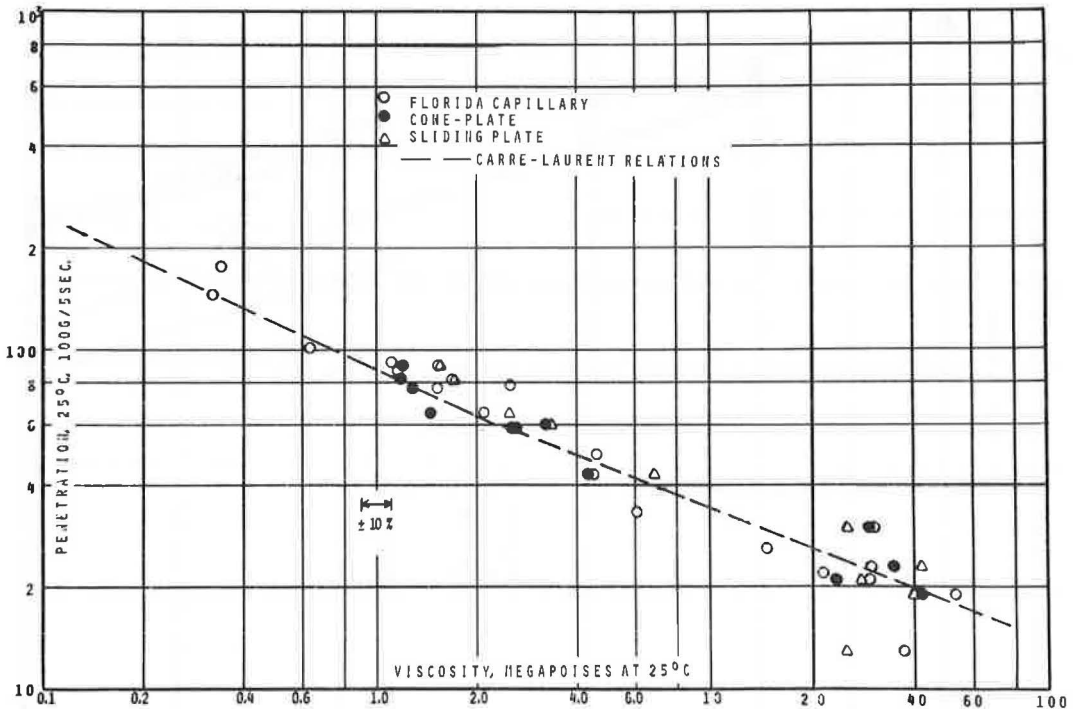


Figure 4. Analysis of Carré-Laurent relation with different methods (9).



There are numerous scientific approaches to evaluating temperature susceptibility, as listed by Jonpier and Kuilman (31). It would seem that the long-run effort to incorporate temperature susceptibility into mix design will require a more quantitative parameter than the empirical PI. It is difficult to believe that temperature susceptibility such as PI evaluated at the high intermediate range of 25 to 60 C can explain asphalt performance at low temperatures, particularly when relative slopes for different asphalts may be reversed. Some PI data are given in Table 4 for the record. Discrepancies are apparent.

STUDIES OF APPLIED RHEOLOGY

Penetration

In 1963, Carré and Laurent (32) presented rheology data on asphalts at temperatures from 15 to 50 C. The authors made an important contribution wherein a rate of shear $\dot{\gamma}_e$, corresponding to a given penetration in the standard test procedure, was proposed at which the equiviscosity η_e should be evaluated. The authors demonstrated a rather elegant mathematical analysis of the flow dynamics of the penetration test that has great merit if the penetrometer could be considered as a viscometer. Each penetration corresponds to a particular rate of shear. The corresponding viscosity at that rate of shear (as determined from viscosity versus rate of shear plots) is called the equishear viscosity of the asphalt. The analysis took into account the shape of the needle where a truncated cone geometry applies from 0 to 54 penetration. Above this rate, the cylindrical geometry effects must be considered. The calculated relation was compared with the results found empirically, showing a break in the plot at 60 penetration with the following results:

For penetration > 60

$$\eta_e = 14,500 P^{-2.15} \text{ megapoises} \quad (5)$$

For penetration < 60

$$\eta_e = 95,000 P^{-2.60} \text{ megapoises} \quad (6)$$

The equation for the relation between equiviscosity shear rate $\dot{\gamma}_e$ and penetration was found to be

$$\dot{\gamma}_e = 0.001441 P^{1.04} \text{ sec}^{-1} \quad (7)$$

These equations are shown in Figure 3 as solid lines with a gauge line of ± 10 percent from any mean viscosity at any given penetration being shown. The relations can be used if the variations shown are acceptable for the sliding-plate instrument.

However, when data from all methods such as the Florida capillary and the cone and plate are used (Fig. 4), the fit may not be as good. In fact, when certain highly blown asphalts or other low-penetration stocks are compared, the fit is not at all good. Single lines for data at different shear rates have been computed. It would appear that, from a linear least-squares fit for the capillary data, the following equations hold for the asphalts used in this study using only one line for the entire range:

At a rate of shear of 0.05 sec^{-1} ,

$$\eta_{05} = 19,100 P^{-2.13} \text{ megapoises} \quad (8)$$

At a constant power input of $10^5 \text{ ergs}/(\text{sec-cm}^2)$,

$$\eta_p = 32,400 P^{-2.32} \text{ megapoises} \quad (9)$$

At an equishear rate corresponding to the penetration,

$$\eta_e = 29,100 P^{-2.26} \text{ megapoises} \quad (10)$$

This analysis is presented for interest only because the author is in favor of direct measurement of viscosity.

Fromm and Phang (33) recently plotted data on viscosity (at 0.05 sec^{-1}) versus penetration and obtained the following relation for asphalts with viscosity at 25 C measured at 0.05 sec^{-1} :

$$\eta = 7,750 P^{-2} \text{ megapoises} \quad (11)$$

They also converted their data at an equishear rate to get

$$\eta = 18,500 P^{-2.198} \text{ megapoises} \quad (12)$$

However, even their 95 percent confidence limits showed allowable variations of ± 40 percent in viscosity.

It would appear from this information (and the fact that the equiviscosity rate of shear varies only from 0.08 to 0.17 sec^{-1} over penetrations from 50 to 100 respectively) that the Carré and Laurent refinement is but a minor correction from a constant shear rate of 0.05 or 0.1 sec^{-1} for most paving asphalts showing some small amount of complex flow. In fact, it is almost the same when penetration is higher than 60 as one proposed in 1933, which did not consider shear rate variations:

$$\eta = 15,800 P^{-2.16} \text{ megapoises} \quad (13)$$

Further analysis of these relations for data at lower temperatures, as will be shown later, indicates that plotting low-temperature data where penetrations are low and $\dot{\gamma}_c$ is very low may approach the range of shear rates where the viscosity is constant. The result is that the shear susceptibility effect disappears, and it may be more practical to compare data at 0.05 sec^{-1} , at a constant power input, or at 1.0 sec^{-1} (9).

Puzinauskas (5) presented a large amount of data on penetration and viscosity at different test temperatures. It was demonstrated with photographs that some asphalts of the same penetration visibly showed appreciable variations in the deformation area around the needle. This effect, which is related to adhesion for the steel needle, also influences the shear rate and volume involved in deformation and negates the use of the penetrometer as a viscometer.

As a final remark regarding penetration tests, it should be pointed out that modern viscosity grading at 60 C and viscosity measurements at 25 C and lower will make all empirical penetration relations obsolete as they are phased out of asphalt technology.

Ductility

For many years, the value of the ductility test on asphalts has been controversial. It has been condemned as worthless by some and praised highly by others. Never has it been shown to be a generally useful measure of asphalt rheology. The truth of the matter is that it is a very esoteric test involving the most complex rheological phenomena and many half-truths. Reiner (12, 19) described some of its mystique, and recent developments in studies of elongational viscosity for polymers may aid in understanding its results.

Most investigators think of ductility only as the length a sample can be extended as some measure of cohesiveness. This length decreases as the consistency increases. However, it is much more complex because the extension is a function of the interaction of test temperature (consistency level), temperature susceptibility, pulling rate and sample geometry (shear susceptibility, transient shear rate, and transient stress), nature of the volume flow (viscoelastic effects), flow mode (relative shear flow or elongational flow), and perhaps other parameters. For these reasons, attempts to measure the test and interpret the results are doomed to confusion unless each interacting test variable can be evaluated independently. For example, it was proposed almost 30 years ago (35) that the test could be explained by shear susceptibility differences, and so it did for the asphalts used as illustrations. Similar relations were reported later (4), but no distinction was made for viscosity modes or nature of the deformation.

Figure 5. Analysis of ductility and viscosity data at different temperatures.

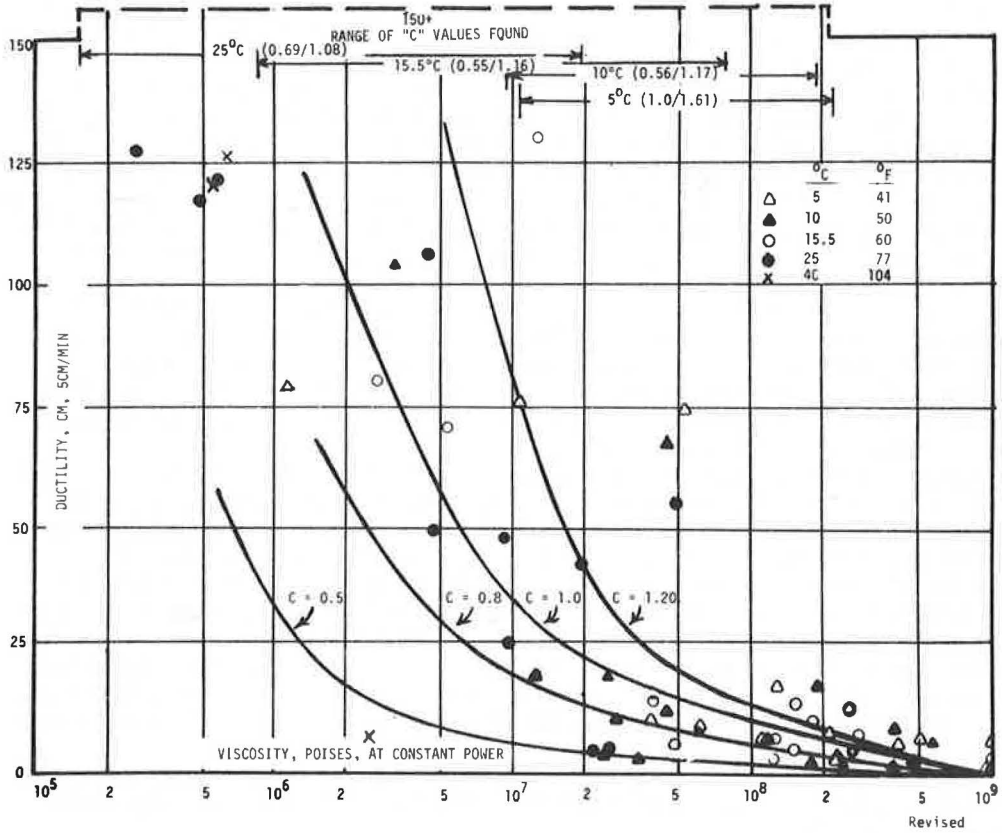


Table 5. Analysis of certain ductility data.

Asphalt		Penetration at 25 C	Penetration (dmm)	Ductility (cm)	Temperature (deg C)	Viscosity*	
Number	Material					Megapoises	C
High Ductility (>150) at Low Penetration at Test Temperature (100 g/5 sec)							
1	S64-8	177	19	>150	5	16.7	1.13
31	S68-3	147	12	>150	5	217	1.61
24	S71-21	108	20	>150	10	17.2	0.70
11	S71-10	92	11	>150	10	110	0.78
18	R72-3	88	12	>150	10	132	1.03
30	S68-2	79	12	>150	10	184	1.17
32	S68-5	93	10	>150	10	45.0	0.62
7	S64-46	43	16	>150	15.5	58.1	0.74
12	S71-13	27	27	>150	25	19.6	0.83
27	R72-5	73	31	>150	15.5	9.42	0.55
BB ^b	Steam ref.	10	10	>150	25	250	1.00
Low Ductility (<125) at High Penetration at Test Temperature (100 g/5 sec)							
9	S71-4	87	29	70	15.5	5.18	0.63
32	S68-5	93	93	122	25	0.568	1.12
2	S64-9	49	49	106	25	4.46	0.76
3	S64-20	101	101	117	25	0.49	0.74
20	S71-18	34	34	49	25	9.28	0.74
34	S71-29	22	47	6.7	40	2.29	0.48
AA ^b	Air blown	44	44	5.5	25	11.8	0.45

*Viscosity data at 10⁶ ergs/(sec cm²).

^bData taken from another publication (35).

Recently, Krchma (36) has proposed a new type of flow test that stretches the asphalt and is related to ductility. The fact that ductility maximizes as soft-asphalt consistencies are increased was noted. This confirms earlier publications (34) of such effects, which are known to experienced asphalt technologists.

Lewis and Welborn (37) demonstrated how, by varying the processing or the test temperature, the ductility maximizes with consistency. It had been demonstrated (34) that the ductility maximized at the region where the asphalt had a viscosity of 1 to 10 megapoises. This was confirmed by the Lewis and Welborn results. Their data maximized in the region of 50 to 75 penetration, which is where many asphalts have viscosity such as noted. It is also the region where the viscosity of the asphalt begins to change rapidly with penetration because the penetration needle truncated cone reverts to a cylinder at 54 penetration.

Lewis and Welborn made a number of ductility tests on selected samples at 15 C using various pulling rates. All samples decreased in ductility as the pull rate increased. Some materials (which probably were highly asphaltic in nature with high viscosities at 25 C) showed only small increases in ductility at low rates. They probably were on the right tail portion of a plot of ductility versus viscosity, and the rate was not slow enough to develop the ductility.

The authors also noted problems of very low ductilities at low temperature even with slow pull rates. Reiner (19) has pointed out that brittle fracture breaking of asphalt is an entirely different matter from a type of creep deformation such as a ductility flow test. His later work (12) is very comprehensive on the subject of a pulling test.

Halstead (38) summarized ductility data and indicated poor service of asphalt pavements when the retained ductility at 25 C dropped to 6 to 13, corresponding to about 20 to 30 penetration. A proposed "critical" ductility-penetration relation was shown, below which pavement distress might be expected. The thin-film test data were suggested as an indicator of pavement hardening for recovered asphalts. The applicability of this concept was illustrated for Virginia and Arkansas experiences as well as for data from the Zaca-Wigmore project on ductility data.

Puzinauskas (5) reported ductility test data at different test temperatures and indicated a relation between maximum tensile strength TS and viscosity η in megapoises approximately as follows:

$$TS = 65 \eta \text{ psi} \quad (13)$$

The author commented on penetration and ductility as follows: "Only a vague relationship exists between these two highly empirical and rheologically poorly controlled test methods."

In Figure 5 an attempt has been made to analyze the ductility data (all at 5 cm/min) in terms of shear susceptibility. Many materials will show a >150 ductility over a range of viscosity and values of shear susceptibility at the top of the figure. The lines drawn on the chart are the best attempt to show how the ductility improves with increased value of C. In general, if the asphalts show a value of C or higher, as designated on the line, the ductility should be at least as high as the line and can be higher.

Certain samples were separated into low and high ductility in Table 5 on the basis of elongational capability. A poor capability was designated as one that would just not string out to a >150 thread even though the material had a low viscosity at the test temperature.

There are a number of asphalts with shear susceptibility substantially above unity ($C > 1$) and high viscosity although this potential is not realized. This could mean that, under stress, a false, relatively hard consistency would be indicated in the penetration or the viscosity test because of dilatancy even though the material is actually relatively fluid at low stress. Accordingly, under the low stress of the ductility test, a good ductility results.

For the asphalts with low ductility, it is noted that, except for asphalt 32, the low ductility is associated with shear thinning ($C < 1$), which causes rapid necking in the ductility test and correspondingly low results. The exception (asphalt 32) is a shale oil residue.

There are two areas of asphalt rheology that are now being investigated in the author's laboratory that may eventually explain some of the anomalies of the ductility results. These relate to high-pressure viscosity measurements and to elongational viscosity, which deals with the filament-producing phenomena for materials, of which asphalt ductility is a good example. The capillary method for viscosity measurement incorporates in part certain geometry where elongational viscosity is involved, and such information when studied in connection with the data given in Table 5 may prove to be valuable. Some preliminary indications of the pressure effects on viscosity of asphalts have been presented (39) and will be extended in a future publication.

CONCLUSIONS

The major efforts of this paper may be summarized as follows:

1. Temperature susceptibility of asphalt cements is a most important material property that can be, and should be, evaluated by absolute viscosity measurements rather than by empirical tests.
2. Temperature susceptibility in the near-transition range varies with shear susceptibility and tends to increase with an increase in the complex flow index.
3. The complex flow index appears to approach unity as the temperature is raised to make the asphalt become essentially fluid. The index may pass through a minimum in the region of 10 to 40 C, and, as glassiness develops, it appears to rise considerably above unity.
4. The relative temperature susceptibilities of asphalts in the near-transition region cannot be predicted from what they exhibit at higher temperature levels.
5. More sophisticated studies are being employed by asphalt technologists in relating asphalt rheology measurements at the lower intermediate temperature ranges to pavement mix design and asphalt pavement performance.
6. Although the penetration test has performed a useful service in asphalt technology, its empiricism confuses all attempts to relate it readily to fundamental rheological studies.
7. The Carré-Laurent relation, which is quite elegant in concept and execution, in reality is not much better than other single-line empirical relations and suffers all the latter's inadequacies.
8. Studies on ductility continue to raise as many questions as they attempt to solve, and recourse should be made to any one or more appropriate tensile strength tests to measure extension properties of asphalts at low temperatures.
9. All research in asphalt technology points to greater recognition of direct viscosity measurements in absolute units for which there are now available satisfactory methods.

REFERENCES

1. Anderson, K. O., and Shields, B. P. Some Alberta Experience With Penetration-Graded Asphalt Cements Having Differing Viscosities at 140 F. Highway Research Record 350, 1971, pp. 15-25.
2. Kandhal, P. S., Sandvig, L. D., Koehler, W. C., and Wenger, M. E. Paper prepared for ASTM annual meeting, Los Angeles, June 1972.
3. Griffin, R. L., Izatt, J. O., and Lettier, J. A. ASTM, Spec. Tech. Pub. 328, 1963, p. 67.
4. Welborn, J. Y., Ogllo, E. R., and Zenewitz, J. A. A Study of Viscosity Graded Asphalt Cement. Public Roads, Vol. 34, No. 2, June 1966.
5. Puzinauskas, V. P. Evaluation of Properties of Asphalt Cements With Emphasis on Consistencies at Low Temperatures. Proc. AAPT, Vol. 36, 1967, pp. 489-540.
6. Fenign, J., and Kroosof, R. C. Proc. Can. Tech. Asphalt Assn., preprint, Nov. 1970.
7. Busby, E. O., and Rader, L. F. Paper prepared for ASTM annual meeting, Los Angeles, June 1972.
8. Lefebvre, J. A., and Robertson, W. D. Viscosity Characteristics of Two Canadian Asphalts. Proc. Canadian Tech. Asphalt Assn., Vol. 15, 1970.
9. Schwyer, H. E. Asphalt Cement Viscosities at Ambient Temperatures By a Rapid Method. Highway Research Record 404, 1972, pp. 86-96.

10. Evans, J. V., and Gorman, J. W. Paper prepared for ASTM annual meeting, Los Angeles, June 1972.
11. ASTM Book of Standards, Part 11. 1970, pp. 929-953.
12. Reiner, M. Deformation Strain and Flow, 3rd Ed. H. K. Lewis and Co., Ltd., London, 1969.
13. Sisko, A. W. Tensile Strength of Asphalt Films and Road Life. Highway Research Record 231, 1969, pp. 62-67.
14. Haas, R. C. G., and Anderson, K. O. Design Subsystem for the Response of Flexible Pavements at Low Temperatures. Proc. AAPT, Vol. 38, 1969, pp. 179-223.
15. Williams, F., Grimmer, L. E., and McAdams, M. M. Ohio Department of Highways, final rept., res. proj. HPS-HPR-1(32), March 1, 1967.
16. Marek, C. R., and Herrin, M. Tensile Behavior and Failure Characteristics of Asphalt Cements in Thin Films. Proc. AAPT, Vol. 37, 1968, pp. 386-421.
17. Heukelom, W. Observations on the Rheology and Fracture of Bitumens and Asphalt Mixes. Proc. AAPT, Vol. 35, 1966, pp. 358-399.
18. Lee, A. R., and Rigden P. J. Jour. Soc. Chem. Ind., Vol. 44, 1945, p. 153.
19. Reiner, M. The Rheological Properties of Bitumen and Asphalt. B.P.I.R., Hebrew Univ., Jerusalem, 1948.
20. Schmidt, R. J., and Santucci, L. E. A Practical Method for Determining the Glass Transition Temperature of Asphalts and Calculations of Their Low Temperature Viscosities. Proc. AAPT, Vol. 35, 1966, pp. 61-90.
21. Dobson, G. R. The Dynamic Mechanical Properties of Bitumen. Proc. AAPT, Vol. 38, 1969, pp. 123-139.
22. Schwyer, H. E., and Busot, J. C. A New Approach in Asphalt Rheology. Highway Research Record 273, 1969, pp. 1-11.
23. Majidzadeh, K., and Schwyer, H. E. Viscoelastic Response of Aged Asphalt Cements. Highway Research Record 231, 1969, pp. 50-61.
24. Sisko, A. W., and Brunstrum, L. C. The Rheological Properties of Asphalts in Relation to Durability and Pavement Performance. Proc. AAPT, Vol. 37, 1968, pp. 448-775.
25. Jonpier, R., and Kuilman, B. Characteristics of the Rheology of Bitumens. Proc. AAPT, Vol. 38, 1969, pp. 98-122.
26. Williams, M. L., Landel, R. F., and Ferry, J. D. The Temperature Dependence of Relaxation Mechanisms in Amorphous Polymers. Jour. Am. Chem. Soc., Vol. 77, 1955, pp. 3701-3707.
27. Sisko, A. W. Determination and Treatment of Asphalt Viscosity Data. Highway Research Record 67, 1965, pp. 27-37.
28. Holmes, A., Collins, J., and Child, W. Ind. Eng. Chem. Anal. Ed., Vol. 8, 1936, p. 100.
29. Pfeiffer, J. P., and Van Doormal, P. M. The Rheological Properties of Asphaltic Bitumen. Jour. Inst. Petrol. Tech., Vol. 22, 1936, p. 414.
30. Griffith, J. M., and Puzinauskas, V. P. Relation of Empirical Tests to Fundamental Viscosity of Asphalt Cement. ASTM STP 328, 1960, pp. 64-88.
31. Jonpier, R., and Kuilman, R. Rheol. Acta. 9, No. 3, 1960, p. 460.
32. Carré, G., and Laurent, D. The Relationship Between the Penetration and Viscosity of Bitumens. Assn. Francais des Techniciens du Petrole, Bull. 157, 1963.
33. Fromm, H. J., and Phang, W. A. Temperature-Susceptibility Control in Asphalt-Cement Specifications. Highway Research Record 350, 1971, pp. 30-39.
34. Traxler, R. N., Schwyer, H. E., and Romberg, J. W. Proc. ASTM, Vol. 40, 1940, p. 1182.
35. Traxler, R. N., Schwyer, H. E., and Romberg, J. W. Ind. Eng. Chem., Vol. 36, 1944, p. 383.
36. Krchma, L. C. Ductility, Flow Limit, and Asphalt Pavement Performance. Proc. AAPT, Vol. 35, 1966, pp. 139-163.
37. Lewis, R. H., and Welborn, J. Y. Public Roads, Vol. 21, No. 1, 1940, p. 1.
38. Halstead, W. J. Relation of Asphalt Ductility to Pavement Performance. Public Roads, Vol. 32, No. 10, Oct. 1963.
39. Schwyer, H. E., Moore, J. P., and Ling, J. K. Paper prepared for ASTM annual meeting, Los Angeles, June 1972.

DISCUSSION

R. L. Davis, Koppers Company, Inc., Pittsburgh

I support the author in his recommendation that rheological measurements on asphalts be made at stresses, strains, and temperatures that are pertinent to the conditions of interest. The importance of realistic testing conditions for measuring the rheological properties of bituminous materials is difficult to overemphasize.

The variation between penetration and various viscosity methods is shown in Figure 4 of Schweyer's paper. Figure 4 is a much fairer comparison than many that have been shown in the past because all methods have been shown at the same shear rates. Many of the other comparisons were made at not only different shear rates but also at different temperatures in some instances. The main objection that I have to Figure 4 is that it compares penetration to three other viscometers. Now each of these viscometers has rather wide precision limits, the variance of which is additive. Therefore, the spread of the three will be considerably wider than for a single method. Any fourth viscometer, when compared to these three, would show up badly on precision. I think that it is surprising that there is not more spread.

It may appear that I prefer the penetrometer to all viscometers. This is not the case. However, I do feel that the penetrometer, which in my view has done a good job over the years, has been unnecessarily maligned. I do think that the penetration test could easily be improved to make it a faster and simpler test method.

AUTHOR'S CLOSURE

The remarks of Davis are appreciated. His comments on variability for two methods compared to one are correct, but I would question that pooled results for other methods necessarily are greater than for any two. Finally, the more I learn about asphalt rheology, the less respect I have for the penetrometer as a potential viscometer.

CRACK DEVELOPMENT IN PAVEMENTS

Joseph E. Soussou and Fred Moavenzadeh, Massachusetts Institute of Technology

This paper discusses methods of analyzing crack development in pavements subjected to random repetitions of various loads in variable operating conditions. The approaches based on Miner's law present the advantage of simplicity. Their principal limitations are that the predicted fatigue life is generally a function of geometry and loading conditions. The data obtained in the laboratory constitute a good approximation to limited types of pavement systems. This law can be modified to account for temperature variations and variations in loading spectrum and material properties. The approaches based on the concepts of fracture mechanics can be viewed as a generalization of Miner's law. Although the latter bases the prediction of crack development on the initial configuration of the system, the fracture mechanics approach incorporates the changes of configuration (i.e., geometry). The application of this approach to linear elastic systems can also be viewed as a special case of a general approach including time-dependent and nonlinear material properties. A simplified extension to viscoelastic systems is also discussed. The modified Miner's law is preferred in the short range because of its simplicity and the availability of data, whereas the approaches based on fracture mechanics concepts are preferred in the long range because of their completeness.

•THE structural damage in pavement systems has two principal indicators: cracking and permanent deformation. The AASHO Road Test (1) indicates that the present serviceability index is not very sensitive to the degree of cracking of the pavement. Cracking may have, however, indirect effects on the accumulation of permanent deformation. These indirect effects are generally ignored in the mathematical models for pavement analyses.

Cracking results from load repetitions or environmental factors. Cracking due to repeated loading occurs primarily as a result of bending deflections. This type of failure is often designated as "fatigue failure." Fatigue in bituminous paving materials has been shown to be a progressive process. Cracks propagate from small flaws inherent in the material until ultimately the amount of cracking reaches an unacceptable level or the remaining section becomes so weak that catastrophic failure occurs.

This study reviews the principal approaches for the analysis of cracking in pavements. These methods are discussed, and two models are proposed.

THEORIES AND LAWS FOR FATIGUE CRACK ANALYSIS

A general law of fatigue crack propagation should take into account the five following factors (2):

1. Geometry (dimension of structure and shape and size of crack),
2. Loads (magnitude and location),
3. Material properties (constitutive equation),
4. Time (number of cycles, duration of loads, and time intervals between loads), and
5. Environment (temperature, moisture, pressure, and surrounding media).

These various factors are aggregated to different degrees depending on the method of analysis. Two broad types of theories are recognized: phenomenological and crack

Publication of this paper sponsored by Committee on Characteristics of Bituminous Materials.

propagation theories. The labeling and distinction between these two classes of approaches is rather arbitrary. The phenomenological theories include the approaches that measure a degree of damage for a homogeneous material without any description of the number, length, and width of cracks. The homogeneous material is assumed to deteriorate uniformly until total failure. These theories focus principally on the life duration of the structure rather than on the description of progressive changes of the damage indicators.

The crack propagation theories recognize the presence of flaws in the material and can describe the number and size of cracks as time elapses. Some of the crack propagation theories could be labeled as phenomenological theories because they try to fit some mathematical model to the macroscopic behavior of the material. However, the preceding definition will be utilized in this text.

PHENOMENOLOGICAL THEORIES

Review of Literature

The phenomenological theories generally assume a failure criterion for a homogeneous material. A general type of failure criterion would predict the failure under any type of loading history. Such a unified criterion is not known for any material. Instead different criteria are developed to account for various classes of loading histories. This approach is used in a number of engineering practices. For example, a maximum shear criterion is used for parts of a structure subjected to a given stress field, whereas a maximum tensile stress criterion is used for other parts of the same structure. Following a rational mechanics approach, it seems that a general criterion should involve combinations of stress or strain tensor invariants. Many analysts (3) use the form

$$F(I_1, I_2, I_3) > F_c \quad (1)$$

where I_1 , I_2 , and I_3 are stress invariants. Novozhilov (4) has given physical interpretation to these invariants. In a more general case, the failure envelope should also contain the time dependence (e.g., for viscoelastic materials). Thus, it could be written as

$$F[I_1(\tau), I_2(\tau), I_3(\tau), t, \text{temperature, etc.}] \geq K \quad (2)$$

Many simplifications are necessary in order to give this relation a tractable form. In particular, the important simplification of neglecting the influence of the past histories of I_1 , I_2 , and I_3 may be achieved. However, general failure envelopes allowing for stress multiaxiality are not known yet. Most of the failure envelopes determined for time-dependent materials correspond to uniaxial loadings. These envelopes are characterized by an indetermination in their values; i.e., statistical variations are the rule rather than the exception. Also, failure envelopes corresponding to long periods of loading (creep type) generally show more variations than failure envelopes corresponding to short times of loading.

Examples of such envelopes are a log stress at failure versus log strain at failure envelope suggested by Smith (5) for constant rate of strain loading histories. This concept, however, applies better to monotonic loading histories than to cycling or otherwise varying loading histories (3, 6). These criteria apply best when the material can be considered continuous (that is, it does not include flaws or other stress concentrators) and when it is subjected to a homogeneous state of stress.

When failure occurs under a large number of repetitions of the load, it is caused by a smaller load level than what would produce failure under a single load application. The failure is classified then as a fatigue failure and is analyzed by special methods. Generally, the main variable is the number of cycles, and it is assumed that every application of the load increases the amount of damage done to the material. The best known phenomenological theory for fatigue is Miner's law (7). This law states that, under constant stress amplitude, the increment of damage per cycle is constant and that this rate is a function of the load level. The law is written in the form

$$\sum_{i=1}^m \frac{n_i}{N_i(\sigma_i)} = 1 \quad (3)$$

where N_i is the number of cycles to failure at stress level σ_i and n_i is the actual number of applied cycles at this stress level. It can be seen readily that a major shortcoming of this law is that it does not account for sequence effects. Nonlinear forms of this law were derived to gain accuracy. These modifications, however, tend to impair the simplicity of the law and do not offer much accuracy and rigor. Indeed, by increasing the number of parameters necessary in a law, one can eventually describe any experimental set of data.

A generalized form of Miner's law is given by Freudenthal (8). The increment of damage F per cycle is assumed to be a function of the number of N or prior load applications:

$$\frac{dF}{dN} = f(N)_s \quad (4)$$

where the function $f(N)$ is also a function of the stress level. Thus, after N cycles, the amount of damage is given by the integral

$$F = \int_{N_{os}}^N f(N)_s dN \quad (5)$$

where N_{os} is the incubation period when the damage is assumed to be zero. This form could account for sequence effects.

Freudenthal and Heller (9) modified it in order to include the interactions between different stress levels. They introduced in Miner's law a stress interaction factor that is a function of the frequency distribution of the random loading. In its modified form, Miner's law is written as follows:

$$\sum_i \frac{n_i}{\omega_i N_i(\sigma_i)} = 1$$

where ω_i are the interaction factors. Another specialized form of Miner's law proposed by Corten and Dolan (10) attempts to account for the effects of prior history.

These different forms of Miner's law have been mainly applied to rate-insensitive materials and result in the determination of an S-N envelope or stress level versus number of cycles to failure at this level.

Williams (11) adapted the concept of Miner's law to rate-sensitive material by replacing the cycle ratio $\frac{n_i}{N_i}$ by a time ratio $\frac{t_i}{T_i}$; t_i is the elapsed time from the start of the test at the strain rate R_i , and T_i is the time to failure under the constant rate of strain R_i . It was observed that Williams' law could be combined with the failure envelope of Smith (5) to relate the results of different types of loading histories. However, its application is mostly successful for monotonic types of loading histories and should not be applied for cyclic loading (fatigue) where the amount of dissipated energy is large compared to the amount of strain energy.

Another phenomenological model was derived by Dong (26). It assumes that the damage function or damage index can be expressed as a nonlinear functional of the stress and strain tensor functions. Dong then proceeds to expand this nonlinear functional into a series of multiple integrals. This model yields Miner's law and Williams' law as particular cases. His model is very general but not very tractable. It can account

for the sequence effects and the interactions of different stress levels; however, as mentioned previously, a model can account for any type of effect when the number of required parameters is increased indefinitely.

Proposed Model

With some assumptions of continuity, the damage functional $F(t)$ can be expanded into a series of multiple integrals (26):

$$F(t) = \int_0^t K_1(t, s)V(s)ds + \int_0^t \int_0^t K_2(t, s_1, s_2)V(s_1)V(s_2)ds_1ds_2 + \dots \\ + \int_0^t \dots \int_0^t K_n(t, s_1, \dots, s_n)V(s_1)\dots V(s_n)ds_1\dots ds_n \quad (6)$$

The measure of damage $F(t)$ is not, however, uniquely defined. The damage may be measured by the density of cracking, or by the value of dynamic modulus of the layer materials at a given frequency, because this modulus decreases as the density of cracking increases (8). The creep compliance of the material can be used as a measure of crack propagation (12) or the number or remaining cycles before complete failure under a given mode of loading can be used for this purpose (7). Any of these measures can be used, and it is convenient to normalize them so that the damage functional equals 0 when the material is intact and increases to 1 at failure. In the preceding equation, $V(s)$ is a function involving stress or strain invariants or both, and s is an arbitrary parameter that may have a meaning of time or cycles. This representation of the damage functional is general and accounts for accumulation of damage, recovery processes such as healing, and aging effects.

The review of literature showed that, for various asphaltic and bituminous mixtures, failure envelopes were related to a strain measure. In the general case of triaxial loading conditions, the strain measure should be expressed as a combination of invariants. In the absence of results of triaxial tests, we will use the derivative of the major principal strain as a strain measure in the damage functional. Thus,

$$F(T) = \int_0^t K_1(t, s)\dot{\epsilon}(s)ds + \int_0^t \int_0^t K_2(t, s_1, s_2)\dot{\epsilon}(s_1)\dot{\epsilon}(s_2)ds_1ds_2 + \dots \quad (7)$$

where the symbol with a dot over it represents a differentiation with respect to the argument. When s has a time meaning, expansion is similar to the representation of the time response of a nonlinear viscoelastic material. When s has a cycle meaning, it may be related to the dynamic representation of a nonlinear viscoelastic material and may be determined as a transfer function of a system subjected to a cyclic loading.

In order to simplify this expansion, we assumed that three different damage processes may be recognized: a damage process depending on the number and amplitude of cycles, a healing process (or a recovery process) depending on the elapsed time since the damage was created, and an aging process where the materials properties are changing with time. The damage functional may now be written as

$$F(t) = \int_0^t K_1(s, t - s)\epsilon(s)ds + \int_0^t \int_0^t K_2(s_1, t - s_1, s_2, t - s_2)\epsilon(s_1)\epsilon(s_2)ds_1ds_2 + \dots \quad (8)$$

This equation implies that the kernels are functions of the running time s (cumulative and aging processes) and of the lapse of time $t - s$ (recovery process).

In a first approach to the problem, the second and higher order kernels will be neglected in the damage expression. We will further assume that the first-order kernel may be factorized:

$$K_1(s, t - s) = K_{\text{cum}}(s) K_{\text{rec}}(t - s, s) \quad (9)$$

i.e., the cumulative and recovery processes are independent. The aging process is included in both K_{cum} and K_{rec} through the dependency on the time s .

Determination of these kernels depends on choosing a measure for the damage and normalizing it as mentioned previously. Let N be the number of cycles to failure (i.e., inadmissible density of cracking) under a given type of random load during relatively short time (no aging or recovery takes place). A damaged material will undergo only N' cycles under the same conditions before failing. The amount of damage is represented by $\frac{N - N'}{N}$. N and N' can be measured on control specimens. Note that in this case $F(t)$ is not a measure of the amount of cracking but is a function of it.

Cumulative Kernel—For a small period of time over which there is neither aging nor damage recovery, we have for the increment of damage $\Delta F(\tau)$ an expression such as

$$\Delta F(\tau) = \sum_{i=1}^m \frac{dn_i}{\omega_i N_i [\Delta \epsilon(\tau), \tau]} \quad (10)$$

where τ indicates that the number of cycles to failure may vary because of aging and that the envelope is to be determined for different values of τ . The increment of damage is also a function of the average strain amplitude applied during the increment of time τ .

Recovery Kernel—The recovery kernel $K_{\text{rec}}(t - \tau, t)$ is a function of the time ($t - \tau$) elapsed since the application of the damage increment and of the age of the material. It is apparent that healing requires the presence of a minimum compressive stress (13). Thus, we will assume that the argument ($t - \tau$) can be replaced by ($t^* - \tau$) and

$$t^* = \tau \int_{\tau}^t H[\sigma(s) - \sigma_{\text{min}}] ds \quad (11)$$

where $H[]$ is the Heaviside step function that is equal to 1 when its argument is positive and zero elsewhere, and σ_{min} is the minimum compressive stress that triggers healing. Thus ($t^* - \tau$) is the accumulated time during which a minimum compressive stress is present.

To determine $K_{\text{rec}}(T)$, two identical specimens (or sets of specimens) should be given the same amount of damage F . F is determined by testing one of the two specimens (control specimen) and measuring the amount of damage that should be applied to cause the specimen to fail. The second specimen is left to rest for a time T and then caused to fail to determine the amount of recovery $K_{\text{rec}}(T)$.

Aging—Aging is accounted for through changes in the characteristics of the constitutive equation and in the cumulative and recovery kernels.

Thus, the complete expression can take the form

$$F(t) = \int_0^t \left\{ \sum_{i=1}^m \frac{dn_i}{\omega_i N_i [\Delta \epsilon(\tau), \tau]} \right\} K_{\text{rec}}(t - \tau, \tau) d\tau \quad (12)$$

CRACK PROPAGATION THEORIES

Review of Literature

A different method of approach is based on the concepts introduced in fracture mechanics. The formulations are based on the balance of energy release and energy

accumulation at the crack tip. Generally, in these formulations the damage index is a crack length. The rate of crack length increase per cycle is given by a relation such as

$$dc/dN = f(\sigma, c, C_1) \quad (13)$$

where C_1 are some material properties. The form of this equation describing the crack growth per cycle of loading is derived from a dimensional analysis, from a work-hardening model, from equations relating the growth rate to the crack opening displacement, or from a molecular theory. The basis of the law could also be empirical.

These approaches are essentially based on the energy balance concept introduced by Griffith (14) for brittle materials. He postulated that a crack will propagate when the rate of release of the strain energy becomes greater than the rate of creating a new surface, i.e., rate of increase of surface energy. Orowan (15) extended this theory to ductile materials by adding to the surface free energy the plastic energy of deformations. Rivlin and Thomas (16) generalized this theory by writing that the release of strain energy does not go entirely to produce new surfaces (surface free energy). In this way, they were able to apply the Griffith theory to rubbers.

The Griffith theory leads to the determination of a critical stress that is given in the following form:

$$\sigma_{cr} = K E \sqrt{T_1/c} \quad (14)$$

where K is a constant of the geometry, E is the material modulus, and c is the crack length. Williams (11) postulates that, to generalize this equation, one may use for the dissipated energy \dot{T}_1 the sum of energies dissipated in the brittle, ductile, and viscoelastic dissipation processes. A better way of extending the Griffith energy balance concept is to use the so-called general power equation (11). This equation may be written as

$$\int_{C_1} T_1 \dot{u}_i d_s = \dot{D} + \dot{U} + \dot{\Gamma} \quad (15)$$

where T_1 and u_i are the surface traction and displacements of a contour C_1 that encloses the crack C , the dots represent a time derivative, U is the free energy (strain energy), D is the energy dissipated in the form of heat, and Γ is the specific surface energy. One can also include in this equation other types of energies such as the kinetic energy as proposed by Blatz (17). There are different methods of applying the power equation to determine the law of crack propagation.

However, as Griffith (14) and Orowan (15) have pointed out, the Griffith energy balance criterion is equivalent to the attainment of specific stresses at the crack tip. In other words, it is the local state of stress at the crack tip that controls cracking. Following this idea, one computes the local stresses ahead of a crack using the results of the theory of elasticity. These local stresses are given in the form of stress intensity factors K_1 , K_2 , and K_3 , which correspond respectively to the opening, in-plane sliding, and tearing modes. K_1 , K_2 , and K_3 are determined by the theory of elasticity as shown by Inglis (18) and Sneddon and Lowengrub (19). Lee (20) showed that, for the case of stress boundary conditions, the elastic constants do not appear in the expression of the stress distribution; thus, the stress distribution is the same for a viscoelastic material as it is for an elastic material. Therefore, Williams (21) solved the problem of the growth of a crack in a viscoelastic material subjected to stress boundary conditions by using the elastic values of the stress intensity factors. The viscoelastic properties are used to deduce the strains at the crack tip. An essential advantage in this approach is that it concentrates on stress or strain criteria rather than energies, and stresses can be superposed whereas energies cannot.

Most of the crack propagation laws obtained for rate-insensitive materials are of the form

$$dc/dN = C \sigma^n c^m \quad (16)$$

where C , m , and n depend on the material properties, the geometry, and the method used for the derivation of the law (i.e., dimensional analysis or work-hardening model).

Proposed Model

It was observed for pavement structures that cracks propagate under the influence of repeated loading rather than under the influence of monotonically varying loading histories. Using these assumptions, one can restrict the study of crack growth in pavement structures to the study of crack growth under the influence of repeated loadings (fatigue).

For fatigue cracking, it is generally convenient to give the probability of crack growth per cycle rather than crack growth per time unit. A cycle is the interval separating two successive troughs or two successive peaks of the load. It is readily seen that, although this representation will be very convenient for sinusoidal loadings, it will not be very useful for some types of random loadings. We will adopt this representation because it is a convenient one for the case of pavement systems where we have loads of different magnitudes that are applied for different durations at various intervals of time.

The use of the number of applied cycles instead of the time increments can be mainly justified when the measure of damage (crack accumulation in this case) varies slowly as a function of the number of applied cycles n . In this case it can be differentiated with respect to n . The probability of a given crack growth per cycle μ_c can be related to the probability of crack growth per unit time μ_t by the expression (22):

$$\mu_c = \mu_t / \omega \quad (17)$$

where ω is the angular frequency.

It appears, however, that, for many materials, the dependence on the past history of the local stress tensor at the tip of the crack can be restricted to the last cycle of a local stress measure. In other words, the crack propagation occurring during the last cycle of load application is exclusively a function of the local stress changes resulting from the last cycle of loading. This is a simplifying assumption, and its degree of validity depends on the type of material.

Because the local stress at the tip of the crack is a function of the nominal stress σ and the crack size c , the rate of crack propagation can be written generally as

$$dc/dn = f(\sigma, c, M_1)_{\text{last cycle}} \quad (18)$$

where M_1 are the materials properties; σ and c can also be combined in the stress intensity factor K :

$$dc/dn = f(K, M_1)_{\text{last cycle}} \quad (19)$$

The best method of approach for the determination of the functional f is to develop a good understanding of the micromechanisms of crack propagation. Otherwise one can only make some educated guesses and check them experimentally. For instance, for non-rate-sensitive materials, one can assume that

$$dc/dn = f[K_n, K_{n-1/2}, K_{n-1}, M_1] \quad (20)$$

where K_n is the last peak value of the stress intensity factor at the tip of the crack, $K_{n-1/2}$ is the last trough, and K_{n-1} is the value of the previous peak. It appears logical to express these three independent variables by another set of independent variables (Fig. 1),

$$\left. \begin{aligned} K &= \frac{1}{3}(K_{n-1} + K_{n-1/2} + K_n) \\ \Delta_1 K &= K_n - K_{n-1/2} \\ \Delta_2 K &= K_n - K_{n-1} \end{aligned} \right\} \quad (21)$$

and to expand f in terms of K , $\Delta_1 K$, and $\Delta_2 K$, and the different combinations of their powers. The influence of K is known to be negligible for non-rate-sensitive materials, $\Delta_1 K$ intervenes by its fourth power (23), and the influence of $\Delta_2 K$ is not well known. It is only known that, when $\Delta_2 K$ is positive, the rate of crack propagation is not much affected. Thus, the rate of crack propagation for many rate-insensitive materials can be written as

$$dc/dn = A(\Delta_2 K) \times \Delta_1 K^m \quad (22)$$

where m is assumed to have the value of 4, and $A(\Delta_2 K)$ is a material property. For rate-sensitive materials, the coefficient A may also become a function of rate and temperature. In this crack law, A and m may become dependent on the structure and the type of loading history. For instance, Ramsamooj (24) finds that it applied better to beams or slabs that were elastically supported than to the same structures with weakened supports. This fact suggests that, for cases where the viscoelastic effects are important, a more complete law of crack propagation will be required. Following the same reasoning to simplify the rate propagation law, we may conclude that, if the rate of crack propagation can be considered a function of the changes in the stress intensity factor during the last cycle, then

$$dc/dn = f(K, \Delta_1 K, \Delta_2 K, t, \Delta_1 t, \Delta_2 t) \quad (23)$$

where K , $\Delta_1 K$, and $\Delta_2 K$ have been defined previously, t is the time corresponding to K_n , and $\Delta_1 t$ is the time lag between K_{n-1} and K_n . Being the parameter accounting mostly for aging and creep rupture, $\Delta_1 t$ represents the time of loading; $\Delta_2 t$ represents the rest period and could correspond to the healing effects. With these assumptions, we may assume a general law of crack propagation for rate-sensitive materials that isolate the most important parameters. This law can be expanded into different forms according to the experimental results that are found. If a simple expansion can result, this relation will be useful. If a complicated expansion is needed, it is preferable to use a more fundamental approach such as the power law described previously. We will assume that such a simplified expression can be found for paving materials:

$$dc/dn = f[(K, t), (\Delta_1 K, \Delta_1 t), (\Delta_2 K, \Delta_2 t)] \quad (24)$$

Such a law can be used to account for random loadings.

For computation purposes, we will use the special case of this propagation law:

$$dc/dn = A(\Delta_1 t, \text{temp}) \Delta_1 K^4 - CH(\Delta_2 t, \text{temp}) \quad (25)$$

where the loading time $\Delta_1 t$ represents the frequency dependence of the coefficient A . More accurate laws will undoubtedly be found when more is known about the fracture of paving materials.

EXAMPLES OF APPLICATIONS

Phenomenological Law

Typical values for the failure envelope were taken from the literature (25). These envelopes were obtained from bending tests under constant stress levels. More accurate failure envelopes should be obtained by trying to simulate typical histories of the triaxial state of stresses that develop at the critical points in the pavements. In the example that was studied, the failure envelope was given by

$$N = K \left(\frac{1}{\Delta \epsilon} \right)^n$$

where $K = 5.10^{-4}$ and $n = 4.5$, and $\Delta \epsilon$ is the strain amplitude and is measured as half the difference between two consecutive peaks and troughs in the strain function. For tem-

Figure 1. Time variations of the stress intensity factor.

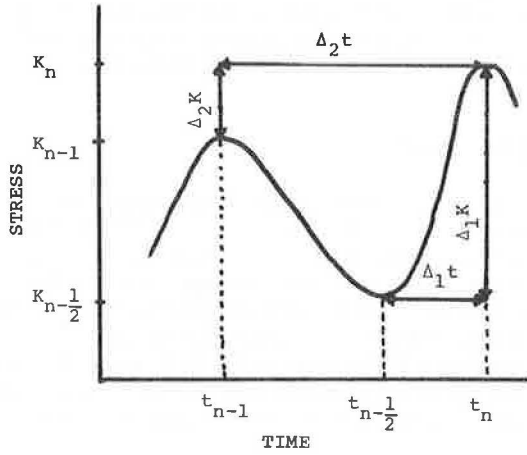


Figure 2. Ratio of tensile strength for damaged and undamaged materials (13).

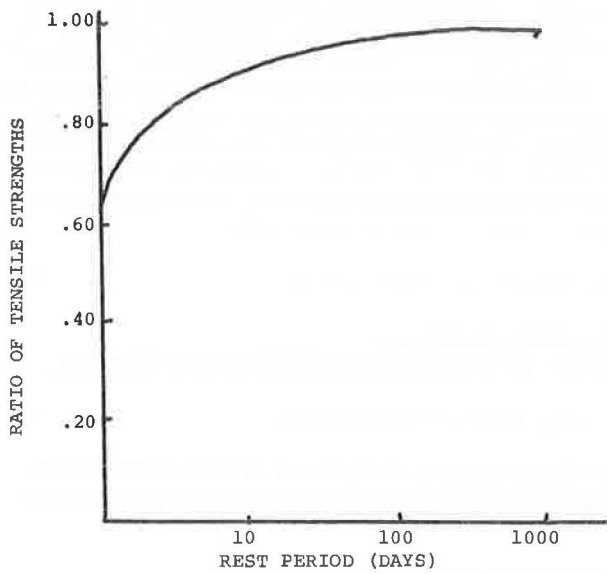


Figure 3. Typical recovery function for a fatigued dense bituminous mix (13).

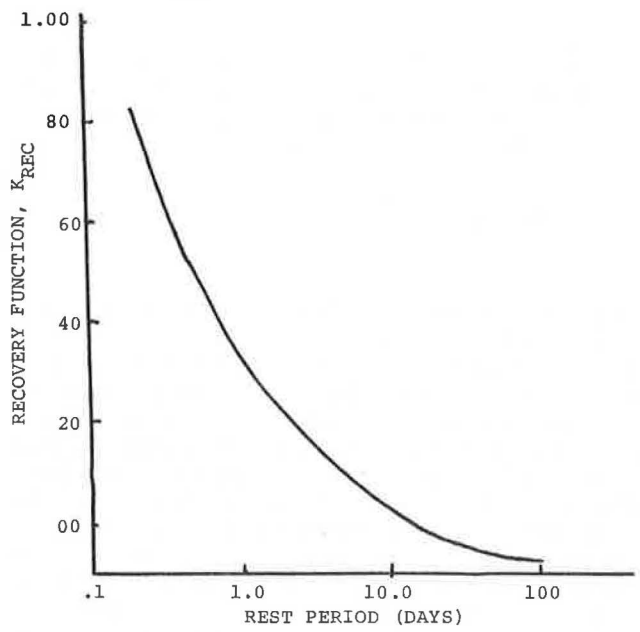
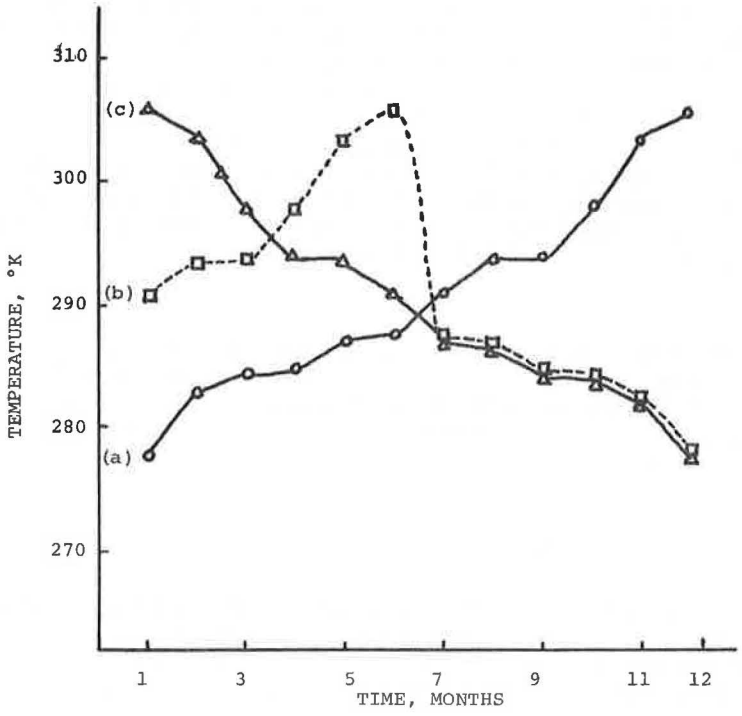


Figure 4. Temperature variations.



peratures above 22 C, K was increased by a function of temperature to account for the fact that, at higher temperatures, very large strains occur but do not contribute to cracking.

The recovery kernel is obtained by curve fitting with a series of exponential experimental results such as shown in Figures 2 and 3 (13). These figures show that, for broken and fatigued bituminous mixes, a complete recovery is obtainable after 3 months at 10 C. This recovery is also a function of temperature. In the example that was treated, the temperature dependence of this function was simplified to

$$K_{r_{oo}}(t) = 0.2 \left(1 + \sum_{i=1}^5 e^{-\alpha_i t} \right)$$

where t^* = total amount of time during which no load is applied and the temperature is above 22 C; α_i were chosen so that the recovery is completed in a period of 3 months.

Twelve different temperatures were generated by the random number generator. These temperatures were arranged by increasing order, then by decreasing order, and finally by a successively increasing and decreasing order [Fig. 4, (a), (b), and (c) respectively]. These series were used as inputs to the analysis, and the number of load applications was assumed constant and equal to 15,000 loads. The resulting residual strains are shown in Figure 5. These residual strains at the first interface were used in lieu of the residual deflections at the surface because they present the same type of behavior and permit the qualitative study of the trends of this behavior. Figure 5 shows that the residual strains after a period of 12 months were almost equal for the series (b) and (c) because the temperatures corresponding to the last 5 months of these series were identical. The effect of the difference of temperature history in the first months was negligible. The residual strains due to the increasing order series (a) were a little different. On the whole, for the assumed materials properties, the residual strains were not very sensitive to changes in the sequence of temperatures.

Figure 5 shows also the strain amplitudes corresponding to each basic unit of time (month). These amplitudes were essentially functions of the present temperatures. Hence, their variations are directly related to the temperature changes.

Figure 5 shows also the damage function, $F(t)$, for the three sequences of temperatures. The irregularities in the shape of $F(t)$ result from the strong nonlinearities arbitrarily introduced by the data used in the formulations. It can be seen, however, that the model accounts for the differences in temperature sequences and that the sequences are more important for the determination of the damage function $F(t)$ than they are for the determination of the residual strains. It is not possible to derive more conclusions from the computed behavior because the data are not real.

Crack Propagation Law

An approximation is used to apply this law. The stress distribution is computed at different temperatures in a multilayered homogeneous viscoelastic system (Fig. 6). The stress intensity factors are approximated by those obtained for simple tension by considering a small volume at the interface between the first and second layer. We find for a penny-shaped crack that

$$K = \frac{2.05}{\sqrt{\pi}} \sqrt{a} \sigma$$

where σ is the nominal stress (Fig. 6) and a is the crack length. The crack is assumed to start at the interface and to propagate toward the surface. The initial flaw size a_0 is given from experimental data, and the final crack size a_r is chosen to be equal to half the thickness of the first layer. Using the Paris (23) crack propagation law, we obtain

$$N_r = \int_{a_0}^{a_r} \frac{1}{A(\Delta K^4)} da = \frac{\pi^2}{A(2.05)^4} \int_{a_0}^{a_r} \frac{d_a}{\sigma^4(c)d_c}$$

Figure 5. Comparison of different sequences of temperatures.

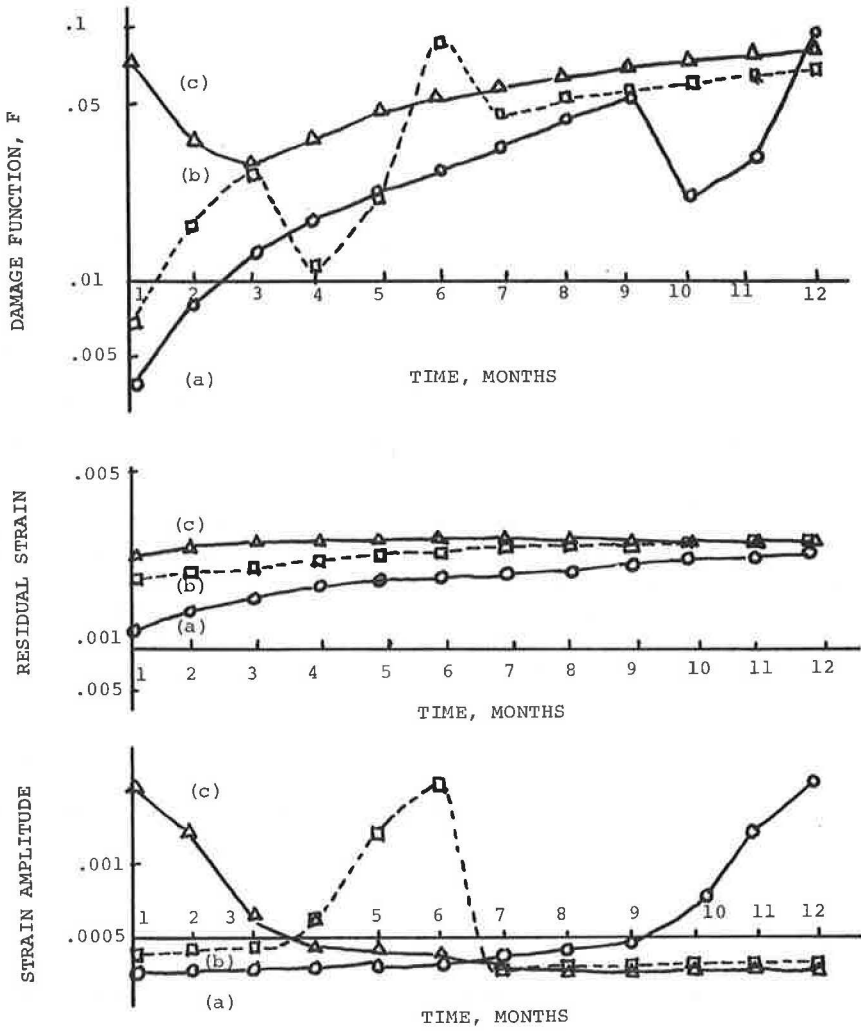
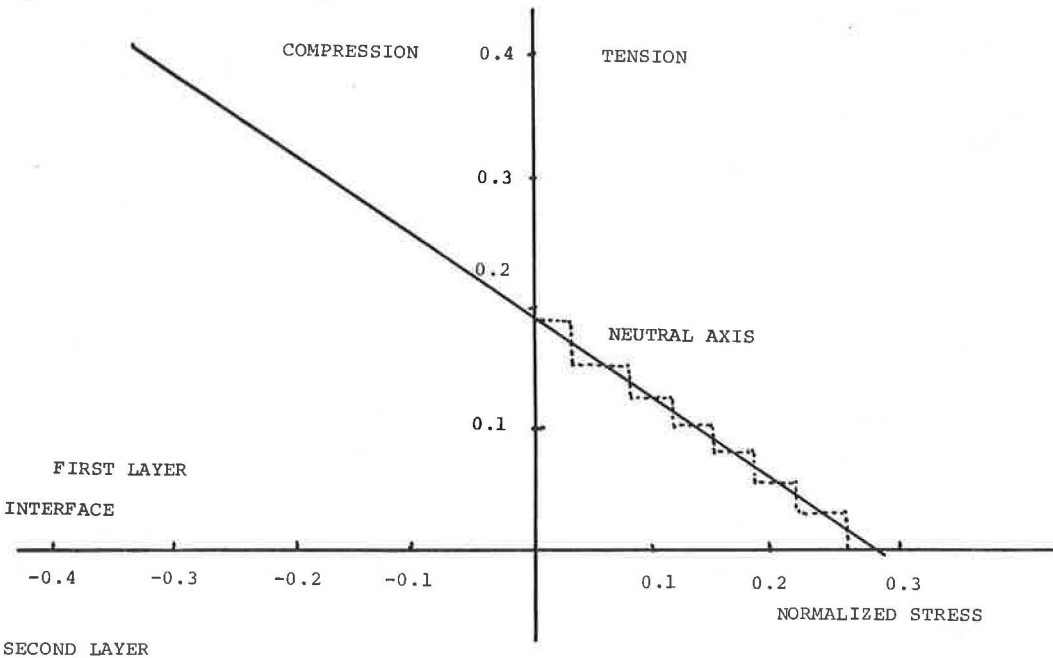


Figure 6. Discretization of crack growth.



where A is a material property.

This integral is broken into a summation of elements representing a small crack propagation during which σ may be assumed to be constant:

$$N_f = \frac{\pi^2}{A(2.05)^2} \sum_{i=1}^m \frac{1}{\sigma^4 \left(\frac{a_i + a_{i-1}}{2} \right)} \left(\frac{1}{a_{i-1}} - \frac{1}{a_i} \right)$$

CONCLUSIONS

The approach based on Miner's law presents the advantage of simplicity. Also, experimental data are readily available for its use. Its principal shortcomings are that it does not account properly for geometry effects and it does not give a physical description of the cracking of the pavement.

The approach based on the crack propagation laws can be viewed as a generalization of Miner's law. The latter bases the prediction of crack development on the initial configuration of the system, and the fracture mechanics approach incorporates changes in configuration. It can be used in a simplified form as shown previously. It is preferred in the long range because it accounts for the five factors previously described (geometry, loads, material properties, time, and environment). It also provides a physical description of the cracking of the system.

ACKNOWLEDGMENT

The work reported here was sponsored by the U.S. Department of Transportation, Federal Highway Administration. The opinions, findings, and conclusions expressed in this paper are those of the authors and not necessarily those of the Federal Highway Administration.

REFERENCES

1. The AASHO Road Test: Report 5—Pavement Research. HRB Spec. Rept. 61E, 1962, 352 pp.
2. Pelloux, R. M. Review of Theories and Laws of Fatigue Crack Propagation. Proc. Conf., Miami Beach, Dec. 15-18, 1969.
3. Williams, M. L. Some General Observations on Failure and Fracture. SRSIA, Vol. 7, No. 1, Jan. 1970.
4. Novozhilov, V. V. The Physical Meaning of the Stress Invariants of the Theory of Plasticity. Applied Math. and Mech., Academy of Science, U.S.S.R., Vol. 16, 1952.
5. Smith, T. L. Ultimate Tensile Properties of Elastomers: Comparison of Failure Envelopes of Unfilled Vulcanizates. Jour. of Applied Physics, Vol. 35, No. 1, Jan. 1964.
6. Knauss, W. G. The Time Dependent Fracture of Viscoelastic Materials. Proc. First Internat. Conf. on Fracture, Sendai, Japan, 1965, Vol. 2, pp. 1139-1166.
7. Miner, M. A. Cumulative Damage in Fatigue. Jour. of Applied Mechanics, Vol. 12, 1945.
8. Freudenthal, A. M. Fatigue. In Handbuch der Physik (Flugge, S., ed.), Vol. 6, Springer-Verlag, 1958, p. 591.
9. Freudenthal, A. M., and Heller, R. Z. On Stress Interactions in Fatigue and a Cumulative Damage Rule. Jour. Aerospace Sciences, Vol. 26, No. 7, July 1959.
10. Corten, H. T., and Dolan, T. J. Cumulative Fatigue Damage. Internat. Conf. on Fatigue, Institute of Mechanical Engineering, London, 1956.
11. Williams, M. L. Initiation and Growth of Viscoelastic Fracture. Proc. First Internat. Conf. on Fracture, Sendai, Japan, 1965, pp. 1111-1133.
12. Majidzadeh, K., et al. Analysis of Fatigue and Fracture of Bituminous Paving Mixtures. Ohio State Univ., Rept. RF 2845, May 1970.
13. Bazin, P., and Saunier, J. B. Deformability, Fatigue and Healing Properties of Asphalt Mixes. Second Internat. Conf. Structural Design of Asphalt Pavement, Ann Arbor, 1967.

14. Griffith, A. A. Proc. First Internat. Congress of Applied Mechanics, Delft, 1924, pp. 55-63.
15. Orowan, E. Fatigue and Fracture of Metals (Murray, W. M., ed.). John Wiley and Sons, 1952, pp. 139-167.
16. Rivlin, R. S., and Thomas, A. G. Jour. of Polymer Science, Vol. 10, No. 3, 1953, p. 291.
17. Blatz, P. J. An Elasto Dynamic Theory of Fracture. Polymer Science Report, North American Aviation Science Center, Thousand Oaks, California, April 1967.
18. Inglis, C. E. Stresses in a Plate Due to the Presence of Cracks and Sharp Corners. Trans. Institute of Naval Architecture, Vol. 55, 1913, p. 219.
19. Sneddon, I. N., and Lowengrub, M. Crack Problems in the Classical Theory of Elasticity. John Wiley and Sons, New York, 1969.
20. Lee, E. H. Structural Mechanics (Goodier, I. H., ed.). Pergamon Press, 1960, pp. 456-482.
21. Williams, M. L. The Fracture of Viscoelastic Materials. In Fracture of Solids (Drucker, D.C., ed.), Interscience Publishers, 1962, pp. 157-188.
22. Yokobori, T. An Interdisciplinary Approach to Fracture and Strength of Solids. Wolters-Noordhoff Scientific Publications, Groningen, The Netherlands, 1968.
23. Paris, P. C. The Fracture Mechanics Approach to Fatigue. In Fatigue: An Interdisciplinary Approach (Burke, J. J., ed.). Proc. 10th Sagamore Army Materials Research Conf., Syracuse Univ. Press, 1964.
24. Ramsamooj, D. V. Analysis and Design of the Flexibility of Pavements. Ohio State Univ., PhD dissertation, 1970.
25. Kasianchuk, D. A. Fatigue Considerations in the Design of Asphalt Concrete Pavements. Univ. of California, Berkeley, PhD dissertation, 1969.
26. Dong, R. G. A Functional Cumulative Damage Theory and Its Relation to Two Well Known Theories. Lawrence Radiation Laboratory, Univ. of California, Jan. 1967.

PROPOSED METHOD OF PRODUCING ASPHALT CONCRETE BEAMS FOR LOW-TEMPERATURE TESTING

L. F. Rader and R. T. Ochalek, University of Wisconsin, Madison; and
E. O. Busby, University of Wisconsin, Platteville

The cracking of asphalt concrete pavements from influences of low temperatures has become an expensive maintenance item to highway departments in cold climates. It has been recognized that flexural tests of beams of bituminous paving mixtures conducted at low temperatures furnish indexes that disclose the thermal sensitivity of the binders. However, the difficulty in reproducing suitable specimens has caused high coefficients of variation in test results. Therefore, the objective of this investigation was to standardize a procedure of making beams that have the characteristics of asphalt concrete wearing courses. The California kneading compactor was modified to form beams 15 by $3\frac{1}{4}$ by $3\frac{1}{2}$ in. in size. Two types of aggregates and five different asphalt cements were used in bituminous mixtures. Viscosity control determined the mixing and the compacting temperatures. A technique of beam making consisting of combinations of tamping blows at different foot pressures and of a static load consistently produced homogeneous specimens of acceptable densities and proper aggregate orientation. From results of this investigation, it appears practicable to form and test beams in state, municipal, and commercial laboratories. The determination of the rheological properties of paving mixtures made with indigenous aggregates and diverse asphalt cements will predict the suitability of the binders at the minimum temperature of a region.

•METEOROLOGICAL records indicate that Wisconsin experienced its worst winter in 100 years during the 1971-72 season: worst in terms of amount of snowfall, number of days of subzero temperatures, and number of freeze-and-thaw cycles. Because some 93 percent of our paved roads are bituminous covered, the transverse cracking of the viscoelastic material induced by low temperatures has become a topic of increasing importance to maintenance departments. This premature non-load-associated cracking has serious implications with respect to accelerating losses in serviceability of these thermoplastic pavements and has become an annual multimillion dollar problem in the northern tier of states in the United States and bordering provinces of Canada.

Cracking of bituminous surfaces may occur from causes other than the excessive tensile stresses developed by high thermal gradients. Other internal forces can result from in-service asphalt cement aging and from moisture absorption and loss in mixes containing absorptive aggregates. External tensile forces in a surface course can be caused by reflective cracking, i.e., volume change of the subgrade or of the base course or both from moisture loss. Tensile stresses are also developed from the bending of the bituminous mat under traffic loadings from loss of support due to settlement of the subgrade and from differential swelling of the subgrade.

Usually, one or more of these causative factors contribute to pavement failure. However, this investigation is confined to the behavior, at low temperatures, of densely graded asphalt concrete.

LABORATORY INVESTIGATIONS

Objective

The primary objective is to standardize a method of making an asphalt concrete beam that, in the laboratory, has the density characteristics, homogeneity, and aggregate orientation of surface courses laid down by current paving equipment. Also, recommendations are made for measuring the rheologic behavior of asphalt concrete at low temperatures utilizing relatively simple equipment.

Justification

Procedures have been developed to measure directly the loading time and temperature dependence of mixtures by testing in compression, tension, and flexure. The types of tests include creep, stress relaxation, and constant rate-of-strain tests and the more complicated dynamic tests that apply sinusoidal loadings to a specimen or the repeated, or pulse-type, loading that simulates vehicle velocity. But whether the equipment utilized in a test is a simple compression machine applying a three-point beam load, a flexural-fatigue machine, or a console-mounted materials testing system with digital processor and analog computer, it is necessary to use a specimen that has "real-life" characteristics and is reproducible within an acceptable index of precision. A literature review indicates that some researchers have been disappointed in what they felt was a high coefficient of variation in test results, especially in flexural-fatigue work. Perhaps some of the deviations were caused by testing beams with nonuniform densities throughout their cross sections.

Because flexural stresses were to be applied to asphalt concrete in subsequent cold-temperature testing, a beam of rectangular cross section was chosen as the geometric form for the specimens. Also, when cutting samples from existing pavements for laboratory correlation, a beam shape is the most suitable for sawing and testing. Under ideal conditions, a bituminous pavement does not act as a beam but rather as a mat on an elastic foundation. Its layered system depends on its base course and subbase to spread traffic loads to the subgrade. But sometimes in the early spring when the wearing course is still frozen and the supporting elements are saturated, the stiffer surface layer resists most of the wheel loads and does indeed act as a beam.

Compaction by static, vibratory, and impact methods was rejected because the resulting beams were not acceptable from the standpoint of proper and uniform densities, particle orientation, and excessive aggregate degradation. Earlier works of beam testing at low temperatures by Davidson (1) and Stauss (2) were handicapped by the inability to produce beams that had uniform densities throughout the cross sections.

Equipment

The California kneading compactor (Fig. 1) was used to form the beams. Monismith (3), Kallas (4), and Hong (5) did pioneer work with the compactor and reported favorable results. The machine applies a kneading action to the hot, loose asphaltic mixture and simulates construction and traffic compaction. Mounted on the mechanical compactor is a sliding plate assembly that laterally moves the steel mold beneath a tamping foot (Fig. 2). Compaction is accomplished by applying a "kneading-like" pressure to the asphaltic mixture in the mold through the tamping foot by means of a controlled slow-speed dynamic force, a balancing air pressure, and the cushioning action of a helical spring. The tamper travels up and down through a distance of about 4 in., alternately applying and releasing a pressure on the mix in a time cycle of 2 sec per stroke. The load exerted by the tamper is regulated by air pressure in the oil reservoir.

Materials

Two types of aggregates were used: a crushed gravel containing a mixture of limestone and igneous material and a crushed stone of dolomite composition. Their grain-size accumulation curves are shown in Figure 3. The gradations were kept constant. The gravel meets Wisconsin specifications and has an acceptable service record in

Figure 1. California kneading compactor.

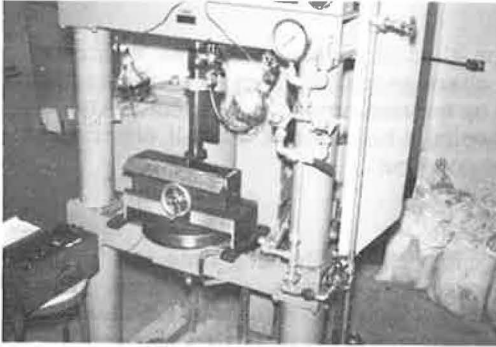


Figure 2. Beam mold assembly.

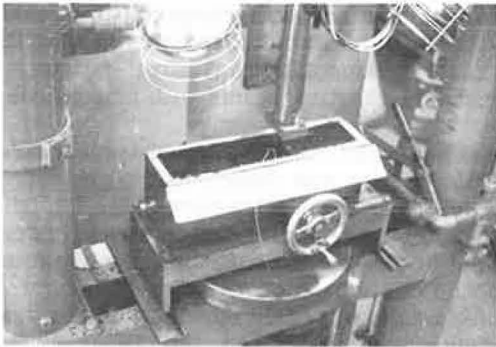
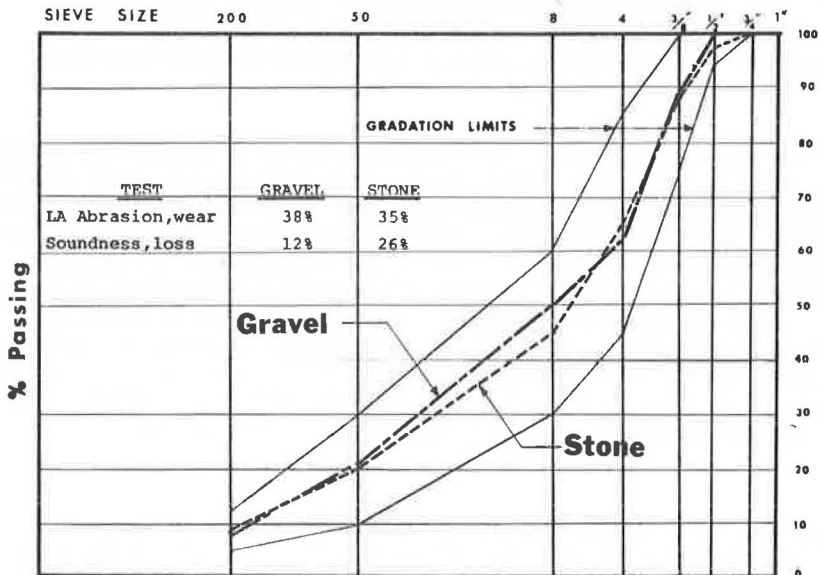


Figure 3. Grain-size accumulation curves.



asphalt pavements in Wisconsin. The crushed stone was rejected as an asphalt concrete aggregate because it failed the five-cycle sodium sulfate soundness test with a weighted loss of 26 percent. Standard specifications of the Wisconsin Division of Highways state that the weighted loss shall not exceed 18 percent, unless 12 percent is specified by special provision. This stone was used in beam making to test the effects of the kneading compactor on aggregate degradation.

Five different asphalt cements were used, ranging from the stiff 40 to 50 penetration grade to the very soft 200 to 300 penetration grade, including 60 to 70, 85 to 100, and 150 to 200 penetration grades. Because viscosity control was used during mixing and compacting operations, the penetration properties of the cements at the standard 77 F were "equalized" during the beam-making process. Mixing was done at the temperature that produced a viscosity of 170 ± 20 cs. This was analogous to mean temperatures varying from 315 F for the 40 to 50 penetration grade to 272 F for the 200 to 300 penetration grade asphalt. Compacting of the mixture was done at 500 ± 50 cs, which corresponds to mean compacting temperature of 275 F for the 40 to 50 penetration grade and 234 F for the 200 to 300 penetration grade asphalt. The higher compaction viscosity is a departure from the present 280 ± 30 cs of ASTM D 1559 (Marshall test). The works of Kallas (6) and Bahri and Rader (7) support the use of the higher compaction viscosity. The range of mixing temperatures and compacting temperatures corresponding to the 170 ± 20 cs and 500 ± 50 are best determined from the plot of log temperature versus log-log viscosity for each asphalt cement. A typical curve is shown in Figure 4.

LABORATORY RESULTS

The finished beams, made by the proposed standard method shown in the Appendix, were examined for acceptable densities, for homogeneity throughout their cross sections, and for particle orientation.

The frequency distribution of the bulk specific gravities of 72 beams is shown in Figure 5. A plot of the accumulative "less than" percentage distribution of the densities on probability graph paper indicates that the data fit the pattern of a normal curve. Using normal curve theory, we found that about 97.5 percent of the beams formed by the proposed procedures had air voids between 2 and 6 percent (Wisconsin Division of Highways' specifications), about 2 percent had less than 2 percent air voids, and 0.5 percent of the beams had more than 6 percent air voids. The mean density of all of the beams was 149.25 lb/ft^3 , with a standard deviation of 1.25 lb/ft^3 , or, as a better measure, a coefficient of variation of 0.84 percent.

The Pearsonian coefficient of skewness of -0.15 indicates a slight tendency toward producing more beams on the "heavy" side (lower air voids content).

The internal dispersion of densities of the beam was checked by cutting into sixths each of the 72 beams—sawed in half along their lengths and transversely at the third points—and obtaining their bulk specific gravities. Here a slightly greater spread of densities was found, with a standard deviation of 1.40 lb/ft^3 and a coefficient of variation of 1.1 percent.

A visual nonquantitative scrutinization of many sawed faces showed that most of the large aggregates were embedded in the mixture with their short axes in the vertical direction. This indicates that the kneading action of the compactor does indeed produce specimens whose particle orientation is similar to that produced in "real life" in pavements.

For a quantitative approach to determine the distribution of coarse aggregates within a beam, a densitometer was utilized. This plotter automatically reads closely spaced optical density gradations of film. The measurements are translated into levels of 10 percent increments that are digitally printed by an electric typewriter. The film reader, consisting of the light source and photodetector, is mounted on top of the typewriter carriage. Output is a voltage directly proportional to the optical density of the film, and an exponential converter linearizes the information on the film. Beams were transversely sawed at four random points, their cross sections were photographed, and the films were enlarged to 8- by 10-in. sheets. At 10 characters per second and 168 units of resolution per square inch, the outputwriter prints out the film densities in 10 incre-

Figure 4. Mixing and compacting temperatures.

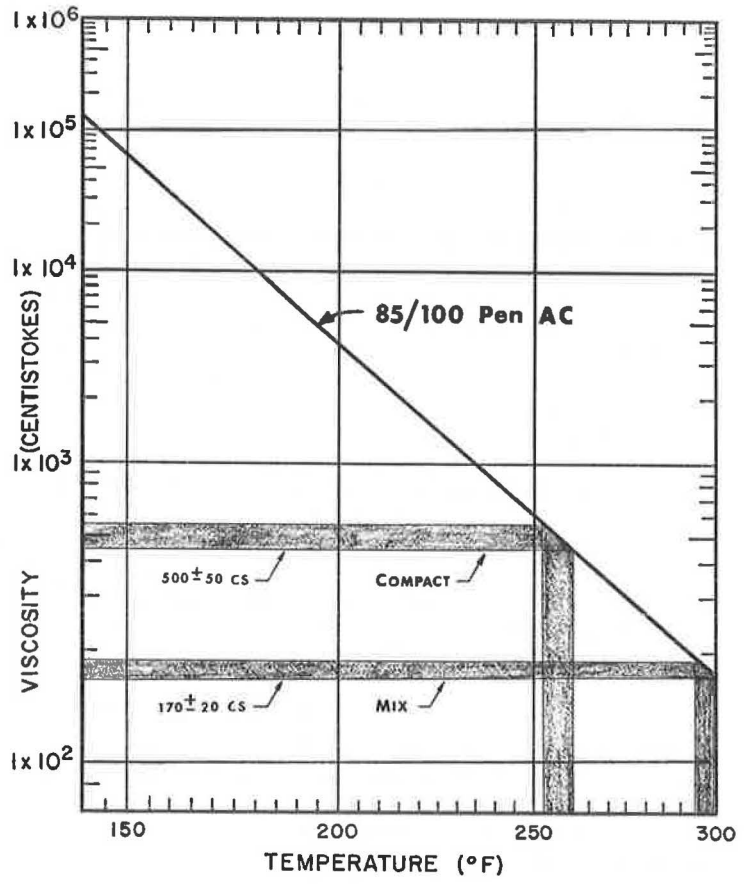
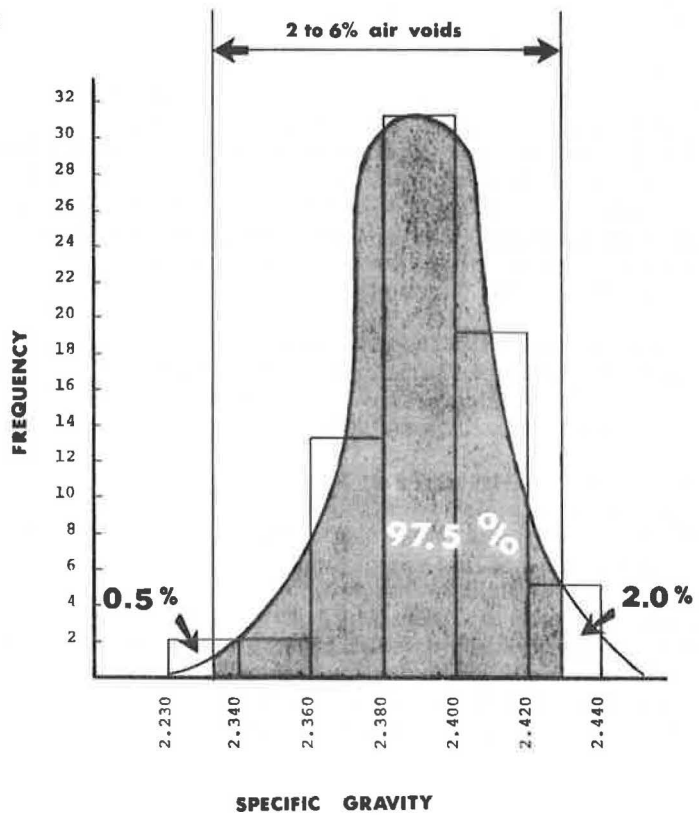


Figure 5. Frequency distribution of specific gravities.



ments from 1 to 0; 1 is white and 0 is black. The light aggregate sections are shown in high contrast within the dark asphaltic binder background, so contouring the course aggregates and obtaining the proportion of their areas to the binder can be readily accomplished. Figure 6 shows a typical beam cross section, and Figure 7 shows its digital densitometer printout.

Readings of the printouts from the four beam cross sections indicated that the coarser aggregates (retained on the No. 8 sieve and larger) occupied 34, 37, 35, and 39 percent of the sawed surface areas. The symbol density of 14 characters per horizontal inch and 12 characters per vertical inch precluded the identification of finer aggregates. The uniformity of the coarse aggregate distribution, as measured by densitometer measurements, suggests that a relatively homogeneous beam was produced.

Specifications dictate that the hot mixture be compacted at a viscosity of 500 ± 50 cs. The heat loss of the mixture during the 11 min required to complete one beam was determined by burying a copper-constantan thermocouple in the hot mix and plotting the millivolt (temperature) versus time curve (Fig. 8). In 11 min, the temperature of the mix dropped 9 F. Referring to Figure 4, the viscosity-temperature curve of the asphalt cement used, the temperature range that corresponds to the viscosity range of 550 to 450 cs is from 253 to 262 F. This means that the beam was compacted entirely within the recommended viscosity limits. It should be noted that asphalt cements of greater temperature sensitivities (steeper slopes) would have smaller temperature tolerances to maintain the 500 ± 50 cs. Figures 1 and 2 show a pair of infrared lamps clamped above the beam apparatus. It was found that the envelope of heat from the two 275-watt bulbs surrounding the mold materially reduced temperature losses during compaction.

The maximum dynamic pressure applied to the mixture during compaction is 300 psi, and, although the tamper blow is cushioned by a spring and is less severe than that from standard impact hammers, some degradation of aggregate does occur. The severity of the degradation was tested by forming beams with acceptable crushed-gravel aggregate and with a rejected crushed stone. A modified extraction process was used to extract and sift the aggregates. The "before and after" curves are shown in Figures 9 and 10. The gravel showed little disintegration, but the crushed stone broke down at all fractions, the percentage finer than the No. 200 sieve increasing from $8\frac{1}{2}$ to 19 percent. The grain-size accumulation curves show that the compacting forces, although producing beams of high densities, are responsive to the strength characteristics of the aggregates.

The specifications state that the beam should be made in two lifts and that three separate and different compactive efforts should be applied to their surfaces as follows:

1. Bottom layer—40 tamps at 75 psi, 40 tamps at 100 psi, and 40 tamps at 200 psi;
2. Top layer—40 tamps at 75 psi, 40 tamps at 100 psi, 40 tamps at 200 psi; and 60 tamps at 300 psi; and
3. Top layer—400 psi static load.

The effects of the three accumulative forces on a beam density, as measured by air voids, are shown in Figure 11. The significance of the static load is evident. It is not merely a cosmetic treatment to the top surface for smoothing the imprints left by the tamping action, but it acts to increase the densities of both layers. More importantly, the static load minimizes the inevitable density differences between top and bottom layers and reduces the relative variations within the beam. In the finished beam, the ends and middle sections of the top layer have air voids contents that vary from the mean by about 0.04 percent; in the bottom layer the deviation is 0.03 percent. Overall, the coefficient of variation among the six segments of the whole beam is approximately 1 percent.

RECOMMENDATIONS

The HRB Committee on Design of Bituminous Paving Mixtures emphasized the importance of bituminous pavements being designed to resist cracking and stated that "the desirability of nonbrittleness at low temperatures in a bituminous pavement has been recognized for many years and is considered to be fully as important as stability from

Figure 6. Typical beam cross section.

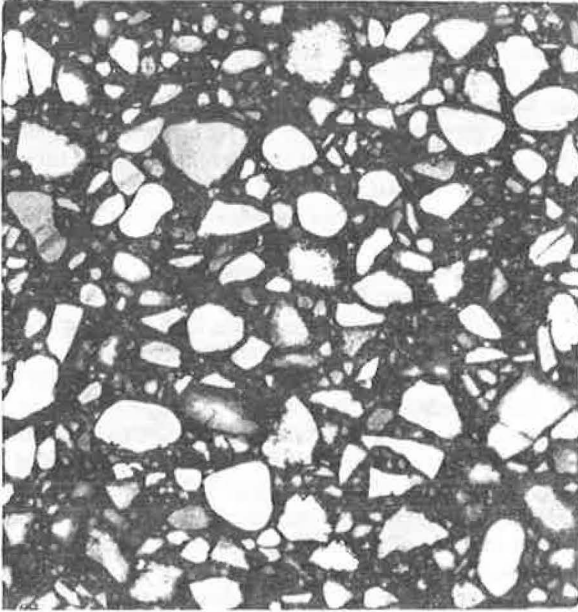


Figure 7. Digital densitometer printout of Figure 6.

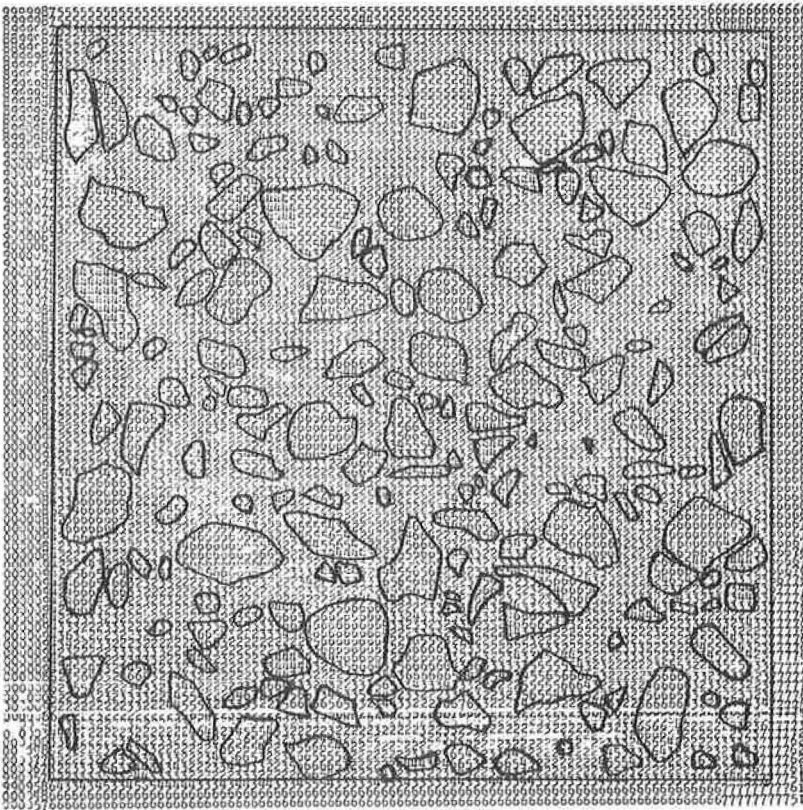


Figure 8. Heat loss during compaction.

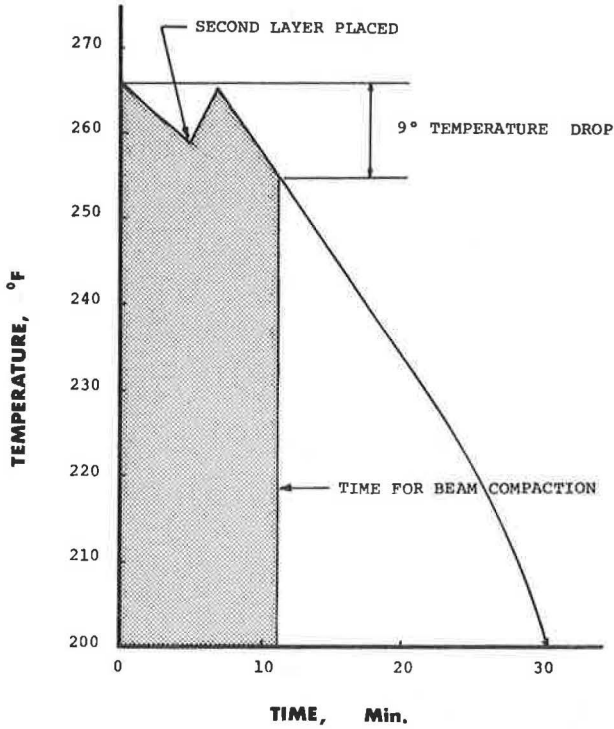


Figure 9. Grain-size accumulation curves (degradation of gravel).

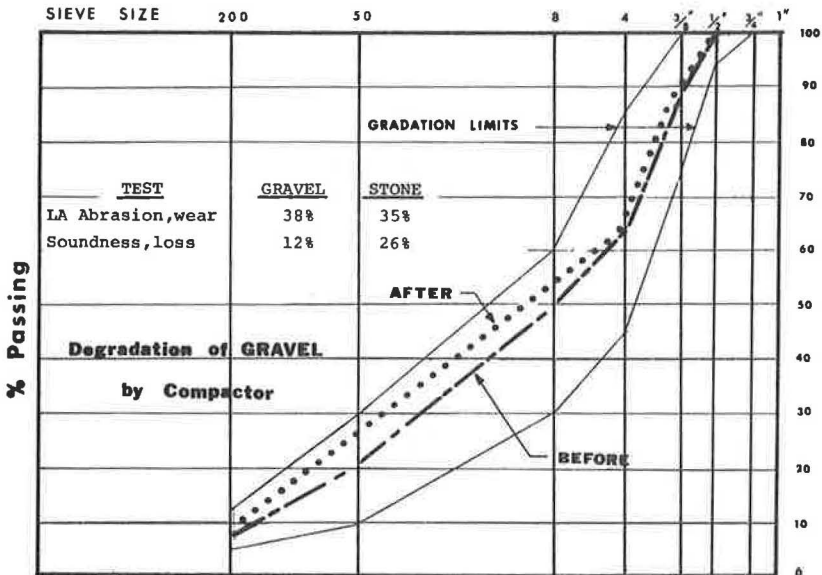


Figure 10. Grain-size accumulation curves (degradation of stone).

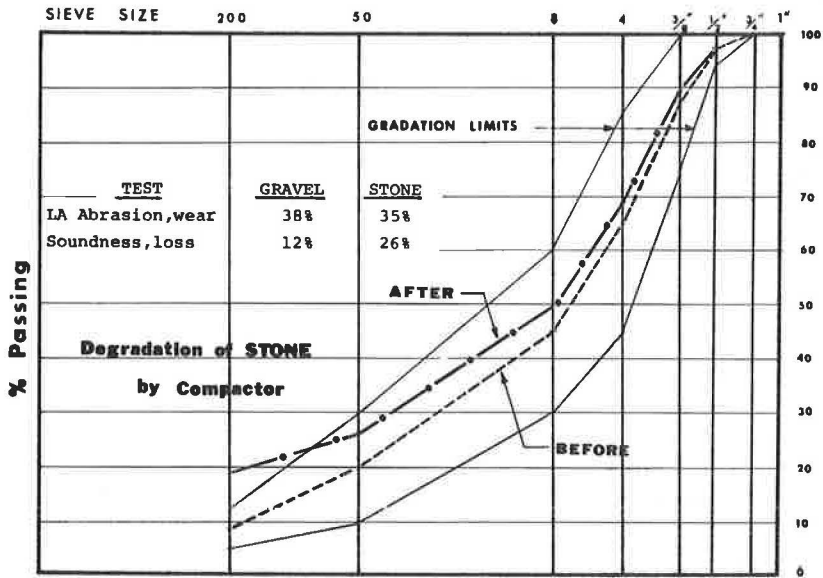
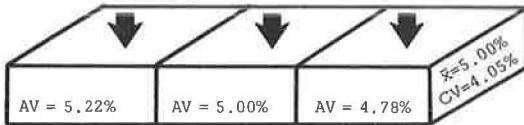


Figure 11. Effects of compact loadings on beam density.

I Loadings

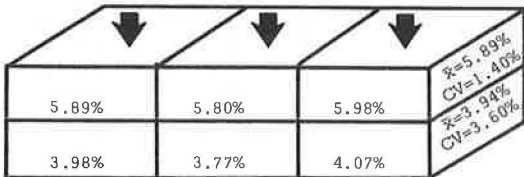
40 tamps @ 75 psi
 40 " @ 100
 40 " @ 200



BOTTOM LAYER (tamping load)

II Loadings

40 tamps @ 75 psi
 40 " @ 100
 40 " @ 200
 60 " @ 300



TOP LAYER (tamping load)

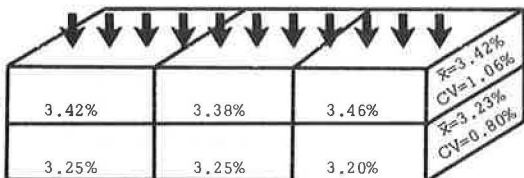
AV = Air Voids

\bar{x} = Mean

CV = Coeff. of Variation

III Loading

Static load of
 400 psi @ 0.25"/min.,
 held for 1 min.



TOP LAYER (static load)

the standpoint of maintaining desirable physical characteristics and rendering good service. Flexural tests conducted on beams of bituminous paving mixtures at low temperatures to establish the modulus of rupture and modulus of elasticity were suggested as possible tests methods. These methods have not received wide acceptance, probably due to a variety of factors, not the least of which is the relative difficulty in preparing suitable specimens." Because it was felt that a method of "preparing suitable specimens" had been devised, the testing of mixtures at low temperatures followed.

Some 37 years ago, Rader (8) wrote: "Quantitative data obtained from low temperature tests should aid engineers in solving problems relating to control of cracking." In 1968, Haas and Topper (9) noted that "The appreciation of this need seems to have lain relatively dormant though until the markedly increased attention given to low-temperature cracking during the past five years." Except for some recent work in Alberta, design supplements for bituminous concrete pavements in cold climates have not been developed.

Current methods of designing paving mixtures seek an end product that has a certain minimum stability at an expected maximum summer temperature, a deformation or flow within limits at the same high temperature, and specified ranges of air voids and voids in the mineral aggregate. Also, various physical and chemical constraints are placed on the asphalt cements and aggregates. In concert, these are supposed to bear some relation to the in-service performance of the asphalt-aggregate system. But most of the criteria are high-temperature oriented and are little related to the range of environmental conditions that the pavement will be subjected to—especially in cold climates. There seems to have been the assumption that high-temperature stability and deformation were the most important considerations and that, because stability increases rapidly with decreasing temperatures, the requirements for design criteria were taken care of.

The search then is for a predictive technique that can foretell the condition of an asphalt paving mixture under a specific low-temperature condition. This procedure should apply to mixtures of different combinations from different sources and having different types of asphalt cement.

From flexural tests on asphalt concrete beams, the moduli of elasticity and moduli of rupture can be calculated. These indexes measure stiffness and bending strengths at the conditions that exist during testing. Formulas from the elastic theory are permissible in the calculations because the specimens are in an elastic state at low temperatures. The full-sized beam (15 by $3\frac{1}{4}$ by $3\frac{1}{2}$ in.) is used. Some researchers have been sawing the beam into quarters, $1\frac{1}{4}$ - by $1\frac{1}{4}$ -in. cross sections; however, Kallas and Puzinauskas (10) found that, by using full-sized beams, the variability of their flexural fatigue tests was reduced. Correlation coefficients ranging from 0.91 to 0.99 were obtained for stress-fracture life and strain-fracture life regression lines.

Busby and Rader (11) have developed procedures for predicting the stiffness of asphalt concrete mixtures at low temperatures. The aggregate gradation was kept constant for any one family of curves, and the beams were formed of mixtures made with various grades of asphalt cements. At some low temperatures (+25, -5, -35 F), the beams were tested in flexure by three-point loadings (loading at center) at a constant rate of strain. The deflection and load at failure together with the geometrics of the beam were used to calculate the moduli of rupture and stiffness. The rupture moduli remained fairly constant at temperatures below -5 F, and a minimum modulus of 800 psi at -5 F was suggested as a design standard for cold-weather areas. Curves of stiffness moduli and temperature were plotted for each mixture, and regression analyses showed high correlation between stiffness and temperature. From the conclusions of McLeod (12) and Phang (13) and working through Van der Poel's stiffness nomographs, it was determined that (for these mixes) cracking could be expected at a flexural stiffness modulus of 300,000 psi minimum. A flexural stiffness modulus of 250,000 psi maximum, which allows for experimental error and in-service hardening, was recommended as a design guide. By placing the limiting 250,000-psi line on the stiffness-temperature curves, the minimum design temperature for thermal crack prevention can be determined for each mixture. From these data, another curve of minimum design temperature and original penetration at 77 F of asphalt cement can be used to

check the minimum penetration grade of asphalt cement that could safely be specified according to the anticipated low temperature of the area. The highest penetration grade cement consistent with high-temperature stability should be selected.

Busby and Rader (14) have also suggested that the slope of the flexural stiffness-temperature curve be used to identify cements that cause premature cracking at low temperatures. This temperature susceptibility slope (TSS), which measures the tendency for a cement to crack, is taken from the -20 F to +20 F segment of the curve and is measured in psi per degree F. A maximum allowable TSS of 6,000 psi/deg F is proposed for a densely graded surface course.

CONCLUSIONS

Upon examining and testing random samples of the finished product, it is evident that the proposed standard method can consistently produce homogeneous beams of acceptable densities and aggregate arrangement. These results are the efforts of two operators working independently in the same laboratory. A series of exercises in several laboratories would more rigorously put the process to the test.

It appears feasible that the forming and testing of beams to determine some of the rheological characteristics of paving mixtures could be conducted in the materials laboratories of state highway departments and municipal and commercial organizations. The equipment described is at hand in laboratories or available at no great cost. Departments could design bituminous pavements to resist low temperatures by working directly with the aggregates and asphalt cements common to the area. Perhaps some asphalt cements that now meet specifications but are deficient in low-temperature considerations would be eliminated from use in surface courses. Some asphalt cements equally graded at 140 F viscosity were shown to behave erratically at low temperatures, and their different susceptibilities could be known only by testing them in mixes. Regional curves could be developed that would restrict bitumens with high sensibilities to thermal variation, and the acceptable asphalt cements could be selected from their temperature-penetration grade relations.

REFERENCES

1. Davidson, B. M. Investigation of Physical Properties of Asphaltic Concrete at Low Temperatures. Univ. of Wisconsin, MS thesis, 1950.
2. Stauss, J. F. Investigations of Physical Properties of Asphaltic Concrete at Low Temperatures. Univ. of Wisconsin, MS thesis, 1950.
3. Monismith, C. L. Correspondence with Rader, 1965.
4. Kallas, B. F. Unpublished report to ASTM Committee D-4, Subcommittee 2a, Jan. 1966.
5. Hong, H. Kneading Compaction of Asphalt Beam Specimens. Jour. of the Highway Div., Proc., ASCE, Nov. 1968.
6. Kallas, B. F. Correspondence with Rader, April 16, 1970.
7. Bahri, G. R., and Rader, L. F. Effects of Asphalt Viscosity on Physical Properties of Asphaltic Concrete. Highway Research Record 67, 1965, pp. 59-83.
8. Rader, L. F. Proc., ASTM, Part II, Vol. 35, 1935.
9. Haas, R. C. G., and Topper, T. H. Thermal Fracture Phenomena in Bituminous Surfaces. HRB Spec. Rept. 101, 1969, pp. 136-153.
10. Kallas, B. F., and Puzinauskas, V. P. Flexural Fatigue Tests on Asphalt Paving Mixtures. Symposium on Fatigue of Compacted Bituminous Aggregate Mixtures, ASTM, July 1971.
11. Busby, E. O., and Rader, L. F. Flexural Stiffness Properties of Asphalt Concrete at Low Temperatures. AAPT Annual Meeting, Feb. 1972.
12. McLeod, N. W. Prepared Discussion. Proc., Canadian Technical Asphalt Assn., 1969.
13. Phang, W. A. Correspondence re Canadian Good Roads Assn. paper, 1970.
14. Busby, E. O., and Rader, L. F. Effect of Penetration Index of Asphalt Cement on Low Temperature Flexural Stiffness of Asphalt Concrete Beams. Proc., Canadian Technical Asphalt Assn., 1971.

APPENDIX

BEAM-FORMING METHOD

This method covers the preparation of beams of bituminous paving mixtures by means of a mechanical compactor that imparts a kneading action compacting the beam by a series of individual impressions made with a ram.

Apparatus

The following equipment is used in the method:

1. California kneading compactor—a mechanical kneading compactor in accordance with ASTM D 1561;
2. Compactor foot—a ram 2.0 by 3.0 in.;
3. Mold—a beam mold with inside dimensions of 15 in. long, $3\frac{1}{4}$ in. wide, and $4\frac{1}{2}$ in. high;
4. Sliding base assembly—an assembly attached to kneading compactor with a hand wheel for moving mold laterally during compaction;
5. Extraction assembly—a beam specimen extraction assembly;
6. Paper—sheets of heavy paper $3\frac{1}{4}$ by 15 in.;
7. Ovens—electric ovens capable of maintaining temperatures of 200 to $325\text{ F} \pm 5\text{ F}$;
8. Testing machine—a comparison testing machine having a minimum capacity of 50,000 lb;
9. Balance—a balance having a capacity of 5 kg or more and sensitive to 1.0 g or less; and
10. Miscellaneous apparatus—thermometer, spatulas, spoons, gloves, metal pans, and mechanical mixer.

Test Specimens

Approximately 6,800 g of the bituminous mixture shall be prepared in accordance with ASTM D 1560, sections 3.1, 3.2, and 3.3 except for specific requirements given in this Appendix.

The beam test specimens shall have a rectangular cross section $3\frac{1}{4}$ in. wide, $3\frac{1}{2}$ in. deep, and 15 in. long.

Procedure

The mixing temperatures shall be those corresponding to an asphalt viscosity of 170 ± 20 cs. Compaction temperatures shall be those corresponding to an asphalt viscosity of 500 ± 50 cs.

Heat the mold to the compaction temperature specified previously. Lightly oil the mold and tamping foot. Place three sheets of $3\frac{1}{4}$ - by 15-in. paper on the mold base-plate. The compactor foot is maintained sufficiently hot to prevent the mixture from adhering to it. Place one-half of the required amount of mixture for one specimen in the mold in a uniform layer. When applying tamping blows to the mixture, turn the base assembly handwheel one-quarter revolution to move the mold laterally $1\frac{1}{2}$ in. after each tamping blow. Apply 40 tamping blows at a foot pressure of 75 psi, followed by 40 blows at 100-psi and 40 blows at 200-psi foot pressure. Place the remaining half of the mixture in the mold and apply 40 tamps at 75 psi to settle the loose mix. Follow with 40 blows at 100-psi, 40 blows at 200-psi, and 60 blows at 300-psi foot pressure. If unstable material is involved and there is undue movement of the mixture under the compactor foot, the foot pressure shall be reduced until the kneading compaction can be accomplished.

Immediately after compaction in the California kneading compactor, place the heated and slightly oiled leveling bar on top of the specimen. Using a compression testing machine, apply a static load on the specimen at the rate of 0.25 in. per min until an applied pressure of 400 psi is reached. Maintain the applied pressure for a period of 1 min and then slowly release the pressure. After the compacted specimen

has cooled sufficiently so that it will not deform on handling, remove it from the mold by means of the extraction assembly. Place the specimen on a smooth, flat surface and allow to cool to room temperature.

Some of the diverse beam fabrication procedures by others are given in Table 1.

Table 1. Beam-making methods.

Study	Layer	Compactive Effort	Mixing Temperature (deg F)	Compaction Temperature (deg F)
A	1	30 tamps at 200 psi	250 to 300	230
	2	45 tamps at 200 psi, 45 tamps at 300 psi		
B	1	20 tamps at 145 psi	250	Not available
	2	25 tamps at 290 psi		
	3	20 tamps at 145 psi, 50 tamps at 290 psi		
C	1	20 tamps at "low pressure"	250	230
	2	45 tamps at 400 psi		
	3	20 tamps at "low pressure," 45 tamps at 400 psi, 75 tamps at 400 psi		
D	1, 2	40 tamps at 50, 120, 190, 260, 330, 400 psi	250 to 300	230
E	1, 2	45 tamps at 400 psi	250	250
	3	115 tamps at 400 psi		
F	1, 2	25 tamps at 400 psi	250	250
	3	100 tamps at 400 psi		

Note: Static leveling load for studies A, C, D, and E was 400 psi; for study B it was 300 psi; and for study F it was 350 psi.

ASPHALT DURABILITY CORRELATION IN IOWA

Dah-yinn Lee, Iowa State University, Ames

Eight asphalt cements and paving projects using these asphalts were evaluated relative to their changes in rheological and chemical properties in pavement service for as long as 48 months. Corresponding changes in these asphalts of the same physical and chemical properties were determined during laboratory aging. The Iowa durability test is a two-stage aging process combining standard TFOT and pressure-oxidation treatment (20 atm in oxygen at 150 F) up to 1,000 hours. Good correlations between field-service aging in Iowa and laboratory aging during the Iowa durability test have been obtained. The master time-equivalency curve between the test in hours and the pavement service life in months, established by combining all asphalts (void levels) and all properties, indicates that 46 hours in test will age asphalts to the equivalent of 60 months in service. Correlation curves for different properties and different levels of pavement voids were also obtained. A tentative specification for paving asphalts, including durability requirements based on the test, is suggested in lieu of current TFOT.

• PUBLIC agencies responsible for the construction and maintenance of highways and airfield pavements and asphalt producers have been interested in the quality of paving asphalts for many years.

The interest in asphalt quality has led to a large amount of research related to asphalt durability and hardening (1, 2, 3). Most of the reported research on asphalt durability has been directed to finding mechanisms or causes of asphalt deterioration, methods for controlling or preventing undue hardening of asphalts or improving the durability of asphalts, and tests to predict the behavior and durability of an asphalt during mixing, laying, and service.

A research project was initiated in Iowa in 1966 as a long-range comprehensive program in the study of asphalt durability. Its ultimate objective was to develop a simple, rapid laboratory test that could be used by highway engineers to select paving asphalt according to quality, to identify inferior asphalts, and to reasonably predict the useful life of asphalts once they are incorporated in the pavements.

The original proposed study on asphalt durability involves work in the following phases:

1. Review of the knowledge of the durability of paving asphalts including the identification of predominant factors causing hardening during mixing, laying, and in-road service;
2. Development of an accelerated laboratory durability test to simulate changes in asphalt during both short-time production and long-term service;
3. Correlation of hardening and other changes in asphalts during the developed laboratory test and changes in the same asphalts in pavements; and
4. Establishment of durability criteria and functional approach specifications by means of established laboratory durability tests on original asphalt.

Work on phases 1 and 2 has been reported elsewhere (2, 3). This paper gives the results of 48-month laboratory-field correlations and offers suggestions as to how the

developed durability test can be applied to realistic asphalt durability evaluation and specifications.

STUDY MATERIALS

A total of eight asphalt paving projects, selected by Iowa State Highway Commission (ISHC) engineers, were included in this study. Asphalt cements, plant mixes, and core (or slabs) samples were obtained from four paving projects during the late 1967 construction season; materials from four more paving projects were obtained during the early 1968 construction season. The locations of the eight pavement projects are given in Table 1. In addition to asphalt received from ISHC, an essentially asphaltene-free asphalt cement (asphalt concrete 5) was obtained from the ESSO Research and Engineering Co. and is included in the study to evaluate the role of asphaltenes in the performance of a paving asphalt.

Four 1-gal asphalt cement samples were taken from each project by district personnel of the ISHC just prior to the asphalt's entry into the mixer. Forty lb of plant mixtures were collected from trucks immediately after they left the mixers and are identified throughout this report as P-samples. The trucks from which the plant mixtures were sampled were tagged. Pavement cores (or slabs) of about 40 lb were cut from the newly finished pavements containing the mixtures from the same tagged trucks. Half of the cores (or slabs) were taken from the wheel track and are identified as f-0-A, and half of the cores (or slabs) were taken from between the wheel tracks and are identified in this report as f-0-B. The same amounts of field core samples were taken from the respective pavement sections every 6 months from the time the pavement was laid and are identified as f-6, -12, -18, . . . , -A, or f-6, -12, -18, . . . , -B.

Pertinent information obtained at each project site by ISHC district personnel was summarized in a standard form by research department personnel and delivered to the Bituminous Research Laboratory, Iowa State University, together with the samples. The general characteristics of the field pavement mixtures studied are given in Table 2. Specific surface, bitumen index, and film thickness were calculated based on data supplied by the project information sheets. The original properties of the nine asphalt cements studied are given in Table 3.

EXPERIMENTAL WORK

Procedures

Experimental work was carried out as shown in Figure 1. When the experimental phase of the project terminated, samples as old as 48 months were tested on six pavements, and 42-month samples were tested on two other projects.

Iowa Durability Test

An Iowa durability test (IDT) was developed (2) to simulate or reproduce the two-stage aging and hardening of the asphalt in the field. The laboratory durability test procedure finally adopted was as follows:

1. Use of BPR thin-film oven test (TFOT) on the original asphalt;
2. Application of pressure-oxidation treatment to the residue from the TFOT in a pressure vessel for as long as 1,000 hours under a film thickness of $\frac{1}{8}$ in., a temperature of 150 F, and a pressure of 20 atm oxygen; and
3. Evaluation of the physical and chemical changes in asphalt during the artificial aging process in relation to the original properties of the asphalt.

Pressure-oxygen treatment was conducted in pressure vessels fabricated of $\frac{1}{2}$ -in. stainless steel. These vessels are capable of simultaneously treating 10 standard TFOT samples to a pressure of 450 psi. The interior dimensions of the vessels are 7.5 in. in diameter and 7.5 in. high. They are equipped with a pressure gauge and a relief valve.

Table 1. Pavement project locations.

Number	County	Location	Project Number	Date Laid
1	Chickasaw	On US-63 north of New Hampton	FN-63-8(1)-20-19	Nov. 1967
2	Dickinson	On Iowa 327 from Iowa 276 east and north	FN-327-1(1)-21-30	Oct. 1967
3	Harrison	On US-75 out of Mo. Valley, north into Mondamin	FN-75-2(3)-21-43	Nov. 1967
4	Story-Polk	On US-69 between Huxley and Ankeny	FN-69-5(2)	Oct. 1967
6	Monona	On US-75 from Harrison Co. line north into Ottawa 11 mi.	FN-3(2)-21-67	April 1968
7	Bremer	On Iowa 3	FN-3-6(5)-21-09	May 1968
8	Keokuk	On Iowa 92 from Sigorney east	FN-92-8(2)-21-54	May 1968
9	Jackson	On US-52 north of Maquoketa	FN-52-1(3)-21-49	June 1968

Table 2. Characteristics of field pavement mixtures.

Characteristic	Asphalt								
	1	2	3	4	6	7	8	9	
Gradation, percent passing sieve									
3/4 in.					100				100
1/2 in.					94				
3/8 in.	100	100	100	100	77	100	100		78
No. 4	81	89	92	78	60	85	85		62
No. 8	62	67	58	59	43	67	63		49
No. 16	44	—	—	—	—	—	—		—
No. 30	30	34	34	31	25	35	35		23
No. 50	16	21	23	18	19	35	25		—
No. 100	12	13	13	13	9	—	13		—
No. 200	9.3	9.9	9.4	9.4	7.1	8.4	8.9		6.7
Percentage of bitumen	7.5	6.3	6.3	7.5	5.0	7.0	5.3		5.5
Specific surface ^a , ft ² /lb	40.59	45.92	44.18	41.86	33.44	51.06	44.34		32.66
Bitumen index ^b , × 10 ⁻³	1.996	1.459	1.517	1.935	1.585	1.469	1.263		1.776
Film thickness ^c , μ	9.72	7.11	7.39	9.24	7.12	7.15	6.15		8.65
Laboratory design voids, percent	6.8	6.1	6.6	9.3	6.8	6.1	3.5		5.8
Hveem side pressure ^d , psi	60	46	63	48	55	61	55		29
Asphalt concrete temperature, deg F	295	300	295	260	267	260	275		300
Aggregate temperature, deg F	300	320	310	310	340	310	375		305
Mix temperature, deg F	290	295	310	310	310	305	306		298
Initial field voids, percent	8.7	9.8	11.5	12.3	5.5	7.1	6.7		5.1
ADT, 1970	2,100	330	590	3,000	500	2,000	1,500		2,400
Condition after 48 months	Transverse cracks	Excellent	Excellent	Severe transverse and longitudinal centerline cracks	Good	Good, some cracks	Good to excellent		Excellent

^aMix Design Methods for Asphalt Concrete. The Asphalt Institute, MS-2, 1962.

^bPercent bitumen (aggregate basic)/specific surface.

^cBitumen index × 4.870.

^dAt 400-psi vertical load.

Table 3. Properties of asphalt studied.

Characteristic	Asphalt								
	1	2	3	4	5	6	7	8	9
Penetration, 77/100/5	89	94	91	90	84	87	95	90	92
Specific gravity, 77/77	1.017	1.026	1.042	1.011	1.017	1.019	1.042	1.003	0.999
Viscosity									
77 F, megapoises	1.16	1.23	1.58	1.10	1.14	1.70	1.15	1.10	1.22
140 F, poises	1,356	1,086	1,316	1,106	1,781	1,455	1,316	1,922	2,060
Softening point, deg F	119.0	116.5	115.5	114.5	113.0	118.0	116.0	118.0	119.5
Flash point, COC, deg F	600	595	630	625	690	615	625	655	655
Fire point, COC, deg F	680	690	705	705	730	670	685	735	735
Microductility at 77 F, cm	63	71	66	77	82	55	68	51	63
TFOT									
Residue penetration	53	51	57	56	67	55	59	60	62
Weight loss, percent	0.02	0.16	+0.01	0.00	+0.01	0.07	0.07	0.24	0.16
Spot test	Negative	Negative	Negative	Negative	Negative	Negative	Negative	Negative	Negative
Source ^a	1	1	2	2	3	4	4	2	2

^a1 = blend of asphalts from Texaco at Casper, Wyoming, and American Petrofina, Big Springs, Texas. 2 = American Oil, Sugar Creek, Missouri. 3 = Esso Research and Engineering Co. 4 = American Petrofina, Big Springs, Texas.

Figure 1. Flow chart of testing procedures.

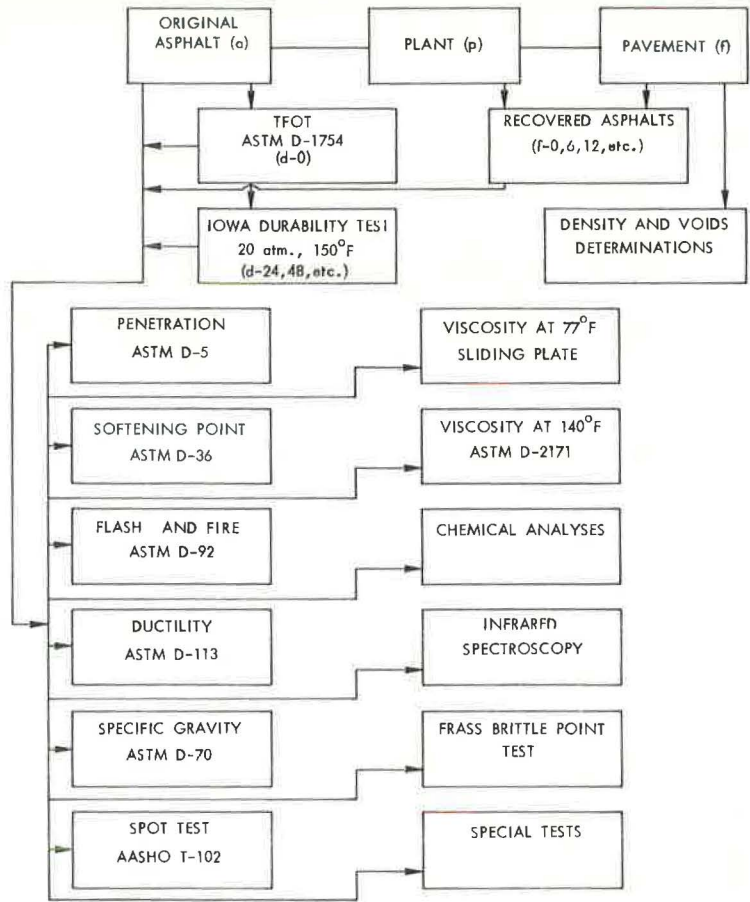


Table 4. Changes in penetration during weathering.

Project Sample	Asphalt Penetration								
	1	2	3	4	5	6	7	8	9
Original	89	94	91	90	84	87	95	90	92
TFOT	53	54	57	56	67	55	59	60	62
Laboratory aging (hours)									
d-24	30	34	36	36 ^a	49 ^a	50	44 ^a	44 ^a	37
d-48	29	30	30	31	41	32	37 ^a	33	27
d-96	26	25	26	25	37	27	29 ^a	30	24
d-240	19	20	20	20	27	22	19 ^a	26	21 ^a
d-480	13 ^a	17	16 ^a	17 ^a	20 ^a	21	16 ^a	22 ^a	23
d-1000	11	13 ^a	8	10	11	14	10	15	—
Field aging (months)									
Plant	60	72	57	67	—	71	76	74	79
f-0									
A ^b	57	67	57	62	—	—	79	71	64
B ^c	57	67	57	62	—	—	—	—	—
f-6									
A	61	56	48	57	—	39	41	43	51
B	56	58	52	62	—	40	41	43	56
f-12									
A	43	37	42	39	—	37	35	42	53
B	39	38	36	35	—	39	42	45	49
f-18									
A	41	38	40	34	—	34	35	35	39
B	43	36	30	36	—	34	35	36	41
f-24									
A	39	35	35	38	—	36	37	38	41
B	36	35	34	29	—	35	36	39	39
f-30									
A	35	33	32	30	—	33	35	35	40
B	33	31	34	32	—	34	33	35	38
f-36									
A	36	34	30	30	—	—	36	36	36
B	37	32	29	30	—	—	35	35	31
f-42									
A	37	33	31	29	—	28	—	34	—
B	39	29	32	28	—	28	—	34	—
f-48									
A	28	28	27	26	—	—	—	—	—
B	31	28	27	26	—	—	—	—	—

^aInterpolated value.

^bA = in wheel tracks.

^cB = between wheel tracks.

Physical Tests

The physical tests selected in this study are mainly for the evaluation of changes in rheological properties of asphalt with aging or hardening and are selected based on the hypothesis that asphalt durability can be related to rheological behaviors.

Tests conducted on the original, laboratory-aged, and recovered field asphalts are shown in Figure 1. Specific gravity, penetration at 77 F (100 g, 5 sec), and ring and ball softening point were determined following standard ASTM procedures. Viscosity at 77 F was determined by the Sheel sliding-plate microviscometer. Plots of log shearing stress and log rate of shear and log viscosity and log rate of shear were made on all asphalts. Viscosities at a rate of shear of $5 \times 10^{-2} \text{ sec}^{-1}$, at a constant energy input of 10^4 ergs (4), and at a constant shearing stress of 167 g/cm^2 (1.63×10^5 dyne/cm²) were calculated (5). Unless otherwise stated, only the viscosity at the rate of shear of $5 \times 10^{-2} \text{ sec}^{-1}$ is reported.

The slope of the log rate of shear versus log shearing stress linear plot is defined as the degree of complex flow, commonly designated by the letter *c* (4). The shear index (SI) or shear susceptibility (*S*) is the tangent of the angle of log shear rate versus log viscosity plot (6). The rate of change in SI of various asphalts during weathering was found to be related to relative durability of asphalt (6-9).

Viscosity at 140 F was determined by Cannon-Manning vacuum viscometers following standard procedures.

Because of the limited quantity of recovered asphalts that would be available, all ductility tests were made at 77 F on $\frac{1}{2}$ - by $\frac{1}{2}$ -in. microductility molds developed by the Phillips Petroleum Co. and used in previous projects (10, 11). The use of microductility specimens also makes the differentiation among asphalts possible within the limits of the ductility machine (150 cm).

The chemical approach to durability studies of asphalts has been criticized as being premature because of a lack of definitive knowledge of chemical composition and asphalt structure. However, this is a fundamental approach. It has been proved that chemical composition does have direct effects on rheological and durability properties of asphalt, that the relation between asphalt durability and chemical composition can be established (12, 13, 14), and that the durability grouping of asphalts by chemical composition is possible (14, 15).

Asphaltene content and oxygen percentage have been used as parameters for chemical changes. Asphaltene content was determined by precipitation with a Skelly F (16), and oxygen content was determined by the combustion method using a Coleman oxygen analyzer.

Chemical analysis of asphalts 1 through 4 was also made by a method suggested by Rostler and White (13) and Halstead et al. (14) to determine the relation between asphalt durability and $(N + A_1)/(A_2 + P)$.

During the second half of this investigation, analysis of asphalts by infrared multiple internal reflection techniques was undertaken to determine the changes in infrared spectra of asphalts during field aging as well as laboratory aging and, if possible, to establish a relation between asphalt durability and its infrared spectrum. The results of infrared analyses have been reported elsewhere (17).

LABORATORY AGING

Changes in Rheological Properties

The results of penetration change with time during laboratory aging (at 77 F, 100 g, and 5 sec) in IDT are given in Table 4 and typical plots are shown in Figure 2. The results of viscosity change measured at 77 F and at $5 \times 10^{-2} \text{ sec}^{-1}$ with time are given in Table 5. Similar results for viscosity at 140 F are given in Table 6. Samples of log viscosity and time plots are shown in Figures 3 and 4. From viscosity at 77 F data, *c* and SI were calculated for all nine asphalts. Results of softening point are given in Table 7, and changes in microductility at 77 F with laboratory aging time are given in Table 8. Except in a few instances for ductility, all the preceding property changes were found to follow the hyperbolic model suggested by Brown et al. (18). This is

Figure 2. Penetration versus time of aging.

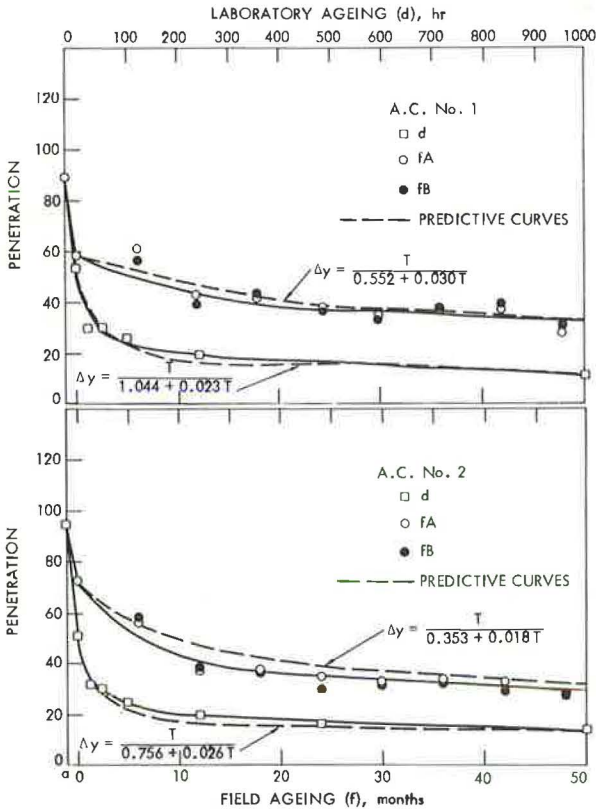


Table 5. Changes in viscosity at 77 F.

Project Sample	Asphalt Viscosity (megapoises)								
	1	2	3	4	5	6	7	8	9
Original	1.16	1.23	1.58	1.10	1.14	1.70	1.15	1.10	1.22
TFOT	4.22	5.35	3.70	3.09	1.68	3.80	3.90	4.15	2.86
Laboratory aging (hours)									
d-24	18.4	11.7	9.50	9.0 ^a	3.50 ^a	—	7.00 ^a	8.30 ^a	10.30
d-48	20.5	19.3	14.2	15.7	5.60	14.60	12.50 ^a	12.60	12.50
d-96	23.9	24.6	19.2	22.6	7.40	21.00	22.00 ^a	14.80	15.00
d-240	44.0	36.2	47.0	36.9	13.50	33.00	51.00 ^a	38.00	27.50 ^a
d-480	64.5 ^a	38.5	76.0 ^a	52.0 ^a	14.70 ^a	37.00	78.50	53.50 ^a	45.00 ^a
d-1000	89.0	—	116.0	64.0	17.30	72.00	99.20	64.00	69.00 ^a
Field aging (months)									
Plant									
f-0									
A ^b	4.87	4.60	3.39	3.01	—	—	2.25	2.14	2.61
D ^c	4.87	4.60	3.39	3.01	—	—	—	—	—
f-6									
A	4.30	5.98	3.40	3.56	—	8.58	8.30	6.40	4.90
B	5.70	5.35	3.78	3.50	—	8.70	8.74	6.40	3.90
f-12									
A	9.80	8.90	9.66	11.2	—	10.60	9.80	14.50	11.50
B	9.54	9.20	—	12.2	—	11.90	9.80	12.50	8.90
f-18									
A	12.7	8.33	12.4	13.9	—	12.10	12.80	11.50	10.50
B	11.5	10.28	12.0	15.5	—	13.80	12.00	10.90	10.50
f-24									
A	12.2	—	12.6	21.0	—	12.70	14.50	9.80	12.00
B	15.0	15.0	11.9	18.6	—	7.80	12.20	8.90	8.40
f-30									
A	14.5	18.5	17.0	20.5	—	13.50	12.00	13.50	9.68
B	18.5	19.2	13.2	21.6	—	17.50	12.00	14.00	9.10
f-36									
A	12.3	13.8	21.0	16.2	—	—	13.80	—	11.50
B	12.5	16.0	19.6	17.7	—	—	—	—	—
f-42									
A	13.4	17.8	18.8	16.2	—	17.50	—	12.50	—
B	9.5	16.5	14.0	22.2	—	—	—	—	—
f-48									
A	19.2	19.6	20.7	21.8	—	—	—	—	—
B	16.4	20.9	16.1	22.0	—	—	—	—	—

^aInterpolated value.

^bA = in wheel tracks.

^cB = between wheel tracks.

Table 6. Changes in viscosity at 140 F.

Project Sample	Asphalt Viscosity (poises)								
	1	2	3	4	5	6	7	8	9
Original	1,356	1,066	1,316	1,106	1,781	1,350	1,316	1,922	2,837
TFOT	2,368	3,448	4,041	3,556	2,341	3,556	3,538	4,376	4,412
Laboratory aging (hours)									
d-24	12,094	10,849	5,812	—	—	—	7,400 ^a	10,500 ^a	12,558
d-48	15,248	17,022	7,979	11,830	4,891	12,457	9,000 ^a	20,199	13,826
d-96	23,276	34,249	12,772	13,930	4,459	19,550	12,800 ^a	24,472	23,497
a-240	81,254	89,639	28,062	23,479	7,727	33,431	26,900 ^a	44,731	—
d-480	—	—	—	—	16,500 ^a	52,000 ^a	53,500 ^a	66,000	—
d-1000	200,000	—	130,000	71,560	37,000	80,000	130,000	120,000	—
Field aging (months)									
Plant									
f-0	2,182	2,045	1,913	2,136	—	2,096	2,070	2,634	3,428
A ^b	2,294	2,931	2,122	1,781	—	—	2,130	2,456	4,001
B ^c	2,294	2,931	2,122	1,781	—	—	—	—	—
f-6									
A	2,716	3,735	2,820	2,582	—	7,546	5,506	7,762	4,824
B	3,555	3,412	3,038	2,525	—	6,227	5,737	9,292	5,852
f-12									
A	5,814	8,165	4,634	5,984	—	5,167	4,634	9,717	4,593
B	6,722	8,098	5,829	5,964	—	8,181	4,597	9,005	5,358
f-18									
A	4,733	6,964	5,331	5,077	—	9,436	6,753	13,468	6,663
B	3,717	7,806	4,799	6,178	—	—	—	—	8,109
f-24									
A	5,158	9,742	6,437	7,672	—	7,797	5,950	9,676	8,653
B	6,675	10,204	6,217	8,526	—	—	—	—	—
f-30									
A	6,710	9,341	6,229	7,960	—	9,250	6,644	13,092	9,392
B	8,506	9,588	5,593	8,605	—	8,567	—	—	—
f-36									
A	5,747	9,991	7,218	7,777	—	—	7,270	10,532	13,940
B	7,031	12,792	8,130	7,484	—	—	—	—	—
f-42									
A	6,448	12,173	6,951	7,598	—	12,384	—	12,925	—
B	4,954	10,054	9,969	—	—	—	—	—	—
f-48									
A	11,044	13,773	8,305	8,490	—	—	—	—	—
B	9,473	14,082	7,549	8,647	—	—	—	—	—

^aInterpolated value.

^bA = in wheel tracks.

^cB = between wheel tracks.

Figure 3. Viscosity at 77 F versus time of aging.

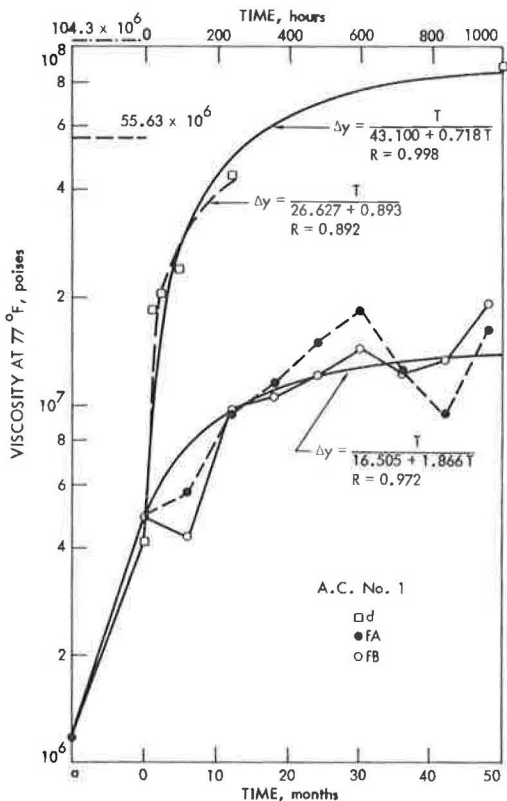


Figure 4. Viscosity at 140 F versus time of aging.

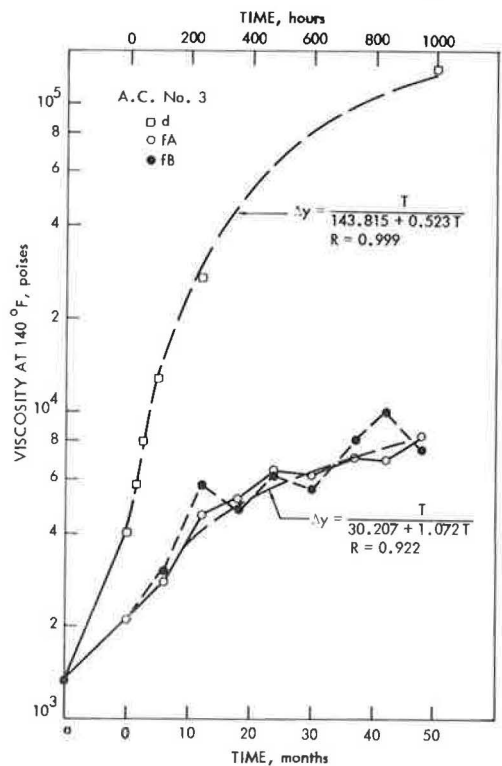


Table 7. Changes in softening point during weathering.

Project Sample	Asphalt Softening Point, Ring and Ball (deg F)								
	1	2	3	4	5	6	7	8	9
Original	119.0	116.5	115.5	114.5	113.0	118.0	116.0	118.0	119.5
TFOT	127.5	131.0	123.0	126.0	119.0	127.0	123.0	129.0	119.5
Laboratory aging (hours)									
d-24	141.0	134.0	131.0	133.5 ^a	121.5 ^a	—	125.5 ^a	136.0 ^a	132.5
d-48	140.5	143.0	138.0	138.0	126.5	140.0	128.5 ^a	142.5	136.0
d-96	143.5	149.0	140.5	141.0	126.0	143.0	134.0 ^a	144.5	145.5
d-240	159.0	152.5	145.0	148.5	134.0	152.0	146.6 ^a	150.0	151.5 ^a
d-480	168.0 ^a	167.0	154.5 ^a	154.5 ^a	143.8 ^a	163.7 ^a	160.5 ^a	164.0 ^a	—
d-1000	175.0	170.0 ^a	171.0	173.5	154.0	174.0	171.0	173.0	—
Field aging (months)									
Plant	130.5	129.0	127.5	122.5	—	118.0	120.0	124.0	116.0
f-0									
A ^b	127.5	125.0	125.0	119.0	—	—	118.0	132.0	124.0
B ^c	127.5	123.0	125.0	119.0	—	—	—	—	—
f-6									
A	124.0	128.0	122.5	120.5	—	133.5	132.0	136.0	132.0
B	125.0	120.5	125.5	120.5	—	133.0	130.0	136.0	126.0
f-12									
A	129.0	135.0	130.0	130.0	—	134.0	129.5	134.0	138.0
B	129.5	137.5	131.0	131.0	—	138.5	130.0	126.0	132.0
f-18									
A	130.0	137.0	—	134.0	—	135.0	132.8	136.4	132.0
B	132.0	136.0	128.0	134.0	—	140.0	132.8	136.0	130.0
f-24									
A	129.5	134.5	136.5	136.5	—	129.0	138.0	138.0	136.0
B	136.0	138.0	136.5	136.5	—	—	—	—	—
f-30									
A	137.0	140.0	136.5	135.5	—	140.0	137.0	141.0	136.0
D	136.0	137.0	—	136.0	—	—	—	—	—
f-36									
A	138.0	143.5	138.0	134.5	—	—	137.0	—	139.0
B	140.0	142.0	138.0	136.5	—	—	—	—	—
f-42									
A	133.0	138.0	140.0	134.5	—	142.0	—	144.0	—
B	129.0	138.2	141.0	134.6	—	—	—	—	—
f-40									
A	134.5	136.5	136.5	136.5	—	—	—	—	—
B	137.3	136.4	134.6	136.4	—	—	—	—	—

^aInterpolated value. ^bA = in wheel tracks. ^cB = between wheel tracks.

Table 8. Changes in microductility at 77 F.

Project Sample	Asphalt (cm)								
	1	2	3	4	5	6	7	8	9
Original	63	71	72	67	81.4	53.0	68.4	51.0	63.0
TFOT	46	36	82	89	91.0	57.0	84.0	60.0	55.0
Laboratory aging (hours)									
d-24	9.2	5.4	59	82	101.0 ^a	16.0 ^a	70.0 ^a	20.0 ^a	11.0
d-48	5.0	3.0	50	41	102.6	5.1	56.0 ^a	7.0	5.5
d-96	2.6	2.0	20	23	122.0	3.0	29.0 ^a	4.0	6.7
d-240	2.0	1.5	5.2	4.7	115.0	0.5	8.0 ^a	2.0	—
d-480	—	—	—	3.8	79.0 ^a	1.0 ^a	4.0 ^a	1.5 ^a	—
d-1000	0.5	—	0.4	1.8	-0.3	1.1	1.3	1.0	—
Field aging (months)									
Plant	48	62	87	93	—	75.0	68.0	67.0	65.0
f-0									
A ^b	69	72	78	81	—	—	60.0	67.0	79.0
B ^c	69	72	78	102	—	—	—	—	68.0
f-6									
A	87	62	102	102	—	23.0	73.0	15.0	37.0
B	87	63	95	101	—	23.0	64.5	14.6	28.0
f-12									
A	63	27	44	58	—	24.4	76.0	25.0	57.0
B	70	—	82	56	—	31.0	101.0	24.0	47.0
f-18									
A	70	33	88	84	—	—	55.5	8.5	16.5
B	76	35	79	85	—	—	80.5	11.0	16.5
f-24									
A	65	14	21	69	—	23.0	57.8	—	—
B	16	9.0	43	55	—	—	—	—	—
f-30									
A	16	7.7	84	65	—	7.2	—	5.9	—
B	17	8.0	69	74	—	—	—	—	—
f-36									
A	15	8.3	35	26	—	—	50.7	—	—
B	17	6.3	35	37	—	—	—	—	—
f-42									
A	16.5	10.0	43	37	—	4.7	—	5.0	—
B	14.0	4.0	34	12	—	—	—	—	—
f-48									
A	4.8	3.8	28	28	—	—	—	—	—
B	6.0	—	29	15	—	—	—	—	—

^aInterpolated value. ^bA = in wheel tracks. ^cB = between wheel tracks.

significant because it agrees with reported actual field hardening in service (18-21). It also suggests that the IDT is realistic and that the correlation between field hardening and hardening of asphalt in the IDT is possible.

According to this theory, the changes in physical properties of asphalt are a hyperbolic function of time and approach a definite limit with time. Brown et al. have suggested the following equation to express the hardening of asphalts in the field:

$$\Delta Y = \frac{T}{a + bT} \quad (1)$$

or

$$\frac{T}{\Delta Y} = a + bT \quad (2)$$

where

ΔY = change in penetration (or softening point or ductility) with time T or the difference between the zero-life value and the value for any subsequent year;

T = time;

a = constant, the intercept of the Eq. 2 line on the ordinate;

b = slope of the Eq. 2 line; and

$1/b$ = the ultimate change (limiting value of change) of penetration at infinite time.

Note that, from the limiting values of change $1/b$, the limiting values of properties Y_u can also be calculated. Both values could be used as numerical measures for comparison of the relative performance of asphalts. Thus, an asphalt with a high value of limiting change of penetration or a low value of limiting penetration could be considered as inferior to one with a low value of limiting change of penetration or a high value of limiting penetration.

Experimental data were fitted to Eq. 2 by the least-squares linear regression methods. Predicted curves were plotted in all pertinent curves in dashed lines and with equations given. Almost without exception, the fittings, as indicated by correlation coefficients R , were excellent. It can thus be concluded that the changes of rheological properties as measured by penetration, viscosity, softening point, and ductility are a hyperbolic function of time during IDT; i.e., the penetration and ductility decrease, and the viscosity and softening point increase, with time approaching definite limiting values.

The limiting values have been suggested by Brown et al. (18) as an index in comparing performance or potential behavior of asphalts. However, as pointed out by the author (2), when it is used as the only index in asphalt durability or quality evaluation, it can be misleading. The reason is that, in reality, asphalt will most likely reach a critical value of penetration, viscosity, ductility, or other controlling property and fail before it reaches the limiting value or infinite time. Therefore, it is the critical value or values of the controlling property or properties and the time the asphalt in question takes to reach this value that are of the utmost practical concern.

From viscosity data, it is shown that aging in IDT resulted in a decrease in c and an increase in S . Here, again, the behavior of asphalts in IDT appeared to be in agreement with other reported field findings (5, 19).

Asphalt hardening can also be expressed in terms of penetration ratio (original penetration/aged penetration) or viscosity ratio (aged viscosity/original viscosity). The viscosity ratio at 77 F is often called the aging index. Results of viscosity ratio for asphalts in IDT were calculated for viscosity at 77 F and for viscosity at 140 F. Linear relations were found between log penetration ratio and log time and between log viscosity ratio and log time during IDT aging. From these plots, relative durability or hardening susceptibility of asphalts of different original penetration or viscosity can be compared.

Aging and Chemical Changes in Asphalts

In this investigation, chemical changes in asphalt during aging were measured by determining the asphaltene content, the chemical composition by the Rostler-White method, and the oxygen content and by spot testing and using IR spectroscopy.

The formation of asphaltenes that results from weathering (oxidation or polymerization or both) has long been observed. The increase in viscosity (hardening of asphalt) and the change in colloidal structure (from sol or sol-gel to gel materials), or the increase in complex flow that accompanies the increase in asphaltene content, have been postulated by many researchers as the cause for asphalt failure by cracking. Thus, the change in asphaltene content was used in this study as an important parameter in asphalt durability evaluation.

The percentage of asphaltenes as given by the Skelly F precipitation method for all asphalts studied is given in Table 9. Three important observations can be made:

1. Aging is accompanied by increase in asphaltene content.
2. Change in asphaltene content is a hyperbolic function of time. Except for asphalt concrete 5, which is an unusual asphaltene-free asphalt, regression coefficients for the plot of $T/\Delta Y$ versus T were all more than 0.90 and were all significant at the 95 percent level.
3. Rates of asphaltene content formation are different for different asphalts (a varied from 5.6 to 32.4 and b varied from 0.05 to 0.99). The ultimate change in asphaltene content varied from 9 to 20 percent.

The data on chemical compositions of asphalts by the Rostler-White method indicated, though not very consistently, general increases in A and A_2 and decreases in A_1 and P with aging in IDT. The N -fraction remained relatively constant.

The composition parameters $(N + A_1)/(A_2 + P)$, the ratios of more reactive to less reactive components, and N/P , the ratio of the most to the least reactive fractions of maltenes, were calculated. The ratio $(N + A_1)/(A_2 + P)$ has been correlated with the durability of asphalts as measured by the tendency of asphalts to harden during aging as determined by the pellet-abrasion test (13, 14). However, the pattern of change in $(N + A_1)/(A_2 + P)$ with aging for asphalts studied could not be defined. The ratios of N/P varied from 1.25 for asphalt 3 to 3.19 for asphalt 4. This parameter was suggested by Halstead et al. (15) as indicative of the quality of asphalt. The significance of this parameter is yet to be determined.

Oxygen content of asphalt and asphaltenes was determined by the combustion method; a gradual increase in oxygen content during aging (both during the durability test and the road service) was observed. The degree and rate of oxidation were also indicated by weight increase during pressure-oxidation treatment.

Data also indicated that aging not only increased asphaltene content and oxygen percentage in asphalt, but it also caused increases in oxygen percentage in asphaltenes.

Results of spot tests during laboratory aging have shown that all original asphalts showed negative spot tests, and, as asphalts aged (except for asphalt 5), all tests became positive at some time during the aging process. The border line between positive and negative spot testing appeared to be about 20 percent asphaltenes.

FIELD AGING

Density and Voids Changes of the Pavements

Changes of density and voids of asphalt pavements were studied because such changes have been found to affect the rate of asphalt hardening, fatigue resistance, and water susceptibility of the mixture. Thus, the changes and voids are two relevant factors to be considered in the final analysis of asphalt durability, correlation, and critical asphalt property values.

Bulk specific gravity d is determined by the water displacement method at 77 F. Percentage of voids V is calculated from bulk specific gravity and maximum theoretical specific gravity D data. The latter is determined following Rice's method, which is essentially that described in the ASTM D2041-64T. Changes in voids content are shown in Figure 5. When the trends are examined and compared with designed mix data, the following observations can be made:

1. There were no appreciable initial differences on density-voids values between specimens in wheel tracks and specimens between wheel tracks,

Table 9. Percentage of asphaltenes.

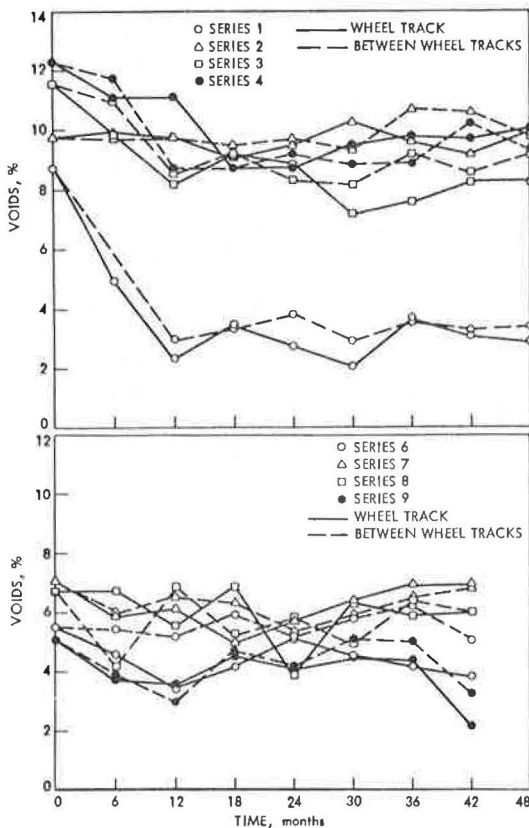
Project Sample	Asphalt									
	1	2	3	4	5	6	7	8	9	
Original	17.72	17.85	15.69	14.52	4.55	15.64	17.80	11.30	11.11	
TFOT	20.60	21.23	19.37	18.33	5.70	19.20	20.20	14.35	14.18	
Laboratory aging (hours)										
d-24	23.34	23.50	21.06	—	6.70 ^a	—	22.00 ^a	16.00 ^a	18.55	
d-48	23.50	23.85	21.67	22.14	8.07	22.30	22.80 ^a	19.20	19.70	
d-96	24.05	24.85	22.69	23.11	7.93	22.68	24.20 ^a	19.15	19.12	
d-240	27.14	26.54	24.57	26.52	10.96	27.13	26.20 ^a	21.06	20.50 ^a	
d-480	27.60 ^a	29.37	27.50 ^a	29.80 ^a	14.40 ^a	27.35	27.50 ^a	22.40 ^a	22.60	
d-1000	28.99	—	34.17	31.10	22.02	28.22	31.10	25.70	—	
Field aging (months)										
Plant	20.26	20.04	19.04	18.83	—	19.48	20.70	13.95	11.96	
f-0										
A ^b	19.96	20.75	18.22	19.10	—	—	19.30	12.35	12.82	
B ^c	—	—	—	19.88	—	—	—	—	—	
f-6										
A	20.11	20.87	19.84	18.38	—	20.39	20.44	17.85	14.48	
B	21.31	20.11	25.97	22.56	—	21.56	20.74	—	15.51	
f-12										
A	20.31	21.86	21.29	21.24	—	20.71	23.07	17.95	16.39	
B	21.26	21.45	—	21.81	—	19.93	—	18.85	16.68	
f-18										
A	23.21	20.69	21.40	21.45	—	23.83	24.59	19.49	18.04	
B	21.88	23.12	20.00	22.20	—	24.95	23.14	19.73	18.80	
f-24										
A	21.16	—	22.02	21.27	—	28.56	23.49	19.73	18.50	
B	23.03	23.95	20.99	24.52	—	28.30	—	18.74	—	
f-30										
A	24.02	22.78	20.99	23.66	—	24.16	24.82	20.73	19.69	
B	24.71	22.85	20.65	23.94	—	—	—	—	—	
f-36										
A	25.08	23.96	21.49	23.83	—	—	23.04	17.88	21.84	
B	25.56	24.30	23.98	23.05	—	—	22.40	—	—	
f-42										
A	24.03	24.91	24.36	23.51	—	28.00	—	21.36	—	
B	—	—	—	—	—	—	—	—	—	
f-48										
A	25.38	24.91	24.15	25.16	—	—	—	—	—	
B	33.23	25.20	24.99	24.97	—	—	—	—	—	

^aInterpolated value.

^bA = in wheel tracks.

^cB = between wheel tracks.

Figure 5. Pavement voids versus time.



2. Pavements constructed during the second period (projects 6 to 9) of warmer weather approached higher density and lower voids relative to design density and voids than those built during the first period (projects 1 to 4),
3. Half of the projects reached design densities and voids at the end of 1 year or after one summer of traffic densification, and
4. Changes of density and voids appeared to have leveled off after 1 year of traffic compaction.

Behavior of Asphalts in the Pavements

Physical and chemical changes in asphalts in pavements were determined for 42 months on four projects and for 48 months on the other four projects. The general changes of physical and chemical properties of recovered asphalts with field aging time were found to follow the time-rate-of-change curves established in laboratory aging during IDT.

Physical Properties—All physical properties (especially rheological) that appeared to be suited to evaluating asphalt durability and that have been conducted on original and laboratory-aged asphalt were also determined on recovered asphalts from plant, p, to just compacted, f-0, and up to 48 months at 6-month intervals.

Within the range of mixing temperatures of 290 to 310 F that were recorded at the plants for the eight paving projects, no appreciable differences were detected in the hardening of asphalt as determined by increase in penetration ratio. The comparison between results of the TFOT, d, and the hardening during mixing, p and f-0, in terms of penetration, penetration ratio, viscosity at 77 and 140 F, aging index (viscosity ratio) at these two temperatures, and softening point showed slightly higher overall hardening in TFOT than in plant mixing for various asphalts used in this project. However, the close parallel between results of these two processes has reconfirmed the ability of the TFOT in simulating hardening of asphalt in an average hot mixing plant.

The changes in penetration softening point, viscosity at 77 and 140 F, and microductility at 77 F for 42 to 48 months of service life are given in Tables 4 through 8. The curves showing drop in penetration have the normally expected shapes of hyperbolic function of time, with a rather rapid rate of hardening in the first 20 months and a tendency for the rate of hardening to decrease thereafter. Hyperbolic fittings were made on all recovered asphalts (both in and between wheel tracks) for all properties between property change ΔY and T time by linear least-squares regression analysis between $T/\Delta Y$ and T. The resulting time-property change curves were indicated by dotted line curves with equations shown in terms of $\Delta Y = (T/a) + bT$. Also shown with the fitted curves is R.

The viscosity at 77 F and the $5 \times 10^{-2} \text{ sec}^{-1}$ increase with time also followed a hyperbolic function, as shown in Figure 3. The effects of field aging were also reflected in c and on S. The general trends of decreasing c and increasing S with field service life can be observed. A hyperbolic increase of viscosity at 140 F with field aging time is shown in Figure 4.

The microductility change with field aging time was less consistent, possibly because of the complex properties that the ductility test measures and the existence of an optimum consistency for ductility. For four of the eight asphalts (1, 3, 4, and 7), the ductility at 77 F remained high or increased up to 30 months and could not be fitted with hyperbolic curves. Only two asphalts (7 and 8) showed a marked decrease in ductility from the beginning of field aging and could be fitted with hyperbolic curves.

Chemical Properties—Changes in the percentage of asphaltenes with time of field service of recovered asphalts are given in Table 9. An increase in asphaltene content with aging or hardening is apparent. Although curve fittings were not as good as were those for rheological data, hyperbolic relations between an increase in asphaltenes and the time of field aging can be established.

Chemical analysis by the Rostler-White method was made on recovered field-aged asphalts 1 to 4. No consistent trends could be found for the two so-called quality parameters, $(N + A_1)/(A_2 + P)$ and N/P .

CORRELATIONS

The value and usefulness of any laboratory durability test depend not only on how logical or realistic the acceleration process is in the laboratory as compared with what actually occurs in the field but also on how good the correlation is between laboratory and field data. One of the major efforts in this investigation was to establish a correlation between hardening and other relevant property changes in asphalts in the developed IDT and changes in the same asphalts in the pavements in Iowa in terms of time-equivalency curves or acceleration factors between aging in IDT in hours and aging in the pavement in months. With the correlation or calibration curves and the selected durability criteria, functional approach specifications of paving asphalt can then be established, and the durability of asphalts in pavement can be predicted in more reasonably exact terms.

Time-equivalency correlation curves were established for each asphalt and for all relevant properties. Correlation curves were drawn from the property-time curves for each asphalt for a certain property. The time in hours in IDT and the equivalent time in months in the pavement required for each asphalt to reach a certain value were determined from the property curves. Seven to fifteen points were taken from each set of property-time curves for each asphalt and each property. They were plotted on semilog-scale with log laboratory time (T_1 , hours) as ordinate and field service time (T_f , months) as abscissa. Sample time-equivalency correlation curves are shown in Figure 6 for penetration.

Because the majority of these curves were of hyperbolic nature, curve fittings for all time-equivalency data for all properties were attempted for all asphalts with the following model:

$$\log T_1 = \frac{T_f}{a + bT_f}$$

where

- T_1 = laboratory IDT time (in hours) to reach certain property value,
- T_f = equivalent field time (in months) to reach same value of same property for the same asphalt, and
- a and b = constants.

In order for the time-equivalency curves to be useful, general correlation curves were established for each property by combining eight individual curves for that property. General time-equivalency curves for penetration, softening point, viscosity at 77 F, viscosity at 140 F, asphaltene content, and microductility are shown in Figure 7. Because each test determines a different asphalt property or behavior, the variation of these curves was to be expected.

Because many other variables—type of aggregate and gradation, asphalt content, mixing temperature, compaction, traffic, and voids—also influence the rate of change of asphalts in pavements, the minor variations among curves of different asphalts for the same property criterion are to be expected.

Because all pavements studied in this project were regular paving projects of the ISHC, materials and construction practices could be safely assumed to have met minimum and acceptable standards. Effects resulting from variations in mixing temperatures were not obvious, as discussed previously. Effects on hardening because of variation in asphalt content and film thickness were examined by correlating the average film thickness (6.2 to 9.7 μ) and viscosity and penetration of 42-month recovered asphalts. No relation was found. Thus, the only variable, in addition to differences among asphalts, that could affect the asphalt hardening rate was voids content. Relations between initial and final voids content and 42-month penetration and viscosity at 77 F are shown in Figure 8. No relation was found between penetration and initial voids; some general trend could be detected between penetration and final voids (correlation was not significant). Though correlations were not good, there was a linear relation between log viscosity and log void content (significant at 5 percent level for

Figure 6. Typical penetration correlation curves.

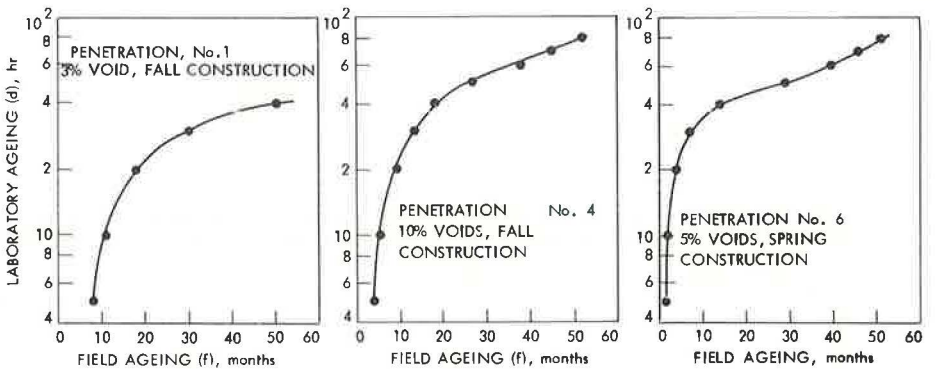


Figure 7. Time-equivalency correlation curves for various properties.

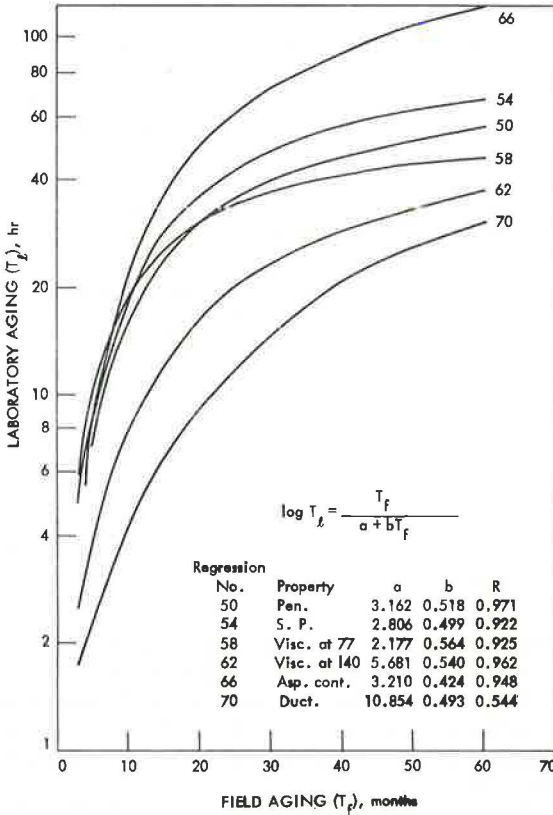
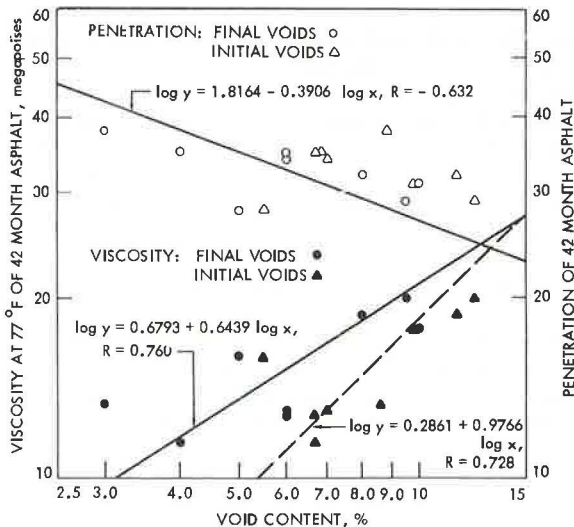


Figure 8. Log viscosity (log penetration) versus log void content of 42-month field asphalts.



both initial and final voids); i.e., there is a general indication of higher viscosity for asphalts recovered from higher voids pavements.

Possible differences resulting from voids content among pavements were accounted for by establishing equations for time-equivalency correlation curves by combining asphalts of different voids level (Fig. 9). The relative positions of the curves are of significance; as percentage of voids in the pavements increases, longer laboratory IDT time is required to reach equivalent field-service hardening. Regression 74, which was obtained by combining all properties and all asphalts and which is a surprisingly good fit (linear correlation significant at 1 percent level), will be called the master time-equivalency curve. For all practical purposes, the use of the master curve for all asphalts used in all acceptable construction procedures should provide reasonable correlation and prediction for Iowa conditions. It is therefore recommended that, at least for a trial period, this curve be used for specification purposes by the IDT method. On the basis of the master curve, 46 hours of aging in IDT will result in hardening in asphalts equivalent to that attained after 60 months of service life in Iowa conditions.

APPLICATION AND ENGINEERING IMPLICATIONS OF RESULTS

It has been shown repeatedly that asphalts meeting the same present-day specifications can and do exhibit a considerable range and variety of behavior, as measured by a number of different parameters, in the field. It appears justifiable to state that, at the present time, standard test procedures and specifications provide no satisfactory means of determining whether or not asphalt will be durable.

Based on results discussed in previous sections, and with the established time-equivalency correlation curves, it is suggested that the IDT can be used to reasonably predict the changes and useful life of asphalt in Iowa pavements. If parameters, tests, and critical values of asphalts are properly selected, the results of this investigation can be applied to asphalt specification to ensure durable paving asphalts.

Selection or establishment of durability criteria and critical values of critical properties are complex problems. Relative durability of asphalts studied in this project were evaluated by using several approaches.

Limiting Values of Selected Properties

Limiting values is based on the hypothesis, which was verified in this study, that changes in asphalt, both in the laboratory IDT and in the field-service aging, are a hyperbolic function of time in the form

$$\Delta Y = \frac{T}{a + bT}$$

When a and b are determined and initial property value Y_0 is known, the ultimate value Y_u can be calculated from the ultimate change

$$\Delta Y_{t \rightarrow \infty} = 1/b$$

Based on this approach, larger ultimate change (or lower ultimate penetration and higher ultimate viscosity and softening point) would be considered properties of less durable asphalts.

Predicted Time to Harden to Certain Critical Values of Selected Properties

Predicted time to critical value is also based on the hyperbolic time-property change curve model as in the preceding approach. But, instead of ultimate change or limiting value, the time it takes for a certain asphalt to harden to a critical value of a selected property is calculated from the predictive equation or from the time-property curve. Times for asphalts to harden to a critical penetration of 20, a critical softening point of 160 F, a critical viscosity at 77 F, and 0.05 sec^{-1} of 20 to 30 megapoises were

Figure 9. Time-equivalency correlation curves by voids level.

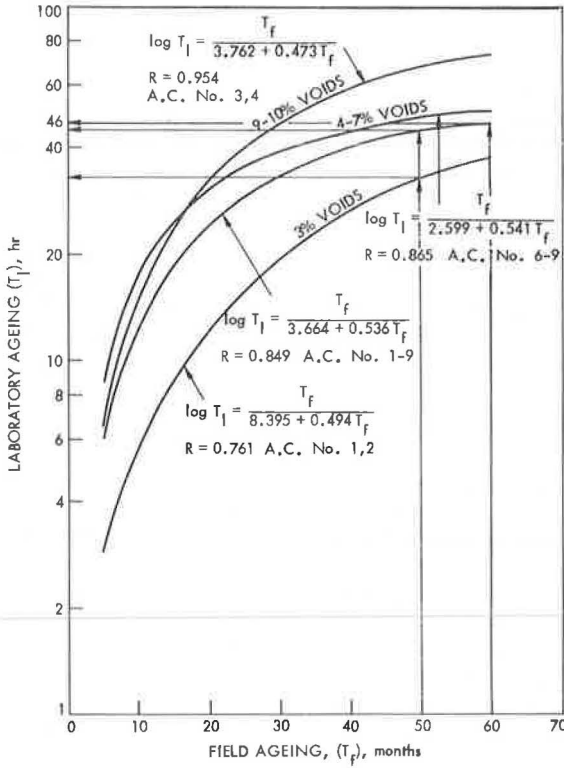


Table 10. Comparison of durability rankings based on different criteria.

Criterion	Asphalt								$\frac{\sum r_n - r_n }{n}$	
	1	2	3	4	5	7	8	9		
Penetration ratio										
r_e	4	2	8	6	5	7	3	1		
r_r	4	7	6	8	3	1	2	5	2.8	
Aging index, 77 F										
r_e	3	1	7	4	5	8	6	2		
r_r	5	6	7	8	2	1	3	4	3.3	
Aging index, 140 F										
r_e	5	7	6	8	4	2	2	1		
r_r	4	8	5	7	3	1	2	6	1.5	
Limiting penetration										
r_e	5	3	8	6	2	7	4	1		
r_r	5	7	8	3	4	1	2	6	2.8	
Limiting viscosity, 77 F										
r_e	4	6	8	5	1	3	7	2		
r_r	3	8	7	6	4	2	5	1	1.5	
Limiting softening point										
r_e	5	3	2	6	7	8	4	1		
r_r	5	3	5	7	4	2	8	1	2.1	
Time to 20 to 30 megapoisies										
r_e	7	4	5	8	2	5	2	1		
r_r	3	6	5	7	4	2	8	1	2.2	
Time to 20 penetration										
r_e	6	7	8	5	3	4	2	1		
r_r	5	4	6	8	2	3	1	7	2.2	
Time to 160-F softening point										
r_e	8	7	2	3	5	4	6	1		
r_r	5	4	6	8	3	2	7	1	2.2	
Total ranking										
R_e	5	4	8	7	2	6	3	1		
R_r	5	6	7	8	2	1	4	3	1.5	

calculated. Rankings of the eight asphalts (longer time to reach a critical value means a more durable asphalt) are given in Table 10.

Penetration Ratio Versus Time Curves

It has been established that log penetration ratio and log time of aging is linear. The slope of such plots, therefore, would be indicative of the relative rate of hardening of various asphalts with time. A small slope will indicate a more durable asphalt. Such an approach can also be applied to retained penetration data.

Aging Index Versus Time Curve

Aging index as defined by the ratio of viscosity of aged and original asphalt can be used as an index of the relative degree of hardening of asphalt. It has also been established that the log aging index and the log time of aging are linear. The slope of such a plot can then be used to indicate the relative rate of hardening of asphalt with time. A small slope will imply a more durable asphalt.

Rankings of the eight asphalts based on the preceding criteria are given in Table 10 (r_l for laboratory-aged and r_f for field-aged asphalts). It can be readily noted that rankings of asphalt durability by different criteria are not consistent, except for asphalt concrete 9, which ranked high by all criteria. The ultimate test in determining which of the criteria is most accurate and suited for Iowa conditions consists of continuing observation of the performance of the eight pavements. At this time, they are essentially all in good condition after 42 to 48 months of field service.

The laboratory- and field-durability rankings of asphalts studied were compared and the ability of various criteria to predict asphalt durability was evaluated to calculate the average laboratory- and field-durability ranking differences of the eight asphalts by each criterion. Based on this index, the aging index based on viscosity at 140 F and the limiting viscosity at 77 F seem to be most indicative of the relative aging of asphalt in the laboratory and the pavement.

The overall durability rankings of all asphalts by all criteria were calculated by totaling all nine rankings for each asphalt for both laboratory-aged and field-aged asphalts and ranked as given in Table 10. The average laboratory and field ranking difference was 1.5, which seems to indicate that the IDT can be used to evaluate and predict pavement performance of asphalts with reasonable accuracy.

Control of durability in terms of IDT can be established by incorporating in paving asphalt cement specifications the following standards: a maximum of 20 megapoises in viscosity at 77 F or a minimum penetration of 20 for residue from 46 hours of IDT or both.

CONCLUSIONS

The following conclusions are based on test data:

1. A laboratory durability method for simulating the weathering of paving asphalts during mixing and pavement service life has been developed and is being correlated with field performance under Iowa conditions.
2. The aging process of paving asphalts follows a hyperbolic function of time both in the field and in the developed IDT laboratory conditions, but at different rates.
3. Good correlations between field service aging in Iowa and laboratory aging during IDT have been obtained. The master time-equivalency curve between IDT in hours and pavement service life in months, established by combining all asphalts (void levels) and properties, indicates that 46 hours in IDT will age asphalts to the equivalent of 60 months in Iowa pavements. Correlation curves for different properties and different levels of pavement voids were also obtained.
4. A tentative specification for paving asphalt, including durability requirements based on IDT, is recommended in lieu of current TFOT.

ACKNOWLEDGMENTS

This report is the end result of a comprehensive 4-year study under a project sponsored by the Iowa Highway Research Board and the Iowa State Highway Commission. This work was also supported, in part, by funds of the Engineering Research Institute, Iowa State University.

REFERENCES

1. Characteristics of Bituminous Materials. Highway Research Board Bibliography 35, 1963, and Highway Research Board Bibliography 40, 1966.
2. Lee, D. Y. Development of a Laboratory Durability Test for Asphalts. Highway Research Record 231, 1968, pp. 34-49.
3. Lee, D. Y. Durability and Durability Test for Paving Asphalt. Engineering Research Institute, Iowa State Univ., 1969.
4. Traxler, R. N. Asphalt: Its Composition, Properties and Uses. Reinhold Publishing Corp., New York, 1961, p. 53.
5. Schmidt, R. J., Painter, L. J., Skog, J. B., and Puzinauskas, V. P. The Precision of Tests Made on Asphalt Residue From Thin Film Oven Exposures. Proc. AAPT, Vol. 37, 1968, pp. 476-509.
6. Hveem, F. N., Zube, E., and Skog, J. Proposed New Tests and Specifications for Paving Asphalts. Proc. AAPT, Vol. 32, 1963, pp. 271-327.
7. Skog, J. "Setting" and Durability Studies on Paving Grade Asphalts. Proc. AAPT, Vol. 36, 1967, pp. 387-420.
8. Chipperfield, C. H., Duthie, J. L., and Girdler, R. B. Asphalt Characteristics in Relation to Road Performance. Proc. AAPT, Vol. 39, 1970, pp. 575-613.
9. Kandhal, P. S., et al. Asphalt Viscosity Related Properties of In-Service Pavements in Pennsylvania. Paper presented at annual meeting of AAPT, 1972.
10. Lee, D. Y., and Csanyi, L. H. Jour. of Materials, Vol. 3, 1968, p. 538.
11. Gotolski, W. H., Ciesielski, S. K., and Heagy, L. N. Progress Report on Changing Asphalt Properties of In-Service Pavements in Pennsylvania. Proc. AAPT, Vol. 33, 1964, pp. 285-319.
12. Vallerger, B. A., and Halstead, W. J. Effects of Field Aging on Fundamental Properties of Paving Asphalts. Highway Research Record 361, 1972, pp. 71-92.
13. Rostler, F. S., and White, R. M. Composition and Changes in Composition of Highway Asphalts, 85-100 Penetration Grade. Proc. AAPT, Vol. 31, 1962, pp. 35-89.
14. Halstead, W. J., Fritz, S. R., and White, R. M. Properties of Highway Asphalts—Part III, Influence of Chemical Composition. Proc. AAPT, Vol. 35, 1966, pp. 91-138.
15. Halstead, W. J., et al. Fingerprinting of Highway Asphalt. Paper presented at annual meeting of AAPT, Feb. 14-16, 1972.
16. Csanyi, L. H., and Fung, H. P. A Rapid Means of Determining the Constituents of Asphalts. Proc. AAPT, Vol. 23, 1954, pp. 64-77.
17. Lee, D. Y., and Huang, R. J. Weathering of Asphalts as Characterized by Infrared Multiple Internal Reflection Spectroscopy. Paper presented at 11th Annual Meeting of Society for Applied Spectroscopy, Dallas, Texas, Sept. 11, 1972.
18. Brown, A. B., Sparks, J. W., and Larsen, O. Rate of Change of Softening Point, Penetration, and Ductility of Asphalt in Bituminous Pavement. Proc. AAPT, Vol. 26, 1957, pp. 66-81.
19. Gallaway, B. M. Durability of Asphalt Cements Used in Surface Treatments. Proc. AAPT, Vol. 26, 1957, pp. 151-173.
20. Pauls, J. T., and Halstead, W. J. Progressive Alterations in a Sheet Asphalt Pavement Over a Long Period of Service. Proc. AAPT, Vol. 27, 1958, pp. 123-154.
21. Heithaus, J. J., and Johnson, R. W. A Microviscometer Study of Road Asphalt Hardening in the Field and Laboratory. Proc. AAPT, Vol. 27, 1958, pp. 17-34.

STORAGE OF BITUMINOUS CONCRETE IN INERT GAS

Prithvi S. Kandhal and Monroe E. Wenger, Pennsylvania Department of Transportation

Possible problems associated with hot storage of bituminous concrete mixes can be migration of asphalt, segregation of the mix, and aging of the asphalt cement due to prolonged storage at high temperature. Laboratory and field investigations were conducted to evaluate the effect of prolonged hot storage on the properties of a bituminous paving mix. No additive was used in the asphalt cement. Storage of mixes was attempted with and without inert gas for as long as 10 days. Field tests were conducted with inert gas only to extend the storage period. Migration of asphalt and segregation of mix did not pose any problem. In the pilot tests, mix stored without inert gas hardened at a faster rate than that stored with an inert atmosphere. If the maximum allowable storage time is determined from the criterion of minimum percentage of retained penetration (AASHO M 20-70) on TFOT residue, this can vary depending on the asphalt source, composition of the bituminous mix, temperature, and time of mixing. No storage might be possible in some cases; however, based on these criteria, the allowable storage period using inert gas was found to be 24 hours in this field study. It is yet to be established to what extent the durability of the pavement is sacrificed because of premature hardening of the asphalt in the hot storage bin.

•THE installation of hot-mix surge and storage-bin systems has considerably increased throughout the United States during the past 2 or 3 years. This study was undertaken to investigate the effects of prolonged storage at high temperature on the properties of a bituminous paving mixture.

The research program consisted of three phases: Phase 1 was the laboratory hot storage study to evaluate the rheological properties of the asphalt cement on being stored at higher temperatures for a considerable length of time, phase 2 was a semi-field test using two pilot storage bins (3 ft in diameter and 3 ft deep) placed in the yard outside the laboratory, and phase 3 was a full-scale field test using 200-ton hot storage bins supplied with inert gas. Phase 3 involved storage of base course and wearing course bituminous mixtures in inert atmosphere for as long as 10 days.

The objectives of this study were to ascertain if there is segregation in the resulting mix; evaluate possible migration of asphalt during storage; determine the effects of storage on the physical properties of the mixture such as Marshall stability, flow, stiffness, and so forth; and evaluate the changes in rheological properties of the asphalt cement caused by prolonged storage at high temperatures.

REVIEW OF LITERATURE

The effect of hot storage on bituminous concrete mixes has been studied by various research agencies with variable results. It has been stated (1) about hot-mix surge storage that safe storage periods are not so much a function of bin design as they are a function of the nature of the mix and its uniformity.

Middleton et al. (2) studied the effects of hot storage on a fine-graded bituminous paving mix (using silicone treated 85 to 100 penetration grade asphalt cement) that was

stored in a silo for a total of 97 hours. Results showed that there was a marked change in the properties of the asphalt cement during mixing but that any change that may have occurred during storage was practically negligible.

Parr (3) has reported about storage of a fine-graded bituminous base course mix using sand-gravel as aggregate and 40 to 50 penetration grade asphalt cement. Two series of tests of storage were conducted: Series A contained asphalt that was untreated, and series B contained asphalt treated with 2 ounces of an additive containing silicone materials for each 5,000 gal of asphalt. With the treated asphalt, no significant change in either penetration or ductility occurred for 72 hours of hot storage. However, with untreated asphalt, significant changes in both penetration and ductility were observed in samples taken after 24-hour storage at the hot-bin temperature.

Vallerga and White (4) reported significant hardening of asphalt cement after 4 hours. The rate of hardening was significantly decreased when silicone fluid was added to the asphalt.

Brock and Cox (5) reviewed the results of tests on actual installations and concluded that hot bituminous mix may be stored without detrimental effects for 10 days in a heated silo blanketed with an inert gas and for more than 14 days if the mix contains silicone and is held in a heated silo blanketed with an inert gas.

A series of gradation tests were conducted (6) on surface-course mix obtained from the silo, but no appreciable change in gradation was noted due to storage.

Four series of 72-hour tests conducted by the National Asphalt Pavement Association (7) indicated that the use of an inert atmosphere increased the storage time from 6 to more than 72 hours for mix made with nontreated asphalt. The use of silicone thus increased storage time from about 24 to more than 72 hours in the inert atmosphere and from about 2 to 6 hours in air.

Parr and Brock (8) conducted a statistical study of effects of hot storage on the composition and properties of a bituminous concrete binder mixture stored for 7 days in a sealed silo equipped with a hot-oil heating jacket and purged with an inert gas inside. They concluded that the mix composition before and after storage was not significantly different. However, some hardening of the asphalt did occur, but it was not severe because the drop in penetration was less than that permitted by specifications for the thin-film oven test (TFOT).

Because the Pennsylvania Department of Transportation does not permit the use of silicones as an additive in the asphalt cement, this additive was excluded from this study.

Effect of hot storage on the rheology of the asphalt cement has not been studied in greater detail. Hardening of asphalt cement because of storage has mostly been observed by noting change in penetration only. Recent research (9, 10, 11) has indicated that, besides absolute viscosity, other parameters such as shear susceptibility and temperature susceptibility are needed to specify the complete rheological behavior of paving grade asphalts. The major factors affecting the durability and performance of the pavements have been observed to be the aging index (based on viscosity at 77 F) and the gain in shear susceptibility of the asphalt cements (12). An attempt has been made in this study, therefore, to evaluate the effects of hot storage on these rheological parameters also.

PRELIMINARY LABORATORY AND SEMI-FIELD TESTS

Laboratory Study

This study was undertaken to simulate the condition when the bituminous concrete mix is stored at high temperature in a sealed silo without inert gas. Bituminous wearing course mix made of limestone aggregates and AC-2000 asphalt cement was stored in 1-quart friction top cans and kept in an oven at 290 F for as long as 15 days. After specified time intervals, the cans were taken out and chilled by immersion in ice water to minimize the effect of continued heat. Asphalt was recovered by the Abson method, and the rheological tests were conducted on the recovered asphalt. Complete data are given elsewhere (13).

Because the cans were sealed, hardening of asphalt continued until the limited oxygen in the air was utilized in about 24 hours of storage, and thereafter further hardening was

negligible for as long as 15 days. During the first 24 hours, penetration dropped from 67 to 53, viscosity at 77 F increased from 3.0 to 4.0 megapoises, viscosity at 140 F increased from 3,450 to 5,290 poises, and viscosity at 275 F increased from 647 to 793 cs.

Semi-Field Study

Bituminous mixes were stored in two CMI pilot bins mounted on a trailer for demonstration purposes. The complete unit, which was placed in the back yard of the BMTR laboratory, consisted of two hot-mix containers 3 ft in diameter and 3 ft deep and an oil heating and inert gas system. One container was supplied with inert gas and jacketed with hot oil; the other was only jacketed with hot oil. Bituminous mixtures were fed in these preheated containers at a temperature of 290 F. The mixtures were stored for as long as 10 days.

Tests similar to the laboratory study were run on the recovered asphalt, and the complete data obtained are given elsewhere (13). The mix stored without inert gas hardened at a faster rate than that stored with inert atmosphere in the bin. However, in both mixes, there was a significant drop in asphalt penetration and ductility and significant increase in viscosity and shear susceptibility during the first 5 to 6 hours. Asphalt cement hardened more than that permitted by specifications for the TFOT. This indicated that the rate of hardening during storage depends primarily on the asphalt source (if storage conditions are held the same). It may be mentioned, however, that, because of problems in maintaining temperature and regulating the inert gas, the data would not relate to the ideal conditions.

FIELD TEST RESULTS

The storage system of the H. R. Imbt Co. (asphalt plant 6) located at Bossardsville, Pennsylvania, was used for this field study. The storage system consisted of the following:

1. Three 200-ton circular bins heated by hot-oil jackets and insulated—Automatic controls were available to maintain the unit at the desired temperature. The bin is a tall, vertical unit on top with a tapered hopper that tends to remix the bituminous concrete while discharging. Each bin is provided with a bottom air lock below a clam-type discharge gate and top air lock to seal the unit and hold the inert gas at a constant low pressure to prevent outside atmosphere from entering.
2. Thermal oil heater—Hot oil from the heater is pumped to the storage unit by a high-volume pump.
3. Inert gas generator—When the generator is operating, inert gas is pulled from the exhaust of the pre-mix burner and is then cooled, dehydrated, compressed, and stored in a pressure tank.
4. Drag chain conveyor—The conveyor is a continuous type and is enclosed to prevent spillage of mix and to maintain temperature.
5. Control room—The room contains consoles consisting of all controls necessary for discharging mix, bin level indicators, and controls for heating and inert gas systems.

Only two bins were used. In one bin, Pennsylvania ID-2 wearing course mix was stored; in the other bin, bituminous concrete base course (BCBC) mix was stored. Sampling of the bituminous concrete was done at specified intervals during the 10-day storage period. Samples were obtained as per ASTM D 979-51. After each storage period, two 1-gal cans were filled with bituminous mix, chilled in cold water, and then shipped to the BMTR laboratory for testing. Samples were also used in compacting three Marshall specimens immediately at the plant laboratory. These were stored for 24 hours and then tested for Marshall stability and flow.

Marshall data obtained on samples of ID-2 wearing course mix are shown in Figure 1. The temperature of discharged mixture from the two bins at the time of sampling is shown in Figure 2.

Asphalt cement was extracted from the duplicate samples of bituminous mix received in the central laboratory. Based on extraction test data, the gradation number, the surface area of the recovered aggregate, and the bitumen index have been determined

Figure 1. Marshall test data (ID-2 wearing course mix).

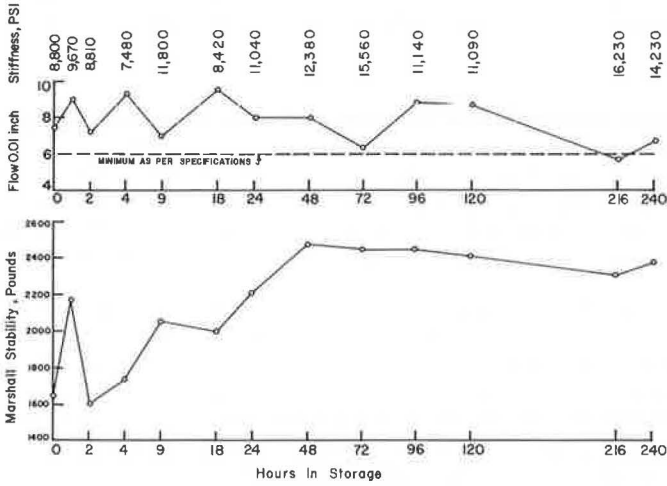


Figure 2. Temperature of discharged mix (field study).

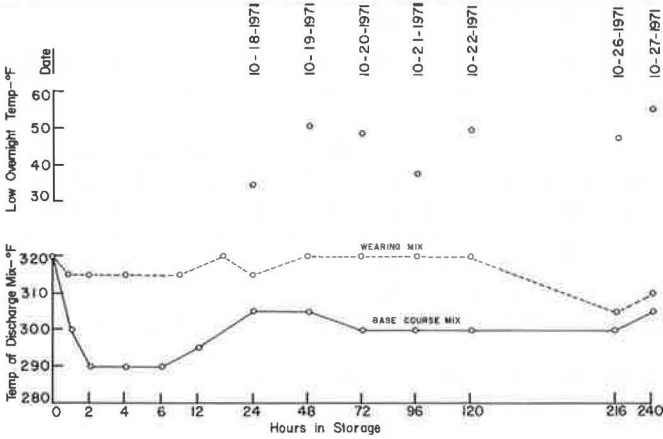


Table 1. Mix data.

Hours in Storage	Asphalt Content (percent)	Gradation Number	Aggregate Surface Area (ft ² /lb)	Bitumen Index (lb/100 ft ²)
0	3.6	2,068	17.74	0.211
1	3.8	2,336	20.18	0.196
2	3.8	2,149	18.49	0.214
4	3.6	2,293	19.66	0.190
6	3.5	2,333	19.38	0.187
12	3.6	2,404	19.81	0.189
24	3.5	2,381	19.27	0.188
48	3.7	2,572	20.09	0.191
72	3.4	2,349	18.07	0.195
96	3.7	2,468	18.98	0.202
120	3.6	2,335	17.86	0.209
216	3.6	2,154	17.34	0.215
240	3.6	2,356	18.64	0.200
Average	3.6	2,323	18.89	0.199
Standard deviation	0.11	0.135	0.936	0.012

to examine the variability in the mix sampled. These data are given in Table 1 for the base course mix. The gradation number is similar to fineness modulus except it is the sum from the $\frac{1}{2}$ -in. and smaller sieves of the percent fractions passing divided by 100.

The recovered asphalt cement was tested for penetration at 77 F; ductility at 60 F, 5 cm/min; absolute viscosity at 77 F, 0.05 sec^{-1} shear rate and shear susceptibility; absolute viscosity at 140 F; and kinematic viscosity at 275 F.

Figures 3, 4, 5, and 6 show these data versus the storage period for both the mixtures.

Absolute viscosity, using the sliding plate microviscometer, was also determined at 50, 104, and 122 F. Temperature susceptibility data based on these results are given in Table 2 for the base course mix only.

Storage aging indexes, based on viscosity at 77 F, have been determined for both mixtures and are shown in Figure 7. These have been determined as follows:

$$\text{Storage aging index} = \frac{\text{viscosity after storage}}{\text{viscosity before storage}}$$

DISCUSSION OF TEST RESULTS

Effect of Storage on Properties of Bituminous Concrete

Changes in the properties of bituminous concrete resulting from storage in the full-scale storage bins are as follows.

Migration of Asphalt Cement—Extraction test data indicate reasonable uniformity of asphalt content in the two mixtures sampled after various storage intervals for as long as 10 days. If the migration of asphalt cement in either of the mixes had taken place toward the bottom of the bins, the asphalt content would have increased with storage period. The standard deviation in the asphalt content for the samples tested was observed to be 0.14 and 0.11 percent for the wearing course and base course mixtures respectively. Migration of asphalt would perhaps occur if the storage is attempted at temperatures higher than 320 F or the bituminous concrete stored is rich in asphalt.

Segregation—Possible segregation of the mixtures due to storage was evaluated by subjecting to sieve analysis the aggregate recovered by the extraction test from the sampled mixtures. The gradation of the recovered aggregate from both the mixtures falls within the tolerance limits as per specifications. Only the normal variation that is inherent in a bituminous concrete plant has been observed.

Gradation number and bitumen index have been used (8) to evaluate the extent of segregation and the uniformity of asphalt film thickness. The aggregate surface area of each sample was calculated to determine the bitumen index. Normally a coarse mix would tend to segregate more than a fine mix. Data given in Table 1 for base course mix do not indicate any segregation problem.

Marshall Stability and Flow—Marshall specimens were compacted from the wearing course mix samples and tested for stability and flow with an automatic recorder. In the specifications for Pennsylvania ID-2 wearing course, a minimum stability of 1,200 lb and a flow value between 6 and 16 are required. The average stability and flow of the mix out of the pug mill was observed to be 1,600 lb and 8 units respectively. Figure 1 shows the changes in these values with the storage period. As would be expected if the asphalt hardens, there was a general trend of increase in stability and decrease in flow due to storage. However, the mix stored for as long as 10 days still met the requirements of the specifications. Most of the increase in stability took place in the first 48 hours of storage. This is explained by a similar increase in asphalt viscosity measured at 140 F (Fig. 5).

Van der Poel developed data indicating that, in case of mixtures containing dense-graded aggregates and asphalt cements, which were well compacted (approximately 3 to 5 percent air voids), the stiffness of a mixture is dependent on the stiffness of the asphalt that it contains and the volume concentration of the aggregate (14). At very short times of loading or low temperatures or both, the behavior of asphaltic concrete is almost elastic in the classical sense, and the stiffness, S , is analogous to an elastic modulus, E . At longer times of loading and higher temperatures, the stiffness is

Figure 3. Penetration and ductility (field study).

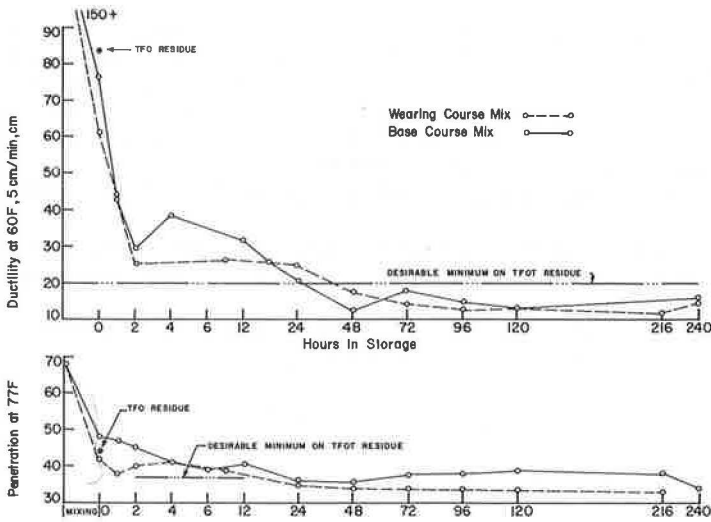


Figure 4. Viscosity and shear susceptibility (field study).

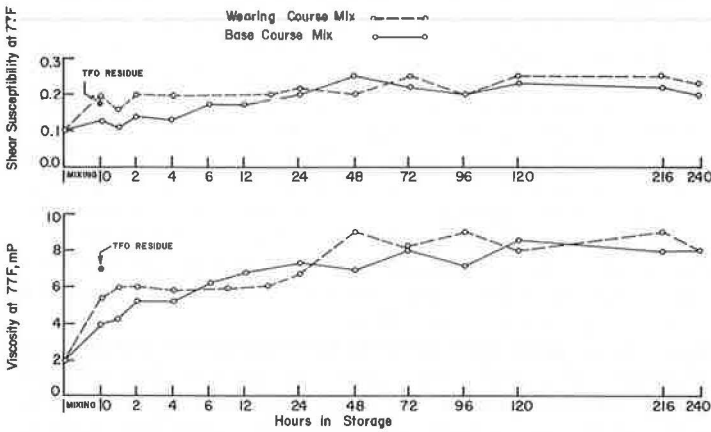


Figure 5. Absolute viscosity at 140 F (field study).

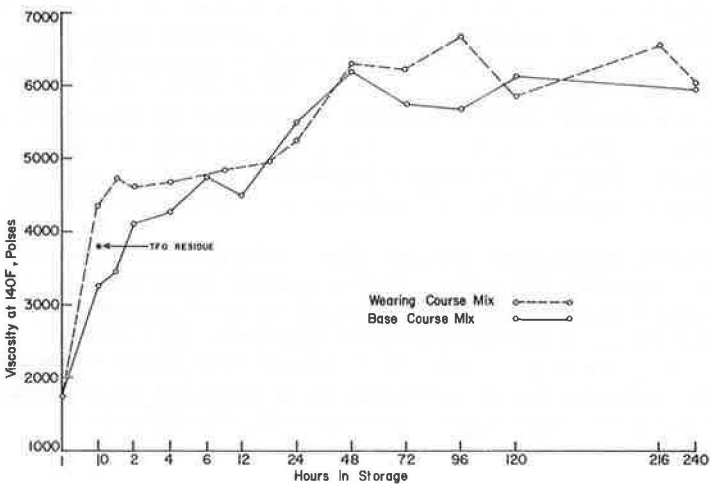


Figure 6. Kinematic viscosity at 275 F (field study).

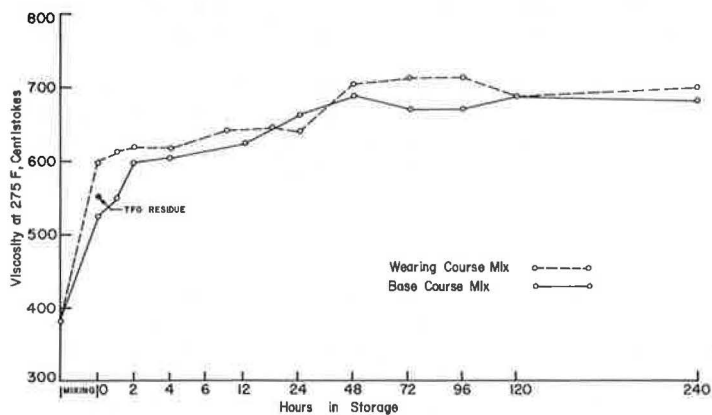
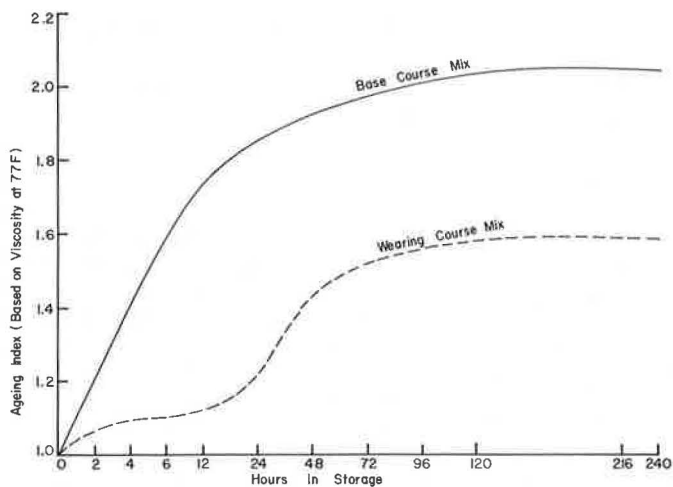


Table 2. Temperature susceptibility of base course mix.

Hours in Storage	Temperature Susceptibility of Recovered Asphalt Cement		
	50 to 77 F	77 to 140 F	140 to 275 F
0 (pug mill)	3.62	3.60	3.48
12	3.16	3.57	3.47
24	3.14	3.40	3.50
72	3.13	3.40	3.51
120	3.12	3.38	3.51
240	3.13	3.20	3.50

Figure 7. Storage aging index (field study).



simply a relation between the applied stress and the resulting strain. Stiffness of the stored wearing course mix, calculated from the stress-strain data obtained in Marshall tests, is shown in Figure 1. Stiffness of the mix increased by 50 percent in the first 48 hours.

Temperature of Stored Mix—Figure 2 shows the temperature of the mix discharged from the storage silo at the time of sampling. There were some initial drops in temperature of base course mix, but the temperature stabilized after 24 hours. On the whole, temperature of the wearing course mix was 15 to 20 F higher than that of the base course mix.

Effect of Storage on Properties of Asphalt Cement

Laboratory and semi-field tests confirmed field tests reported by others that inert gas extends storage time, and, because the intent was to extend the storage to 10 days, only inert gas was tested in the field. No problems with respect to the functioning of the heating and inert gas systems were encountered, so the results can be considered as realistic in a practical sense. However, the results would be valid only for the asphalt cement actually used in the two mixtures. Though the same asphalt cement was used in the wearing course and base course mixes, more hardening occurred in the pug mill in case of wearing course mix. The effect of storage on the various properties of asphalt cement is discussed in the following.

Penetration—Penetration of original asphalt cement was 68. After mixing in the pug mill, the penetration of asphalt was noted to be 42 and 48 in the wearing course and base course mixes respectively. Drop in penetration of asphalt cement (Fig. 3) occurred from 42 to 34 in the wearing course mix and from 48 to 36 in the base course mix during the first 48 hours of storage period, and then there was no appreciable change. Most of the drop in penetration took place in the first 24 hours. According to AASHTO M 20-70 on penetration graded asphalt cements, penetration of residue after TFOT for the asphalt cement used can be permitted as low as 37 (that is, 54 percent of original). If this is assumed as a criterion for acceptance, these mixes would be acceptable if stored for 24 hours or less (Fig. 3). However, this may not be applicable in general. More hardening in the pug mill itself can take place in some cases, and thus storage may not be possible at all. The following data taken from two projects (15) using an asphalt cement from the same source would indicate this:

Mix	Penetration Values			Percentage Retained Penetration		
	Original	After Mixing	After Compaction	Original	After Mixing	After Compaction
LR 219	59	36	31	100	61	53
LR 101	59	44	40	100	75	68

It would not have been possible to store the LR 219 mix to meet the same criterion, whereas LR 101 mix could possibly be stored for some period. Asphalt from the same source was used in these projects, but different aggregate sources and aggregate gradations were used. Thus, it would seem that the allowable storage time depends on the asphalt source and the composition of the bituminous mix. It is evident that hardening in 24 hours of storage can be equivalent to about 20 months of hardening in the pavement based on penetration (Fig. 8). The two asphalts compared are from different sources but had almost the same penetration after pug mill mixing. These asphalts had almost identical viscosity at 77 and 140 F.

Ductility—There was significant drop in ductility (60 F) in the first 2 hours of storage (Fig. 3). The ductility dropped to 25 and 30 cm in the wearing course and base course mixtures respectively. The desirable minimum ductility on the TFOT residue is 20 cm at 60 F; therefore, these mixtures would not be acceptable after 24 hours. The change in ductility value beyond 48 hours was negligible.

Viscosity at 140 F and 275 F—Viscosity at 140 F of asphalt cement increased from 4,350 to 6,300 poises in wearing course mix and from 3,250 to 6,200 poises in the base

Figure 8. Penetration and viscosity of asphalt (silo versus pavement).

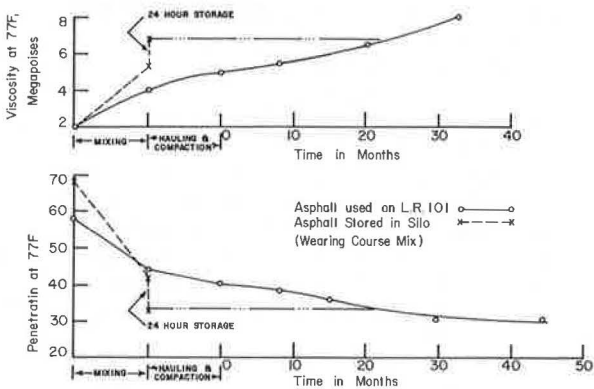
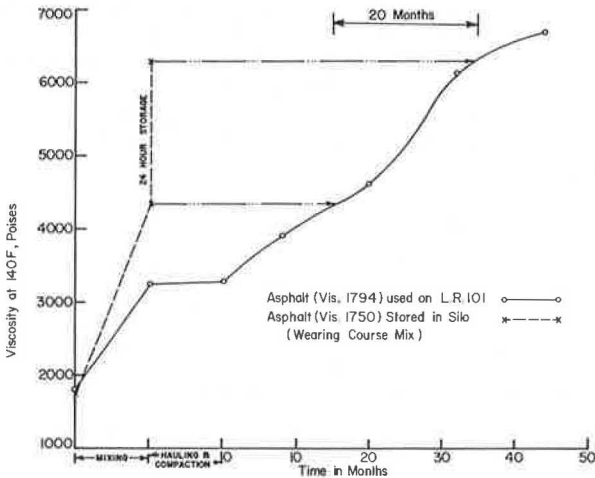


Figure 9. Viscosity at 140 F of asphalt (silo versus pavement).



course mix during 48 hours of storage, and then it leveled off (Fig. 5). Maximum permissible viscosity after the TFOT is 8,000 poises, which was not reached in 10 days of storage. However, when compared to hardening in the pavement based on viscosity, the hardening due to 24 hours of storage is equivalent to that that occurred in pavement in about 20 months (Fig. 9).

Viscosity data at 275 F also indicate the same trend (Fig. 6).

Absolute Viscosity at 77 F—Increase in absolute viscosity at 77 F was noted during the first 48 hours of storage, most of which occurred in the first 24 hours. Thereafter, no significant increase took place (Fig. 4). Increased viscosity at 77 F reduces the capability of the pavements to compact under traffic at ambient temperatures (12). Hardening in 24 hours of storage can be equivalent to about 20 months of hardening in the pavement based on viscosity at 77 F (Fig. 8). The two asphalts compared had original viscosity of 2.0 megapoises.

Because the same asphalt in the wearing and base course mixes did not harden to the same extent in the pug mill, storage aging index is a better indicator of relative hardening in the storage silo. Asphalt in the base course mix hardened at a faster rate than the asphalt in the wearing course mix (Fig. 7) as would normally be expected. How-

ever, ultimate hardening of the asphalt was greater in the wearing course mix than the base course mix.

Shear Susceptibility—There was no significant increase in shear susceptibility (77 F) of the asphalt in the wearing course mix, whereas the shear susceptibility increased during the first 24 hours of storage in the base course mix (Fig. 4). However, in both cases, the shear susceptibility does not seem to be excessive.

Temperature Susceptibility—Temperature susceptibility data for asphalt in the base course mix are given in Table 2, based on the viscosity data at 50, 77, 104, 122, 140, and 175 F. Because of shear dependent viscosities at temperatures lower than 140 F, slopes of the temperature viscosity lines deviate from those obtained between 140 F and higher temperatures. Therefore, the temperature susceptibility of the asphalts has been determined in three temperature ranges: 50 to 77 F, 77 to 140 F, and 140 to 275 F. It will be observed that the temperature susceptibility values of the asphalt have shown a decreasing trend with storage aging in the first two temperature ranges, whereas the increase in the range of 140 to 275 F is not significant.

General Data—Most of the hardening during the 10-day storage period in inert atmosphere occurred in the first 24 to 48 hours. It seems that some air is trapped by the mixture when it is dropped from the pug mill onto the conveyor used in charging the silo. The oxygen in this air is not displaced by the inert silo atmosphere and undoubtedly oxidizes the asphalt of the stored mix at the high-temperature storage conditions. This was also observed by Parr and Brock (8). The significant increase in asphalt viscosity (77 and 140 F) and drop in penetration because of 24 hours of storage in inert atmosphere has been observed to be equivalent to 20 months of hardening in the pavement using asphalt of the same consistency based on viscosity. Though the drop in penetration and increase in viscosity is less than that permitted by AASHO specifications for the TFOT (AASHO M 20-70 and M 226-70), the amount of hardening that should be classed as detrimental is a moot question.

CONCLUSIONS

The following conclusions were drawn with regard to laboratory and semi-field tests:

1. Mix stored without inert gas hardened at a faster rate than that stored with inert atmosphere in the bin, and
2. The aging index is a better indicator of relative hardening when asphalts from different sources are used or mixtures of different composition are stored.

Full-scale field tests were conducted using inert gas only, and the following conclusions are drawn:

1. No migration of asphalt cement in the bituminous concrete was observed during 10-day storage.
2. All silo discharge samples met the specification requirements for gradation of wearing and base course mixes, so there was no segregation problem.
3. Wearing course mix samples obtained from the storage silo for as long as 10 days still met the specification requirements for Marshall stability and flow. However, the stiffness of the mix increased by 50 percent in the first 48 hours because of increased Marshall stability and reduced flow.
4. Based on the aging index, base course mix hardened at a faster rate than the wearing course mix.
5. Most of the hardening during the 10-day storage period occurred in the first 48 hours. It seems the air entrapped in the mix is not displaced completely by the inert silo atmosphere and thus oxidation continues for a limited period.

The following general conclusions were made:

1. If the maximum allowable storage time is determined from the criterion of minimum percentage of retained penetration (AASHO M 20-70) on TFOT residue, it can vary depending on the asphalt source, composition of bituminous mix, temperature, and time of mixing. Although no storage might be possible in some cases, based on these criteria, the allowable storage period using inert gas was found to be 24 hours in this study.

2. Asphalt hardening (aging) during 24 hours of storage of bituminous concrete in inert atmosphere can be equivalent to 20 months of hardening in the pavement. It is yet to be established to what extent the durability of the pavement is sacrificed because of this premature hardening in the hot storage bin. Further investigations should be attempted to include comparison of asphalt properties from pavements laid from silo-stored materials with those of asphalt from pavements laid directly from the pug mill.

ACKNOWLEDGMENTS

This report is the result of a research project sponsored by the Pennsylvania Department of Transportation. The opinions, findings, and conclusions expressed are those of the authors and not necessarily those of the Pennsylvania Department of Transportation. CMI Systems, Chattanooga, Tennessee, and the Pennsylvania Asphalt Pavement Association cooperated in this study.

Thanks are due to W. S. Myers for assistance in the field study, P. G. Kaiser for physical testing of the bituminous mixtures, and H. R. Basso, Jr., for the testing of recovered asphalt.

Appreciation is also expressed to Edward Macko for illustrations and June Viozzi for compilation of research data.

REFERENCES

1. Rheinfrank, L. Common Sense on Hot-Mix Surge Storage. Standard Havens System, Glasgow, Missouri, Dec. 1969.
2. Middleton, S. C., et al. The Effect of Hot Storage on an Asphaltic Concrete Mix. Proc. Assn. of Asphalt Paving Technologists, Vol. 36, Feb. 1967.
3. Parr, W. K. Discussion of Middleton, S. C., et al., The Effect of Hot Storage on an Asphaltic Concrete Mix. Proc. Assn. of Asphalt Paving Technologists, Vol. 36, Feb. 1967.
4. Vallerga, B. A., and White, R. M. Discussion of Middleton, S. C., et al., The Effect of Hot Storage on an Asphaltic Concrete Mix. Proc. Assn. of Asphalt Paving Technologists, Vol. 36, Feb. 1967.
5. Brock, J. D., and Cox, R. B. Safe Hot-Storage Time Extended With Silicone and Inert Gas. Roads and Streets, July 1968.
6. Triplett, G. S. Storage of Asphalt Concrete Mixtures as Practiced in North Carolina. The Asphalt Institute, Raleigh District, March 1967.
7. Foster, C. R. More on Hot Storage of Asphalt Paving Mixtures. Annual Convention of National Asphalt Pavement Assn., Feb. 1968.
8. Parr, W. K., and Brock, J. D. Statistical Study of Effect of Hot Storage on the Composition and Properties of Asphaltic Concrete. Annual Meeting of the Assn. of Asphalt Paving Technologists, Cleveland, Feb. 14-16, 1972.
9. Gzemski, F. C. Viscoelastic Properties of Paving Asphalts. ASTM STP 328, 1962.
10. Skog, J. Setting and Durability Studies on Paving Grade Asphalts. Proc. Assn. of Asphalt Paving Technologists, Vol. 36, Feb. 1967.
11. Chipperfield, C. H., Duthie, J. L., and Girdler, R. B. Asphalt Characteristics in Relation to Road Performance. Proc. Assn. of Asphalt Paving Technologists, Vol. 39, Feb. 1970.
12. Kandhal, P. S., Sandvig, L. D., Koehler, W. C., and Wenger, M. E. Asphalt Viscosity Related Properties of In-Service Pavements in Pennsylvania. Annual Meeting of ASTM, Los Angeles, June 25-29, 1972.
13. Kandhal, P. S., and Wenger, M. E. Vertical Hot Bin Storage of Bituminous Concrete Mixes. Bureau of Materials, Testing and Research, Pennsylvania Department of Transportation, Research Report (project 70-29), May 1972.
14. Finn, F. N. Factors Involved in the Design of Asphaltic Pavement Surfaces. NCHRP Rept. 39, 1967, 112 pp.
15. Gotolski, W. H., et al. A Study of Physical Factors Affecting the Durability of Asphaltic Pavements. Pennsylvania Department of Transportation, Research Report IR-9, Sept. 1968.

DISCUSSION

R. L. Davis, Koppers Company, Inc.

The authors of this paper are to be congratulated on bringing information on such an interesting and timely subject to us. The use of hot storage bins has increased rapidly in the past few years, and the reduction in cost that comes from greater flexibility in scheduling hot-mix operations should not be ignored. It is my understanding that the reduction in cost is significant, and, in a competitive market, this reduction will soon be passed on to the buyer.

This paper points out the importance of silicone fluid in reducing the rate of hardening of asphalt binders, thus making possible longer storage periods without significant hardening of the mix. Previous papers (2, 3, 5, 7) have shown that asphalt mix could be stored for several days with only negligible hardening. The authors point out that silicone liquid was used in each case in contrast to the present paper where silicone was not used and where a storage period of only a day or less would be allowable. It is interesting to note that the data of this paper like those of other papers (2, 3, 5, 7) show no migration of asphalt cement in the mixture and no segregation problem.

The matter that causes me the greatest concern in this paper is that there is no indication of the random variation of the testing procedures. This is not so much a criticism of the paper or the authors as it is of the general current practice in the bituminous field. We know that the precision of our bituminous testing methods such as the Abson recovery method, Marshall stability, flow, penetration, ductility, viscosity, and shear susceptibility are poor. When they are added together as they are here, the errors become very large. Some indication of the confidence spread about each of the time series lines in Figures 1 through 9 would be a tremendous help in evaluating the meaning of these figures.

AUTHORS' CLOSURE

Samples were tested in duplicate, and reported results are the average of these values. It is realized that precision of bituminous testing methods is poor. It must be pointed out that each of the specific tests cited was performed by only one trained operator in each case. This procedure should tend to cancel the influence of variances among operators.

We admit that it would be highly desirable to have data that would permit establishment of the confidence spread about each of the time series lines. However, the scope of this investigation and the manpower and testing hours precluded development of these data.

Any future work on this study will be expanded to permit determination of the confidence limits. We are also considering the Orsat analysis of the inert gases to determine the effect of oxygen and carbon monoxide on the asphalt properties.

IRRECOVERABLE AND RECOVERABLE NONLINEAR VISCOELASTIC PROPERTIES OF ASPHALT CONCRETE

James S. Lai, University of Utah; and
Douglas Anderson, Utah State Department of Highways

The results are reported of a series of uniaxial compression creep tests of an asphalt mixture under constant loadings, multiple-step loadings, and repeated loadings of as many as 100 cycles. It has been shown that the nonlinear viscoelastic behavior of the asphalt concrete can be represented by a nonlinear generalized Kelvin model that consists of a nonlinear dash-pot connected in series with a nonlinear Kelvin chain. Thus, the nonlinear creep strains are separated into irrecoverable and recoverable strains. It has been shown that the constitutive equation can be determined by the use of both the creep and the recovery parts of the constant loading creep test results. The accuracy in predicting the creep behavior of the asphalt concrete under the multiple-step loadings and the repeated loadings has been shown to be very satisfactory. The importance of the irrecoverable strains to the practical implementation of asphalt pavements subjected to traffic loading is discussed. A possible way of relating the irrecoverable strains to the fatigue life of the material is also discussed.

•IN the past 10 years, considerable interest has been developed in an attempt to characterize the time and temperature dependence of the mechanical properties of asphalt paving mixtures within the framework of viscoelastic theory, especially the linear viscoelastic theory. Most of the test results reported so far on the viscoelastic characterization of asphalt mixtures have been obtained from the constant stress creep tests, or constant strain relaxation tests (1-4), and the sinusoidal loading tests (5-8). In most cases, the linear viscoelastic behavior of the asphalt concrete was assumed, and, henceforth, the linear viscoelastic material properties in terms of creep compliance, relaxation modulus, and complex compliance and complex modulus were obtained. For example, the phenomenon of creep can be represented by the following equation under a uniaxial stress state:

$$\epsilon(t) = \int_0^t J(t - \xi) \frac{\partial \sigma(\xi)}{\partial \xi} d\xi \quad (1)$$

where ϵ and σ are uniaxial strain and stress respectively. $J(t)$ is the uniaxial creep compliance and is usually determined from constant stress creep tests. For a given constant stress, Eq. 1 becomes

$$\epsilon(t) = J(t)\sigma_0 \quad \text{or} \quad J(t) = \frac{\epsilon(t)}{\sigma_0} \quad (2)$$

In this equation, $\epsilon(t)$ is the measured creep strain under the constant stress σ_0 , and the creep compliance $J(t)$ can be obtained according to Eq. 2. In principle, if a material

is truly linearly viscoelastic, Eq. 1 with $J(t)$ determined from Eq. 2 can be used to predict the creep behavior of the material under any kind of uniaxial loading history. However, this is not always true when the material is subjected to a more complex loading history.

In this report, the time-dependent properties of asphalt concrete are investigated under multiple-step loading histories, including several cyclic loading histories, in an effort to verify the applicability of linear viscoelastic theory in predicting the creep behavior under multiple-step loadings and also to construct a workable constitutive equation to describe more closely the time-dependent behavior of asphalt concrete under time-dependent loading histories.

In this report, the emphasis is also placed on distinction between the recoverable and irrecoverable creep under loading. This is important from a practical viewpoint because the irrecoverable creep strain contributes a large portion of the creep strain of asphalt concrete under external loading, and the irrecoverable strain is accumulative under repeated loading, whereas the recoverable creep is not necessarily.

MATERIALS AND SPECIMENS

A single asphalt mixture was utilized for the investigations. The asphalt cement used in preparing test specimens was from the American Oil Co. with 85 to 100 penetration grade. The asphalt content was 9 percent by weight. The gradation of aggregates is shown as follows:

<u>Sieve Size</u>	<u>Percentage Passing</u>
$\frac{3}{8}$ in.	100
No. 4	95.0
No. 8	60.0
No. 16	33.0
No. 50	15.0
No. 200	6.0

The test specimens used in this study were made of compressed asphalt concrete cylinders 2-in. in diameter and 3-in. in length. The asphalt mixture was pressed in a 2-in. diameter mold at 3,000 psi for 5 min at a temperature of 220 F. The specimens were cured in an oven at 140 F for 72 hours prior to the testing. Also, the randomness of the strain response of each specimen was minimized by subjecting each specimen to a 50-psi prestress for 12 min.

EXPERIMENTAL APPARATUS PROCEDURES

The basic test equipment shown in Figure 1 consists of a rigid frame A, a loading head B, a 1-to-10 ratio loading lever C, and the deformation measuring devices. A linear variable differential transducer (LVDT) was used to measure the deformation of the specimen. The output from LVDT, which is directly related to the total deformation, could be automatically recorded on a strip-chart recorder.

During the test, the specimen was placed directly under the loading head, and the LVDT was properly set. A selected dead weight was then put on the loading lever to produce a constant load on the specimen. The temperature during the test was kept at 75 ± 2 F.

RESULTS AND ANALYSIS

Nine tests at three stress levels (10, 30, and 50 psi) were performed on prestressed samples. Duration of the loading period varied from 10 to 1,000 sec (i.e., 10, 100, and 1,000 sec). The results of the constant stress creep tests at three stress levels at three loading periods are shown in Figures 2, 3, and 4. Each solid line is the average of several repeated test results. In these figures, the recovery strains following each creep test are also shown.

Using Eq. 2, we can obtain the creep compliance $J(t)$ as follows. Once the creep

Figure 1. Basic equipment for unconfined compressive creep test.

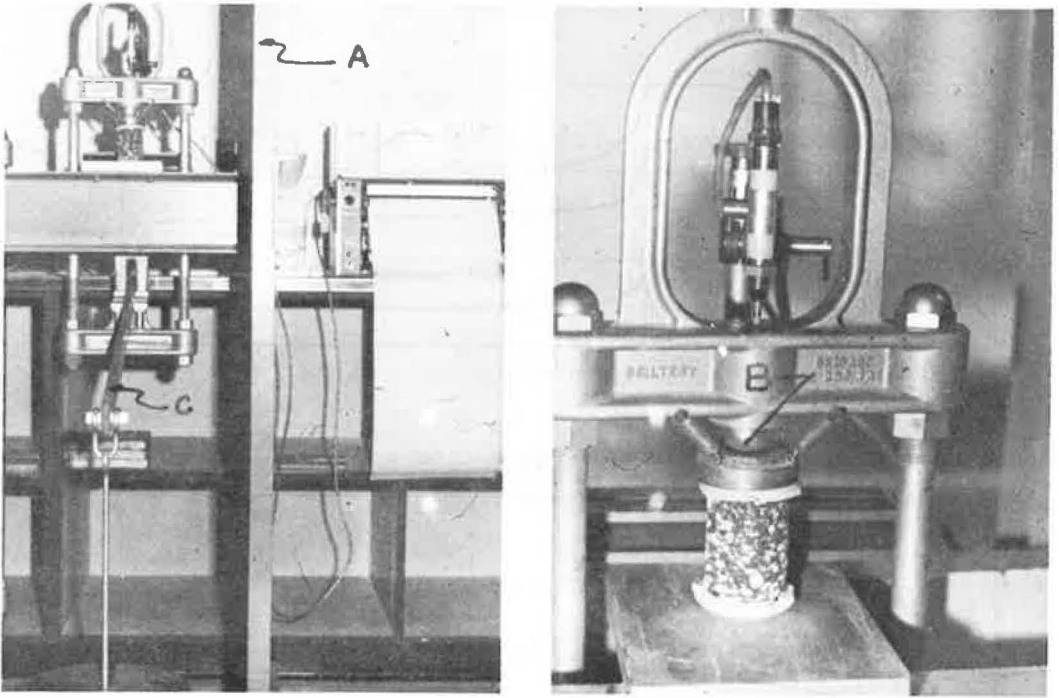


Figure 2. Creep and recovery of constant stress creep tests ($t_i = 10$ sec).

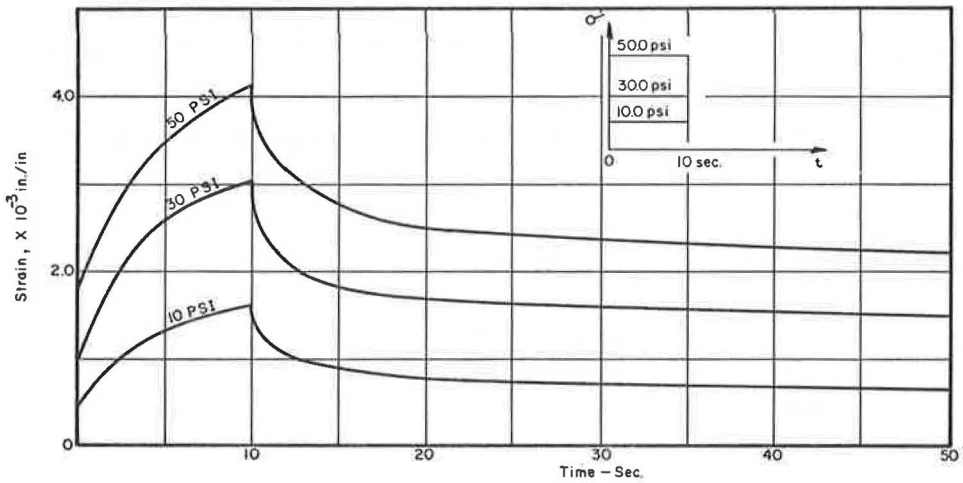


Figure 3. Creep and recovery of constant stress creep tests ($t_i = 100$ sec).

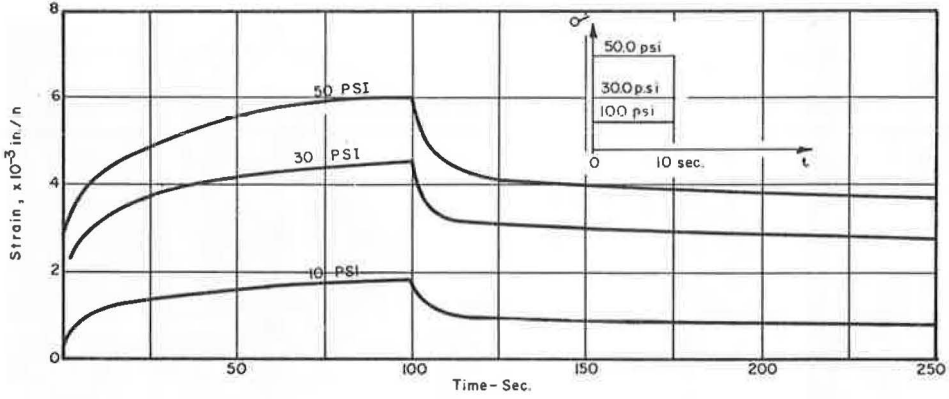


Figure 4. Creep and recovery of constant stress creep tests ($t_i = 1,000$ sec).

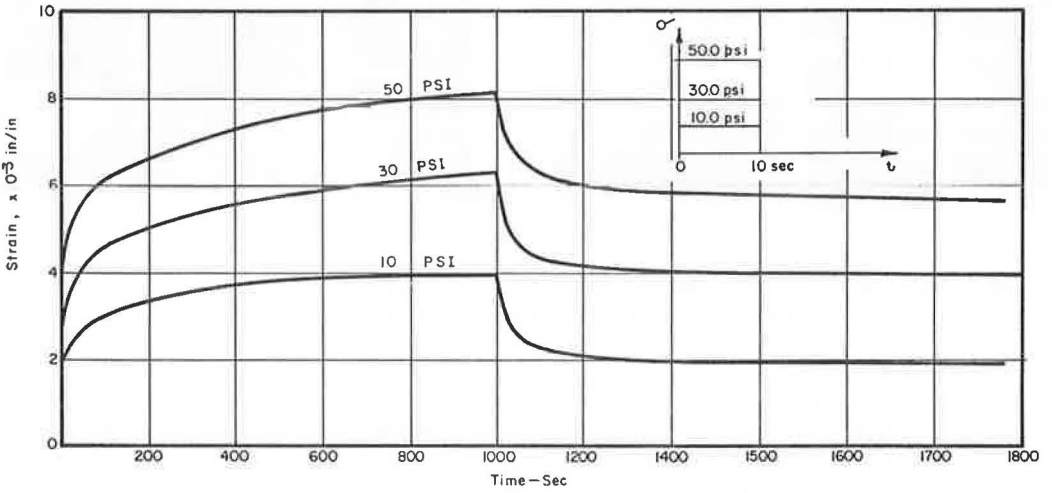
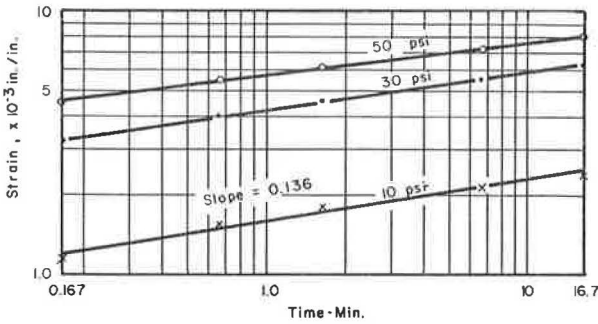


Figure 5. Constant stress creep curves plotted in log-log scale.



curves on the log-strain versus log-time base were replotted, they appeared to be straight lines as shown in Figure 5. Because the straight lines at three stress levels (Fig. 5) have nearly the same slope (0.136), the creep behavior could be expressed in the following form:

$$\epsilon_r(t) = A_r t^{n_T} \quad (3)$$

where ϵ_r is the total creep strain, and A_r is the strain at unit time ($t = 1$ min). The fact that A_r varies with stress can be seen by cross-plotting the strain values at $t = 1$ min of Figure 5 and the stress as shown in Figure 6 (open circles) and can be represented by the following relation:

$$\left. \begin{aligned} \epsilon_r(t) &= A_r(\sigma) t^{n_T} \\ A_r(\sigma) &= a_1 \sigma + a_2 \sigma^2 \\ a_1 &= 0.159 \times 10^{-3} \\ a_2 &= -0.857 \times 10^{-6} \end{aligned} \right\} \quad (4)$$

The creep compliance $J(t)$, which is defined as $\frac{\epsilon(t)}{\sigma_0}$, can be obtained from Eq. 4 as follows:

$$J(t) = (a_1 + a_2 \sigma) t^{n_T} \quad (5)$$

In view of Eq. 4 or 5, the asphalt concrete exhibits nonlinear behavior. Although a more popular form of power-law representation, such as σ^n , can be used as accurately as Eq. 4 to represent the stress dependence of A_r , this type of representation violates the basic invariance requirements as imposed from the continuum mechanics standpoint. Furthermore, Eq. 4 can be extended readily to represent the creep behavior under multiple stress states (11), whereas the power-law representation cannot.

Because the asphalt concrete was found to be nonlinear from the constant stress creep test, the second linearity requirement, the linear superposition principle, is not applicable any more. However, the modified superposition method (9-13) has been used to describe the nonlinear creep behavior and has been shown to be applicable in describing the creep behavior under arbitrary loading from the constant stress creep test results of many nonlinear viscoelastic materials. This modified superposition method is employed here to describe the recovery behavior. The modified superposition method yields the following form (9) for the recovery after constant stress creep:

$$\epsilon_r(t) = \epsilon[\sigma(t)] - \epsilon[\sigma(t - t_1)] \quad (6)$$

$t > t_1$

where $\epsilon[\sigma(t)]$ represents the creep strain under constant stress input, such as Eq. 4, and t_1 the unloading time. Inserting Eq. 4 into Eq. 6 yields

$$\epsilon_r(t) = (a_1 \sigma + a_2 \sigma^2) \left[t^{n_T} - (t - t_1)^{n_T} \right] \quad (7)$$

For n_T less than 1, as shown in Eq. 4 for the asphalt concrete, Eq. 7 predicts that the recovery strain approaches zero. The recovery curves shown in Figures 2, 3, and 4 indicate, however, a large irrecoverable strain (permanent set). Apparently Eq. 7 is not capable of describing the recovery behavior because either the modified superposition principle is not applicable for this material or Eq. 4, determined from the constant stress creep test results, does not represent the actual constitutive relation of the material. Therefore, an attempt was made using both the creep curves and the recovery curves of Figures 2, 3, and 4 to obtain a better representation of the constitutive relation of the material.

Because of the large portion of the unrecoverable strain of each creep test and because the amount of unrecoverable strain is dependent on the length of the loading period,

Figure 6. Creep strain-stress at unit time.

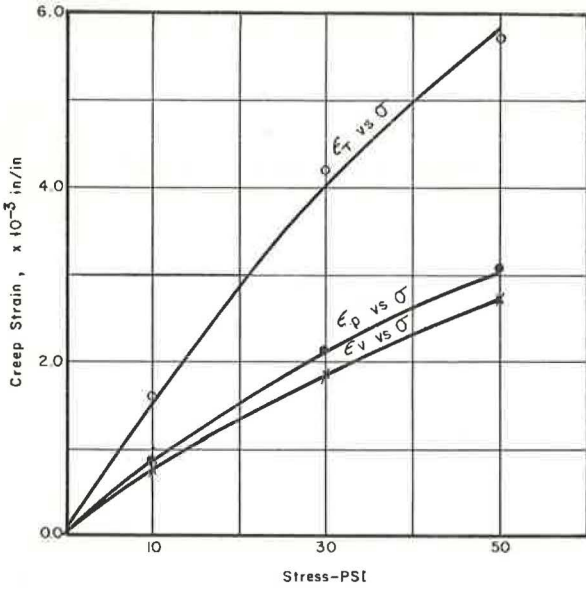


Figure 7. Nonlinear generalized Kelvin model.

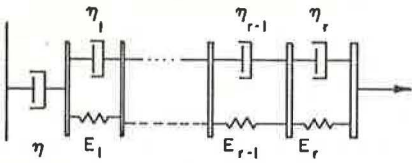
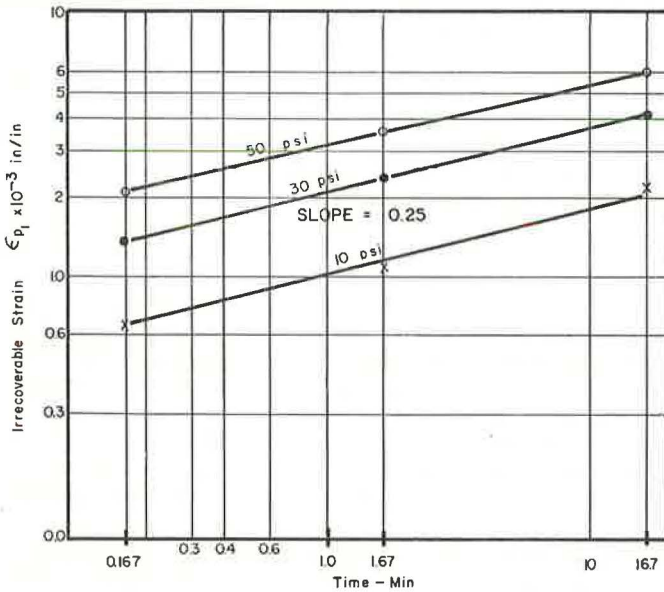


Figure 8. Irrecoverable strain versus time.



the creep behavior may be represented by a generalized nonlinear Kelvin model as shown in Figure 7. Here, the nonlinear dashpot may contribute to the irrecoverable strain, and the series of Kelvin models (Kelvin chain) may contribute to the power-law creep behavior (11). Therefore, the total creep strains (ϵ_T) of each test were separated into two parts, the irrecoverable strains (ϵ_p) due to the nonlinear dashpot and the completely recoverable strains (ϵ_v) due to the nonlinear Kelvin chain. The irrecoverable strains versus the length of the loading period (10, 100, and 1,000 sec) at each stress level on a log-log scale were plotted to form three straight lines as shown in Figure 8. Because these three straight lines have nearly the same slope of 0.25, the following expression can be obtained for irrecoverable strains:

$$\epsilon_p(t) = A_p t^{n_p} \quad (8)$$

Again, by cross-plotting the ϵ_p at $t = 1.0$ min and the stress as shown in Figure 6 (closed circles) and using the stress polynomial to fit those points, we can obtain the following equation:

$$\left. \begin{aligned} \epsilon_p(t) &= (b_1 \sigma + b_2 \sigma^2) t^{n_p} \\ b_1 &= 0.0844 \times 10^{-3} \\ b_2 &= -0.454 \times 10^{-6} \\ n_p &= 0.25 \end{aligned} \right\} \quad (9)$$

The rate of the irrecoverable strain $\dot{\epsilon}_p$ can be obtained from Eq. 9 as follows:

$$\dot{\epsilon}_p(t) = n_p (b_1 \sigma + b_2 \sigma^2) t^{n_p-1} \quad (10)$$

Instead of using Eq. 10, it was found that the "strain hardening theory" that relates the rate of the irrecoverable strain to the current stress and irrecoverable strain yielded a better description of the irrecoverable strain. The rate of the irrecoverable strain can be obtained by eliminating the time variable from Eqs. 7 and 10, which yields

$$\dot{\epsilon}_p(t) = n_p (b_1 \sigma + b_2 \sigma^2)^{1/n_p} \epsilon_p^{(n_p-1)/n_p} \quad (11)$$

or

$$\dot{\epsilon}_p(t) = \eta(\sigma, \epsilon_p) \sigma \quad (12)$$

$$\eta(\sigma, \epsilon_p) = n_p \left[\frac{1}{\sigma} (b_1 \sigma + b_2 \sigma^2)^{1/n_p} \right] \epsilon_p^{(n_p-1)/n_p} \quad (12a)$$

Equations 12 and 12a show that the dashpot is nonlinear and that the "coefficient of viscosity" η is dependent on the stress and the irrecoverable strain.

The recoverable strains ϵ_v due to the Kelvin chain were then obtained by subtracting the irrecoverable strains ϵ_p from the total strains ϵ_T . Thus, the total creep strains were separated into the recoverable part and the irrecoverable part.

Again, by using the same technique of plotting the ϵ_v versus time in the log-log scale, as shown in Figure 9, and cross-plotting in Figure 6, we can express the recoverable strains in the following form:

$$\left. \begin{aligned} \epsilon_v(t) &= (C_1 \sigma + C_2 \sigma^2) t^{n_v} \\ C_1 &= 0.0748 \times 10^{-3} \\ C_2 &= -0.412 \times 10^{-6} \\ n_v &= 0.093 \end{aligned} \right\} \quad (13)$$

The constitutive relation for the asphalt concrete using the generalized Kelvin model is summarized as follows for the constant stress creep:

$$\epsilon_{\tau}(t) = \epsilon_p(t) + \epsilon_v(t) \quad (14)$$

where ϵ_p is given by Eq. 12, and ϵ_v is given by Eq. 13. For the time-dependent stress input, the following equation is utilized:

$$\epsilon_{\tau}(t) = \int_0^t \dot{\epsilon}_p(\xi) d\xi + \int_0^t (t - \xi)^{n_v} [C_1 + 2C_2\sigma(\xi)] \dot{\sigma}(\xi) d\xi \quad (15)$$

In Eq. 15, the modified superposition method was again used (in the second integral) to describe the recoverable part of the creep strains under time-dependent stress input (10, 11, 12).

RESULTS AND PREDICTION OF CREEP UNDER MULTIPLE-STEP LOADING

In order to test and improve the application of Eq. 15 to the creep behavior of the asphalt concrete, we performed four multiple-step loading creep tests. The results are shown in Figures 10 through 13.

Equations 12, 13, and 15 were utilized to predict the creep behavior under multiple-step loading as follows. The stress inputs of the multiple steps can be expressed in a single algebraic equation using the Heaviside's unit function

$$\sigma(t) = \sum_{i=0}^n (\sigma_i - \sigma_{i-1}) H(t - t_i) \quad (15a)$$

where $H(t - t_i)$ is the Heaviside's unit function, which has the value of 1 when $t \geq t_i$, 0 when $t < 0$, $\sigma_{-1} = 0$, and $t_0 = 0$. Inserting Eq. 15a into Eq. 15, after performing the integration, yields the following for the total strain at each loading step where

$$\epsilon_{\tau}(t) = \epsilon_p(t) + \epsilon_v(t) \quad (16)$$

For $0 < t < t_1$,

$$\epsilon_p(t) = [(b_1\sigma_0 + b_2\sigma_0^2)^{1/n_p} t]^{n_p} \quad (17a)$$

$$\epsilon_v(t) = (C_1\sigma_0 + C_2\sigma_0^2) t^{n_v} \quad (17b)$$

For $t_1 < t < t_2$,

$$\epsilon_p(t) = [(b_1\sigma_0 + b_2\sigma_0^2)^{1/n_p} t_1 + (b_1\sigma_1 + b_2\sigma_1^2)^{1/n_p} (t - t_1)]^{n_p} \quad (18a)$$

$$\begin{aligned} \epsilon_v(t) = & (C_1\sigma_0 + C_2\sigma_0^2) [t^{n_v} - (t - t_1)^{n_v}] \\ & + (C_1\sigma_1 + C_2\sigma_1^2) (t - t_1)^{n_v} \end{aligned} \quad (18b)$$

For $t_{r-1} < t < t_r$, $r = 1, 2, 3, \dots$,

$$\begin{aligned} \epsilon_p(t) = & [(b_1\sigma_0 + b_2\sigma_0^2)^{1/n_p} t_1 + \dots + (b_1\sigma_{r-2} + b_2\sigma_{r-2}^2)^{1/n_p} (t_{r-1} - t_{r-2}) \\ & + (b_1\sigma_{r-1} + b_2\sigma_{r-1}^2)^{1/n_p} (t - t_{r-1})]^{n_p} \end{aligned} \quad (19a)$$

Figure 9. Recoverable strain versus time.

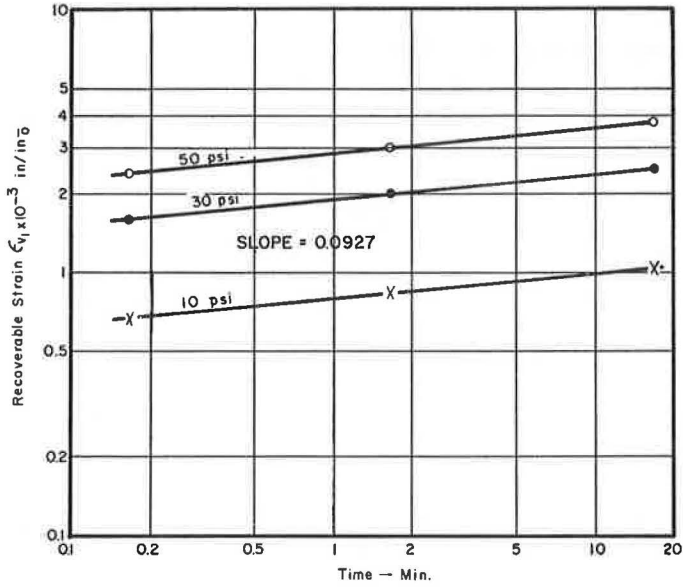


Figure 10. Results and predictions of creep behavior under step loading.

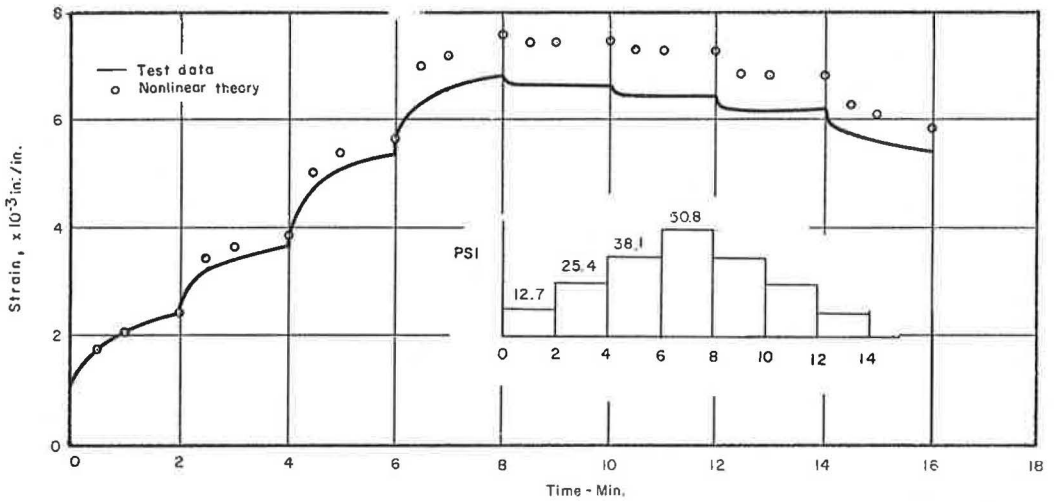


Figure 11. Results and predictions of creep behavior under step loading.

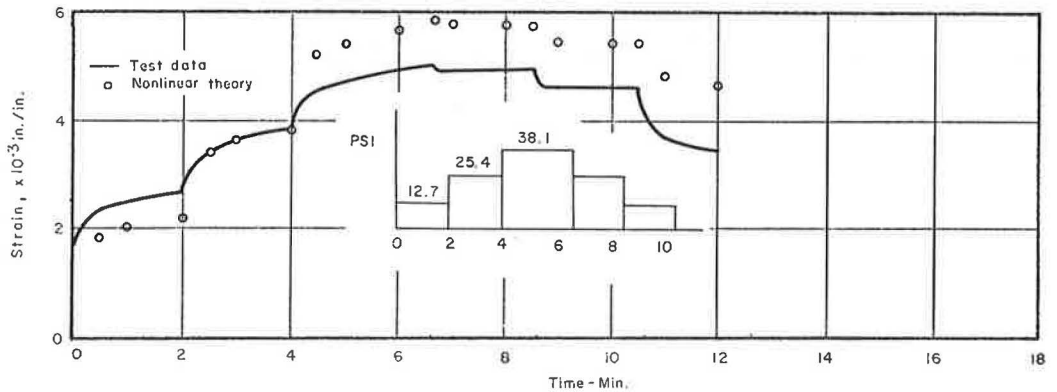


Figure 12. Results and predictions of creep behavior under step loading.

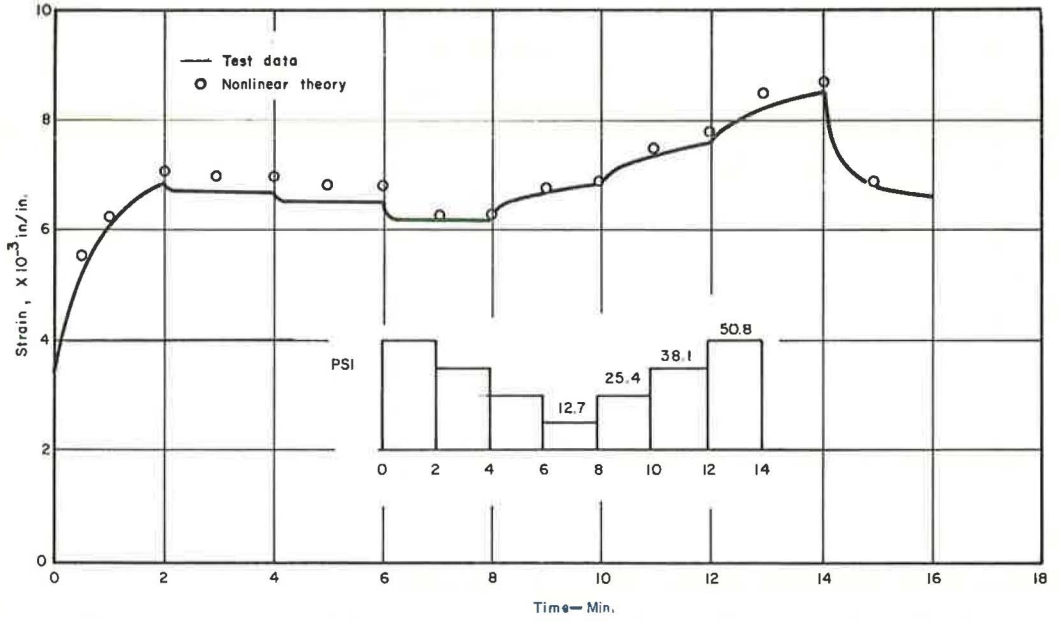
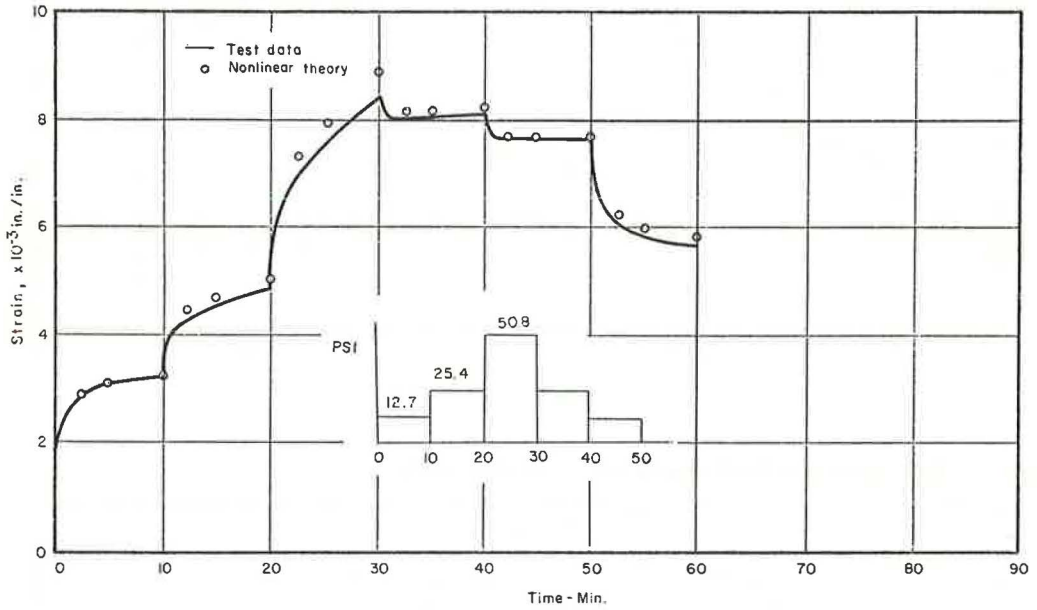


Figure 13. Results and predictions of creep behavior under step loading.



$$\begin{aligned} \epsilon_v(t) = & (C_1\sigma_0 + C_2\sigma_0^2) [t^{n_v} - (t - t_1)^{n_v}] + \dots \\ & + (C_1\sigma_{r-2} + C_2\sigma_{r-2}^2) [(t - t_{r-2})^{n_v} - (t - t_{r-1})^{n_v}] \\ & + (C_1\sigma_{r-1} + C_2\sigma_{r-1}^2) (t - t_{r-1})^{n_v} \end{aligned} \quad (19b)$$

By adding the predicted irrecoverable strains ϵ_p and the predicted recoverable strains ϵ_v , the predicted total creep strains ϵ_r under multiple-step loading can be obtained and are shown as the open circles in Figures 10 through 13 together with the experimental results that are depicted by the solid lines. The overall comparisons are quite satisfactory.

RESULTS AND PREDICTION OF CREEP UNDER REPEATED LOADING

The theory for a loading-unloading type of input was tested by loading specimens for 1 min and allowing them to recover in an unloaded state for 3 min before reloading. Cycles of this type were applied to specimens of 10, 20, 30, 40, and 50 psi, up to eight cycles. In addition, a 40-psi, 100-cycle repeated test was also conducted. The results are shown in Figures 14 through 19.

Again, using Eqs. 15, 19a, and 19b, the creep strains under the repeated loading were calculated as shown in Figures 14 through 18 for the eight-cycle tests. The theory predicts well for both the loading period and the unloading period of each cycle, though no deviation was observed in the recovery period.

These periodic loading tests are particularly important in the evaluation of asphalt concrete because pavements are constantly subjected to a similar loading pattern. Traffic passing over the pavement creates a loading period that is followed by an unloaded period. The loading time and stress are of primary importance to the total creep strain; thus, heavier, slower moving traffic causes greater "permanent" deformation. Although the total strain (or the shape of the total creep strain output with each loading cycle) is interesting and in many ways useful, the main concern when dealing with this type of material and stress pattern must lie not with the recoverable portion but with the irrecoverable strain introduced with each cycle. It can be seen from Figures 20 and 21 that the irrecoverable portion causes the accumulation of the total strain. Therefore, when the material is subjected to a large number of cyclic loadings, it may seem justified to deal mainly with expressions for the irrecoverable strain and to neglect the recoverable strain. In Figure 20, the theoretical and the experimental total strains and the irrecoverable strains at the end of each loading cycle were plotted against the number of cycles. The difference between total strain and the irrecoverable strain, which equals the recoverable, is small in comparison with the total strain or the irrecoverable strain. This figure also points out the range in which the theory is applicable. The increase in strain for each cycle remains fairly constant up to approximately 60 cycles. At this point, the rate begins to increase, and more deformation is observed with each cycle than in the previous cycle as shown in Figures 19 and 20. This is also where the theory and the observed strains begin to differ, leading to the conclusion that the equations predict the output within about 2.2 percent strain in this case, which is reached at about 60 cycles. A significant change in the shape of the specimen was also observed at about 60 cycles. The sample began to take on a barrel shape, increasing the cross-sectional area and most likely weakening a great deal of the internal bonds. In the region lower than 2.2 percent strain, where the increase in total deformation from one cycle to the next remains nearly constant, the cycles are very uniform in shape. Both the loading and recovery periods, after the first few cycles, demonstrate constant strain rates and magnitudes.

By letting N be the cycle number, Δt be the duration of the loading period of each cycle, and σ_0 be the constant stress at the load period, Eq. 19a becomes

$$\epsilon_p = (b_1\sigma_0 + b_2\sigma_0^2) [N(\Delta t)]^{n_p} \quad (20)$$

where ϵ_p represents the irrecoverable strains at the end of the N th loading cycle. The parameters contribute to the buildup of the irrecoverable strain, which is shown in

Figure 14. Results and predictions of creep behavior under cyclic loading (10-psi stress amplitude).

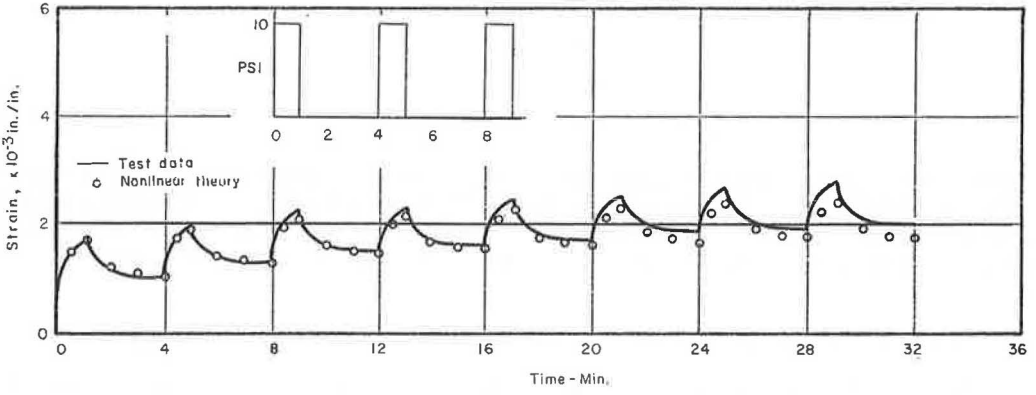


Figure 15. Results and predictions of creep behavior under cyclic loading (20-psi stress amplitude).

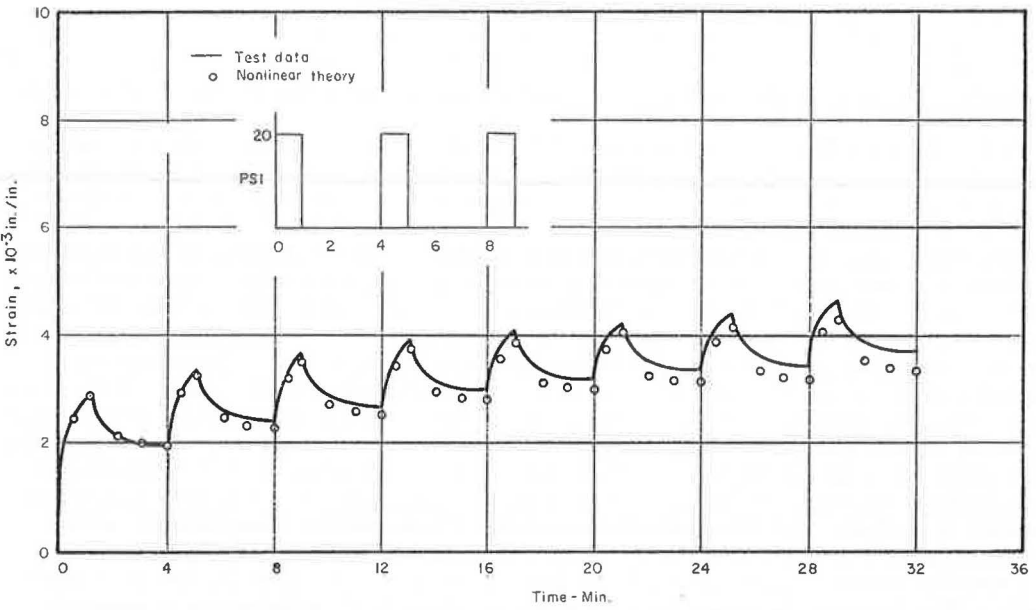


Figure 16. Results and predictions of creep behavior under cyclic loading (30-psi stress amplitude).

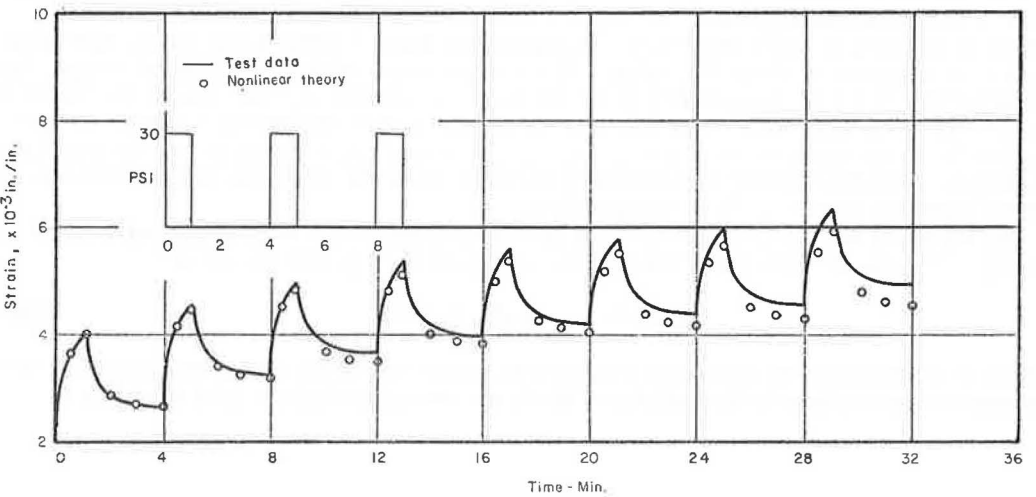


Figure 17. Results and predictions of creep behavior under cyclic loading (40-psi stress amplitude).

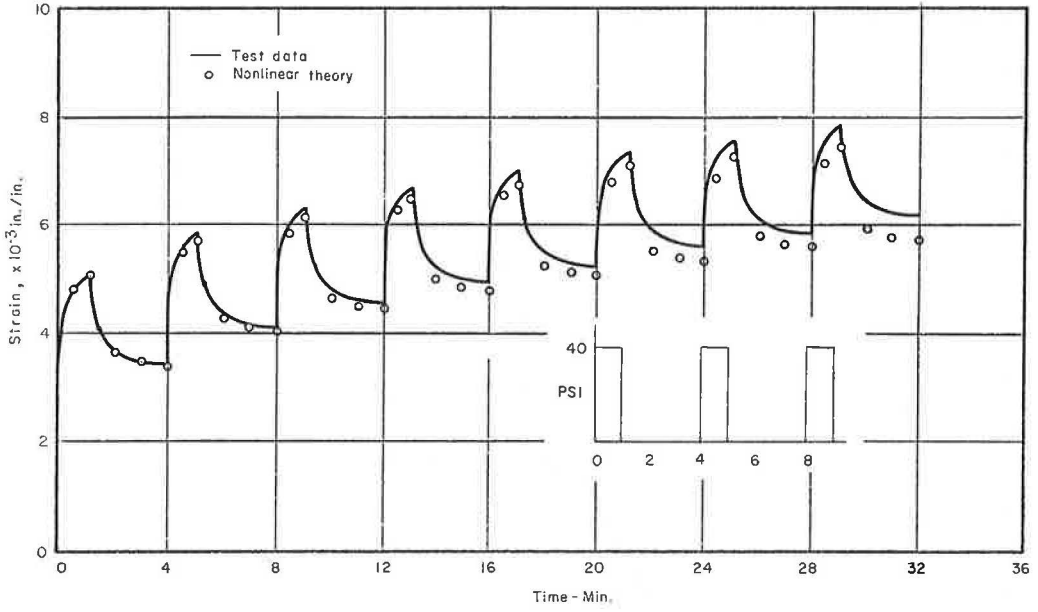


Figure 18. Results and predictions of creep behavior under cyclic loading (50-psi stress amplitude).

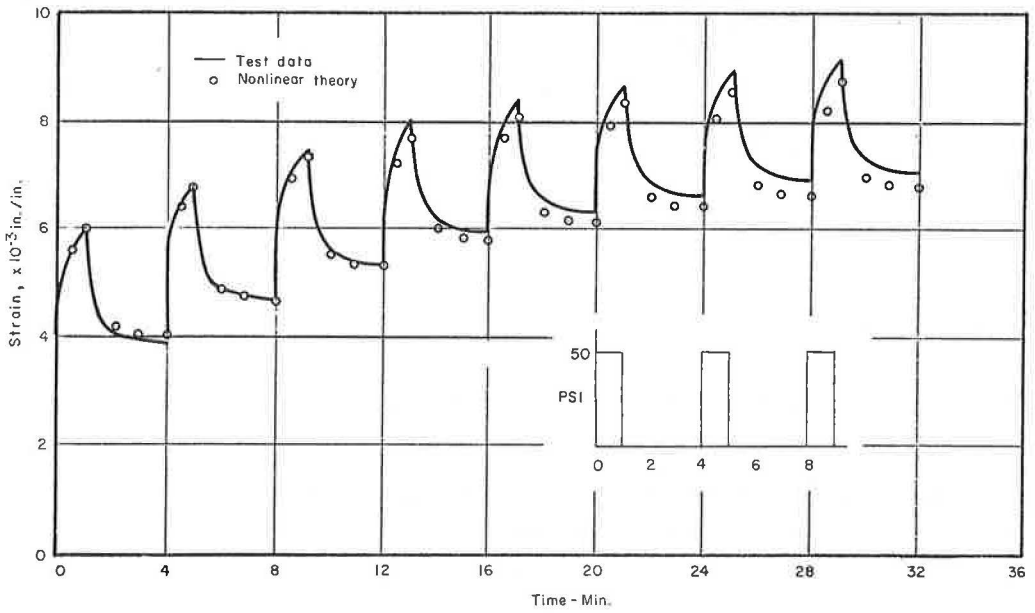


Figure 19. Results and predictions of creep behavior under cyclic loading (40-psi stress amplitude, 100 cycles).

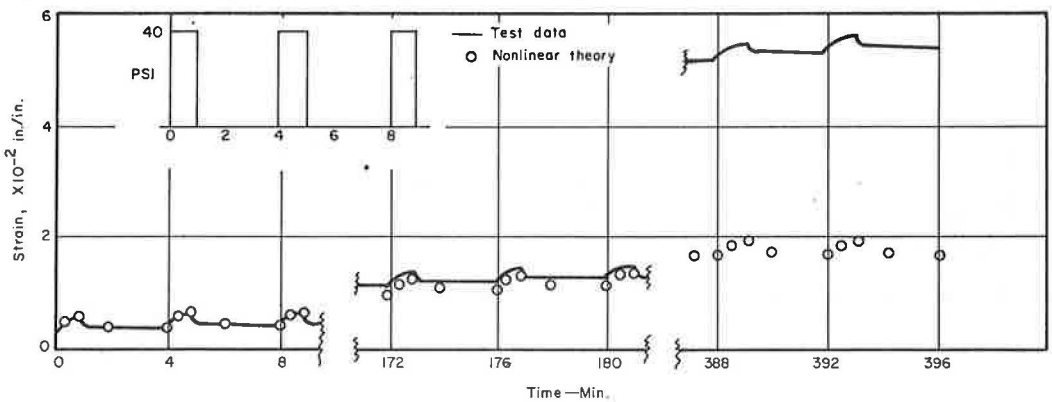


Figure 20. Irrecoverable and theoretical strains versus cycle number.

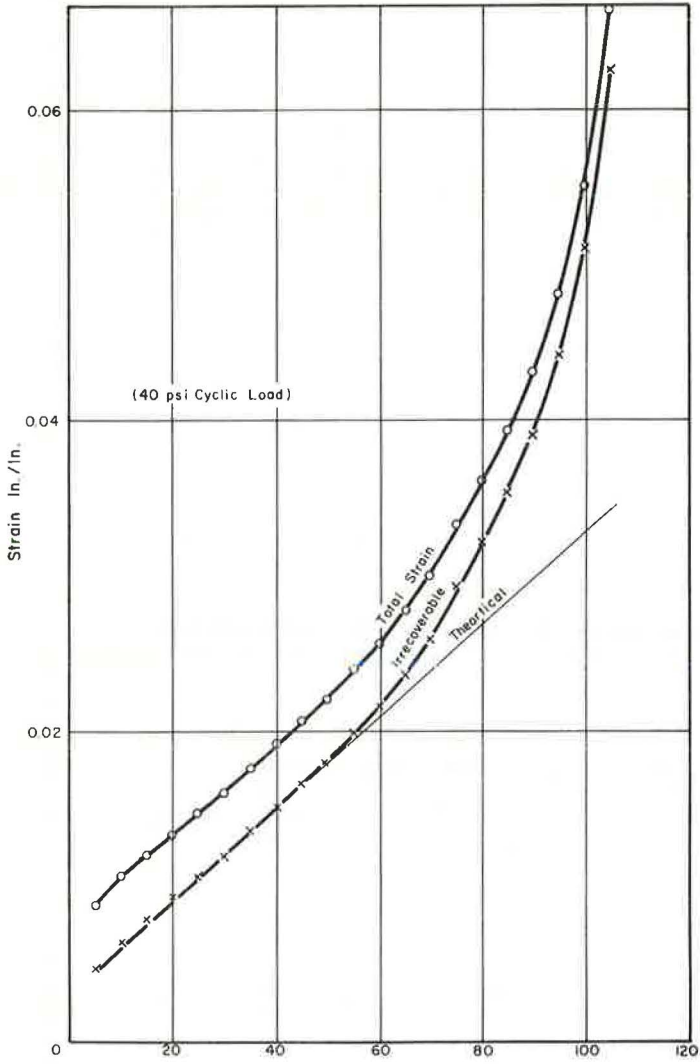
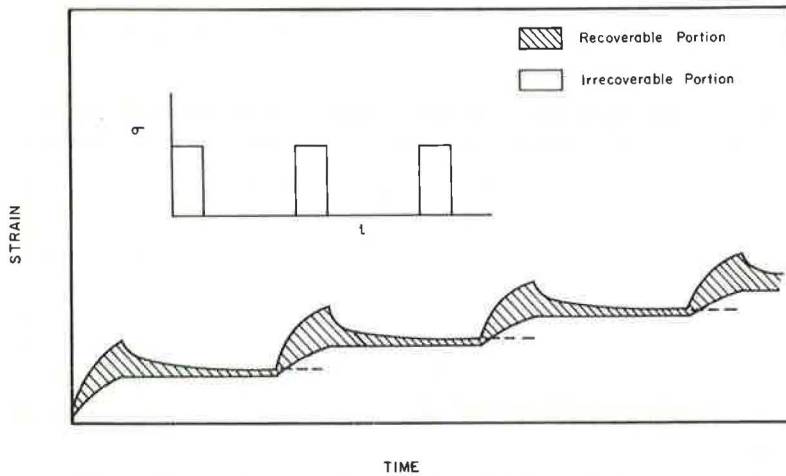


Figure 21. Irrecoverable and recoverable portions of total strain in a repeated loading test.



Eq. 20. Furthermore, if the maximum strain ϵ_{\max} (as approximated by the $\epsilon_{p\max}$) is chosen to be the failure criterion of a material, Eq. 20, after rewriting into the following form, implies that

$$N = \frac{1}{(\Delta t)} \left(\frac{\epsilon_{p\max}}{b_1 \sigma + b_2 \sigma^2} \right)^{1/n_p} \quad (21)$$

The longer the loading time during each cycle and the larger the stress amplitude are, the fewer the number of cycles the material can withstand. Although Eq. 21 is derived from the viscoelastic characterization of asphalt concrete, some similar conclusions, such as the effect of load duration, effect of ultimate strain (tensile strain), and magnitude of stress amplitude on the fatigues life of asphalt concrete, have been reached in other fatigue studies (14, 15).

CONCLUSION

It has been shown that the nonlinear viscoelastic behavior of an asphalt concrete can be represented by a nonlinear generalized Kelvin model that is made of a nonlinear dashpot connected in series with a nonlinear Kelvin chain. The nonlinear dashpot accounts for the time-dependent irrecoverable strain (viscous flow), and the nonlinear Kelvin chain accounts for the power-law time-dependent recoverable strain. It has been shown that the constitutive equation can be determined relatively simply by utilizing both the creep and recovery parts of the constant stress creep test results. The accuracy in predicting the creep behavior of the asphalt concrete under multiple-step loading and repeated loadings using the proposed constitutive equation is very satisfactory.

It has also been shown that an equation relating the number of cycles to failure to the applied stress amplitude and the duration of each cycle similar to the existing fatigue theories can be derived from the irrecoverable creep strains. It is hoped that this study will lead to a better understanding of the time-dependent behavior of asphalt concrete.

In this report, only a single asphalt concrete mixture was utilized for the investigations, which were conducted under only one temperature ($75 \pm F$). Though it is anticipated that varying the mixtures and the testing temperatures would definitely affect the creep behavior of asphalt concrete, some of the preliminary experimental results indicate that the difference of the creep behavior of different asphalt concrete mixtures at different temperatures (above the glass transition temperature) is more quantitative than qualitative.

REFERENCES

1. Secor, K. E., and Monismith, C. L. Analysis of Triaxial Test Data on Asphalt Concrete Using Viscoelastic Principles. HRB Proc., Vol. 40, 1961, pp. 259-314.
2. Monismith, C. L., and Secor, K. E. Viscoelastic Behavior of Asphalt Concrete Pavements. Proc. Internat. Conf. on the Structural Design of Asphalt Pavements, Univ. of Michigan, 1963.
3. Pagen, C. A. An Analysis of the Thermorheological Response of Bituminous Concrete. Ohio State Univ., PhD thesis, 1963.
4. Fitzgerald, J. E., and Lai, J. S. Initial Evaluation of the Effect of Synthetic Rubber Additives on the Thermorheological Properties of Asphalt Mixtures. Highway Research Record 313, 1970, pp. 18-31.
5. Pagazian, H. S. The Response of Linear Viscoelastic Materials in the Frequency Domain With Emphasis on Asphalt Concrete. Proc. Internat. Conf. on the Structural Design of Asphalt Pavement, Univ. of Michigan, 1962.
6. Pagen, C. A. Rheological Response of Bituminous Concrete. Highway Research Record 67, 1965, pp. 1-26.
7. Kallas, B. F., and Riley, S. C. Mechanical Properties of Asphalt Pavement Materials. Proc. Second Internat. Conf. on the Structural Design of Asphalt Pavements, Univ. of Michigan, 1967.

8. Swami, S. A., Goetz, W. H., and Harr, M. E. Time and Load Independent Properties of Bituminous Mixtures. Highway Research Record 313, 1970, pp. 63-78.
9. Findley, W. N., and Lai, J. S. A Modified Superposition Principle Applied to Creep of Nonlinear Viscoelastic Material. Trans. Soc. of Rheology, Vol. 11, No. 2, 1967, pp. 361-380.
10. Lai, J. S., and Findley, W. N. Stress Relaxation of Nonlinear Viscoelastic Material Under Uniaxial Strain. Trans. Soc. of Rheology, Vol. 12, No. 2, 1968, pp. 259-280.
11. Findley, W. N., Lai, J. S., and Onaian, K. Creep and Stress Relaxation of Nonlinear Viscoelastic Materials. To be published.
12. Pipkin, A. C., and Rogers, T. G. A Nonlinear Integral Representation for Viscoelastic Behavior. Jour. of Mechanics and Physics of Solids, Vol. 16, 1968, pp. 59-72.
13. Stafford, R. O. On Mathematical Forms for the Material Functions in Nonlinear Viscoelasticity. Jour. Mechanics and Physics of Solids, 1969, pp. 339-358.
14. Deacon, J. A. Materials Characterization—Experimental Behavior. HRB Spec. Rept. 126, 1971, pp. 150-179.
15. Finn, F. N. Factors Involved in the Design of Asphalt Pavement Surfaces. NCHRP Rept. 39, 1967, 112 pp.

RAPID DETERMINATION OF ASPHALT CONTENT USING PENNSYLVANIA PYCNOMETER

Prithvi S. Kandhal, William C. Koehler, and Monroe E. Wenger,
Pennsylvania Department of Transportation

This paper describes the development and testing of the Pennsylvania pycnometer proposed for rapid determination of asphalt content. The method is based on the procedures of ASTM D2041-67, which have been modified to achieve greater accuracy and precision essential for asphalt content determinations. The Pennsylvania pycnometer has been found to be practical in use and free of operating inconveniences. Asphalt content is determined in approximately 30 min by weight-volume relation and by the aid of nomographs. Paving mixtures containing limestone, sand, gravel, and slag aggregates have been tested for asphalt content. Results are compared to those obtained by use of the reflux equipment. The test data have been analyzed statistically. Greater accuracy is indicated in the results obtained by the Pennsylvania pycnometer. For highly absorptive aggregates, which present problems in complete retrieval of the asphalt, the pycnometer method has better proficiency than the reflux method.

•ASPHALT content is one of the most important factors in the overall quality of asphaltic concrete pavements. As little as 0.5 percent too much asphalt can cause flushing and rutting; an asphalt deficiency of 0.5 percent may cause premature cracking or raveling of the pavement. Thus, a close control of asphalt content is essential for optimum durability and serviceability. The amount of asphalt cement is also important economically because it is the most expensive ingredient in the mix.

Current methods for quantitative extraction of bitumen from bituminous paving mixtures (AASHTO T 164-70) consist of four procedures. Although these procedures are relatively simple and have been used for many years, they are extremely time-consuming to perform, and the results obtained are often of questionable value. With the high production capacity of modern asphalt plants, it is essential that test methods be available that can provide an accurate measure of asphalt content within minutes if a meaningful degree of control is to be employed. It is not uncommon for a modern plant to produce 100 to 200 tons of mixture per hour. Therefore, one can readily visualize the possible difficulties that could arise if 3 or 4 hours were required to obtain a test result. The problem could be complicated even further if a check test or tests are necessary. By this time, several hundred tons of mixture would be laid and compacted, thereby making appropriate adjustments in asphalt content impossible for the mixture already placed on the grade.

There is need, therefore, to devise a method that can strike a proper balance among accuracy of test results, cost of equipment, speed with which the test can be performed, and technician training required. To be of optimum value, such a method must be readily adaptable to both laboratory and field use.

REVIEW OF LITERATURE

Various methods (1, 2) have been investigated for extracting asphalt from asphaltic concrete, some of which were adopted as ASTM or AASHTO standard tests subsequently. Besides being time-consuming, these methods have too much variation in the asphalt content results. Steele and Krieger (3) conducted statistical evaluation of equipment and operator effects on the results of asphalt extraction tests and reported significant differences among operators and among laboratories.

In a study (4) undertaken by the Pennsylvania Department of Transportation in 1969 for determining the variations of results among asphalt plant laboratories, significant differences were noted.

Several improvements have been suggested to reduce the time required for extraction. Jones et al. (5) suggested vacuum extraction of asphalt from paving mixtures using methylene chloride as a reagent.

The principle of using nuclear radiation to measure the asphalt content of paving mixtures was established several years ago by Lamb and Zoller (6); since then, it has been investigated by many researchers. Some drawbacks have been reported by Hughes (7) in this method. An improved nuclear gauge for determining asphalt content in the field has also been studied recently (8).

Stain method (9) has been proposed for fine-graded asphaltic concrete mixtures, but it has several limitations such as operator technique and errors related to the amount of fines in the paving mixture. Flask method (10) requires constant attention to ensure complete dissolution of the asphalt by the solvent. The ignition method (11), in which the weight of a sample before and after removal of the asphalt by burning is used, has been reported to show an operator effect associated with the test method.

Steele and Hudson (12) attempted the asphalt content determination by weight-volume relation based on the procedure of ASTM D 2041. The research work under report is also based on the same concept, but a new apparatus and procedure have been developed and tested involving mixtures containing different types of aggregates and varying asphalt contents.

BACKGROUND AND DEVELOPMENT OF TEST APPARATUS

The concept of determining the maximum specific gravity of bituminous paving mixtures was developed by James M. Rice under the auspices of the National Crushed Stone Association. This contribution is growing in importance as the use of absorptive aggregates becomes increasingly necessary. The vacuum saturation technique employed in this method makes possible the determination of the effective specific gravities of the aggregate and both the effective and total asphalt content of the paving mixture. It has been recognized that, when the average specific gravities of the aggregate remain constant, the major factor affecting the maximum specific gravity of the paving mixture is the volume of asphalt. Under these conditions, the vacuum saturation procedure affords a rapid means for determining asphalt content.

MATHEMATICAL COMPUTATIONS

There are two parts to the required computations (12). The first part is to find the specific gravity of the asphalt-aggregate mixture and then to determine the ratio of asphalt to total mix that corresponds to this specific gravity.

The maximum specific gravity of the mixture is computed by the use of Eq. 2 in ASTM C 2041:

$$\text{Specific gravity } G_m = \frac{A}{A + D - E} \quad (1)$$

where

A = weight of specimen (mix) in air,

D = weight of pycnometer filled with water at test temperature, and

E = weight of pycnometer filled with water and specimen at test temperature.

Figure 1. Work sheet 1.

BITUMEN CONTENT OF PAVING MIXTURES—PENNSYLVANIA PYCNOMETER METHOD

Project No. _____
 Type Aggregate _____
 Mix Type _____
 Producer _____
 Plant _____
 Location _____

Line		Sample Identification				
1	Wt. Pyc. + Mix					
2	Wt. dry Pyc.					
3	(1-2) = Wt. of Mix (A)					
4	Wt. Pyc. + Water (D)					
5	Line 3 + Line 4					
6	Wt. Pyc. + Mix + Water (E)					
7	(5-6) = Vol. of voidless Mix					
8	(3 ÷ 7) = Max. Sp. Gr. of Mix, G_m					
9	($G_a \div P$)-1					
10	(J x 9) = % Bitumen					

G_a	Effective Specific Gravity - Aggregate =
G_b	Specific Gravity - Asphalt =
F	$G_a - G_b =$
J	$(100 \times G_b) \div F =$

Operator _____ Date _____
 Laboratory _____

Figure 2. Work sheet 2.

EFFECTIVE SPECIFIC GRAVITY OF AGGREGATE (G_a)

Type Aggregate _____
 Mix Type _____
 Producer _____
 Plant _____

Line			Sample Identification			
1	Line 8 (G_m) of Sheet No. 1	G_m				
2	Known % bitumen	P				
3	Sp. Gr. of bitumen	G_b				
4	Line 2 ÷ Line 3	P/G_b				
5	100.0 - Percent bitumen	$100-P$				
6	Line 1 x Line 4	$(G_m \times P)/G_b$				
7	Line 1 x Line 5	$G_m (100-P)$				
8	100.0 - Line 6	$100-G_m P/G_b$				
9	Line 7 ÷ Line 8 = Eff. Sp. Gr.	G_a				

Operator _____
 Date _____

both initial and final voids); i.e., there is a general indication of higher viscosity for asphalts recovered from higher voids pavements.

Possible differences resulting from voids content among pavements were accounted for by establishing equations for time-equivalency correlation curves by combining asphalts of different voids level (Fig. 9). The relative positions of the curves are of significance; as percentage of voids in the pavements increases, longer laboratory IDT time is required to reach equivalent field-service hardening. Regression 74, which was obtained by combining all properties and all asphalts and which is a surprisingly good fit (linear correlation significant at 1 percent level), will be called the master time-equivalency curve. For all practical purposes, the use of the master curve for all asphalts used in all acceptable construction procedures should provide reasonable correlation and prediction for Iowa conditions. It is therefore recommended that, at least for a trial period, this curve be used for specification purposes by the IDT method. On the basis of the master curve, 46 hours of aging in IDT will result in hardening in asphalts equivalent to that attained after 60 months of service life in Iowa conditions.

APPLICATION AND ENGINEERING IMPLICATIONS OF RESULTS

It has been shown repeatedly that asphalts meeting the same present-day specifications can and do exhibit a considerable range and variety of behavior, as measured by a number of different parameters, in the field. It appears justifiable to state that, at the present time, standard test procedures and specifications provide no satisfactory means of determining whether or not asphalt will be durable.

Based on results discussed in previous sections, and with the established time-equivalency correlation curves, it is suggested that the IDT can be used to reasonably predict the changes and useful life of asphalt in Iowa pavements. If parameters, tests, and critical values of asphalts are properly selected, the results of this investigation can be applied to asphalt specification to ensure durable paving asphalts.

Selection or establishment of durability criteria and critical values of critical properties are complex problems. Relative durability of asphalts studied in this project were evaluated by using several approaches.

Limiting Values of Selected Properties

Limiting values is based on the hypothesis, which was verified in this study, that changes in asphalt, both in the laboratory IDT and in the field-service aging, are a hyperbolic function of time in the form

$$\Delta Y = \frac{T}{a + bT}$$

When a and b are determined and initial property value Y_0 is known, the ultimate value Y_u can be calculated from the ultimate change

$$\Delta Y_{t \rightarrow \infty} = 1/b$$

Based on this approach, larger ultimate change (or lower ultimate penetration and higher ultimate viscosity and softening point) would be considered properties of less durable asphalts.

Predicted Time to Harden to Certain Critical Values of Selected Properties

Predicted time to critical value is also based on the hyperbolic time-property change curve model as in the preceding approach. But, instead of ultimate change or limiting value, the time it takes for a certain asphalt to harden to a critical value of a selected property is calculated from the predictive equation or from the time-property curve. Times for asphalts to harden to a critical penetration of 20, a critical softening point of 160 F, a critical viscosity at 77 F, and 0.05 sec^{-1} of 20 to 30 megapoises were

Figure 9. Time-equivalency correlation curves by voids level.

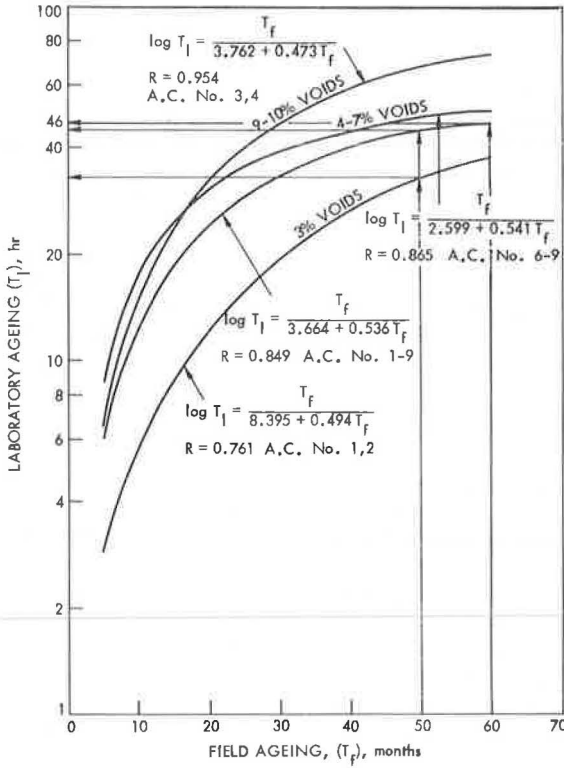


Table 10. Comparison of durability rankings based on different criteria.

Criterion	Asphalt								$\frac{\sum r_n - r_n }{n}$	
	1	2	3	4	5	7	8	9		
Penetration ratio										
r_e	4	2	8	6	5	7	3	1		2.8
r_r	4	7	6	8	3	1	2	5		
Aging index, 77 F										
r_e	3	1	7	4	5	8	6	2		3.3
r_r	5	6	7	8	2	1	3	4		
Aging index, 140 F										
r_e	5	7	6	8	4	2	2	1		1.5
r_r	4	8	5	7	3	1	2	6		
Limiting penetration										
r_e	5	3	8	6	2	7	4	1		2.8
r_r	5	7	8	3	4	1	2	6		
Limiting viscosity, 77 F										
r_e	4	6	8	5	1	3	7	2		1.5
r_r	3	8	7	6	4	2	5	1		
Limiting softening point										
r_e	5	3	2	6	7	8	4	1		2.1
r_r	5	3	5	7	4	2	8	1		
Time to 20 to 30 megapoisies										
r_e	7	4	5	8	2	5	2	1		2.2
r_r	3	6	5	7	4	2	8	1		
Time to 20 penetration										
r_e	6	7	8	5	3	4	2	1		2.2
r_r	5	4	6	8	2	3	1	7		
Time to 160-F softening point										
r_e	8	7	2	3	5	4	6	1		2.2
r_r	5	4	6	8	3	2	7	1		
Total ranking										
R_e	5	4	8	7	2	6	3	1		1.5
R_r	5	6	7	8	2	1	4	3		

calculated. Rankings of the eight asphalts (longer time to reach a critical value means a more durable asphalt) are given in Table 10.

Penetration Ratio Versus Time Curves

It has been established that log penetration ratio and log time of aging is linear. The slope of such plots, therefore, would be indicative of the relative rate of hardening of various asphalts with time. A small slope will indicate a more durable asphalt. Such an approach can also be applied to retained penetration data.

Aging Index Versus Time Curve

Aging index as defined by the ratio of viscosity of aged and original asphalt can be used as an index of the relative degree of hardening of asphalt. It has also been established that the log aging index and the log time of aging are linear. The slope of such a plot can then be used to indicate the relative rate of hardening of asphalt with time. A small slope will imply a more durable asphalt.

Rankings of the eight asphalts based on the preceding criteria are given in Table 10 (r_l for laboratory-aged and r_f for field-aged asphalts). It can be readily noted that rankings of asphalt durability by different criteria are not consistent, except for asphalt concrete 9, which ranked high by all criteria. The ultimate test in determining which of the criteria is most accurate and suited for Iowa conditions consists of continuing observation of the performance of the eight pavements. At this time, they are essentially all in good condition after 42 to 48 months of field service.

The laboratory- and field-durability rankings of asphalts studied were compared and the ability of various criteria to predict asphalt durability was evaluated to calculate the average laboratory- and field-durability ranking differences of the eight asphalts by each criterion. Based on this index, the aging index based on viscosity at 140 F and the limiting viscosity at 77 F seem to be most indicative of the relative aging of asphalt in the laboratory and the pavement.

The overall durability rankings of all asphalts by all criteria were calculated by totaling all nine rankings for each asphalt for both laboratory-aged and field-aged asphalts and ranked as given in Table 10. The average laboratory and field ranking difference was 1.5, which seems to indicate that the IDT can be used to evaluate and predict pavement performance of asphalts with reasonable accuracy.

Control of durability in terms of IDT can be established by incorporating in paving asphalt cement specifications the following standards: a maximum of 20 megapoises in viscosity at 77 F or a minimum penetration of 20 for residue from 46 hours of IDT or both.

CONCLUSIONS

The following conclusions are based on test data:

1. A laboratory durability method for simulating the weathering of paving asphalts during mixing and pavement service life has been developed and is being correlated with field performance under Iowa conditions.
2. The aging process of paving asphalts follows a hyperbolic function of time both in the field and in the developed IDT laboratory conditions, but at different rates.
3. Good correlations between field service aging in Iowa and laboratory aging during IDT have been obtained. The master time-equivalency curve between IDT in hours and pavement service life in months, established by combining all asphalts (void levels) and properties, indicates that 46 hours in IDT will age asphalts to the equivalent of 60 months in Iowa pavements. Correlation curves for different properties and different levels of pavement voids were also obtained.
4. A tentative specification for paving asphalt, including durability requirements based on IDT, is recommended in lieu of current TFOT.

ACKNOWLEDGMENTS

This report is the end result of a comprehensive 4-year study under a project sponsored by the Iowa Highway Research Board and the Iowa State Highway Commission. This work was also supported, in part, by funds of the Engineering Research Institute, Iowa State University.

REFERENCES

1. Characteristics of Bituminous Materials. Highway Research Board Bibliography 35, 1963, and Highway Research Board Bibliography 40, 1966.
2. Lee, D. Y. Development of a Laboratory Durability Test for Asphalts. Highway Research Record 231, 1968, pp. 34-49.
3. Lee, D. Y. Durability and Durability Test for Paving Asphalt. Engineering Research Institute, Iowa State Univ., 1969.
4. Traxler, R. N. Asphalt: Its Composition, Properties and Uses. Reinhold Publishing Corp., New York, 1961, p. 53.
5. Schmidt, R. J., Painter, L. J., Skog, J. B., and Puzinauskas, V. P. The Precision of Tests Made on Asphalt Residue From Thin Film Oven Exposures. Proc. AAPT, Vol. 37, 1968, pp. 476-509.
6. Hveem, F. N., Zube, E., and Skog, J. Proposed New Tests and Specifications for Paving Asphalts. Proc. AAPT, Vol. 32, 1963, pp. 271-327.
7. Skog, J. "Setting" and Durability Studies on Paving Grade Asphalts. Proc. AAPT, Vol. 36, 1967, pp. 387-420.
8. Chipperfield, C. H., Duthie, J. L., and Girdler, R. B. Asphalt Characteristics in Relation to Road Performance. Proc. AAPT, Vol. 39, 1970, pp. 575-613.
9. Kandhal, P. S., et al. Asphalt Viscosity Related Properties of In-Service Pavements in Pennsylvania. Paper presented at annual meeting of AAPT, 1972.
10. Lee, D. Y., and Csanyi, L. H. Jour. of Materials, Vol. 3, 1968, p. 538.
11. Gotolski, W. H., Ciesielski, S. K., and Heagy, L. N. Progress Report on Changing Asphalt Properties of In-Service Pavements in Pennsylvania. Proc. AAPT, Vol. 33, 1964, pp. 285-319.
12. Vallerga, B. A., and Halstead, W. J. Effects of Field Aging on Fundamental Properties of Paving Asphalts. Highway Research Record 361, 1972, pp. 71-92.
13. Rostler, F. S., and White, R. M. Composition and Changes in Composition of Highway Asphalts, 85-100 Penetration Grade. Proc. AAPT, Vol. 31, 1962, pp. 35-89.
14. Halstead, W. J., Fritz, S. R., and White, R. M. Properties of Highway Asphalts—Part III, Influence of Chemical Composition. Proc. AAPT, Vol. 35, 1966, pp. 91-138.
15. Halstead, W. J., et al. Fingerprinting of Highway Asphalt. Paper presented at annual meeting of AAPT, Feb. 14-16, 1972.
16. Csanyi, L. H., and Fung, H. P. A Rapid Means of Determining the Constituents of Asphalts. Proc. AAPT, Vol. 23, 1954, pp. 64-77.
17. Lee, D. Y., and Huang, R. J. Weathering of Asphalts as Characterized by Infrared Multiple Internal Reflection Spectroscopy. Paper presented at 11th Annual Meeting of Society for Applied Spectroscopy, Dallas, Texas, Sept. 11, 1972.
18. Brown, A. B., Sparks, J. W., and Larsen, O. Rate of Change of Softening Point, Penetration, and Ductility of Asphalt in Bituminous Pavement. Proc. AAPT, Vol. 26, 1957, pp. 66-81.
19. Gallaway, B. M. Durability of Asphalt Cements Used in Surface Treatments. Proc. AAPT, Vol. 26, 1957, pp. 151-173.
20. Pauls, J. T., and Halstead, W. J. Progressive Alterations in a Sheet Asphalt Pavement Over a Long Period of Service. Proc. AAPT, Vol. 27, 1958, pp. 123-154.
21. Heithaus, J. J., and Johnson, R. W. A Microviscometer Study of Road Asphalt Hardening in the Field and Laboratory. Proc. AAPT, Vol. 27, 1958, pp. 17-34.

STORAGE OF BITUMINOUS CONCRETE IN INERT GAS

Prithvi S. Kandhal and Monroe E. Wenger, Pennsylvania Department of Transportation

Possible problems associated with hot storage of bituminous concrete mixes can be migration of asphalt, segregation of the mix, and aging of the asphalt cement due to prolonged storage at high temperature. Laboratory and field investigations were conducted to evaluate the effect of prolonged hot storage on the properties of a bituminous paving mix. No additive was used in the asphalt cement. Storage of mixes was attempted with and without inert gas for as long as 10 days. Field tests were conducted with inert gas only to extend the storage period. Migration of asphalt and segregation of mix did not pose any problem. In the pilot tests, mix stored without inert gas hardened at a faster rate than that stored with an inert atmosphere. If the maximum allowable storage time is determined from the criterion of minimum percentage of retained penetration (AASHO M 20-70) on TFOT residue, this can vary depending on the asphalt source, composition of the bituminous mix, temperature, and time of mixing. No storage might be possible in some cases; however, based on these criteria, the allowable storage period using inert gas was found to be 24 hours in this field study. It is yet to be established to what extent the durability of the pavement is sacrificed because of premature hardening of the asphalt in the hot storage bin.

•THE installation of hot-mix surge and storage-bin systems has considerably increased throughout the United States during the past 2 or 3 years. This study was undertaken to investigate the effects of prolonged storage at high temperature on the properties of a bituminous paving mixture.

The research program consisted of three phases: Phase 1 was the laboratory hot storage study to evaluate the rheological properties of the asphalt cement on being stored at higher temperatures for a considerable length of time, phase 2 was a semi-field test using two pilot storage bins (3 ft in diameter and 3 ft deep) placed in the yard outside the laboratory, and phase 3 was a full-scale field test using 200-ton hot storage bins supplied with inert gas. Phase 3 involved storage of base course and wearing course bituminous mixtures in inert atmosphere for as long as 10 days.

The objectives of this study were to ascertain if there is segregation in the resulting mix; evaluate possible migration of asphalt during storage; determine the effects of storage on the physical properties of the mixture such as Marshall stability, flow, stiffness, and so forth; and evaluate the changes in rheological properties of the asphalt cement caused by prolonged storage at high temperatures.

REVIEW OF LITERATURE

The effect of hot storage on bituminous concrete mixes has been studied by various research agencies with variable results. It has been stated (1) about hot-mix surge storage that safe storage periods are not so much a function of bin design as they are a function of the nature of the mix and its uniformity.

Middleton et al. (2) studied the effects of hot storage on a fine-graded bituminous paving mix (using silicone treated 85 to 100 penetration grade asphalt cement) that was

stored in a silo for a total of 97 hours. Results showed that there was a marked change in the properties of the asphalt cement during mixing but that any change that may have occurred during storage was practically negligible.

Parr (3) has reported about storage of a fine-graded bituminous base course mix using sand-gravel as aggregate and 40 to 50 penetration grade asphalt cement. Two series of tests of storage were conducted: Series A contained asphalt that was untreated, and series B contained asphalt treated with 2 ounces of an additive containing silicone materials for each 5,000 gal of asphalt. With the treated asphalt, no significant change in either penetration or ductility occurred for 72 hours of hot storage. However, with untreated asphalt, significant changes in both penetration and ductility were observed in samples taken after 24-hour storage at the hot-bin temperature.

Vallerga and White (4) reported significant hardening of asphalt cement after 4 hours. The rate of hardening was significantly decreased when silicone fluid was added to the asphalt.

Brock and Cox (5) reviewed the results of tests on actual installations and concluded that hot bituminous mix may be stored without detrimental effects for 10 days in a heated silo blanketed with an inert gas and for more than 14 days if the mix contains silicone and is held in a heated silo blanketed with an inert gas.

A series of gradation tests were conducted (6) on surface-course mix obtained from the silo, but no appreciable change in gradation was noted due to storage.

Four series of 72-hour tests conducted by the National Asphalt Pavement Association (7) indicated that the use of an inert atmosphere increased the storage time from 6 to more than 72 hours for mix made with nontreated asphalt. The use of silicone thus increased storage time from about 24 to more than 72 hours in the inert atmosphere and from about 2 to 6 hours in air.

Parr and Brock (8) conducted a statistical study of effects of hot storage on the composition and properties of a bituminous concrete binder mixture stored for 7 days in a sealed silo equipped with a hot-oil heating jacket and purged with an inert gas inside. They concluded that the mix composition before and after storage was not significantly different. However, some hardening of the asphalt did occur, but it was not severe because the drop in penetration was less than that permitted by specifications for the thin-film oven test (TFOT).

Because the Pennsylvania Department of Transportation does not permit the use of silicones as an additive in the asphalt cement, this additive was excluded from this study.

Effect of hot storage on the rheology of the asphalt cement has not been studied in greater detail. Hardening of asphalt cement because of storage has mostly been observed by noting change in penetration only. Recent research (9, 10, 11) has indicated that, besides absolute viscosity, other parameters such as shear susceptibility and temperature susceptibility are needed to specify the complete rheological behavior of paving grade asphalts. The major factors affecting the durability and performance of the pavements have been observed to be the aging index (based on viscosity at 77 F) and the gain in shear susceptibility of the asphalt cements (12). An attempt has been made in this study, therefore, to evaluate the effects of hot storage on these rheological parameters also.

PRELIMINARY LABORATORY AND SEMI-FIELD TESTS

Laboratory Study

This study was undertaken to simulate the condition when the bituminous concrete mix is stored at high temperature in a sealed silo without inert gas. Bituminous wearing course mix made of limestone aggregates and AC-2000 asphalt cement was stored in 1-quart friction top cans and kept in an oven at 290 F for as long as 15 days. After specified time intervals, the cans were taken out and chilled by immersion in ice water to minimize the effect of continued heat. Asphalt was recovered by the Abson method, and the rheological tests were conducted on the recovered asphalt. Complete data are given elsewhere (13).

Because the cans were sealed, hardening of asphalt continued until the limited oxygen in the air was utilized in about 24 hours of storage, and thereafter further hardening was

negligible for as long as 15 days. During the first 24 hours, penetration dropped from 67 to 53, viscosity at 77 F increased from 3.0 to 4.0 megapoises, viscosity at 140 F increased from 3,450 to 5,290 poises, and viscosity at 275 F increased from 647 to 793 cs.

Semi-Field Study

Bituminous mixes were stored in two CMI pilot bins mounted on a trailer for demonstration purposes. The complete unit, which was placed in the back yard of the BMTR laboratory, consisted of two hot-mix containers 3 ft in diameter and 3 ft deep and an oil heating and inert gas system. One container was supplied with inert gas and jacketed with hot oil; the other was only jacketed with hot oil. Bituminous mixtures were fed in these preheated containers at a temperature of 290 F. The mixtures were stored for as long as 10 days.

Tests similar to the laboratory study were run on the recovered asphalt, and the complete data obtained are given elsewhere (13). The mix stored without inert gas hardened at a faster rate than that stored with inert atmosphere in the bin. However, in both mixes, there was a significant drop in asphalt penetration and ductility and significant increase in viscosity and shear susceptibility during the first 5 to 6 hours. Asphalt cement hardened more than that permitted by specifications for the TFOT. This indicated that the rate of hardening during storage depends primarily on the asphalt source (if storage conditions are held the same). It may be mentioned, however, that, because of problems in maintaining temperature and regulating the inert gas, the data would not relate to the ideal conditions.

FIELD TEST RESULTS

The storage system of the H. R. Imbt Co. (asphalt plant 6) located at Bossardsville, Pennsylvania, was used for this field study. The storage system consisted of the following:

1. Three 200-ton circular bins heated by hot-oil jackets and insulated—Automatic controls were available to maintain the unit at the desired temperature. The bin is a tall, vertical unit on top with a tapered hopper that tends to remix the bituminous concrete while discharging. Each bin is provided with a bottom air lock below a clam-type discharge gate and top air lock to seal the unit and hold the inert gas at a constant low pressure to prevent outside atmosphere from entering.
2. Thermal oil heater—Hot oil from the heater is pumped to the storage unit by a high-volume pump.
3. Inert gas generator—When the generator is operating, inert gas is pulled from the exhaust of the pre-mix burner and is then cooled, dehydrated, compressed, and stored in a pressure tank.
4. Drag chain conveyor—The conveyor is a continuous type and is enclosed to prevent spillage of mix and to maintain temperature.
5. Control room—The room contains consoles consisting of all controls necessary for discharging mix, bin level indicators, and controls for heating and inert gas systems.

Only two bins were used. In one bin, Pennsylvania ID-2 wearing course mix was stored; in the other bin, bituminous concrete base course (BCBC) mix was stored. Sampling of the bituminous concrete was done at specified intervals during the 10-day storage period. Samples were obtained as per ASTM D 979-51. After each storage period, two 1-gal cans were filled with bituminous mix, chilled in cold water, and then shipped to the BMTR laboratory for testing. Samples were also used in compacting three Marshall specimens immediately at the plant laboratory. These were stored for 24 hours and then tested for Marshall stability and flow.

Marshall data obtained on samples of ID-2 wearing course mix are shown in Figure 1. The temperature of discharged mixture from the two bins at the time of sampling is shown in Figure 2.

Asphalt cement was extracted from the duplicate samples of bituminous mix received in the central laboratory. Based on extraction test data, the gradation number, the surface area of the recovered aggregate, and the bitumen index have been determined

Figure 1. Marshall test data (ID-2 wearing course mix).

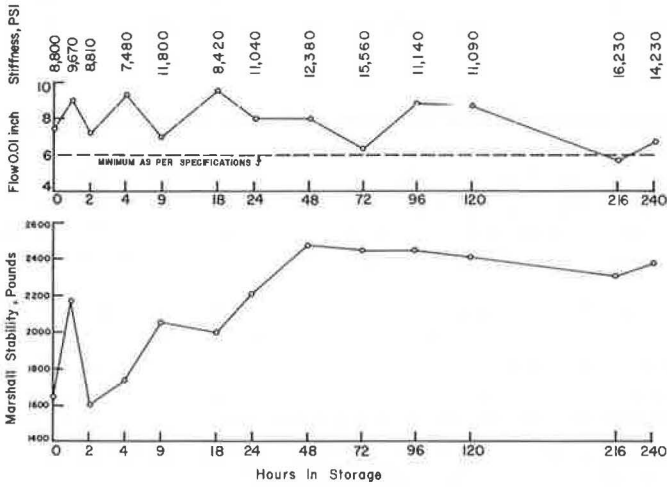


Figure 2. Temperature of discharged mix (field study).

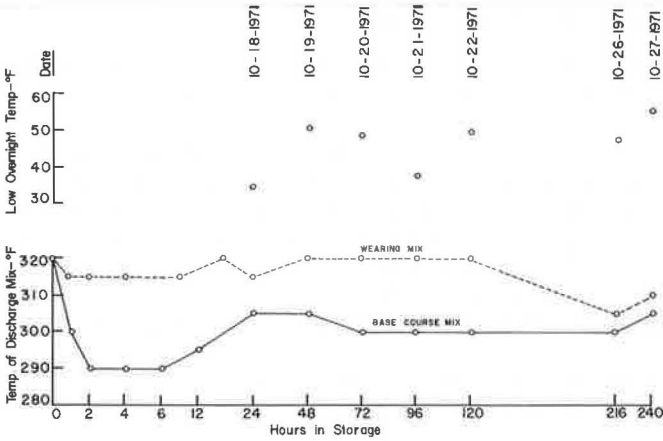


Table 1. Mix data.

Hours in Storage	Asphalt Content (percent)	Gradation Number	Aggregate Surface Area (ft ² /lb)	Bitumen Index (lb/100 ft ²)
0	3.6	2,068	17.74	0.211
1	3.8	2,336	20.18	0.196
2	3.8	2,149	18.49	0.214
4	3.6	2,293	19.66	0.190
6	3.5	2,333	19.38	0.187
12	3.6	2,404	19.81	0.189
24	3.5	2,381	19.27	0.188
48	3.7	2,572	20.09	0.191
72	3.4	2,349	18.07	0.195
96	3.7	2,468	18.98	0.202
120	3.6	2,335	17.86	0.209
216	3.6	2,154	17.34	0.215
240	3.6	2,356	18.64	0.200
Average	3.6	2,323	18.89	0.199
Standard deviation	0.11	0.135	0.936	0.012

to examine the variability in the mix sampled. These data are given in Table 1 for the base course mix. The gradation number is similar to fineness modulus except it is the sum from the $\frac{1}{2}$ -in. and smaller sieves of the percent fractions passing divided by 100.

The recovered asphalt cement was tested for penetration at 77 F; ductility at 60 F, 5 cm/min; absolute viscosity at 77 F, 0.05 sec^{-1} shear rate and shear susceptibility; absolute viscosity at 140 F; and kinematic viscosity at 275 F.

Figures 3, 4, 5, and 6 show these data versus the storage period for both the mixtures.

Absolute viscosity, using the sliding plate microviscometer, was also determined at 50, 104, and 122 F. Temperature susceptibility data based on these results are given in Table 2 for the base course mix only.

Storage aging indexes, based on viscosity at 77 F, have been determined for both mixtures and are shown in Figure 7. These have been determined as follows:

$$\text{Storage aging index} = \frac{\text{viscosity after storage}}{\text{viscosity before storage}}$$

DISCUSSION OF TEST RESULTS

Effect of Storage on Properties of Bituminous Concrete

Changes in the properties of bituminous concrete resulting from storage in the full-scale storage bins are as follows.

Migration of Asphalt Cement—Extraction test data indicate reasonable uniformity of asphalt content in the two mixtures sampled after various storage intervals for as long as 10 days. If the migration of asphalt cement in either of the mixes had taken place toward the bottom of the bins, the asphalt content would have increased with storage period. The standard deviation in the asphalt content for the samples tested was observed to be 0.14 and 0.11 percent for the wearing course and base course mixtures respectively. Migration of asphalt would perhaps occur if the storage is attempted at temperatures higher than 320 F or the bituminous concrete stored is rich in asphalt.

Segregation—Possible segregation of the mixtures due to storage was evaluated by subjecting to sieve analysis the aggregate recovered by the extraction test from the sampled mixtures. The gradation of the recovered aggregate from both the mixtures falls within the tolerance limits as per specifications. Only the normal variation that is inherent in a bituminous concrete plant has been observed.

Gradation number and bitumen index have been used (8) to evaluate the extent of segregation and the uniformity of asphalt film thickness. The aggregate surface area of each sample was calculated to determine the bitumen index. Normally a coarse mix would tend to segregate more than a fine mix. Data given in Table 1 for base course mix do not indicate any segregation problem.

Marshall Stability and Flow—Marshall specimens were compacted from the wearing course mix samples and tested for stability and flow with an automatic recorder. In the specifications for Pennsylvania ID-2 wearing course, a minimum stability of 1,200 lb and a flow value between 6 and 16 are required. The average stability and flow of the mix out of the pug mill was observed to be 1,600 lb and 8 units respectively. Figure 1 shows the changes in these values with the storage period. As would be expected if the asphalt hardens, there was a general trend of increase in stability and decrease in flow due to storage. However, the mix stored for as long as 10 days still met the requirements of the specifications. Most of the increase in stability took place in the first 48 hours of storage. This is explained by a similar increase in asphalt viscosity measured at 140 F (Fig. 5).

Van der Poel developed data indicating that, in case of mixtures containing dense-graded aggregates and asphalt cements, which were well compacted (approximately 3 to 5 percent air voids), the stiffness of a mixture is dependent on the stiffness of the asphalt that it contains and the volume concentration of the aggregate (14). At very short times of loading or low temperatures or both, the behavior of asphaltic concrete is almost elastic in the classical sense, and the stiffness, S , is analogous to an elastic modulus, E . At longer times of loading and higher temperatures, the stiffness is

Figure 3. Penetration and ductility (field study).

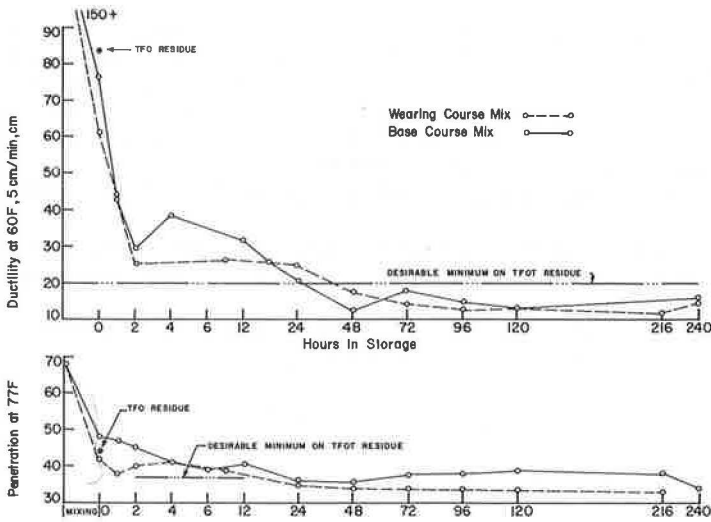


Figure 4. Viscosity and shear susceptibility (field study).

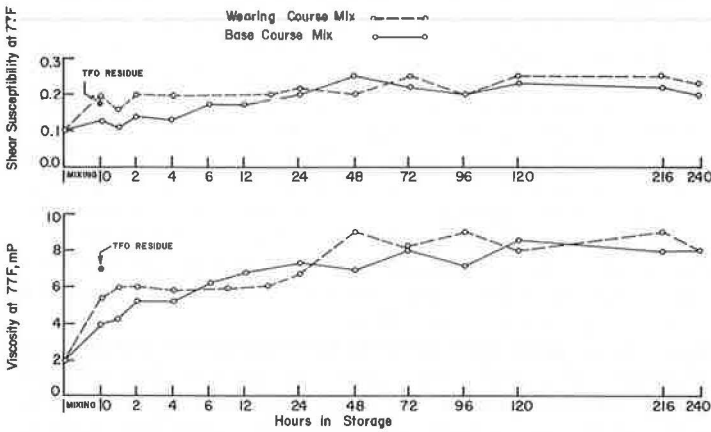


Figure 5. Absolute viscosity at 140 F (field study).

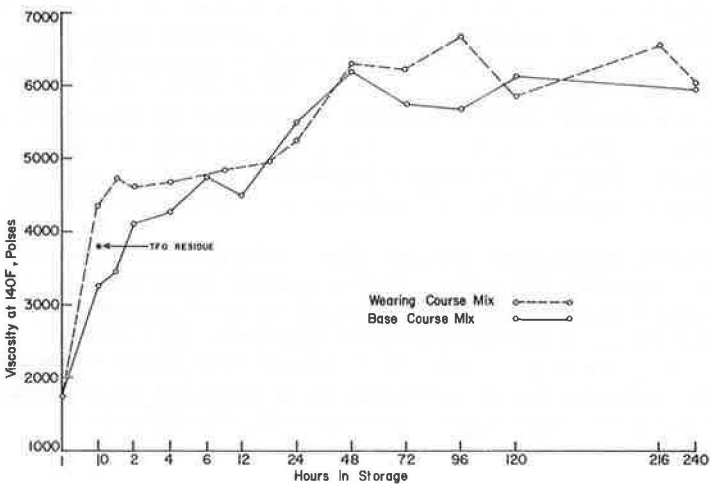


Figure 6. Kinematic viscosity at 275 F (field study).

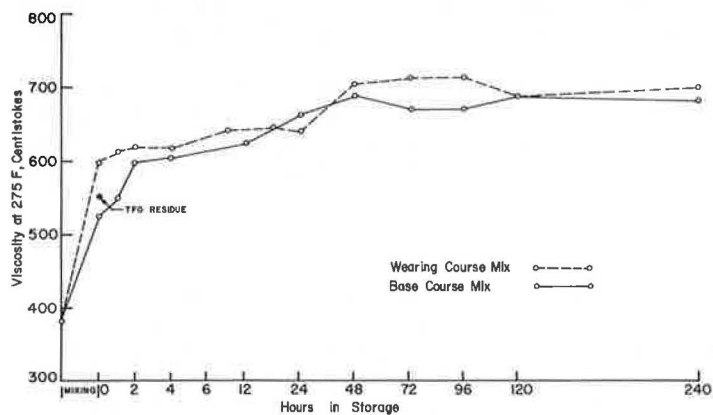
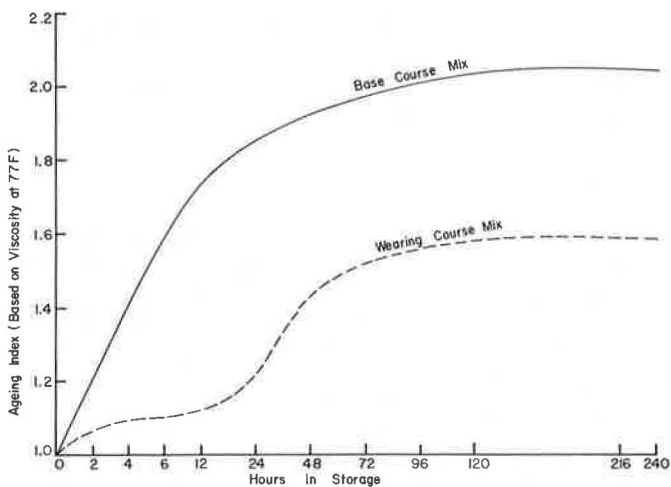


Table 2. Temperature susceptibility of base course mix.

Hours in Storage	Temperature Susceptibility of Recovered Asphalt Cement		
	50 to 77 F	77 to 140 F	140 to 275 F
0 (pug mill)	3.62	3.60	3.48
12	3.16	3.57	3.47
24	3.14	3.40	3.50
72	3.13	3.40	3.51
120	3.12	3.38	3.51
240	3.13	3.20	3.50

Figure 7. Storage aging index (field study).



simply a relation between the applied stress and the resulting strain. Stiffness of the stored wearing course mix, calculated from the stress-strain data obtained in Marshall tests, is shown in Figure 1. Stiffness of the mix increased by 50 percent in the first 48 hours.

Temperature of Stored Mix—Figure 2 shows the temperature of the mix discharged from the storage silo at the time of sampling. There were some initial drops in temperature of base course mix, but the temperature stabilized after 24 hours. On the whole, temperature of the wearing course mix was 15 to 20 F higher than that of the base course mix.

Effect of Storage on Properties of Asphalt Cement

Laboratory and semi-field tests confirmed field tests reported by others that inert gas extends storage time, and, because the intent was to extend the storage to 10 days, only inert gas was tested in the field. No problems with respect to the functioning of the heating and inert gas systems were encountered, so the results can be considered as realistic in a practical sense. However, the results would be valid only for the asphalt cement actually used in the two mixtures. Though the same asphalt cement was used in the wearing course and base course mixes, more hardening occurred in the pug mill in case of wearing course mix. The effect of storage on the various properties of asphalt cement is discussed in the following.

Penetration—Penetration of original asphalt cement was 68. After mixing in the pug mill, the penetration of asphalt was noted to be 42 and 48 in the wearing course and base course mixes respectively. Drop in penetration of asphalt cement (Fig. 3) occurred from 42 to 34 in the wearing course mix and from 48 to 36 in the base course mix during the first 48 hours of storage period, and then there was no appreciable change. Most of the drop in penetration took place in the first 24 hours. According to AASHTO M 20-70 on penetration graded asphalt cements, penetration of residue after TFOT for the asphalt cement used can be permitted as low as 37 (that is, 54 percent of original). If this is assumed as a criterion for acceptance, these mixes would be acceptable if stored for 24 hours or less (Fig. 3). However, this may not be applicable in general. More hardening in the pug mill itself can take place in some cases, and thus storage may not be possible at all. The following data taken from two projects (15) using an asphalt cement from the same source would indicate this:

<u>Mix</u>	<u>Penetration Values</u>			<u>Percentage Retained Penetration</u>		
	<u>Original</u>	<u>After Mixing</u>	<u>After Compaction</u>	<u>Original</u>	<u>After Mixing</u>	<u>After Compaction</u>
LR 219	59	36	31	100	61	53
LR 101	59	44	40	100	75	68

It would not have been possible to store the LR 219 mix to meet the same criterion, whereas LR 101 mix could possibly be stored for some period. Asphalt from the same source was used in these projects, but different aggregate sources and aggregate gradations were used. Thus, it would seem that the allowable storage time depends on the asphalt source and the composition of the bituminous mix. It is evident that hardening in 24 hours of storage can be equivalent to about 20 months of hardening in the pavement based on penetration (Fig. 8). The two asphalts compared are from different sources but had almost the same penetration after pug mill mixing. These asphalts had almost identical viscosity at 77 and 140 F.

Ductility—There was significant drop in ductility (60 F) in the first 2 hours of storage (Fig. 3). The ductility dropped to 25 and 30 cm in the wearing course and base course mixtures respectively. The desirable minimum ductility on the TFOT residue is 20 cm at 60 F; therefore, these mixtures would not be acceptable after 24 hours. The change in ductility value beyond 48 hours was negligible.

Viscosity at 140 F and 275 F—Viscosity at 140 F of asphalt cement increased from 4,350 to 6,300 poises in wearing course mix and from 3,250 to 6,200 poises in the base

Figure 8. Penetration and viscosity of asphalt (silo versus pavement).

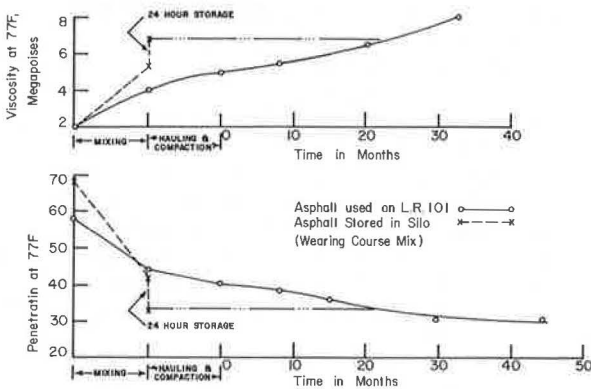
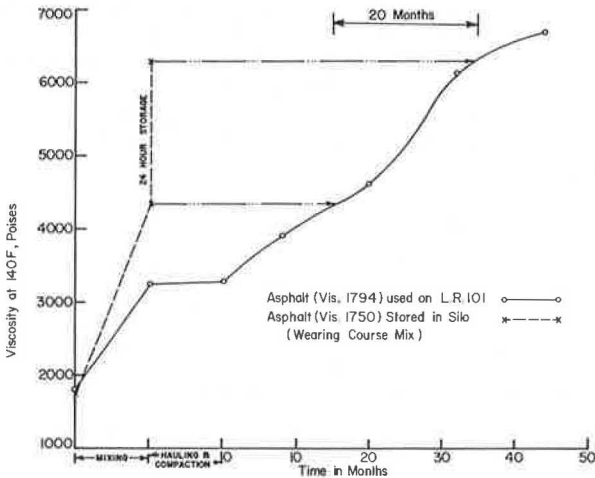


Figure 9. Viscosity at 140 F of asphalt (silo versus pavement).



course mix during 48 hours of storage, and then it leveled off (Fig. 5). Maximum permissible viscosity after the TFOT is 8,000 poises, which was not reached in 10 days of storage. However, when compared to hardening in the pavement based on viscosity, the hardening due to 24 hours of storage is equivalent to that that occurred in pavement in about 20 months (Fig. 9).

Viscosity data at 275 F also indicate the same trend (Fig. 6).

Absolute Viscosity at 77 F—Increase in absolute viscosity at 77 F was noted during the first 48 hours of storage, most of which occurred in the first 24 hours. Thereafter, no significant increase took place (Fig. 4). Increased viscosity at 77 F reduces the capability of the pavements to compact under traffic at ambient temperatures (12). Hardening in 24 hours of storage can be equivalent to about 20 months of hardening in the pavement based on viscosity at 77 F (Fig. 8). The two asphalts compared had original viscosity of 2.0 megapoises.

Because the same asphalt in the wearing and base course mixes did not harden to the same extent in the pug mill, storage aging index is a better indicator of relative hardening in the storage silo. Asphalt in the base course mix hardened at a faster rate than the asphalt in the wearing course mix (Fig. 7) as would normally be expected. How-

ever, ultimate hardening of the asphalt was greater in the wearing course mix than the base course mix.

Shear Susceptibility—There was no significant increase in shear susceptibility (77 F) of the asphalt in the wearing course mix, whereas the shear susceptibility increased during the first 24 hours of storage in the base course mix (Fig. 4). However, in both cases, the shear susceptibility does not seem to be excessive.

Temperature Susceptibility—Temperature susceptibility data for asphalt in the base course mix are given in Table 2, based on the viscosity data at 50, 77, 104, 122, 140, and 175 F. Because of shear dependent viscosities at temperatures lower than 140 F, slopes of the temperature viscosity lines deviate from those obtained between 140 F and higher temperatures. Therefore, the temperature susceptibility of the asphalts has been determined in three temperature ranges: 50 to 77 F, 77 to 140 F, and 140 to 275 F. It will be observed that the temperature susceptibility values of the asphalt have shown a decreasing trend with storage aging in the first two temperature ranges, whereas the increase in the range of 140 to 275 F is not significant.

General Data—Most of the hardening during the 10-day storage period in inert atmosphere occurred in the first 24 to 48 hours. It seems that some air is trapped by the mixture when it is dropped from the pug mill onto the conveyor used in charging the silo. The oxygen in this air is not displaced by the inert silo atmosphere and undoubtedly oxidizes the asphalt of the stored mix at the high-temperature storage conditions. This was also observed by Parr and Brock (8). The significant increase in asphalt viscosity (77 and 140 F) and drop in penetration because of 24 hours of storage in inert atmosphere has been observed to be equivalent to 20 months of hardening in the pavement using asphalt of the same consistency based on viscosity. Though the drop in penetration and increase in viscosity is less than that permitted by AASHTO specifications for the TFOT (AASHTO M 20-70 and M 226-70), the amount of hardening that should be classed as detrimental is a moot question.

CONCLUSIONS

The following conclusions were drawn with regard to laboratory and semi-field tests:

1. Mix stored without inert gas hardened at a faster rate than that stored with inert atmosphere in the bin, and
2. The aging index is a better indicator of relative hardening when asphalts from different sources are used or mixtures of different composition are stored.

Full-scale field tests were conducted using inert gas only, and the following conclusions are drawn:

1. No migration of asphalt cement in the bituminous concrete was observed during 10-day storage.
2. All silo discharge samples met the specification requirements for gradation of wearing and base course mixes, so there was no segregation problem.
3. Wearing course mix samples obtained from the storage silo for as long as 10 days still met the specification requirements for Marshall stability and flow. However, the stiffness of the mix increased by 50 percent in the first 48 hours because of increased Marshall stability and reduced flow.
4. Based on the aging index, base course mix hardened at a faster rate than the wearing course mix.
5. Most of the hardening during the 10-day storage period occurred in the first 48 hours. It seems the air entrapped in the mix is not displaced completely by the inert silo atmosphere and thus oxidation continues for a limited period.

The following general conclusions were made:

1. If the maximum allowable storage time is determined from the criterion of minimum percentage of retained penetration (AASHTO M 20-70) on TFOT residue, it can vary depending on the asphalt source, composition of bituminous mix, temperature, and time of mixing. Although no storage might be possible in some cases, based on these criteria, the allowable storage period using inert gas was found to be 24 hours in this study.

2. Asphalt hardening (aging) during 24 hours of storage of bituminous concrete in inert atmosphere can be equivalent to 20 months of hardening in the pavement. It is yet to be established to what extent the durability of the pavement is sacrificed because of this premature hardening in the hot storage bin. Further investigations should be attempted to include comparison of asphalt properties from pavements laid from silo-stored materials with those of asphalt from pavements laid directly from the pug mill.

ACKNOWLEDGMENTS

This report is the result of a research project sponsored by the Pennsylvania Department of Transportation. The opinions, findings, and conclusions expressed are those of the authors and not necessarily those of the Pennsylvania Department of Transportation. CMI Systems, Chattanooga, Tennessee, and the Pennsylvania Asphalt Pavement Association cooperated in this study.

Thanks are due to W. S. Myers for assistance in the field study, P. G. Kaiser for physical testing of the bituminous mixtures, and H. R. Basso, Jr., for the testing of recovered asphalt.

Appreciation is also expressed to Edward Macko for illustrations and June Viozzi for compilation of research data.

REFERENCES

1. Rheinfrank, L. Common Sense on Hot-Mix Surge Storage. Standard Havens System, Glasgow, Missouri, Dec. 1969.
2. Middleton, S. C., et al. The Effect of Hot Storage on an Asphaltic Concrete Mix. Proc. Assn. of Asphalt Paving Technologists, Vol. 36, Feb. 1967.
3. Parr, W. K. Discussion of Middleton, S. C., et al., The Effect of Hot Storage on an Asphaltic Concrete Mix. Proc. Assn. of Asphalt Paving Technologists, Vol. 36, Feb. 1967.
4. Vallerga, B. A., and White, R. M. Discussion of Middleton, S. C., et al., The Effect of Hot Storage on an Asphaltic Concrete Mix. Proc. Assn. of Asphalt Paving Technologists, Vol. 36, Feb. 1967.
5. Brock, J. D., and Cox, R. B. Safe Hot-Storage Time Extended With Silicone and Inert Gas. Roads and Streets, July 1968.
6. Triplett, G. S. Storage of Asphalt Concrete Mixtures as Practiced in North Carolina. The Asphalt Institute, Raleigh District, March 1967.
7. Foster, C. R. More on Hot Storage of Asphalt Paving Mixtures. Annual Convention of National Asphalt Pavement Assn., Feb. 1968.
8. Parr, W. K., and Brock, J. D. Statistical Study of Effect of Hot Storage on the Composition and Properties of Asphaltic Concrete. Annual Meeting of the Assn. of Asphalt Paving Technologists, Cleveland, Feb. 14-16, 1972.
9. Gzemski, F. C. Viscoelastic Properties of Paving Asphalts. ASTM STP 328, 1962.
10. Skog, J. Setting and Durability Studies on Paving Grade Asphalts. Proc. Assn. of Asphalt Paving Technologists, Vol. 36, Feb. 1967.
11. Chipperfield, C. H., Duthie, J. L., and Girdler, R. B. Asphalt Characteristics in Relation to Road Performance. Proc. Assn. of Asphalt Paving Technologists, Vol. 39, Feb. 1970.
12. Kandhal, P. S., Sandvig, L. D., Koehler, W. C., and Wenger, M. E. Asphalt Viscosity Related Properties of In-Service Pavements in Pennsylvania. Annual Meeting of ASTM, Los Angeles, June 25-29, 1972.
13. Kandhal, P. S., and Wenger, M. E. Vertical Hot Bin Storage of Bituminous Concrete Mixes. Bureau of Materials, Testing and Research, Pennsylvania Department of Transportation, Research Report (project 70-29), May 1972.
14. Finn, F. N. Factors Involved in the Design of Asphaltic Pavement Surfaces. NCHRP Rept. 39, 1967, 112 pp.
15. Gotolski, W. H., et al. A Study of Physical Factors Affecting the Durability of Asphaltic Pavements. Pennsylvania Department of Transportation, Research Report IR-9, Sept. 1968.

DISCUSSION

R. L. Davis, Koppers Company, Inc.

The authors of this paper are to be congratulated on bringing information on such an interesting and timely subject to us. The use of hot storage bins has increased rapidly in the past few years, and the reduction in cost that comes from greater flexibility in scheduling hot-mix operations should not be ignored. It is my understanding that the reduction in cost is significant, and, in a competitive market, this reduction will soon be passed on to the buyer.

This paper points out the importance of silicone fluid in reducing the rate of hardening of asphalt binders, thus making possible longer storage periods without significant hardening of the mix. Previous papers (2, 3, 5, 7) have shown that asphalt mix could be stored for several days with only negligible hardening. The authors point out that silicone liquid was used in each case in contrast to the present paper where silicone was not used and where a storage period of only a day or less would be allowable. It is interesting to note that the data of this paper like those of other papers (2, 3, 5, 7) show no migration of asphalt cement in the mixture and no segregation problem.

The matter that causes me the greatest concern in this paper is that there is no indication of the random variation of the testing procedures. This is not so much a criticism of the paper or the authors as it is of the general current practice in the bituminous field. We know that the precision of our bituminous testing methods such as the Abson recovery method, Marshall stability, flow, penetration, ductility, viscosity, and shear susceptibility are poor. When they are added together as they are here, the errors become very large. Some indication of the confidence spread about each of the time series lines in Figures 1 through 9 would be a tremendous help in evaluating the meaning of these figures.

AUTHORS' CLOSURE

Samples were tested in duplicate, and reported results are the average of these values. It is realized that precision of bituminous testing methods is poor. It must be pointed out that each of the specific tests cited was performed by only one trained operator in each case. This procedure should tend to cancel the influence of variances among operators.

We admit that it would be highly desirable to have data that would permit establishment of the confidence spread about each of the time series lines. However, the scope of this investigation and the manpower and testing hours precluded development of these data.

Any future work on this study will be expanded to permit determination of the confidence limits. We are also considering the Orsat analysis of the inert gases to determine the effect of oxygen and carbon monoxide on the asphalt properties.

IRRECOVERABLE AND RECOVERABLE NONLINEAR VISCOELASTIC PROPERTIES OF ASPHALT CONCRETE

James S. Lai, University of Utah; and
Douglas Anderson, Utah State Department of Highways

The results are reported of a series of uniaxial compression creep tests of an asphalt mixture under constant loadings, multiple-step loadings, and repeated loadings of as many as 100 cycles. It has been shown that the nonlinear viscoelastic behavior of the asphalt concrete can be represented by a nonlinear generalized Kelvin model that consists of a nonlinear dash-pot connected in series with a nonlinear Kelvin chain. Thus, the nonlinear creep strains are separated into irrecoverable and recoverable strains. It has been shown that the constitutive equation can be determined by the use of both the creep and the recovery parts of the constant loading creep test results. The accuracy in predicting the creep behavior of the asphalt concrete under the multiple-step loadings and the repeated loadings has been shown to be very satisfactory. The importance of the irrecoverable strains to the practical implementation of asphalt pavements subjected to traffic loading is discussed. A possible way of relating the irrecoverable strains to the fatigue life of the material is also discussed.

•IN the past 10 years, considerable interest has been developed in an attempt to characterize the time and temperature dependence of the mechanical properties of asphalt paving mixtures within the framework of viscoelastic theory, especially the linear viscoelastic theory. Most of the test results reported so far on the viscoelastic characterization of asphalt mixtures have been obtained from the constant stress creep tests, or constant strain relaxation tests (1-4), and the sinusoidal loading tests (5-8). In most cases, the linear viscoelastic behavior of the asphalt concrete was assumed, and, henceforth, the linear viscoelastic material properties in terms of creep compliance, relaxation modulus, and complex compliance and complex modulus were obtained. For example, the phenomenon of creep can be represented by the following equation under a uniaxial stress state:

$$\epsilon(t) = \int_0^t J(t - \xi) \frac{\partial \sigma(\xi)}{\partial \xi} d\xi \quad (1)$$

where ϵ and σ are uniaxial strain and stress respectively. $J(t)$ is the uniaxial creep compliance and is usually determined from constant stress creep tests. For a given constant stress, Eq. 1 becomes

$$\epsilon(t) = J(t)\sigma_0 \quad \text{or} \quad J(t) = \frac{\epsilon(t)}{\sigma_0} \quad (2)$$

In this equation, $\epsilon(t)$ is the measured creep strain under the constant stress σ_0 , and the creep compliance $J(t)$ can be obtained according to Eq. 2. In principle, if a material

is truly linearly viscoelastic, Eq. 1 with $J(t)$ determined from Eq. 2 can be used to predict the creep behavior of the material under any kind of uniaxial loading history. However, this is not always true when the material is subjected to a more complex loading history.

In this report, the time-dependent properties of asphalt concrete are investigated under multiple-step loading histories, including several cyclic loading histories, in an effort to verify the applicability of linear viscoelastic theory in predicting the creep behavior under multiple-step loadings and also to construct a workable constitutive equation to describe more closely the time-dependent behavior of asphalt concrete under time-dependent loading histories.

In this report, the emphasis is also placed on distinction between the recoverable and irrecoverable creep under loading. This is important from a practical viewpoint because the irrecoverable creep strain contributes a large portion of the creep strain of asphalt concrete under external loading, and the irrecoverable strain is accumulative under repeated loading, whereas the recoverable creep is not necessarily.

MATERIALS AND SPECIMENS

A single asphalt mixture was utilized for the investigations. The asphalt cement used in preparing test specimens was from the American Oil Co. with 85 to 100 penetration grade. The asphalt content was 9 percent by weight. The gradation of aggregates is shown as follows:

<u>Sieve Size</u>	<u>Percentage Passing</u>
$\frac{3}{8}$ in.	100
No. 4	95.0
No. 8	60.0
No. 16	33.0
No. 50	15.0
No. 200	6.0

The test specimens used in this study were made of compressed asphalt concrete cylinders 2-in. in diameter and 3-in. in length. The asphalt mixture was pressed in a 2-in. diameter mold at 3,000 psi for 5 min at a temperature of 220 F. The specimens were cured in an oven at 140 F for 72 hours prior to the testing. Also, the randomness of the strain response of each specimen was minimized by subjecting each specimen to a 50-psi prestress for 12 min.

EXPERIMENTAL APPARATUS PROCEDURES

The basic test equipment shown in Figure 1 consists of a rigid frame A, a loading head B, a 1-to-10 ratio loading lever C, and the deformation measuring devices. A linear variable differential transducer (LVDT) was used to measure the deformation of the specimen. The output from LVDT, which is directly related to the total deformation, could be automatically recorded on a strip-chart recorder.

During the test, the specimen was placed directly under the loading head, and the LVDT was properly set. A selected dead weight was then put on the loading lever to produce a constant load on the specimen. The temperature during the test was kept at 75 ± 2 F.

RESULTS AND ANALYSIS

Nine tests at three stress levels (10, 30, and 50 psi) were performed on prestressed samples. Duration of the loading period varied from 10 to 1,000 sec (i.e., 10, 100, and 1,000 sec). The results of the constant stress creep tests at three stress levels at three loading periods are shown in Figures 2, 3, and 4. Each solid line is the average of several repeated test results. In these figures, the recovery strains following each creep test are also shown.

Using Eq. 2, we can obtain the creep compliance $J(t)$ as follows. Once the creep

Figure 1. Basic equipment for unconfined compressive creep test.

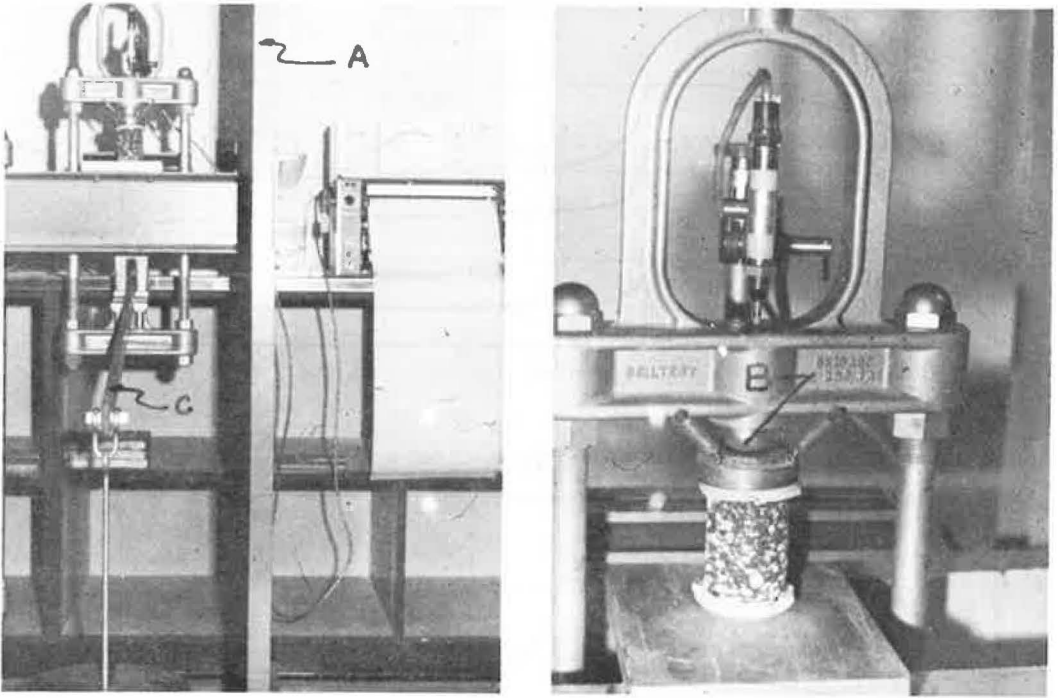


Figure 2. Creep and recovery of constant stress creep tests ($t_i = 10$ sec).

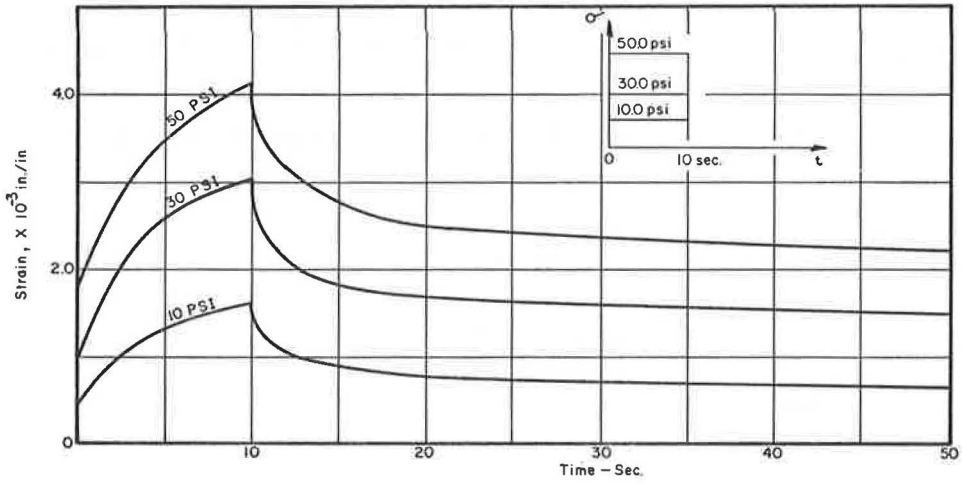


Figure 3. Creep and recovery of constant stress creep tests ($t_i = 100$ sec).

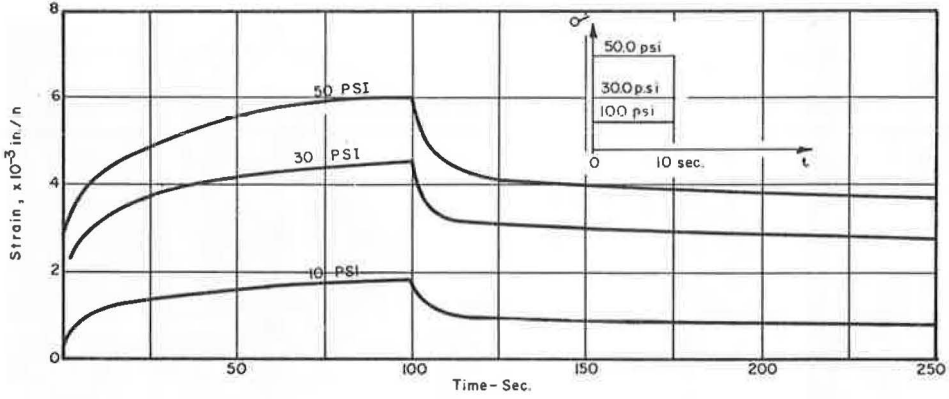


Figure 4. Creep and recovery of constant stress creep tests ($t_i = 1,000$ sec).

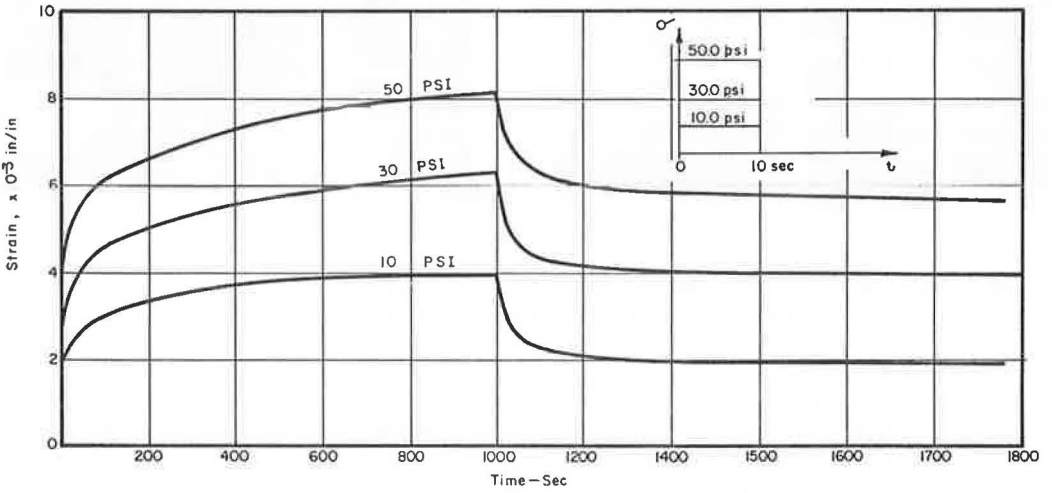
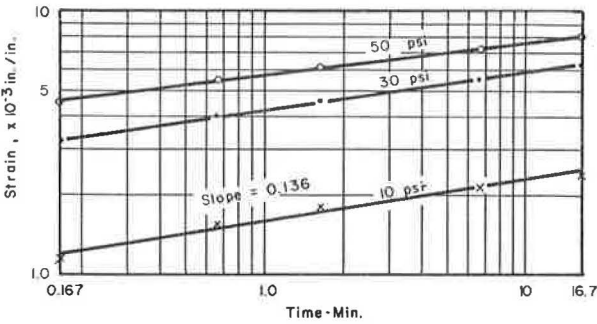


Figure 5. Constant stress creep curves plotted in log-log scale.



curves on the log-strain versus log-time base were replotted, they appeared to be straight lines as shown in Figure 5. Because the straight lines at three stress levels (Fig. 5) have nearly the same slope (0.136), the creep behavior could be expressed in the following form:

$$\epsilon_r(t) = A_r t^{n_T} \quad (3)$$

where ϵ_r is the total creep strain, and A_r is the strain at unit time ($t = 1$ min). The fact that A_r varies with stress can be seen by cross-plotting the strain values at $t = 1$ min of Figure 5 and the stress as shown in Figure 6 (open circles) and can be represented by the following relation:

$$\left. \begin{aligned} \epsilon_r(t) &= A_r(\sigma) t^{n_T} \\ A_r(\sigma) &= a_1 \sigma + a_2 \sigma^2 \\ a_1 &= 0.159 \times 10^{-3} \\ a_2 &= -0.857 \times 10^{-6} \end{aligned} \right\} \quad (4)$$

The creep compliance $J(t)$, which is defined as $\frac{\epsilon(t)}{\sigma_0}$, can be obtained from Eq. 4 as follows:

$$J(t) = (a_1 + a_2 \sigma) t^{n_T} \quad (5)$$

In view of Eq. 4 or 5, the asphalt concrete exhibits nonlinear behavior. Although a more popular form of power-law representation, such as σ^n , can be used as accurately as Eq. 4 to represent the stress dependence of A_r , this type of representation violates the basic invariance requirements as imposed from the continuum mechanics standpoint. Furthermore, Eq. 4 can be extended readily to represent the creep behavior under multiple stress states (11), whereas the power-law representation cannot.

Because the asphalt concrete was found to be nonlinear from the constant stress creep test, the second linearity requirement, the linear superposition principle, is not applicable any more. However, the modified superposition method (9-13) has been used to describe the nonlinear creep behavior and has been shown to be applicable in describing the creep behavior under arbitrary loading from the constant stress creep test results of many nonlinear viscoelastic materials. This modified superposition method is employed here to describe the recovery behavior. The modified superposition method yields the following form (9) for the recovery after constant stress creep:

$$\epsilon_r(t) = \epsilon[\sigma(t)] - \epsilon[\sigma(t - t_1)] \quad (6)$$

$t > t_1$

where $\epsilon[\sigma(t)]$ represents the creep strain under constant stress input, such as Eq. 4, and t_1 the unloading time. Inserting Eq. 4 into Eq. 6 yields

$$\epsilon_r(t) = (a_1 \sigma + a_2 \sigma^2) \left[t^{n_T} - (t - t_1)^{n_T} \right] \quad (7)$$

For n_T less than 1, as shown in Eq. 4 for the asphalt concrete, Eq. 7 predicts that the recovery strain approaches zero. The recovery curves shown in Figures 2, 3, and 4 indicate, however, a large irrecoverable strain (permanent set). Apparently Eq. 7 is not capable of describing the recovery behavior because either the modified superposition principle is not applicable for this material or Eq. 4, determined from the constant stress creep test results, does not represent the actual constitutive relation of the material. Therefore, an attempt was made using both the creep curves and the recovery curves of Figures 2, 3, and 4 to obtain a better representation of the constitutive relation of the material.

Because of the large portion of the unrecoverable strain of each creep test and because the amount of unrecoverable strain is dependent on the length of the loading period,

Figure 6. Creep strain-stress at unit time.

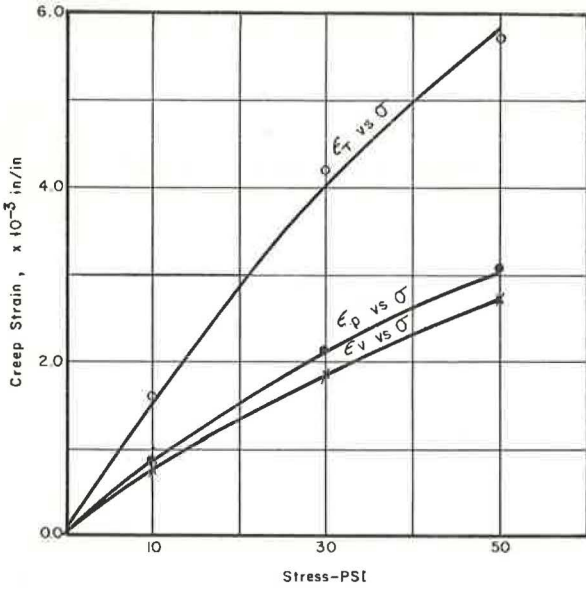


Figure 7. Nonlinear generalized Kelvin model.

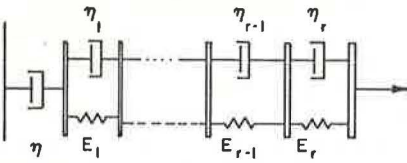
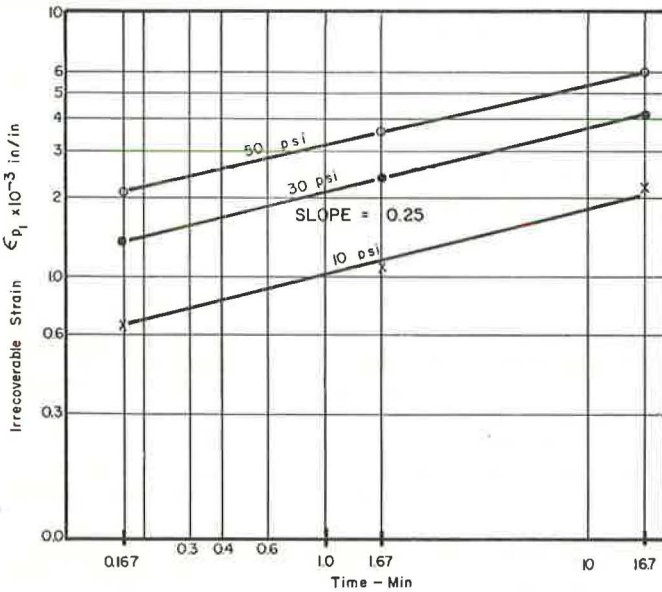


Figure 8. Irrecoverable strain versus time.



the creep behavior may be represented by a generalized nonlinear Kelvin model as shown in Figure 7. Here, the nonlinear dashpot may contribute to the irrecoverable strain, and the series of Kelvin models (Kelvin chain) may contribute to the power-law creep behavior (11). Therefore, the total creep strains (ϵ_T) of each test were separated into two parts, the irrecoverable strains (ϵ_p) due to the nonlinear dashpot and the completely recoverable strains (ϵ_v) due to the nonlinear Kelvin chain. The irrecoverable strains versus the length of the loading period (10, 100, and 1,000 sec) at each stress level on a log-log scale were plotted to form three straight lines as shown in Figure 8. Because these three straight lines have nearly the same slope of 0.25, the following expression can be obtained for irrecoverable strains:

$$\epsilon_p(t) = A_p t^{n_p} \quad (8)$$

Again, by cross-plotting the ϵ_p at $t = 1.0$ min and the stress as shown in Figure 6 (closed circles) and using the stress polynomial to fit those points, we can obtain the following equation:

$$\left. \begin{aligned} \epsilon_p(t) &= (b_1 \sigma + b_2 \sigma^2) t^{n_p} \\ b_1 &= 0.0844 \times 10^{-3} \\ b_2 &= -0.454 \times 10^{-6} \\ n_p &= 0.25 \end{aligned} \right\} \quad (9)$$

The rate of the irrecoverable strain $\dot{\epsilon}_p$ can be obtained from Eq. 9 as follows:

$$\dot{\epsilon}_p(t) = n_p (b_1 \sigma + b_2 \sigma^2) t^{n_p-1} \quad (10)$$

Instead of using Eq. 10, it was found that the "strain hardening theory" that relates the rate of the irrecoverable strain to the current stress and irrecoverable strain yielded a better description of the irrecoverable strain. The rate of the irrecoverable strain can be obtained by eliminating the time variable from Eqs. 7 and 10, which yields

$$\dot{\epsilon}_p(t) = n_p (b_1 \sigma + b_2 \sigma^2)^{1/n_p} \epsilon_p^{(n_p-1)/n_p} \quad (11)$$

or

$$\dot{\epsilon}_p(t) = \eta(\sigma, \epsilon_p) \sigma \quad (12)$$

$$\eta(\sigma, \epsilon_p) = n_p \left[\frac{1}{\sigma} (b_1 \sigma + b_2 \sigma^2)^{1/n_p} \right] \epsilon_p^{(n_p-1)/n_p} \quad (12a)$$

Equations 12 and 12a show that the dashpot is nonlinear and that the "coefficient of viscosity" η is dependent on the stress and the irrecoverable strain.

The recoverable strains ϵ_v due to the Kelvin chain were then obtained by subtracting the irrecoverable strains ϵ_p from the total strains ϵ_T . Thus, the total creep strains were separated into the recoverable part and the irrecoverable part.

Again, by using the same technique of plotting the ϵ_v versus time in the log-log scale, as shown in Figure 9, and cross-plotting in Figure 6, we can express the recoverable strains in the following form:

$$\left. \begin{aligned} \epsilon_v(t) &= (C_1 \sigma + C_2 \sigma^2) t^{n_v} \\ C_1 &= 0.0748 \times 10^{-3} \\ C_2 &= -0.412 \times 10^{-6} \\ n_v &= 0.093 \end{aligned} \right\} \quad (13)$$

The constitutive relation for the asphalt concrete using the generalized Kelvin model is summarized as follows for the constant stress creep:

$$\epsilon_{\tau}(t) = \epsilon_p(t) + \epsilon_v(t) \quad (14)$$

where ϵ_p is given by Eq. 12, and ϵ_v is given by Eq. 13. For the time-dependent stress input, the following equation is utilized:

$$\epsilon_{\tau}(t) = \int_0^t \dot{\epsilon}_p(\xi) d\xi + \int_0^t (t - \xi)^{n_v} [C_1 + 2C_2\sigma(\xi)] \dot{\sigma}(\xi) d\xi \quad (15)$$

In Eq. 15, the modified superposition method was again used (in the second integral) to describe the recoverable part of the creep strains under time-dependent stress input (10, 11, 12).

RESULTS AND PREDICTION OF CREEP UNDER MULTIPLE-STEP LOADING

In order to test and improve the application of Eq. 15 to the creep behavior of the asphalt concrete, we performed four multiple-step loading creep tests. The results are shown in Figures 10 through 13.

Equations 12, 13, and 15 were utilized to predict the creep behavior under multiple-step loading as follows. The stress inputs of the multiple steps can be expressed in a single algebraic equation using the Heaviside's unit function

$$\sigma(t) = \sum_{i=0}^n (\sigma_i - \sigma_{i-1}) H(t - t_i) \quad (15a)$$

where $H(t - t_i)$ is the Heaviside's unit function, which has the value of 1 when $t \geq t_i$, 0 when $t < 0$, $\sigma_{-1} = 0$, and $t_0 = 0$. Inserting Eq. 15a into Eq. 15, after performing the integration, yields the following for the total strain at each loading step where

$$\epsilon_{\tau}(t) = \epsilon_p(t) + \epsilon_v(t) \quad (16)$$

For $0 < t < t_1$,

$$\epsilon_p(t) = [(b_1\sigma_0 + b_2\sigma_0^2)^{1/n_p} t]^{n_p} \quad (17a)$$

$$\epsilon_v(t) = (C_1\sigma_0 + C_2\sigma_0^2) t^{n_v} \quad (17b)$$

For $t_1 < t < t_2$,

$$\epsilon_p(t) = [(b_1\sigma_0 + b_2\sigma_0^2)^{1/n_p} t_1 + (b_1\sigma_1 + b_2\sigma_1^2)^{1/n_p} (t - t_1)]^{n_p} \quad (18a)$$

$$\begin{aligned} \epsilon_v(t) = & (C_1\sigma_0 + C_2\sigma_0^2) [t^{n_v} - (t - t_1)^{n_v}] \\ & + (C_1\sigma_1 + C_2\sigma_1^2) (t - t_1)^{n_v} \end{aligned} \quad (18b)$$

For $t_{r-1} < t < t_r$, $r = 1, 2, 3, \dots$,

$$\begin{aligned} \epsilon_p(t) = & [(b_1\sigma_0 + b_2\sigma_0^2)^{1/n_p} t_1 + \dots + (b_1\sigma_{r-2} + b_2\sigma_{r-2}^2)^{1/n_p} (t_{r-1} - t_{r-2}) \\ & + (b_1\sigma_{r-1} + b_2\sigma_{r-1}^2)^{1/n_p} (t - t_{r-1})]^{n_p} \end{aligned} \quad (19a)$$

Figure 9. Recoverable strain versus time.

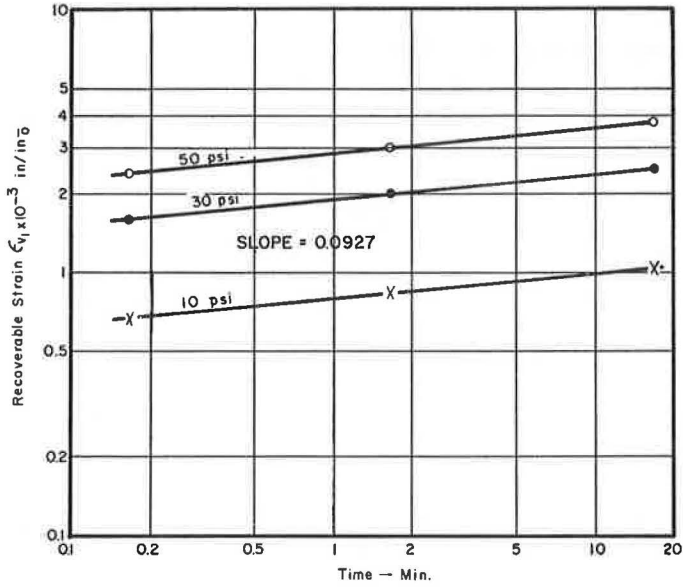


Figure 10. Results and predictions of creep behavior under step loading.

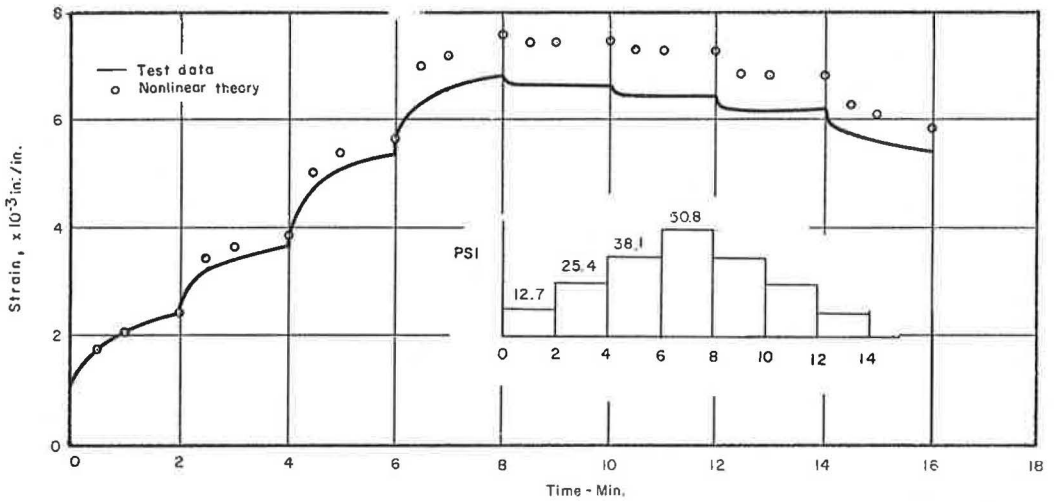


Figure 11. Results and predictions of creep behavior under step loading.

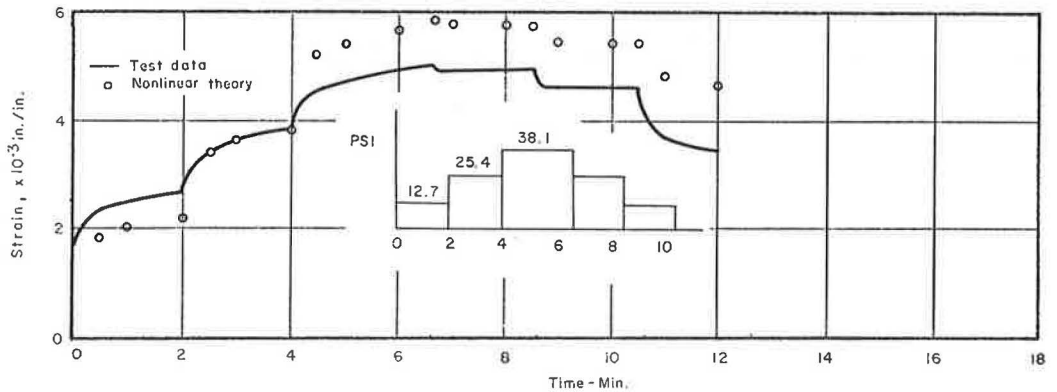


Figure 12. Results and predictions of creep behavior under step loading.

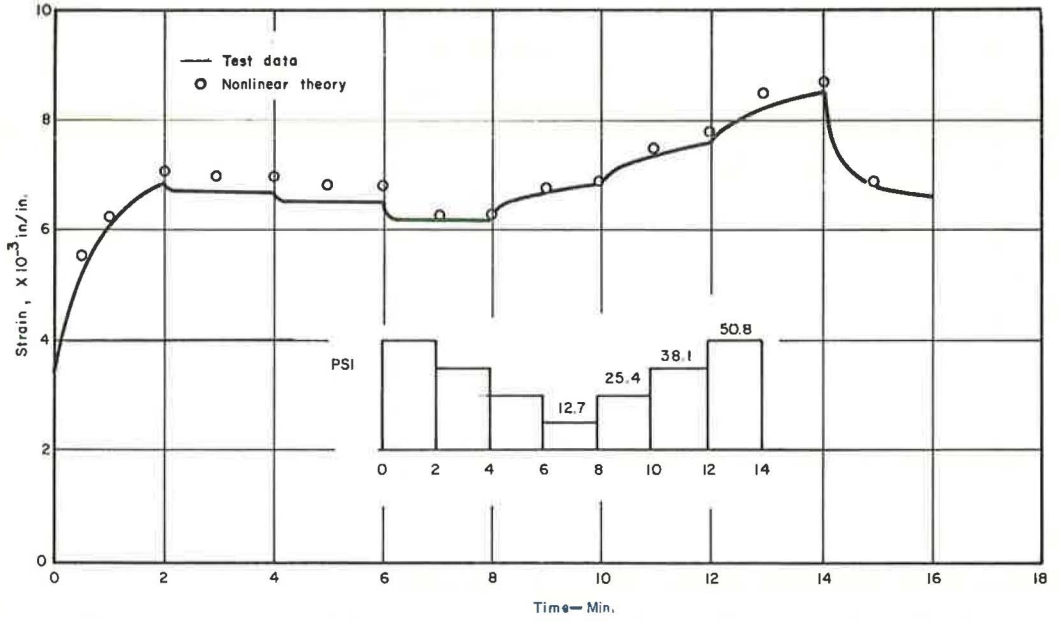
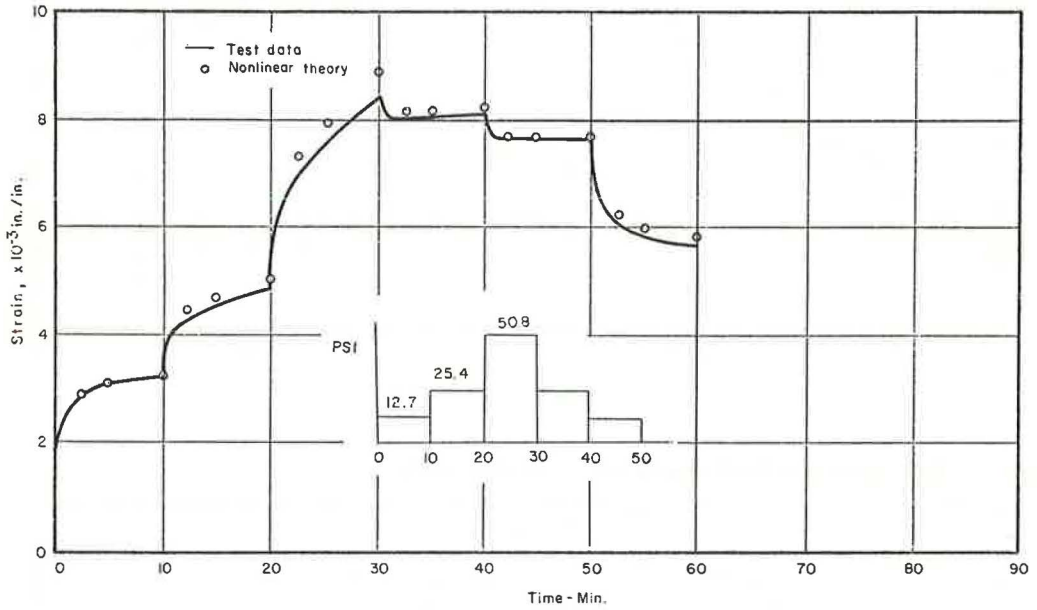


Figure 13. Results and predictions of creep behavior under step loading.



$$\begin{aligned} \epsilon_v(t) = & (C_1\sigma_0 + C_2\sigma_0^2) [t^{n_v} - (t - t_1)^{n_v}] + \dots \\ & + (C_1\sigma_{r-2} + C_2\sigma_{r-2}^2) [(t - t_{r-2})^{n_v} - (t - t_{r-1})^{n_v}] \\ & + (C_1\sigma_{r-1} + C_2\sigma_{r-1}^2) (t - t_{r-1})^{n_v} \end{aligned} \quad (19b)$$

By adding the predicted irrecoverable strains ϵ_p and the predicted recoverable strains ϵ_v , the predicted total creep strains ϵ_r under multiple-step loading can be obtained and are shown as the open circles in Figures 10 through 13 together with the experimental results that are depicted by the solid lines. The overall comparisons are quite satisfactory.

RESULTS AND PREDICTION OF CREEP UNDER REPEATED LOADING

The theory for a loading-unloading type of input was tested by loading specimens for 1 min and allowing them to recover in an unloaded state for 3 min before reloading. Cycles of this type were applied to specimens of 10, 20, 30, 40, and 50 psi, up to eight cycles. In addition, a 40-psi, 100-cycle repeated test was also conducted. The results are shown in Figures 14 through 19.

Again, using Eqs. 15, 19a, and 19b, the creep strains under the repeated loading were calculated as shown in Figures 14 through 18 for the eight-cycle tests. The theory predicts well for both the loading period and the unloading period of each cycle, though no deviation was observed in the recovery period.

These periodic loading tests are particularly important in the evaluation of asphalt concrete because pavements are constantly subjected to a similar loading pattern. Traffic passing over the pavement creates a loading period that is followed by an unloaded period. The loading time and stress are of primary importance to the total creep strain; thus, heavier, slower moving traffic causes greater "permanent" deformation. Although the total strain (or the shape of the total creep strain output with each loading cycle) is interesting and in many ways useful, the main concern when dealing with this type of material and stress pattern must lie not with the recoverable portion but with the irrecoverable strain introduced with each cycle. It can be seen from Figures 20 and 21 that the irrecoverable portion causes the accumulation of the total strain. Therefore, when the material is subjected to a large number of cyclic loadings, it may seem justified to deal mainly with expressions for the irrecoverable strain and to neglect the recoverable strain. In Figure 20, the theoretical and the experimental total strains and the irrecoverable strains at the end of each loading cycle were plotted against the number of cycles. The difference between total strain and the irrecoverable strain, which equals the recoverable, is small in comparison with the total strain or the irrecoverable strain. This figure also points out the range in which the theory is applicable. The increase in strain for each cycle remains fairly constant up to approximately 60 cycles. At this point, the rate begins to increase, and more deformation is observed with each cycle than in the previous cycle as shown in Figures 19 and 20. This is also where the theory and the observed strains begin to differ, leading to the conclusion that the equations predict the output within about 2.2 percent strain in this case, which is reached at about 60 cycles. A significant change in the shape of the specimen was also observed at about 60 cycles. The sample began to take on a barrel shape, increasing the cross-sectional area and most likely weakening a great deal of the internal bonds. In the region lower than 2.2 percent strain, where the increase in total deformation from one cycle to the next remains nearly constant, the cycles are very uniform in shape. Both the loading and recovery periods, after the first few cycles, demonstrate constant strain rates and magnitudes.

By letting N be the cycle number, Δt be the duration of the loading period of each cycle, and σ_0 be the constant stress at the load period, Eq. 19a becomes

$$\epsilon_p = (b_1\sigma_0 + b_2\sigma_0^2) [N(\Delta t)]^{n_p} \quad (20)$$

where ϵ_p represents the irrecoverable strains at the end of the N th loading cycle. The parameters contribute to the buildup of the irrecoverable strain, which is shown in

Figure 14. Results and predictions of creep behavior under cyclic loading (10-psi stress amplitude).

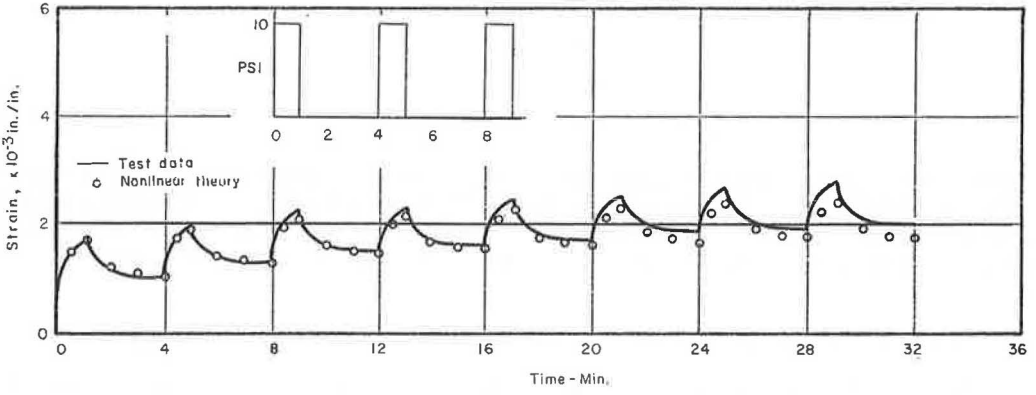


Figure 15. Results and predictions of creep behavior under cyclic loading (20-psi stress amplitude).

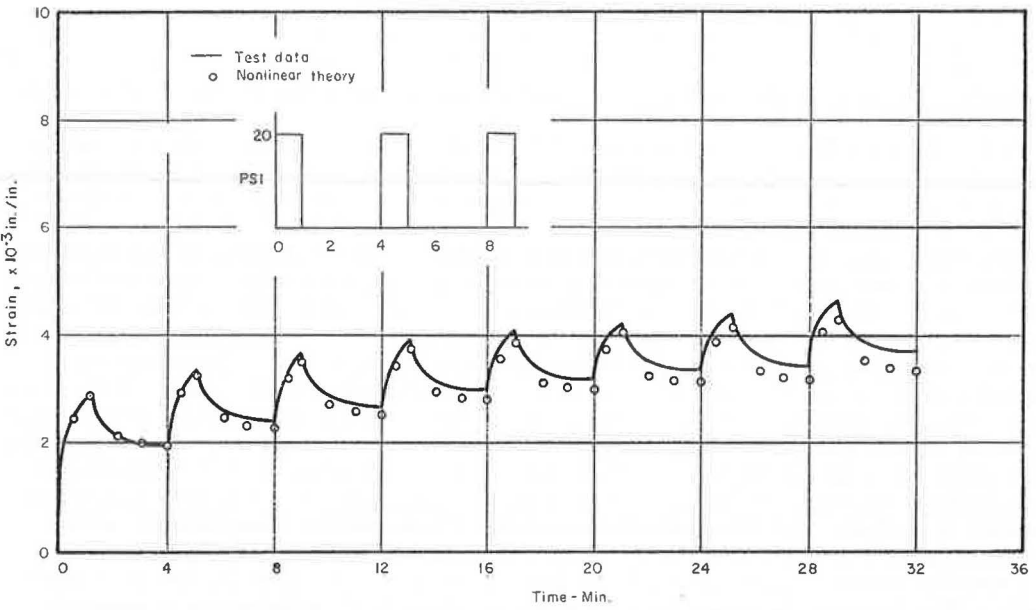


Figure 16. Results and predictions of creep behavior under cyclic loading (30-psi stress amplitude).

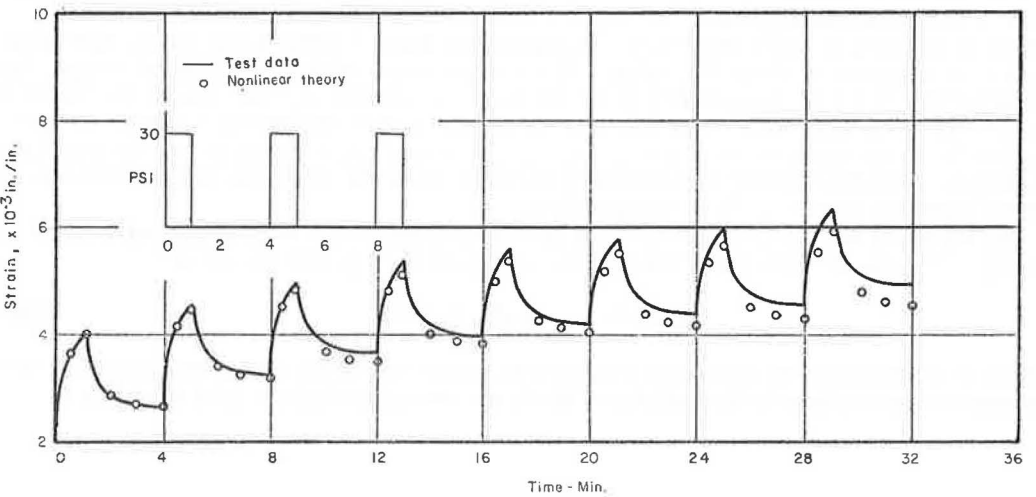


Figure 17. Results and predictions of creep behavior under cyclic loading (40-psi stress amplitude).

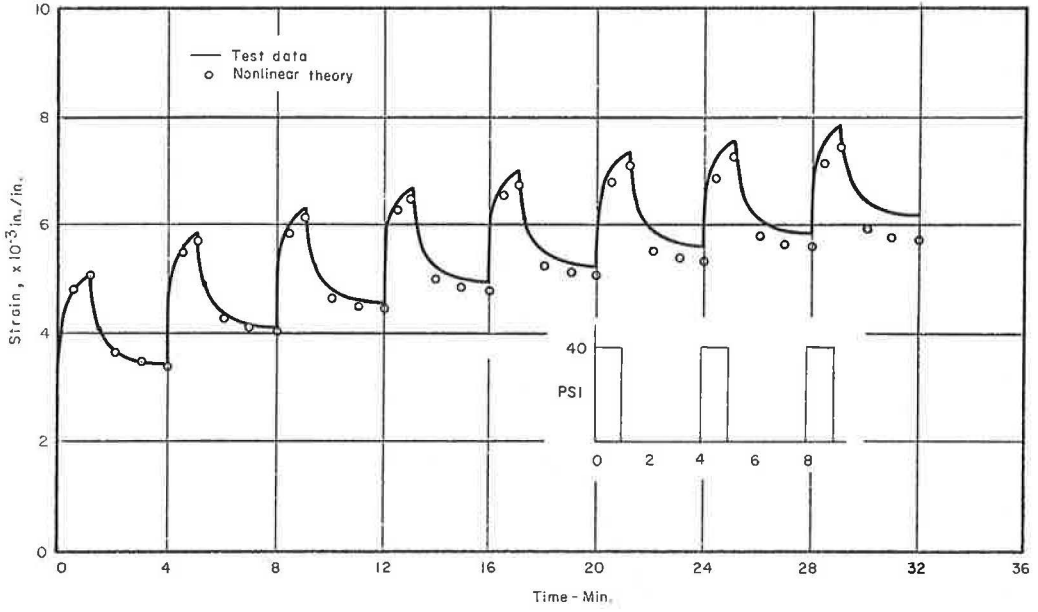


Figure 18. Results and predictions of creep behavior under cyclic loading (50-psi stress amplitude).

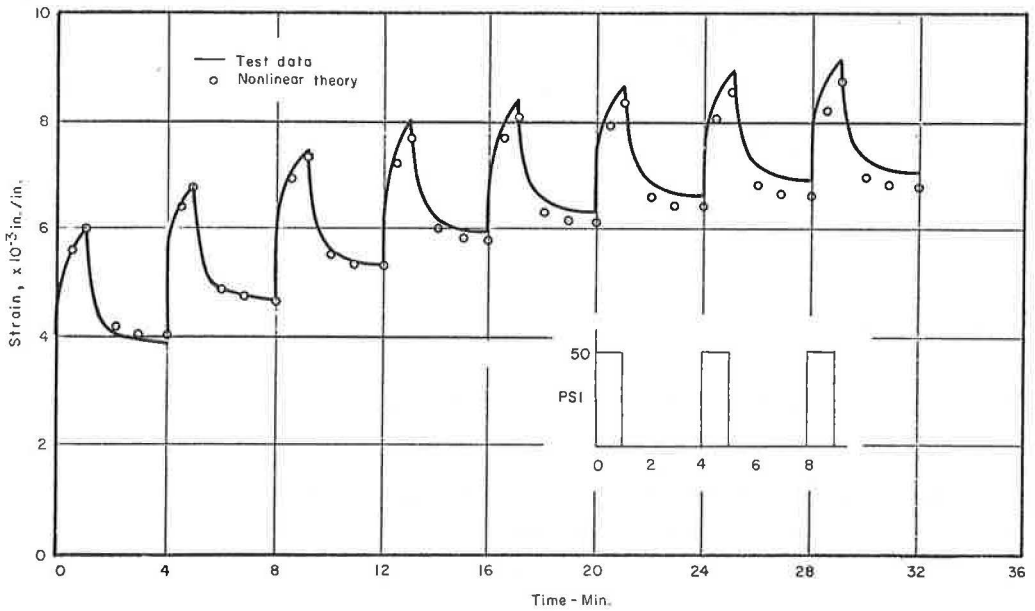


Figure 19. Results and predictions of creep behavior under cyclic loading (40-psi stress amplitude, 100 cycles).

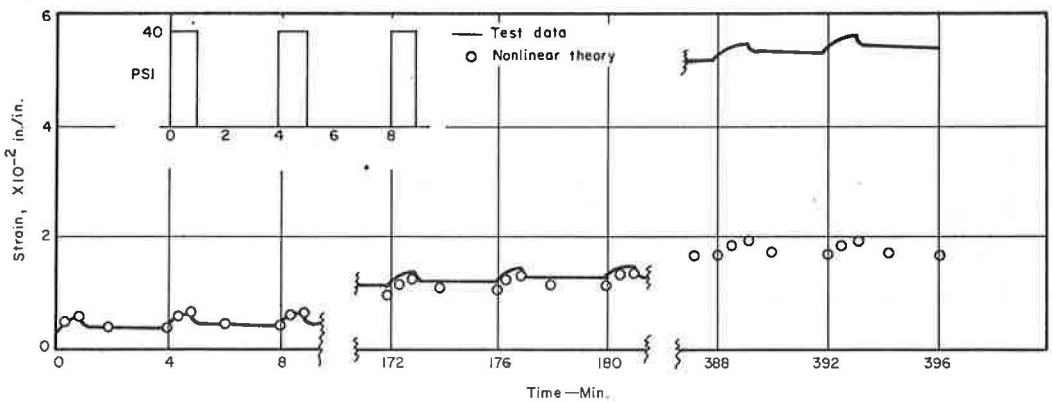


Figure 20. Irrecoverable and theoretical strains versus cycle number.

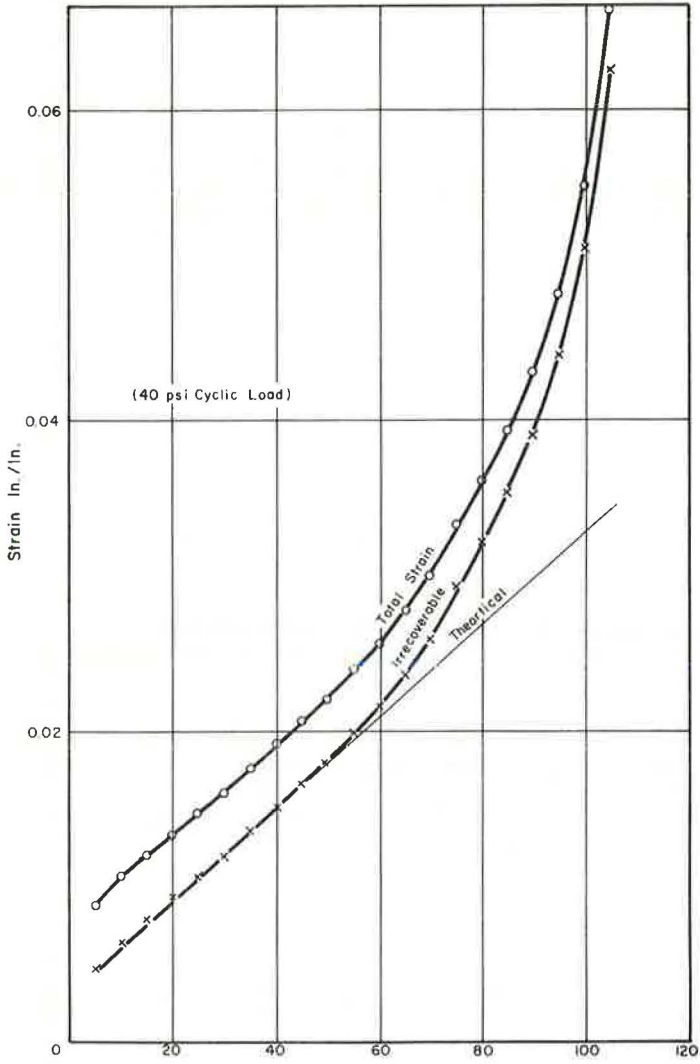
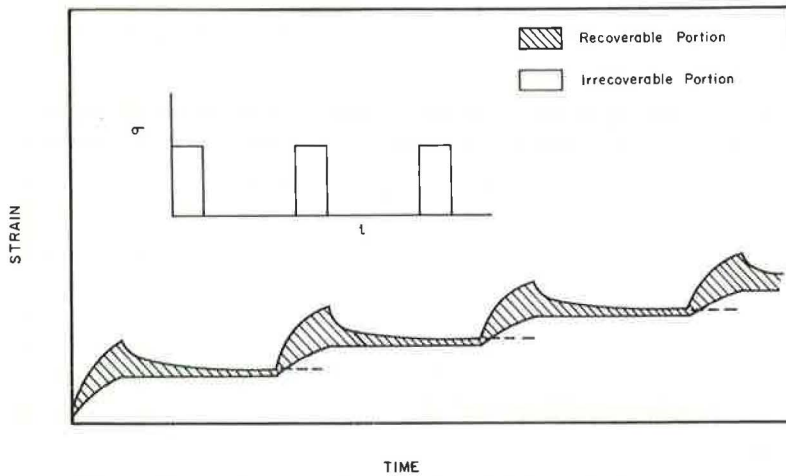


Figure 21. Irrecoverable and recoverable portions of total strain in a repeated loading test.



Eq. 20. Furthermore, if the maximum strain ϵ_{\max} (as approximated by the $\epsilon_{p\max}$) is chosen to be the failure criterion of a material, Eq. 20, after rewriting into the following form, implies that

$$N = \frac{1}{(\Delta t)} \left(\frac{\epsilon_{p\max}}{b_1 \sigma + b_2 \sigma^2} \right)^{1/n_p} \quad (21)$$

The longer the loading time during each cycle and the larger the stress amplitude are, the fewer the number of cycles the material can withstand. Although Eq. 21 is derived from the viscoelastic characterization of asphalt concrete, some similar conclusions, such as the effect of load duration, effect of ultimate strain (tensile strain), and magnitude of stress amplitude on the fatigues life of asphalt concrete, have been reached in other fatigue studies (14, 15).

CONCLUSION

It has been shown that the nonlinear viscoelastic behavior of an asphalt concrete can be represented by a nonlinear generalized Kelvin model that is made of a nonlinear dashpot connected in series with a nonlinear Kelvin chain. The nonlinear dashpot accounts for the time-dependent irrecoverable strain (viscous flow), and the nonlinear Kelvin chain accounts for the power-law time-dependent recoverable strain. It has been shown that the constitutive equation can be determined relatively simply by utilizing both the creep and recovery parts of the constant stress creep test results. The accuracy in predicting the creep behavior of the asphalt concrete under multiple-step loading and repeated loadings using the proposed constitutive equation is very satisfactory.

It has also been shown that an equation relating the number of cycles to failure to the applied stress amplitude and the duration of each cycle similar to the existing fatigue theories can be derived from the irrecoverable creep strains. It is hoped that this study will lead to a better understanding of the time-dependent behavior of asphalt concrete.

In this report, only a single asphalt concrete mixture was utilized for the investigations, which were conducted under only one temperature ($75 \pm F$). Though it is anticipated that varying the mixtures and the testing temperatures would definitely affect the creep behavior of asphalt concrete, some of the preliminary experimental results indicate that the difference of the creep behavior of different asphalt concrete mixtures at different temperatures (above the glass transition temperature) is more quantitative than qualitative.

REFERENCES

1. Secor, K. E., and Monismith, C. L. Analysis of Triaxial Test Data on Asphalt Concrete Using Viscoelastic Principles. HRB Proc., Vol. 40, 1961, pp. 259-314.
2. Monismith, C. L., and Secor, K. E. Viscoelastic Behavior of Asphalt Concrete Pavements. Proc. Internat. Conf. on the Structural Design of Asphalt Pavements, Univ. of Michigan, 1963.
3. Pagen, C. A. An Analysis of the Thermorheological Response of Bituminous Concrete. Ohio State Univ., PhD thesis, 1963.
4. Fitzgerald, J. E., and Lai, J. S. Initial Evaluation of the Effect of Synthetic Rubber Additives on the Thermorheological Properties of Asphalt Mixtures. Highway Research Record 313, 1970, pp. 18-31.
5. Pagazian, H. S. The Response of Linear Viscoelastic Materials in the Frequency Domain With Emphasis on Asphalt Concrete. Proc. Internat. Conf. on the Structural Design of Asphalt Pavement, Univ. of Michigan, 1962.
6. Pagen, C. A. Rheological Response of Bituminous Concrete. Highway Research Record 67, 1965, pp. 1-26.
7. Kallas, B. F., and Riley, S. C. Mechanical Properties of Asphalt Pavement Materials. Proc. Second Internat. Conf. on the Structural Design of Asphalt Pavements, Univ. of Michigan, 1967.

8. Swami, S. A., Goetz, W. H., and Harr, M. E. Time and Load Independent Properties of Bituminous Mixtures. Highway Research Record 313, 1970, pp. 63-78.
9. Findley, W. N., and Lai, J. S. A Modified Superposition Principle Applied to Creep of Nonlinear Viscoelastic Material. Trans. Soc. of Rheology, Vol. 11, No. 2, 1967, pp. 361-380.
10. Lai, J. S., and Findley, W. N. Stress Relaxation of Nonlinear Viscoelastic Material Under Uniaxial Strain. Trans. Soc. of Rheology, Vol. 12, No. 2, 1968, pp. 259-280.
11. Findley, W. N., Lai, J. S., and Onaian, K. Creep and Stress Relaxation of Nonlinear Viscoelastic Materials. To be published.
12. Pipkin, A. C., and Rogers, T. G. A Nonlinear Integral Representation for Viscoelastic Behavior. Jour. of Mechanics and Physics of Solids, Vol. 16, 1968, pp. 59-72.
13. Stafford, R. O. On Mathematical Forms for the Material Functions in Nonlinear Viscoelasticity. Jour. Mechanics and Physics of Solids, 1969, pp. 339-358.
14. Deacon, J. A. Materials Characterization—Experimental Behavior. HRB Spec. Rept. 126, 1971, pp. 150-179.
15. Finn, F. N. Factors Involved in the Design of Asphalt Pavement Surfaces. NCHRP Rept. 39, 1967, 112 pp.

RAPID DETERMINATION OF ASPHALT CONTENT USING PENNSYLVANIA PYCNOMETER

Prithvi S. Kandhal, William C. Koehler, and Monroe E. Wenger,
Pennsylvania Department of Transportation

This paper describes the development and testing of the Pennsylvania pycnometer proposed for rapid determination of asphalt content. The method is based on the procedures of ASTM D2041-67, which have been modified to achieve greater accuracy and precision essential for asphalt content determinations. The Pennsylvania pycnometer has been found to be practical in use and free of operating inconveniences. Asphalt content is determined in approximately 30 min by weight-volume relation and by the aid of nomographs. Paving mixtures containing limestone, sand, gravel, and slag aggregates have been tested for asphalt content. Results are compared to those obtained by use of the reflux equipment. The test data have been analyzed statistically. Greater accuracy is indicated in the results obtained by the Pennsylvania pycnometer. For highly absorptive aggregates, which present problems in complete retrieval of the asphalt, the pycnometer method has better proficiency than the reflux method.

•ASPHALT content is one of the most important factors in the overall quality of asphaltic concrete pavements. As little as 0.5 percent too much asphalt can cause flushing and rutting; an asphalt deficiency of 0.5 percent may cause premature cracking or raveling of the pavement. Thus, a close control of asphalt content is essential for optimum durability and serviceability. The amount of asphalt cement is also important economically because it is the most expensive ingredient in the mix.

Current methods for quantitative extraction of bitumen from bituminous paving mixtures (AASHTO T 164-70) consist of four procedures. Although these procedures are relatively simple and have been used for many years, they are extremely time-consuming to perform, and the results obtained are often of questionable value. With the high production capacity of modern asphalt plants, it is essential that test methods be available that can provide an accurate measure of asphalt content within minutes if a meaningful degree of control is to be employed. It is not uncommon for a modern plant to produce 100 to 200 tons of mixture per hour. Therefore, one can readily visualize the possible difficulties that could arise if 3 or 4 hours were required to obtain a test result. The problem could be complicated even further if a check test or tests are necessary. By this time, several hundred tons of mixture would be laid and compacted, thereby making appropriate adjustments in asphalt content impossible for the mixture already placed on the grade.

There is need, therefore, to devise a method that can strike a proper balance among accuracy of test results, cost of equipment, speed with which the test can be performed, and technician training required. To be of optimum value, such a method must be readily adaptable to both laboratory and field use.

REVIEW OF LITERATURE

Various methods (1, 2) have been investigated for extracting asphalt from asphaltic concrete, some of which were adopted as ASTM or AASHTO standard tests subsequently. Besides being time-consuming, these methods have too much variation in the asphalt content results. Steele and Krieger (3) conducted statistical evaluation of equipment and operator effects on the results of asphalt extraction tests and reported significant differences among operators and among laboratories.

In a study (4) undertaken by the Pennsylvania Department of Transportation in 1969 for determining the variations of results among asphalt plant laboratories, significant differences were noted.

Several improvements have been suggested to reduce the time required for extraction. Jones et al. (5) suggested vacuum extraction of asphalt from paving mixtures using methylene chloride as a reagent.

The principle of using nuclear radiation to measure the asphalt content of paving mixtures was established several years ago by Lamb and Zoller (6); since then, it has been investigated by many researchers. Some drawbacks have been reported by Hughes (7) in this method. An improved nuclear gauge for determining asphalt content in the field has also been studied recently (8).

Stain method (9) has been proposed for fine-graded asphaltic concrete mixtures, but it has several limitations such as operator technique and errors related to the amount of fines in the paving mixture. Flask method (10) requires constant attention to ensure complete dissolution of the asphalt by the solvent. The ignition method (11), in which the weight of a sample before and after removal of the asphalt by burning is used, has been reported to show an operator effect associated with the test method.

Steele and Hudson (12) attempted the asphalt content determination by weight-volume relation based on the procedure of ASTM D 2041. The research work under report is also based on the same concept, but a new apparatus and procedure have been developed and tested involving mixtures containing different types of aggregates and varying asphalt contents.

BACKGROUND AND DEVELOPMENT OF TEST APPARATUS

The concept of determining the maximum specific gravity of bituminous paving mixtures was developed by James M. Rice under the auspices of the National Crushed Stone Association. This contribution is growing in importance as the use of absorptive aggregates becomes increasingly necessary. The vacuum saturation technique employed in this method makes possible the determination of the effective specific gravities of the aggregate and both the effective and total asphalt content of the paving mixture. It has been recognized that, when the average specific gravities of the aggregate remain constant, the major factor affecting the maximum specific gravity of the paving mixture is the volume of asphalt. Under these conditions, the vacuum saturation procedure affords a rapid means for determining asphalt content.

MATHEMATICAL COMPUTATIONS

There are two parts to the required computations (12). The first part is to find the specific gravity of the asphalt-aggregate mixture and then to determine the ratio of asphalt to total mix that corresponds to this specific gravity.

The maximum specific gravity of the mixture is computed by the use of Eq. 2 in ASTM C 2041:

$$\text{Specific gravity } G_m = \frac{A}{A + D - E} \quad (1)$$

where

A = weight of specimen (mix) in air,

D = weight of pycnometer filled with water at test temperature, and

E = weight of pycnometer filled with water and specimen at test temperature.

Figure 1. Work sheet 1.

BITUMEN CONTENT OF PAVING MIXTURES—PENNSYLVANIA PYCNOMETER METHOD

Project No. _____
 Type Aggregate _____
 Mix Type _____
 Producer _____
 Plant _____
 Location _____

Line		Sample Identification				
1	Wt. Pyc. + Mix					
2	Wt. dry Pyc.					
3	(1-2) = Wt. of Mix (A)					
4	Wt. Pyc. + Water (D)					
5	Line 3 + Line 4					
6	Wt. Pyc. + Mix + Water (E)					
7	(5-6) = Vol. of voidless Mix					
8	(3 ÷ 7) = Max. Sp. Gr. of Mix, G_m					
9	($G_a \div P$)-1					
10	(J x 9) = % Bitumen					

G_a	Effective Specific Gravity - Aggregate =
G_b	Specific Gravity - Asphalt =
F	$G_a - G_b =$
J	$(100 \times G_b) \div F =$

Operator _____ Date _____
 Laboratory _____

Figure 2. Work sheet 2.

EFFECTIVE SPECIFIC GRAVITY OF AGGREGATE (G_a)

Type Aggregate _____
 Mix Type _____
 Producer _____
 Plant _____

Line			Sample Identification			
1	Line 8 (G_m) of Sheet No. 1	G_m				
2	Known % bitumen	P				
3	Sp. Gr. of bitumen	G_b				
4	Line 2 ÷ Line 3	P/G_b				
5	100.0 - Percent bitumen	$100-P$				
6	Line 1 x Line 4	$(G_m \times P)/G_b$				
7	Line 1 x Line 5	$G_m (100-P)$				
8	100.0 - Line 6	$100-G_m P/G_b$				
9	Line 7 ÷ Line 8 = Eff. Sp. Gr. G_a	G_a				

Operator _____
 Date _____

Figure 1, steps 1 through 8, can be used to solve this equation.

The relation of this specific gravity G_m to the specific gravities of the asphalt and the combined mineral aggregates, and their respective percentages in the mixture, is expressed by the following equation:

$$G_m = \frac{100}{\frac{P}{G_b} + \frac{100 - P}{G_a}} \quad (2)$$

where

G_m = specific gravity of the mixture as determined by Eq. 1,

G_b = specific gravity of the asphalt at test temperature,

G_a = effective specific gravity of the combined mineral aggregate at test temperature, and

P = percentage of total mix by weight of asphalt.

For convenience in repeated use, Eq. 2 can be rearranged algebraically (12) and written as follows:

$$P = \frac{100 G_b}{G_m - G_b} \left(\frac{G_a}{G_b} - 1 \right) \quad (3)$$

The effective specific gravity G_a of the combined aggregates is not necessarily the specific gravity as determined by standard methods. It is found experimentally by testing specimens of known asphalt content and substituting in Eq. 3 the known values of P, G_b , and G_m . G_a is determined by Eq. 1. Effective specific gravity of the aggregates can be conveniently determined by completing steps 1 through 9, Figure 2.

The first part of Eq. 3 is a constant for any particular asphalt-aggregate combination, and is computed using Figure 1. The percentage of asphalt is computed in steps 9 and 10, Figure 1.

Steele and Hudson (12) used this concept and were able to determine the asphalt content with much success, though their adaption of a vacuum dessicator as a pycnometer resulted in some operating inconveniences.

There was a need to develop an apparatus for practical use in the field as well as in the central laboratory. It was desired to have the following features to eliminate operating inconveniences and to obtain better reproducibility of the test results:

1. The pycnometer should be of such size that its manual handling to release the air bubbles is easy and convenient. A pycnometer of 4,000-ml capacity was considered to be suitable.

2. The pycnometer should be transparent, strong, and reasonably resistant to scratching. This would facilitate the observation of air bubbles while applying vacuum. Therefore, a heavy-wall glass pycnometer was considered. As compared to plastic or other material, glass is more resistant to scratching by the aggregates in the mix. Being inexpensive, it can be replaced when too much scratching is caused by prolonged use.

3. The construction of the pycnometer should be such that a stirring rod is accessible to all the areas within the pycnometer to manipulate air bubbles. The proposed Pennsylvania pycnometer (Fig. 3) has a wide mouth and a tapered shape to meet this requirement.

4. The pycnometer should be of rigid construction. Flexibility is not desirable because the pycnometer can distort under stresses when handled, introducing error in its constant volume.

5. A fine capillary stopper and overflow cap were desired to have increased precision in calibration and testing.

To meet these requirements, the authors developed the Pennsylvania pycnometer (Fig. 3) for practical use in both the field and the laboratory. The apparatus and its accessories are shown in Figure 4. Approximate total cost is \$80.00. It is possible to determine the asphalt content in approximately 30 min.

Figure 3. Pennsylvania pycnometer, 4,000-ml capacity.

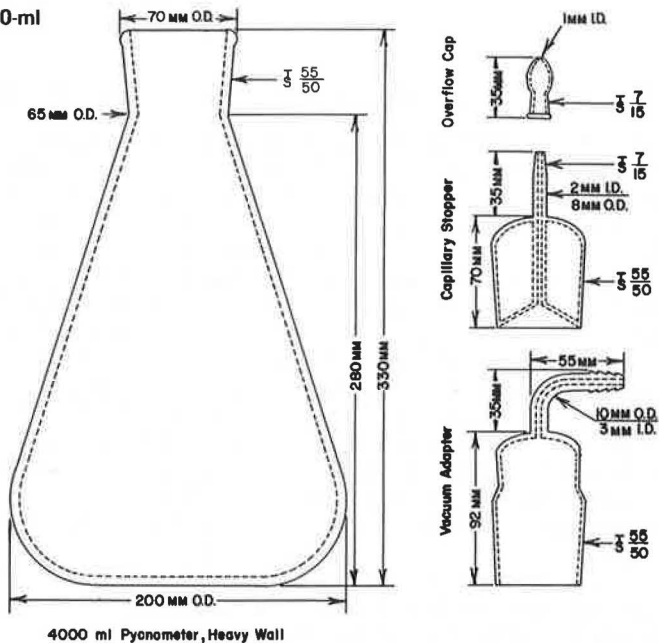


Figure 4. Pennsylvania pycnometer assembly with accessories.

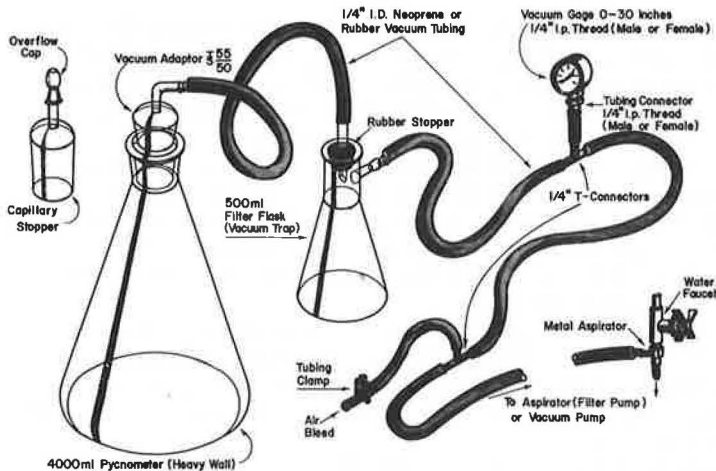


Table 1. Asphalt content test data.

Limestone			Sand and Gravel			Slag		
Actual	Extraction	Pycnometer	Actual	Extraction	Pycnometer	Actual	Extraction	Pycnometer
4.96	5.10	4.75	5.94	5.90	6.14	6.96	6.80	6.56
4.96	4.90	4.87	5.95	5.70	5.88	6.98	7.10	6.93
4.96	4.90	5.15	5.96	5.90	6.01	7.02	7.10	6.68
5.95	5.60	6.01	6.94	7.30	6.84	7.96	8.30	7.54
6.00	6.00	6.01	6.94	6.70	7.16	7.98	8.00	7.72
6.01	6.10	5.96	6.94	6.90	6.08	7.99	7.70	7.85
6.88	6.80	6.87	7.89	7.70	8.06	8.95	9.20	9.07
6.92	6.90	6.87	7.92	7.70	7.80	8.97	9.00	8.89
7.04	7.00	7.04	7.93	7.70	8.12	9.96	10.00	10.54
7.91	7.91	8.02	8.81	8.50	8.95	9.97	10.40	10.36
7.93	7.93	8.02	8.86	8.60	8.83	10.05	9.90	10.54
8.13	8.20	8.19	8.91	8.60	9.08	-	-	-
Average difference from actual	-0.026	+0.009	-0.149	-0.003	-	+0.104	-0.010	-

Note: All materials 1D-2 wearing course mixtures.

TEST PROCEDURE AND DISCUSSION OF RESULTS

The detailed test procedure is given in the Appendix. The proposed method was attempted on Pennsylvania ID-2 and FJ-1 wearing course mixtures containing known asphalt contents. Series of mixtures were prepared with limestone, sand, gravel, and slag aggregates to check if the method is applicable to all types of aggregate. One highly absorptive sand and gravel aggregate that had posed problems in complete extraction of the asphalt was also included in the study. Quantitative extraction of asphalt from these paving mixtures was also carried out by AASHTO T 164-70 (method D) with some modifications. Test data on asphalt content by these two methods are given in Tables 1 and 2 together with the actual asphalt content.

For statistical comparisons, the asphalt contents obtained by the two procedures have been paired with the actual asphalt content. By using this approach, as suggested by Snedecor and Cochran (13), it is possible to discover and evaluate the differences among results rather than the results themselves. With only a single pair, it is impossible to say whether the difference in behavior is to be attributed to the difference in treatment, to the natural variability of the mixes, or partly to both. Therefore, several pairs of test data from mixtures containing different asphalt contents have been used in the statistical analysis. Besides test of significance of differences between the actual and obtained data, this analysis gives 95 percent confidence interval for the mean difference. Table 3 gives an example of detailed statistical analysis of the differences for one type of mixture.

Table 4 gives the summary of statistical analyses performed on the data (Tables 1 and 2) obtained in this study. The differences from actual asphalt contents are not significant in all cases.

From the values of mean of differences \bar{D} , it would appear that the results obtained by Pennsylvania pycnometer have greater accuracy than those by the reflux method. The negative value of \bar{D} in most cases obtained by the latter method indicates a bias that is not revealed in the pycnometer method. This is most evident in the extraction results on the mix containing highly absorptive sand and gravel aggregates.

On comparison of 95 percent confidence limits for the mean difference, it appears that the pycnometer method is more precise for the mixtures containing limestone aggregates. This can be attributed to the uniformity of limestone aggregates resulting in consistent, effective specific gravity values. The pycnometer method seems to have better precision when dealing with highly absorptive aggregates from which all the binder is difficult to retrieve by reflux method.

In case of slag and gravel aggregates, the effective specific gravity in individual samples is not as consistent as in limestone aggregates, so the results obtained by the Pennsylvania pycnometer method are less precise but still acceptable. As mentioned in the appended test method, for ± 0.01 variation in the effective specific gravity, the asphalt content will vary ± 0.1 percent.

Table 4 also gives the estimated percentage of results within ± 0.4 percent of actual asphalt contents. These results appear to indicate that the proficiency of the pycnometer method is comparable to the reflux method.

It may be mentioned that all the data reported in this study were obtained at random by three operators and include a working range of asphalt content for each type of mix. Thus, the final results reflect variability among operators and among samples. Better results would expectedly be obtained if the testing were done by a single operator on mixtures containing the same asphalt content.

CONCLUSIONS

The design features of the Pennsylvania pycnometer have proved to be practical and convenient for the operators.

Results obtained by the Pennsylvania pycnometer, using the recommended procedure, appear to have greater accuracy than those obtained by the conventional reflux method. Precision seems to be equal to or better than the reflux method for the mixtures containing limestone aggregates or highly absorptive gravel aggregates. Accord-

Table 2. Test data.

Limestone ^a			Slag ^b			Absorptive Sand and Gravel ^b			
Actual	Extraction	Pycnometer	Actual	Extraction	Pycnometer	Actual	Extraction	Actual	Pycnometer
5.93	6.00	5.94	7.99	8.10	7.58	5.20	4.90	5.50	5.90
5.97	6.10	5.83	7.99	7.90	7.64	5.20	4.80	5.50	5.70
5.98	6.10	5.66	8.01	7.90	7.98	5.20	5.00	5.50	5.40
6.71	6.70	6.69	9.00	9.20	9.19	5.20	4.90	5.50	5.40
7.01	7.30	7.09	9.04	9.10	8.67	5.20	5.00	5.50	5.90
7.01	6.90	6.97	9.06	9.20	9.30	5.20	4.80	5.50	5.80
7.95	8.00	8.17	9.92	9.90	10.39	5.20	4.80	5.50	5.30
7.95	8.00	8.06	10.00	10.00	10.34	5.20	4.70	5.50	5.40
7.95	8.00	8.00	10.06	9.90	10.17	5.20	4.90	5.50	5.60
8.87	8.60	8.80	11.00	10.80	11.31	5.20	4.90	—	—
8.91	8.80	9.03	11.05	10.40	11.08	—	—	—	—
8.98	8.80	9.20	11.11	11.00	10.68	—	—	—	—
Average difference from actual	+0.007	+0.018		-0.069	+0.008		-0.330		+0.433

^aFJ-1 wearing course mix.^bID-2 wearing course mix.

Table 3. Typical statistical analysis of differences (FJ-1 wearing course mix).

Pair Number	Actual Asphalt Content (percent)	Asphalt Concrete, Pycnometer Method (percent)	Difference, $D = X_2 - X_1$	Deviation, $d = D - \bar{D}$	Squared Deviation
1	5.93	5.94	+0.01	-0.0083	0.0001
2	5.97	5.83	-0.14	-0.1583	0.0250
3	5.98	5.66	-0.32	-0.3383	0.1144
4	6.71	6.69	-0.02	-0.0383	0.0015
5	7.01	7.09	+0.08	0.0617	0.0038
6	7.01	6.97	-0.04	-0.0583	0.0034
7	7.95	8.17	+0.22	+0.2017	0.0407
8	7.95	8.06	+0.11	+0.0917	0.0084
9	7.95	8.00	+0.05	+0.0317	0.0010
10	8.87	8.80	-0.07	-0.0883	0.0078
11	8.91	9.03	+0.12	+0.1017	0.0103
12	8.98	9.20	+0.22	+0.2017	0.0407

Note: $\bar{D} = +0.0183$ and $n = 12$. $S_d [\sum d^2 / (n - 1)]^{0.5} = [0.2751 / (12 - 1)]^{0.5} = 0.152$. $S_D = S_d / n^{0.5} = 0.152 / 12^{0.5} = 0.0439$. $t = \bar{D} / S_D = 0.0183 / 0.0439 = 0.4168$. $t_{\alpha/2, n-1} = 2.201$; 11 degrees of freedom, so differences are not significant. 95 percent confidence limits $= \bar{D} \pm t (S_D) = +0.0180 \pm 0.097 = +0.12$ and -0.08 (rounded).

Table 4. Summary of statistical analysis of differences.

Type of Mix	Analytical Method	Range of Known Asphalt Content	\bar{D}	t	$t_{\alpha/2, n-1}$	Significant Difference	95 Percent Confidence Limits	Percent Within ± 0.4 Percent of Actual
ID-2 W (limestone)	Pycnometer	4.96 to 8.13	+0.009	0.030	2.201 ^a	No	+0.07 -0.06	100
	Extraction	4.96 to 8.13	-0.026	0.745	2.201	No	+0.05 -0.10	100
FJ-1 (limestone)	Pycnometer	5.93 to 8.98	+0.018	0.417	2.201	No	+0.12 -0.08	89
	Extraction	5.93 to 8.98	+0.007	0.159	2.201	No	+0.10 -0.09	82
ID-2 W (sand and gravel)	Pycnometer	5.94 to 8.91	-0.003	0.035	2.201	No	+0.19 -0.19	82
	Extraction	5.94 to 8.91	-0.112	1.836	2.201	No	+0.29 -0.51	91
ID-2 W (slag)	Pycnometer	6.96 to 10.05	-0.010	0.092	2.228 ^b	No	+0.23 -0.25	73
	Extraction	6.96 to 10.05	+0.064	0.985	2.228	No	+0.21 -0.08	87
FJ-1 (slag)	Pycnometer	7.99 to 11.11	+0.008	0.086	2.201	No	+0.21 -0.20	73
	Extraction	7.99 to 11.11	-0.069	0.312	2.201	No	+0.02 -0.11	91
ID-2 W (absorptive sand and gravel)	Pycnometer	5.50	+0.100	1.282	2.306 ^c	No	+0.28 -0.08	88
	Extraction	5.20	-0.330	11.000	2.262 ^d	Yes	-0.26 -0.40	57

^a11 degrees of freedom.^b10 degrees of freedom.^c8 degrees of freedom.^d9 degrees of freedom.

ing to the theoretical percentage within the range of ± 0.4 from actual, the proficiency of this method is comparable to the reflux method.

In comparison to the reflux method the time required for testing by this method is appreciably reduced.

The initial cost of the Pennsylvania pycnometer is reasonable. No expenditure on solvents is involved in this method.

Use of the Pennsylvania pycnometer should be considered as a more rapid and economical means of determining asphalt content of paving mixtures.

ACKNOWLEDGMENTS

This report is the result of a research project sponsored by the Pennsylvania Department of Transportation. The opinions, findings, and conclusions expressed are those of the authors and not necessarily those of the Pennsylvania Department of Transportation.

Thanks are due to L. D. Sandvig for his encouragement and to J. R. Basso, Jr., for assisting in the development of the Pennsylvania pycnometer.

Appreciation is expressed to P. G. Kaiser for supervision of tests, Edward Macko for illustrations, and June Viozzi for compilation of data. Review of statistical analysis by R. M. Nicotera is also appreciated.

REFERENCES

1. Hubbard, F. A Cooperative Investigation of Certain Test Methods as Applied to Asphalt Concrete Mixtures. Proc. Assn. of Asphalt Paving Technologists, Vol. 18, 1949.
2. Wood, J. E. A Method of Extracting Asphalt From Large Samples of Asphaltic Concrete. Proc. Assn. of Asphalt Paving Technologists, Vol. 18, 1949.
3. Steele, G. W., and Krieger, F. L. Statistical Evaluation of Equipment and Operator Effects on the Results of Asphalt Extraction Tests. Proc. Assn. of Asphalt Paving Technologists, Vol. 36, 1967.
4. Schmidt, G. H., and Wenger, M. E. Experimental Extraction of Bitumen. Pennsylvania Dept. of Transportation, Feb. 1970.
5. Jones, G. M., et al. Vacuum Extraction of Bitumen From Pavement Mixtures. ASTM STP 461, July 1969.
6. Lamb, D. R., and Zoller, J. H. Determination of Asphalt Content of Bituminous Mixtures by Means of Radioactive Isotopes. HRB Proc., Vol. 35, 1956, pp. 322-326.
7. Hughes, C. S. The Use of a Nuclear Asphalt Content Gauge. ASTM STP 461, July 1969.
8. Klotz, R. C. Asphalt Content Determination Using Nuclear Techniques. Pennsylvania Dept. of Transportation, Res. Proj. 70-13, March 1972.
9. Smith, W. F. The Supplementing of Laboratory Control of Hot Mix Plants by Simple Manual Tests. Proc. Assn. of Asphalt Paving Technologists, Vol. 24, 1955.
10. Holland, L. E. Asphalt Content of Bituminous Mixtures. Paper presented at the annual meeting of ASTM, Chicago, June 1964.
11. Antrim, J. D., et al. Rapid Test Methods for Field Control of Highway Construction. NCHRP Rept. 103, 1970, 89 pp.
12. Steele, G. W., and Hudson, S. B. A Pycnometer Test Procedure for Determining Asphalt Content of Paving Mixture. ASTM STP 461, July 1969.
13. Snedecor, G. W., and Cochran, W. G. Statistical Methods. Iowa State Univ. Press, Ames, 1967.

APPENDIX

METHOD OF TEST FOR BITUMEN CONTENT OF BITUMINOUS CONCRETE MIXTURES (PENNSYLVANIA PYCNOMETER METHOD)

Scope

This method of test is intended for determining the bitumen content of bituminous concrete mixtures.

Apparatus

1. A balance sensitive to 0.1 g at the maximum weight to be determined.
2. A 4,000-ml heavy-wall glass pycnometer (Pennsylvania pycnometer) fitted with a vacuum adapter, capillary stopper, and overflow cap (Fig. 3). The pycnometer shall be sufficiently strong to withstand a partial vacuum (air pressure less than 30 mm of mercury).
3. Vacuum pump or water aspirator for evacuating air from the pycnometer.
4. Dial-type vacuum gauge (0 to 30 in. of mercury vacuum) or mercury-filled absolute pressure manometer calibrated to at least 1-mm divisions.
5. Vacuum trap consisting of a 500-ml glass filter flask fitted with a rubber stopper.
6. Tubing and connectors assembly as shown in Figure 4.
7. Constant-temperature water bath maintained at a temperature of 77 ± 0.9 F (25 ± 0.5 C).
8. Thermometer range 66 to 80 F as prescribed in ASTM specifications E-1.

Calibration of Pycnometer

Calibrate the pycnometer by accurately determining the weight of water at 77 ± 0.9 F (25 ± 0.5 C) required to fill it with the capillary stopper and overflow cap in place. Allow some water to overflow through capillary tube while inserting the capillary stopper. Make certain that the capillary tube is filled to the top and that no air bubbles are present after the pycnometer is kept immersed in the constant-temperature water bath for 1 hour. Dry the outside of the pycnometer with an absorbent paper or cloth towel prior to weighing.

Test Data

The following data must be obtained in order to calculate the bitumen content:

1. Specific gravity of bitumen G_b at 77 F (AASHTO T 228-68), and
2. Effective specific gravity of combined aggregate G_a (this is determined by testing samples having a known bitumen content).

Test Samples

1. The sample shall be obtained in accordance with AASHTO T 168-55 on sampling bituminous paving mixtures.
2. The size of the sample of bituminous concrete mixture shall be from 1,000 to 2,000 g. In no case should the selection of a sample of a predetermined weight be attempted.

Procedure

1. Separate the particles of the sample, using care not to fracture the mineral particles, so that the particles of the fine-aggregate portion are not larger than $\frac{1}{4}$ in. If the mixture is not sufficiently soft to be separated manually, place it in a large, flat pan, and warm it in an oven until it can be so handled.
2. Cool the sample to room temperature, place it in the pycnometer, and weigh it. Add sufficient water at approximately 77 F (25 C) to cover the sample.
3. Remove entrapped air by subjecting the contents to a partial vacuum (less than

29 in. mercury vacuum or less than 30-mm mercury absolute pressure) for 10 ± 2 min. Agitate the container and contents either continuously by mechanical device or manually by vigorous shaking at intervals of about 2 min.

Note: The release of entrapped air may be facilitated by the addition of a suitable wetting agent such as Aerosol OT in the concentration of 0.01 percent, or 1 ml of 10 percent solution in 1,000 ml of water.

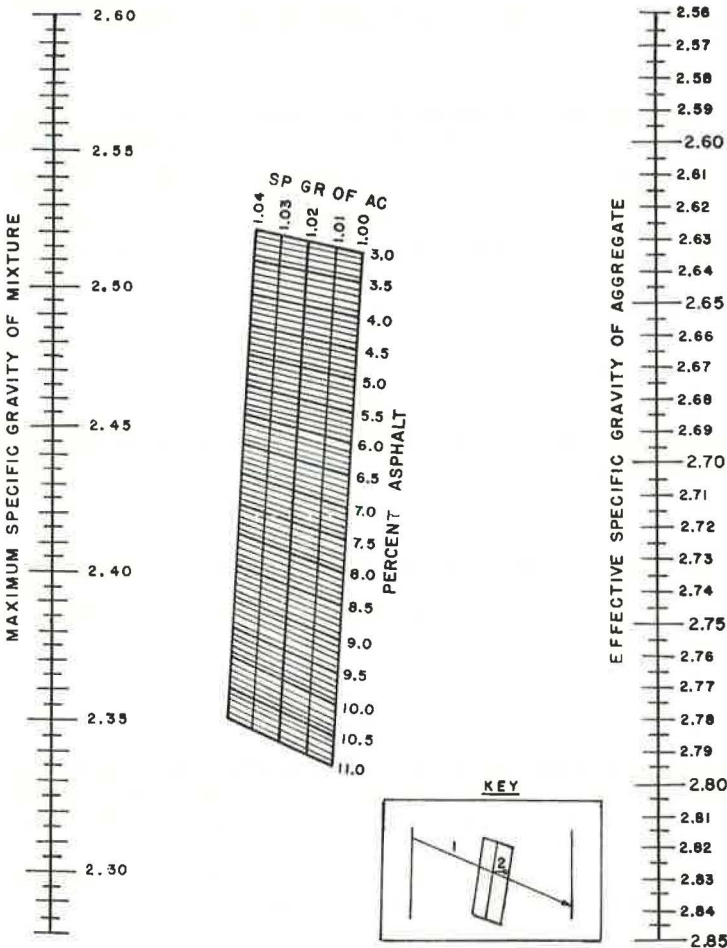
4. Fill the flask with water. If air bubbles are caused by filling, these should be removed by means of a stirring rod. Bring the contents to a temperature of $77 \text{ F} \pm 0.9 \text{ F}$ ($25 \pm 0.5 \text{ C}$) in a constant-temperature bath. Determine the weight of the pycnometer (completely filled) and contents 10 ± 1 min after completing previous step. Ensure that the capillary tube is filled to the top and that the capillary cap is in place. Dry the outside of the pycnometer prior to weighing.

Note: For rapid determinations, warm bituminous mix can be introduced in the pycnometer and then sufficiently cold ice water added to regulate and obtain a resulting temperature of $77 \text{ F} \pm 0.9 \text{ F}$.

Calculations

1. The maximum specific gravity of the voidless mix G_m is determined using Eq. 1. The equation can be solved by operations in steps 1 through 8, Figure 1.

Figure 5. Asphalt content using Pennsylvania pycnometer method.



2. G_a shall be determined as explained later, and G_b shall be determined using AASHTO T 228-68. Knowing G_a , G_b and G_m , the percentage of bitumen content P can be determined by operations shown in steps 9 and 10, Figure 1, or by solving Eq. 3.

3. Knowing the values G_a , G_b , and G_m , the bitumen content can also be determined by the use of Figure 5, which has been prepared to solve Eq. 3. G_m and G_a are connected by a straight line. At the point where this line crosses the 1.02 specific gravity of AC line, proceed horizontally to the line applicable to the specific gravity of the asphalt being used and read the percentage of asphalt by weight in the total mix.

Effective Specific Gravity of Aggregate

1. G_a is determined by testing a sample of the mix that has been prepared in the laboratory with a known P . Accurate results can be obtained if the gradation and asphalt content of the sample match, as closely as possible, the gradation and asphalt content of the mix being produced at the plant. The sample should be of about the same size as the samples that are tested for bitumen content.

2. Transfer the prepared mix to the pycnometer and determine G_m as outlined previously using Figure 1. Once P and specific G_b are known, G_a can be determined by Eq. 3, which has been rearranged algebraically as Eq. 4:

$$G_a = \frac{G_m(100 - P)}{100 - \frac{G_m \times P}{G_b}} \quad (4)$$

This equation can be conveniently solved by operations in steps 1 through 9, Figure 2.

3. At least 10 bituminous mix samples of known asphalt content should be tested to establish G_a for an asphalt plant. Calculate the average of the 10 determinations and then determine the maximum plus and minus variations from this average. If the values vary more than ± 0.010 , discard these values, recalculate the average, and redetermine the variation. A minimum of 6 values should be used to establish the average finally.

4. The specific gravity of the aggregate may change during production. G_a should be redetermined if the type of source of any of the aggregates being used in the mix is changed, or if the gradation of the mix changes enough to require a change in the job mix formula.

Note: While transferring the mix from the mixing bowl to the pycnometer, some fine materials will still be stuck to the bowl and spatula. This should be accounted for to determine P in the mix.

Accuracy of Method

The bitumen content of the bituminous mixture will vary by ± 0.10 percent for the following variations in measurements: weight of specimen, ± 1.0 g; weight of displaced water, ± 0.5 g; maximum specific gravity of mix, ± 0.003 units; specific gravity of bitumen, ± 0.010 units; and effective specific gravity of aggregate, ± 0.010 units.

EVALUATION OF MINERAL FILLERS FOR ASPHALT PAVING MIXTURES

S. K. Rao and B. R. Sen, Indian Institute of Technology, Kharagpur-2, India

Rigden's fractional volume voids was used in the evaluation of three fillers. The filler of specified weight (10 g) is compacted in a small cylinder under a definite compactive effort given by a rammer (350 g in weight) falling from a fixed height (4 in.) a specified number (100) of times. After compaction, the volume of voids in the compacted bulk volume of filler is calculated and is expressed as a fraction of unit volume. The amount of asphalt in excess of the volume of voids in the compacted filler is used by Rigden as a measure of the stiffness of the filler-asphalt mix. In the compaction of asphalt and filler to form a mastic, the asphalt content imparts a fluid or solid character to the mix. Observation of the behavior of a mixture of asphalt with different types of fillers leads to the concept that a portion of the asphalt gets fixed up in the inter- or intra-granular pores of the filler forming a solid phase with the filler, and the excess asphalt, termed fluid phase, acts as a binder on the solid phase. Maximum stiffness results as a particular proportion of the fluid phase or excess asphalt. If the demand for additional asphalt, because of the inclusion of the fine aggregate, is kept constant, the comparison of the optimum binder (filler and asphalt) contents for maximum strength of sheet-asphalt mixes can be made in terms of the optimum fluid phases for the filler-asphalt mastics alone.

•MOST of the asphalt paving specifications in use today specify the inclusion of fine powders, such as portland cement, that are referred to as mineral fillers.

Although the quantity of a filler for a paving mix is specified as a percent fraction of the aggregate, no distinction is drawn among the fillers on the basis of physical characteristics such as fineness, specific gravity, and surface area. Because it is difficult to assess the effectiveness of a filler in quantitative terms based on these individual properties, a simple filler characteristic that bears a direct relation to its performance in a paving mix is of significant value. Rigden's fractional volume voids is one such characteristic.

The present investigation refers to the study of three fillers with different fineness characteristics that were evaluated by Rigden's test for use in paving mixes. The differences in the effectiveness of the fillers are interpreted in terms of Rigden's fractional volume voids. It has been observed that, by comparing the dry compaction characteristics of fillers, the optimum filler content of a given filler for a paving mix can be ascertained without resorting to strength tests.

Fillers are included in paving mixtures to impart greater stability and strength. As the literature on this subject indicates, there are two viewpoints to explain the stabilizing influence of fillers. According to the first one, filler (because of its fine particle size distribution) serves to fill the voids in the fine aggregate or coarse and fine aggregate combinations, thereby increasing the density and strength of the compacted mixture. The second viewpoint presumes that the fine particles of filler become suspended in the asphaltic binder forming a mastic. The suspended filler particles adsorb

asphalt components, giving rise to increased viscosity of the binder and, consequently, to tougher mixes.

It is reasonable to presume that, in the case of any filler, both functions come into play. Either of the two functions predominates, depending on the characteristics of the aggregate, the fineness characteristics of the filler, and the relative proportions of filler and asphalt in the mix.

EVALUATION OF FILLERS FOR PAVING MIXTURES BY RIGDEN'S TEST

Regardless of which is the predominant function, what must be known is the extent to which a filler affects the strength and stability of a paving mix. A simple filler characteristic that bears a direct relation to its performance in a paving mix is of essential value. Studies by other investigators (1, 2) toward such an end have indicated that, in a general way, the influence of a filler on an asphaltic binder can be assessed by their bulking or packing properties. Researchers have expressed this in various ways, for example, by the bulk density in benzene and the fractional volume voids in dry compacted filler. Rigden, who devised the latter test, claimed (3) that it gives a direct indication of the viscosity of filler-asphalt mixtures for all types of fillers. Heukelom (4) explained the quantitative differences in the effects of fillers on paving mixtures with the help of this test parameter.

The fractional voids test is one in which filler of a specified weight (10 g) is compacted in a small cylinder under a definite compactive effort given by a rammer (350 g in weight), falling from a fixed height (4 in.), for a specified number (100) of times. After compaction, the volume of voids in the compacted bulk volume of filler is calculated and expressed as a fraction of the unit bulk volume.

OPTIMUM ASPHALT CONTENT FOR A FILLER-ASPHALT MASTIC

The packing properties of a filler depend on its physical and geometric properties, such as particle shape, size distribution, and surface texture. Under a given compaction, a filler will enclose some voids depending on these properties. If filler and asphalt are mixed and compacted to form a mastic, the asphalt will go into the voids of the filler. If the quantity of asphalt is less, a stiff dry product is obtained without adequate bond between the filler particles. If the asphalt content is excessive, it imparts a fluid character to the mixture. The amount of asphalt in excess of the volume of voids in the compacted filler is adopted by Rigden as a measure of the stiffness of the filler-asphalt mix. Mixtures of asphalt with different types of filler gave a rather uniform viscosity when this excess amount of asphalt was of the same proportion of the total volume of filler and asphalt in each case, irrespective of the actual volumes of fillers used. This concept supposes that a portion of the asphalt gets fixed up in the inter- and intra-granular pores of the filler, forming a sort of solid phase with the filler, and the excess asphalt, which may be termed the fluid phase, acts like a binder on the solid phase. This is shown in Figure 1A.

It is obvious that a filler with large compacted bulk volume fixes up a large proportion of asphalt because of the large fraction of voids in it; the same proportions of solid and fluid phases can be obtained (and, hence, the same stiffness according to Rigden) where a small quantity of the former is sufficient when mixed with the same quantity of asphalt. It then remains to be seen at what proportions of solid and fluid phases a filler-asphalt mastic gives the maximum stiffness. The following reasoning appears to be valid in this connection.

When the asphalt content is just sufficient to fill the voids in the compacted filler (that is, when the fluid phase is zero), the mix cannot have the maximum stiffness because, in this condition, the amount of asphalt is not adequate to envelop the filler particles fully. The asphalt only occupies the void spaces available in the particles. The increased stiffness of a filler-asphalt mastic over simple asphalt must be partly due to the filler particles adsorbing layers of asphalt around them (1, 5). This condition can be achieved by coating fully the filler particles. In this case, more asphalt

is needed than is necessary just to fill the voids. On the other hand, if the asphalt content is too much, the coated filler particles cannot have close packing but are pushed apart and kept floating in the abundant asphalt, thus decreasing the stiffness of the mix. It may be construed that, when the amount of excess asphalt is of such a proportion as to coat the filler particles fully and permit a close packing of them, the mix offers maximum resistance to deformation. A greater or lesser asphalt content results in a weaker mix. This means that the maximum stiffness results at a particular proportion of the fluid phase or excess asphalt. This may be termed the optimum fluid phase (Fig. 1B).

Optimum Binder Content for a Paving Mix

A filler-asphalt mastic, proportioned to have maximum stiffness in accordance with the preceding plan when mixed with fine aggregate (as in the case of this investigation) to form a paving mix, does not impart maximum strength to the mix because the asphalt content that was just adequate to coat the filler particles and to fill its voids would now be required to coat the particles of fine aggregate and fill the additional voids created by its inclusion. This would create a deficit in the asphalt content, lowering the strength. In terms of functional volumes, it means that the inclusion of sand has increased the solid phase, and, for maximum strength of the mix, the asphalt content and the fluid phase should correspondingly be increased. It may be construed that, in this case, the fluid phase or excess asphalt has to serve as a binder to the sand, filler, and fixed-asphalt solid-phase system.

In the present investigation, the amount and grading of sand are kept the same for all the sheet-asphalt mixes prepared with different filler-asphalt mastics. The increased solid phase in each case is thus the same, and the excess asphalt necessary to cover the increased solid phase for maximum strength of sheet-asphalt mixes is also the same. If the demand for additional asphalt, because of the inclusion of the fine aggregate, is kept constant, the comparison of the optimum binder (filler and asphalt) contents for maximum strength of sheet-asphalt mixes can be made in terms of the optimum fluid phases for the filler-asphalt mastics alone.

Study Purpose and Scope

The object of this investigation is to ascertain whether the reasoning given previously is valid and to assess Rigden's test as a tool for evaluation of fillers for paving mixtures.

For this purpose, three fillers with different fineness characteristics were selected and used in sheet-asphalt mixtures. The sheet-asphalt mixtures were designed on a volumetric basis, so that each one of them has the same volumes of sand and binder (filler and asphalt). Thus, the voids in the sand were filled by a fixed volume of filler and asphalt, regardless of the proportions of filler and asphalt (F-A ratios) in the mixes. Six different mixes were formed with each filler by varying the F-A ratio within the constant volume of filler-asphalt binder.

In order to eliminate densification as a variable, all the mixes were compacted to have the same volume fraction of air voids by using different compactive efforts.

It was felt that creep tests, rather than quick tests like Marshall stability, would reveal the influence of the binder more appropriately. The sheet-asphalt mixtures, formed into cylindrical specimens, were thus tested in unconfined compression creep, under four different loads. The minimum rates of deformation from the creep curves were taken as a measure of the mixture resistance to the applied loads.

The fractional voids content for each of the three fillers was determined by Rigden's test. These values were used to determine the functional volumes (the solid and fluid phases) for the filler-asphalt binder of each of the sheet-asphalt mixtures. The binders of those mixes giving maximum resistance to deformation with each of the fillers were then compared in terms of their functional volumes.

Figure 1. Basic concepts of fractional voids in a filler-asphalt system.

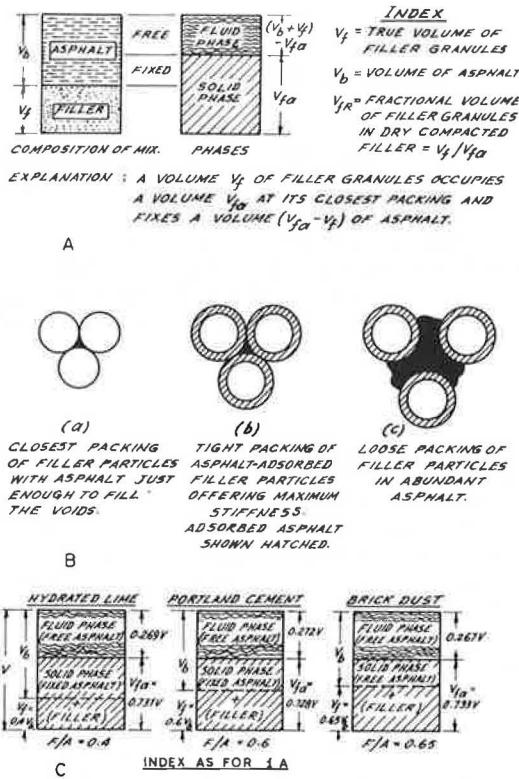


Table 1. Physical properties of mineral fillers.

Filler	Specific Gravity	Specific Surface Area ^a (cm ² /g)	Bulk Density in Benzene (g/cm ³)	Fractional Void Volume in Dry Compacted State ^b	Percent <0.001 cm
Hydrated lime	2.408	3,965	0.267	0.609	42
Portland cement	3.114	2,765	0.625	0.485	22
Brick dust	2.738	1,375	0.833	0.463	6

^aDetermined by using Blaine's air permeability apparatus.
^bDetermined by using Rigden's fractional voids test.

Table 2. Compositional and physical properties of sheet-asphalt mixtures.

Filler	F-A Ratio by Volume	Mix Composition, Percent by Volume of Total Mix ^a			Bulk Specific Gravity of Compacted Specimens ^a	Functional Volumes, Percent by Volume of Filler and Asphalt		Minimum Rate of Strain Min ⁻¹ × 10 ⁻⁶ , at Applied Stress of			
		Aggregate	Binder (filler and asphalt)	Air Voids		Solid Phase	Fluid Phase	17.5 psi	35 psi	52.5 psi	70 psi
Hydrated lime	0.2	65.0	30.0	5.0	2.11	42.6	57.4	5.5	23.5	46.9	92.0
	0.3	65.1	30.0	4.9	2.14	59.0	41.0	1.4	8.0	20.0	42.7
	0.4	65.0	30.0	5.0	2.16	73.1	26.9 ^b	0.8	5.1	13.3	29.4
	0.45	65.0	30.0	5.0	2.17	79.5	20.5	1.1	6.0	15.7	34.9
	0.5	65.0	30.0	5.0	2.18	85.3	14.7	2.5	10.6	25.1	47.6
	0.55	65.0	30.0	5.0	2.19	90.8	9.2	3.7	15.7	34.7	54.5
Portland cement	0.3	65.1	30.0	4.9	2.19	44.8	55.2	9.1	108.0	364.0	1,040.0
	0.4	65.0	30.0	5.0	2.22	56.5	43.5	5.7	56.0	250.0	670.0
	0.5	65.0	30.0	5.0	2.25	64.8	35.2	4.1	39.6	128.0	400.0
	0.6	65.1	30.0	4.9	2.28	72.8	27.2 ^b	2.2	21.3	75.0	202.5
	0.7	65.0	30.0	5.0	2.30	80.0	20.0	2.8	26.5	87.5	262.5
	0.8	64.7	29.8	5.5	2.31	86.4	13.6	3.2	28.7	99.0	310.0
Brick dust	0.4	65.0	30.0	5.0	2.19	53.2	46.8	15.8	208.0	1,040.0	2,470.0
	0.5	64.9	29.9	5.2	2.21	62.0	38.0	9.2	101.6	483.0	1,347.0
	0.6	64.9	29.9	5.2	2.23	69.8	30.2	4.7	52.1	260.0	600.0
	0.65	64.9	29.9	5.2	2.24	73.3	26.7 ^b	4.3	37.5	205.0	500.0
	0.7	64.9	29.9	5.2	2.25	76.7	23.3	5.1	55.7	296.0	620.0
	0.8	65.0	30.0	5.0	2.27	82.8	17.2	7.8	87.5	375.0	1,250.0

^aAverage test values for three specimens.

^bOptimum binder content.

EXPERIMENTAL PROCEDURES

Materials

In this study, filler is considered as the fraction of the material passing the No. 200 sieve. The fillers used were hydrated lime, portland cement, and brick dust. The physical properties of the fillers are given in Table 1.

The asphalt cement used was Mexphalte, an 80 to 100 penetration grade asphalt.

The fine aggregate was a locally available river sand. The fraction of the sand passing the No. 200 sieve was removed by sifting; it was not included in the sheet-asphalt mixes. All of the fraction that is finer than the No. 200 sieve was thus contributed by one of the three fillers.

Preparation of Mixtures

Uniform gradation of sand in all the mixtures was achieved by sifting the sand into respective sizes and recombining by weight to get a size distribution that conforms closely to type VIIIa (fine sheet) Asphalt Institute classification.

All the mixtures were designed to contain 30 percent of binder (taken as filler and asphalt), 65 percent of sand, and 5 percent of air voids by total volume of the mix. While maintaining these constant proportions, volumetric F-A ratios were varied within the constant volume of filler-asphalt binder.

The mixtures were formed into cylindrical specimens 2 in. in diameter and 4 in. in height. The specimens were prepared by heating calculated quantities of aggregates and asphalt separately to 325 and 300 F respectively and then combining them in a mixing operation for a period of 2 min. The mixture was placed in a molding cylinder in three layers, each rodded 25 times with a small metal rod. Then, it was compacted in a static load compression machine, and the load was maintained for 1½ min on both faces. The specimens were compacted to a constant height of 4 in., with the help of a mark on the plunger, thus ensuring the stipulated volume percentages of aggregate, binder, and voids. However, small differences in heights of specimens were observed after extrusion from the molds because of variations in specimen rebound. These were responsible for the slight variations in the volume proportions of the mixture components (Table 2). The use of different proportions of filler and asphalt in the different mixes necessitated variations in the compacting pressures (which ranged from 1,000 to 5,000 psi) to achieve constant volumes for the specimens. The specimens, after extrusion from the molds, were allowed to cure in air at a temperature of about 80 F for 2 days before testing. The volumes of the specimens were determined by using the water displacement method, and their weights were obtained for bulk specific gravity calculations and determination of voids.

The compositional and physical properties of the mixtures are given in Table 2.

Creep Tests

Two Soiltest consolidometers were adapted for applying static loads on the specimens. The tests were carried out in an air-conditioned room, and the temperature was held at 85 F during the period of testing.

The deformations were measured at chosen time intervals ranging from 6 sec elapsed time to 12 hours or until the specimens failed, in cases of earlier failure.

The sheet-asphalt specimens were tested for creep under four constant loads corresponding to 17.5, 35, 52.5, and 70 psi. Six different mixtures were formed with each filler corresponding to six different F-A ratios. Because the filler-asphalt volume is kept constant for all the mixes, very low percentages of filler, especially in the cases of portland cement and brick dust, resulted in mixes that were too plastic and yielded too quickly under the applied loads to give accurate results. On the other hand, higher F-A ratios, particularly with hydrated lime, gave mixes that were very dry and unworkable. The F-A ratios with each of the fillers were thus suitably selected so as to include at least two concentrations on either side of that giving the maximum resistance to deformation. The F-A ratios utilized in the study are given in Table 2.

Figure 2. Strain versus time at different concentrations of hydrated lime filler.

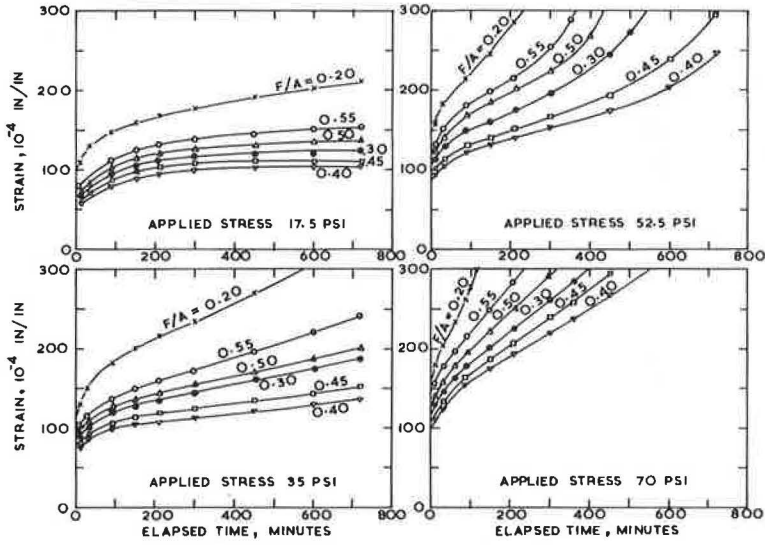


Figure 3. Strain versus time at different concentrations of portland cement filler.

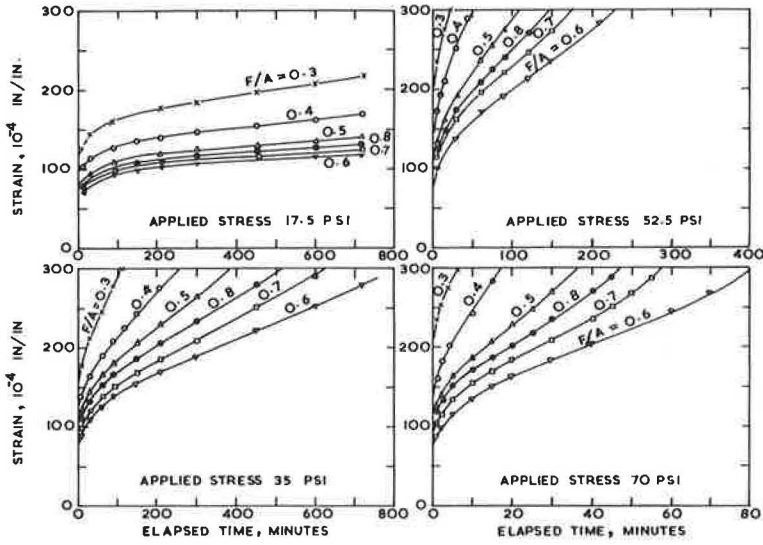


Figure 4. Strain versus time at different concentrations of brick dust filler.

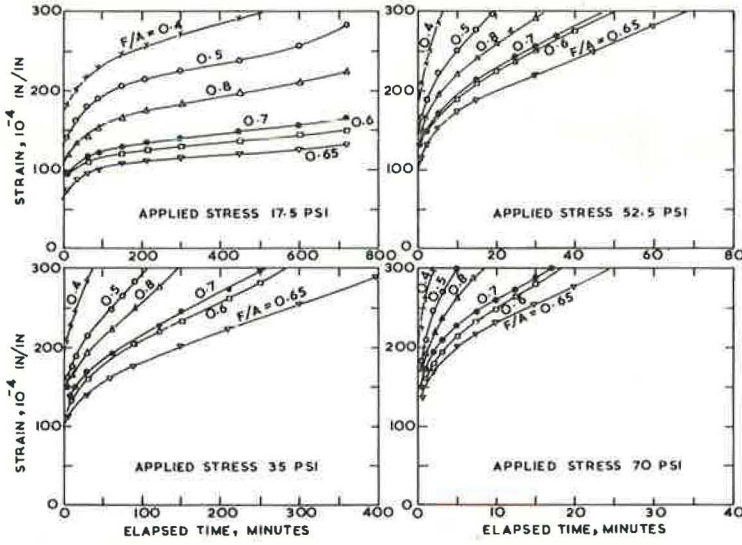
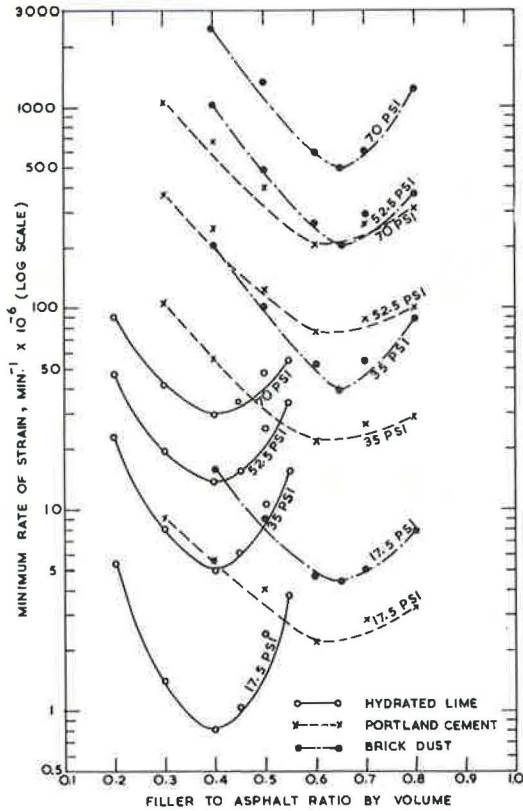


Figure 5. Relation between minimum rate of strain and F-A ratio under different stresses.



Voids in Dry Compacted Filler

Void content in each of the fillers in the dry compacted state was determined according to BS 812 with an apparatus fabricated to the specifications laid therein. Values of the fractional void content in unit bulk volume of the compacted filler are given in Table 1 for the different fillers.

Other Physical Properties of Fillers

The particle size distributions of the fillers, which were determined by a hydrometer, are not shown here, but the percentages of fillers finer than 10 microns are given in Table 1.

The surface areas of the fillers were determined by Blaine's air permeability apparatus according to ASTM C 204-51.

The bulk densities of the fillers in benzene were determined according to BS 812. These physical properties of the fillers are given in Table 1.

ANALYSES OF TEST RESULTS

The time-versus-strain data obtained from the creep tests on the different mixes under the four different loads are shown in Figures 2 through 4. The minimum rate of strain for each of the mixes under the different loads is given in Table 2. Figure 5 shows the minimum rate of strain and the F-A ratio for the three fillers under the different loads.

It is observed that, under any of the loads, the maximum resistance to deformation has occurred at a particular F-A ratio with each of the fillers. This ratio, which may be called the optimum F-A ratio, is 0.4 for hydrated lime, 0.6 for portland cement, and 0.65 for brick dust.

The fluid phase or excess asphalt calculated for the filler and asphalt binder volume for each of the mixes is given in Table 2. It is observed that the fluid phase at the optimum F-A ratio is 26.9, 27.2, and 26.7 percent for hydrated lime, portland cement, and brick dust respectively. The functional volumes (the solid and fluid phases) at the optimum F-A ratio for the three fillers are shown in Figure 1C.

It suggests that, with the chosen fine aggregate and type of asphalt, any of the fillers gives the maximum resistance to deformation when the filler and asphalt are proportioned so as to yield nearly 27 percent of excess asphalt. However, it may be noted that the minimum rate of strain (corresponding to maximum strength) at the optimum F-A ratio is different for the different fillers. These differences among the fillers could be due to other properties such as chemical composition. What then is the use of Rigden's test? The use of Rigden's test lies in interpreting the optimum F-A ratio for maximum resistance of a sheet-asphalt mixture with any filler, in terms of the optimum F-A ratio with a known filler, by comparing dry compaction characteristics alone, without resorting to strength tests. Regardless of the absolute strengths that result by using different fillers, the optimum F-A ratio with any of the fillers is dependent on an optimum proportion of the excess asphalt necessary for the chosen aggregate fraction and can be ascertained by Rigden's fractional volume voids test.

REFERENCES

1. Mitchell, J. G., and Lee, A. R. The Evaluation of Fillers for Tar and Other Bituminous Surfacing. *Jour. Society of Chemical Industry*, Vol. 58, 1939, pp. 299-306.
2. Lee, A. R., and Rigden, P. J. The Use of Mechanical Tests in the Design of Bituminous Road-Surfacing Mixtures. *Jour. Society of Chemical Industry*, Vol. 64, 1945, pp. 153-161.
3. Rigden, P. J. The Use of Fillers in Bituminous Road Surfacing: A Study of Filler-Binder Systems in Relation to Filler Characteristics. *Jour. Society of Chemical Industry*, Vol. 66, 1965, pp. 299-309.
4. Heukelom, W. The Role of Filler in Bituminous Mixes. *Proc. AAPT*, Vol. 20, 1965, pp. 396-429.

5. Richardson, C. The Theory of the Perfect Sheet Asphalt Surface. Jour. of Industrial and Engineering Chemistry, Vol. 7, No. 6, 1915.
6. Kallas, B. F., Puzinauskas, V. P., and Krieger, H. C. Mineral Fillers in Asphalt Paving Mixtures. HRB Bull. 329, 1962, pp. 6-29.

STUDY OF MINERAL FILLERS FOR SHEET-ASPHALT MIXTURES

V. Venkatasubramanian and T. S. Venkataraman, Regional Engineering College, Tiruchirapalli-15, India

Three fillers, fly ash, hydrated lime, and quarry dust, were evaluated on the basis of simple beam tests that reflect the viscous resistance of the mix. Indian standard sand and asphalt of standard specification were used. The 10-in. long test specimen was supported on mild-steel rollers 20 cm (8 in.) apart and allowed to deflect under its own weight only. The deflection was measured at different time intervals until the specimens failed. A generalized form of creep law was used in estimation of the resistance offered by the different mixes to deformation. For a given percentage of binder with increasing concentration of filler, the resulting mix becomes stiff with decreasing deformation characteristics in the creep curve. The optimum F-A ratio is that at which creep constants are minimum. A measure of the greatest resistance is described, and fly ash is rated highest.

• AMONG the various tests available to study the flow properties of sheet-asphalt mixtures, the tensile and beam tests are most common. It is well known that the main influence of mineral fillers is on the rheological properties of asphalt mixes. An attempt is made in this study to evaluate three mineral fillers on the basis of simple beam tests that reflect the viscous resistance of the mix.

The three fillers studied were fly ash, hydrated lime, and quarry dust, which were sifted through a No. 200 mesh sieve. The fly ash contained 62 percent silica and 16 percent calcium oxide; the hydrated lime contained 60 percent calcium oxide and no silica. The quarry dust contained 93 percent silica with a trace of calcium oxide. The physical properties of the fillers are given in Table 1.

Indian standard sand was used throughout the investigation. Asphalt of 80 to 100 penetration grade, conforming to The Asphalt Institute's specification for 85 to 100 paving asphalt, was used as a binder, and its percentage was kept at 9 percent for all mixes, which is within the recommended limits of The Asphalt Institute's specifications (1).

The test specimens were 10 in. long, 2 in. wide, and 1 in. deep and were similar to those used by Lee and Rigden in their tensile strength studies (2). The design of the asphalt mixture was based on the recommendations made in The Asphalt Institute manual series. The hot mix was spread evenly inside the hot mold, and a static load of 12 tons was applied for 2 min. The specimens were air-cured for 7 days before test. Curing and testing was done at 30 ± 1 C. The bulk density of the test specimens using the three types of fillers is given in Table 1.

The test specimen was simply supported on mild-steel rollers 20 cm (8 in.) apart and allowed to deflect under its own weight only. The central deflection was measured at different time intervals until the specimen failed. The deflection was measured every 6 sec during the first minute and thereafter every $\frac{1}{2}$ min. From the measured deflections, the maximum tensile strains were computed; the derivation of this relation is given in the Appendix. Typical strain-time curves are shown in Figures 1, 2, and 3.

Table 1. Physical properties of the fillers and test beam.

Filler	Specific Gravity	Bulk Density in Toluene (g/cc)	Specific Surface (cm ² /g)	Voids in the Dry Compacted Filler	Bulk Density of Test Beam* (lb/ft ³)
Fly ash	2.13	0.500	4,184	0.520	116 to 119
Hydrated lime	2.56	0.220	11,760	0.644	112 to 115
Quarry dust	2.67	0.833	1,959	0.400	125 to 131

*10- by 2- by 1-in. beam.

Figure 1. Typical experimental creep curve, fly ash.

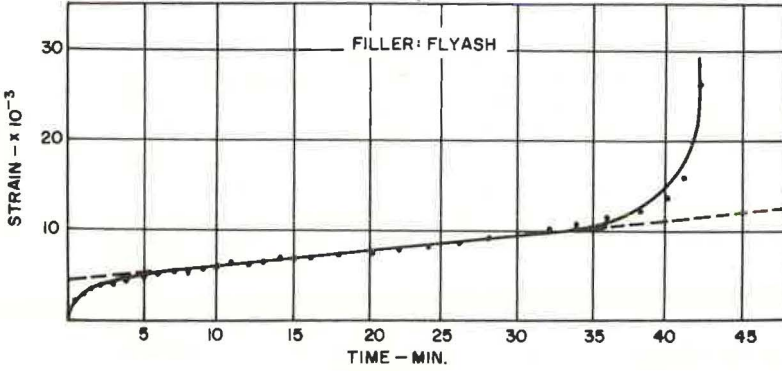


Figure 2. Typical experimental creep curve, hydrated lime.

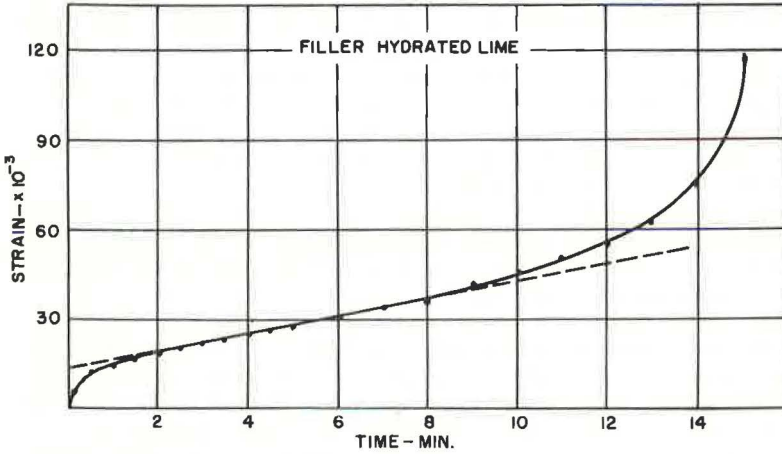
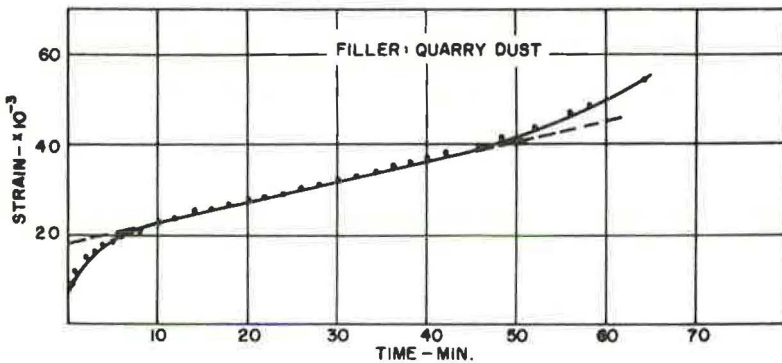


Figure 3. Typical experimental creep curve, quarry dust.



EVALUATION OF MINERAL FILLERS FROM AN ANALYSIS OF CREEP DEFORMATION

Based on Seth's (3) generalized strain measure, Rao (4) has developed a generalized form of creep law that deals with the strains in the initial transient stage and the subsequent steady-state deformation. The total strain ϵ at any time t can be expressed as

$$\epsilon = Kt_s^{1/m} + \alpha(t - t_s)$$

where K and $1/m$ are material constants characterizing the transient state deformation, t_s is time for limiting transient strain, t is total time, and α is constant rate of strain in the steady-state deformation.

The values of α , K , and $1/m$, derived from the experimental curves, give a measure of the resistance offered by the different mixes to deformation. The strains during the transient state of deformation are plotted on log-log scale in Figures 4 through 6. The straight-line relation seems to justify the use of the transient-state creep relation given in the preceding equation. The material constants K and $1/m$ computed from Figures 4 through 6 for different filler-asphalt (F-A) ratios are given in Tables 2 through 4. The variation of these material constants with different F-A ratios for the three fillers investigated is shown in Figures 7 through 9.

The material constants K and $1/m$ indicate definite trends with different F-A ratios, and their critical values are obtained for the optimum F-A ratio. An analysis of the data shows that the logarithmic law of transient creep holds good in the first minute, after which the steady-state creep conditions tend to dominate. Furthermore, the transient condition is not ordinarily a critical factor in the design, as it is for the comparative evaluation of the fillers. The minimum rate of strain during the steady-state creep α was considered more significant and was taken as a measure of the viscous resistance of the mix to deformation.

In general, it can be seen that, for a given percentage of binder with increasing concentration of filler, the resulting mix becomes stiff with decreasing deformation characteristics in the creep curve. The F-A ratio at which these creep constants are minimum can be taken as the optimum F-A ratio for the particular filler. These optimum values are 1.01, 0.425, and 1.33 for fly ash, hydrated lime, and quarry dust respectively. The filler having the lowest among the minimum values of α can be considered to exhibit the greatest resistance. Accordingly, the fillers may be rated in the order of fly ash, hydrated lime, and quarry dust (from the standpoint of resistance to deformation under the steady-state condition). This conclusion also appears to be justifiable from physical properties of the filler as given in Table 1.

REFERENCES

1. The Asphalt Institute. U.S.A. Manual Series 6, 1959.
2. Lee, A. R., and Rigden, P. J. The Use of Mechanical Tests in the Design of Bituminous Road Surfacing Mixtures, Part 1. Jour. of the Society of Chemical Industry, June 1945.
3. Seth, B. R. Generalised Strain Measure With Applications to Physical Problems. Proc. Internat. Symp. on Second Order Effects in Elasticity, Plasticity and Fluid Dynamics. Haifa, Israel, 1962.
4. Rao, S. K. A Study of Some Mineral Fillers for Sheet Asphalt Mixes With Particular Reference to Their Evaluation by Creep Tests. Indian Institute of Technology, Kharagpur, PhD thesis, 1969.
5. Timoshenko, S. Strength of Materials, Part 2, Advanced Theory and Problems. East-West Student Ed., D. Van Nostrand Co., Inc., 1965.
6. Secor, K. E., and Monismith, C. L. Viscoelastic Response of Asphalt Paving Slabs Under Creep Loading. Highway Research Record 67, 1964, pp. 84-97.
7. Lee, A. R., and Markwick, A. H. D. The Mechanical Properties of Bituminous Surfacing Materials Under Constant Stress. Jour. of the Society of Chemical Industry, London, May 1937.

Table 2. Material constants with varying F-A ratios, fly ash.

Filler by Weight of Total Mix (percent)	F-A Ratio by Volume	Material Constants		
		$\alpha \times 10^{-6}$	$k \times 10^{-4}$	1/m
12	0.62	5.52	104.0	0.532
14	0.72	4.53	83.0	0.445
16	0.83	0.335	25.0	0.354
18	0.91	0.083	7.5	0.306
20	1.01	0.046	5.4	0.384
22	1.12	0.133	13.2	0.268
24	1.24	2.74	28.0	0.384

Table 3. Material constants with varying F-A ratios, hydrated lime.

Filler by Weight of Total Mix (percent)	F-A Ratio by Volume	Material Constants		
		$\alpha \times 10^{-6}$	$k \times 10^{-4}$	1/m
6	0.26	33.30	138	0.589
8	0.35	0.83	82	0.466
10	0.43	0.33	36	0.296
12	0.52	0.71	32	0.306
16	0.68	5.00	14	0.374

Table 4. Material constants with varying F-A ratios, quarry dust.

Filler by Weight of Total Mix (percent)	F-A Ratio by Volume	Material Constants		
		$\alpha \times 10^{-6}$	$k \times 10^{-4}$	1/m
26	1.076	7.64	135	0.5095
28	1.160	2.77	100	0.4142
30	1.240	2.36	58	0.4986
32	1.320	1.45	44	0.4987
38	1.570	7.33	73	0.5206

Figure 4. Log time and strain during transient creep, fly ash.

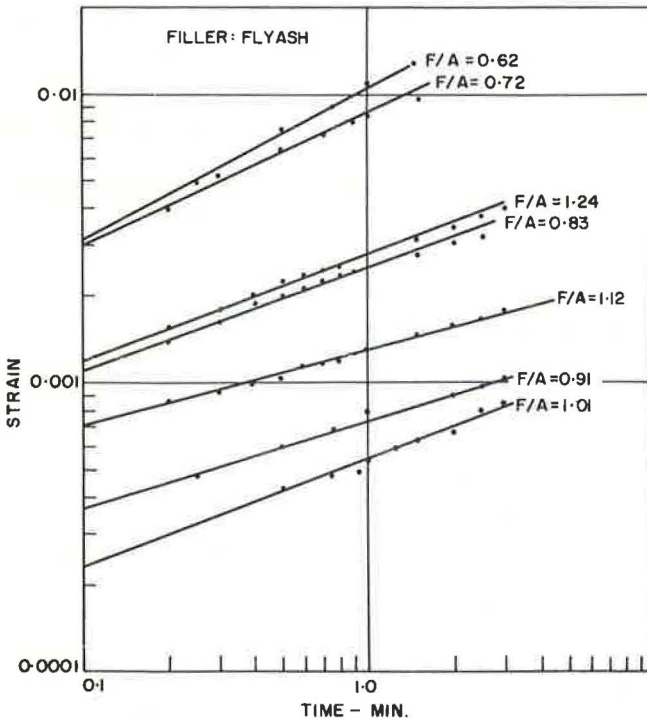


Figure 5. Log time and strain during transient creep, hydrated lime.

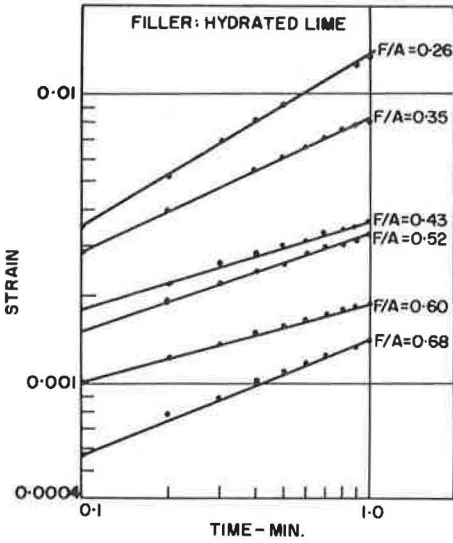


Figure 6. Log time and strain during transient creep, quarry dust.

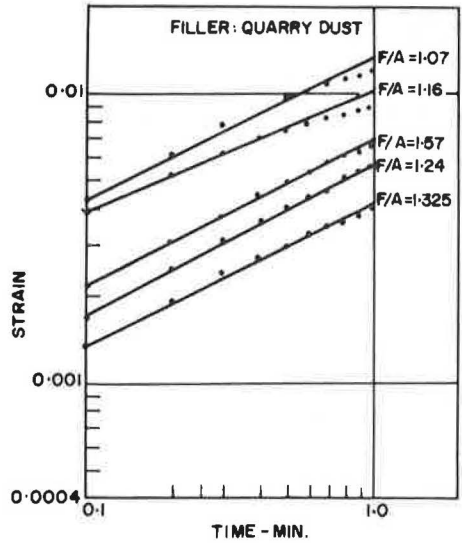


Figure 7. Relation between K under transient creep conditions and F-A ratio for different fillers.

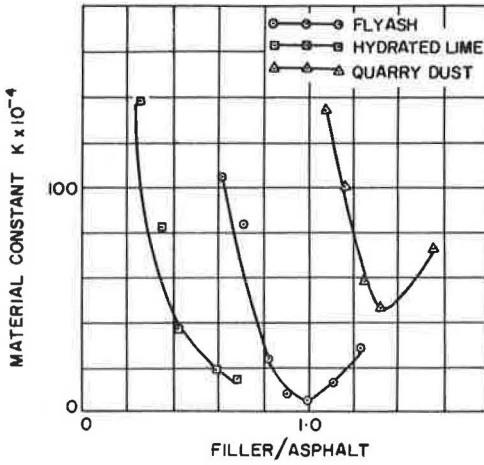


Figure 9. Relation between minimum rate of strain and F-A ratio for different fillers.

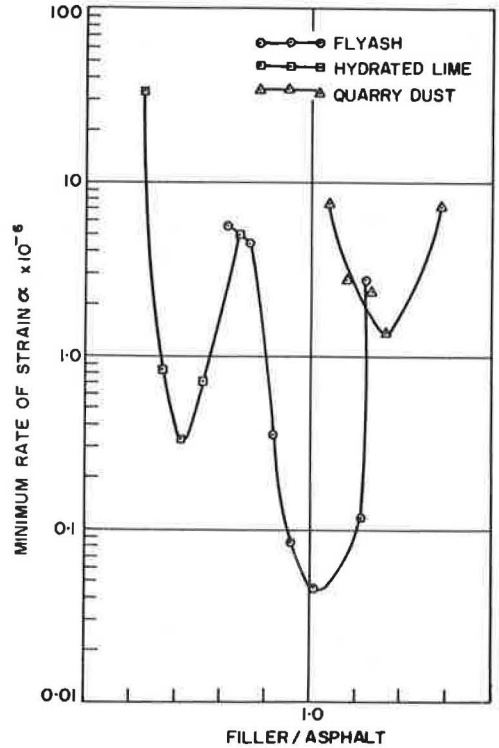
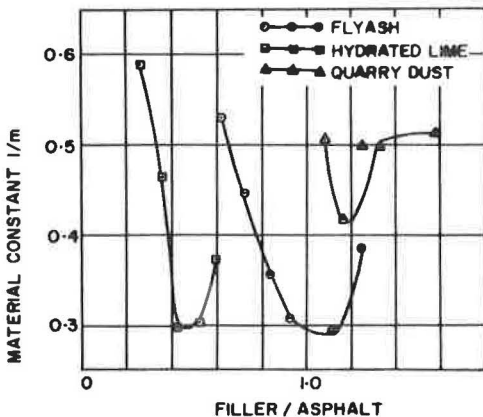


Figure 8. Relation between 1/m under transient creep conditions and F-A ratio for different fillers.



APPENDIX

DERIVATION OF MAXIMUM TENSILE STRAINS

From the theory of simple bending of beams, which does not follow Hooke's law (5),

$$\epsilon = \frac{y}{R}$$

where

- ϵ = strain of the fiber considered,
- y = depth of the fiber considered below the neutral axis, and
- R = radius of curvature of the neutral axis of the deflected beam.

Secor and Monismith (6) have observed that the neutral axis is above the geometrical axis; Lee and Markwick (7) have experimentally verified that the neutral axis is very near the top of the deflected beam. Hence, the tensile strain of the bottom fiber can be approximately taken as

$$\epsilon \approx \frac{h}{R}$$

where h = the depth of the beam. The actual strain shall be less than the estimated strain, depending on the position of the neutral axis above the geometrical axis of the beam.

From the geometry of the deflected beam, assuming it to be an arc of a circle, it is evident that

$$R_c = L^2/8\delta$$

where

- R_b = radius of curvature of the bottom fiber,
- L = simply supported span, and
- δ = observed deflection of the bottom fiber.

Because the span is 20 cm in the present study,

$$R_c = 50/\delta$$

Because the depth of the beam is very small compared to the radius of curvature, it can be safely assumed that

$$R = R_c = 50/\delta$$

Hence,

$$\epsilon = \frac{h}{50/\delta} = \frac{h\delta}{50}$$

In about 50 specimens tested in the study, it was found that the minimum radius of curvature observed was so large in comparison with the thickness of the specimen that the error involved in the assumption $R = R_b$ was less than 2 percent.

ASPHALT CONTENT DETERMINATION USING NUCLEAR TECHNIQUES

Robert C. Klotz, Pennsylvania Department of Transportation

An evaluation was made of the application of the Troxler nuclear asphalt content gauge, model 2226, to determine the asphalt content of hot bituminous mixes using neutron thermalization. Parallel data were acquired, where convenient, by the use of a Nuclear-Chicago asphalt content gauge, model 9999, previously evaluated. Data were first acquired for variables of mix design (gradation), aggregate types, and asphalt producers for bituminous mixes with various representative asphalt contents. These initial samples were mixed under controlled laboratory conditions. Comparisons were made of design asphalt contents, Immerex extraction values on the same samples, and the values determined with the two nuclear units. Field tests of the Troxler gauge were also conducted at various batch plants with resulting values compared to extracted asphalt content on the same sample.

•DURING the past 15 years, various nuclear techniques and instrumentation have been applied to the task of determining the asphalt content of bituminous concrete mixes in an accurate and swift manner (2-4). The standard reflux extraction is an accepted method for obtaining asphalt content; however, considerable time (as much as 1½ hours) is required for the test to be accurately performed, and the material represented by the tested mix may have been placed and compacted before the extraction results are known. In addition, mixes determined by this method yield a standard deviation of 0.2 percent of bitumen content (ASTM D 2172-65T, Method C). With the evolution of solid-state circuitry and detecting devices of greater sensitivity, studies of nuclear techniques progressed until units were designed specifically for the purpose of determining the asphalt content of hot bituminous concrete mixes while maintaining a sufficient degree of portability such that field use became practical. Initial studies of such a gauge by the department were reported in 1968 (1). Early in 1970, a Troxler asphalt content gauge, model 2226, was purchased, and an investigative study was undertaken to evaluate this new gauge.

THE TROXLER GAUGE

The 16- by 16- by 16-in. Troxler gauge (Fig. 1) consists of a one-piece unit weighing about 125 lb. All components are enclosed within the single unit, and a sliding-drawer arrangement is provided such that stainless steel pans containing the bituminous test sample can be inserted into the gauge. Three He-3 neutron detector tubes were utilized to monitor the thermal neutrons from a test specimen. Two of these tubes were sample detector tubes, positioned beneath the test specimen pan in the sliding drawer. The other tube was situated near the top of the gauge and acted as a reference detector (Fig. 2).

The counts monitored by the reference detector were used as a continuous internal standard count and were electronically compared with the sample count. Thus, any

electronic drift caused by temperature variation or component aging could be accounted for during the actual test count. Because of this system of continuous standardization, no auxiliary standard was provided.

PRINCIPLE OF OPERATION

The basic principle of operation of an asphalt content gauge of this type relies on neutron thermalization. It is first necessary to produce a sufficient number of neutrons. A convenient source of neutrons is provided when beryllium metal is bombarded with alpha particles emitting from a radioactive source. With this gauge the source consisted of 300 mC of americium-241. This source emits a wide variety of beta and gamma radiation of relatively low energies; in addition alpha particles in the energy range of 5.31 to 5.50 MeV are emitted. These alpha particles are of importance in neutron production because they have sufficient energy to initiate the beryllium-alpha reaction, ${}_4\text{Be}^9 + {}_2\text{He}^4 \rightarrow {}_0\text{n}^1 + {}_6\text{C}^{12}$, when they collide with beryllium metal mixed with the americium-241 in the sealed source. In terms of alpha particles with the energy value of 5.3 MeV, about 1 alpha particle in 10^4 produces a neutron; therefore, the number of neutrons from a 300-mC source would be approximately

$$3.7 \times 10^7 \frac{\text{alpha disintegration}}{\text{millicurie}} \times 300 \text{ mC} \times 10^{-4} \frac{\text{neutron}}{\text{alpha disintegration}}$$

$$= 11.1 (10^5) \text{ neutrons with about 2.5 MeV of energy}$$

When charged particles react with matter, electrostatic forces and radiation emission are most important; however, the emitted neutrons are uncharged, and their interaction with matter consists almost entirely of collisions with nuclei of the matter. Such collisions can be divided into three classes: elastic scattering, where the incident neutron is deflected by the nucleus with a loss of kinetic energy; inelastic scattering, where the incident neutron and nucleus interact such that a new neutron is emitted with a lower energy than the incident neutron; and neutron capture, where the neutron is absorbed by the nucleus with the usual emission of a photon. The two scattering interactions are of importance in the determination of asphalt content in bituminous mixes. With scattering, the nucleus maintains its lowest energy state, and the resulting collisions with nuclei are of the "billiard ball" type and easily analyzed with familiar laws of mechanics, based on the principles of energy and momentum conservation.

Useful data can be obtained from an asphalt content gauge by slowing sufficient numbers of "fast" neutrons (energies from 0.5 to 10 MeV) to "thermal" levels (0.025 eV). Only at thermal levels can the neutrons be successfully counted by the He-3 detector tubes. After a sufficient number of scattering collisions, a neutron's velocity is reduced to where its kinetic energy is the same as that of the atoms of the scattering medium. Thermal neutrons are thus in thermal equilibrium with the atoms of the asphaltic mix under test in a nuclear gauge.

THEORETICAL CONSIDERATIONS

The scattering collisions that occur over a timed counting period are a function of the macroscopic cross section for the number of nuclei of the test material. This is expressed for a single element as

$$\Sigma = \frac{\rho N_a}{A} \sigma_s \quad (1)$$

where

- Σ = macroscopic cross section in barns (1 barn = 10^{-24} cm²),
- A = atomic weight of element,
- ρ = density of element in g/cm³,
- N_a = number of atoms per gram atom (0.602×10^{24}), and
- σ_s = microscopic scattering cross section for a single atomic nucleus in barns.

For a compound consisting of i -elements, the cross section for scattering can be written as

$$\sum_i = \frac{\rho N_a}{M} \gamma_i \sigma_{si} \quad (2)$$

where

M = the compound molecular weight, and

γ_i = the number of i th atoms in the compound molecule.

Thus, for a material scattering consisting of a single compound with i atoms, we have

$$\sum_i = \frac{\rho N_a}{M} [\gamma_1 \sigma_{s1} + \gamma_2 \sigma_{s2} + \dots + \gamma_i \sigma_{si}] \quad (3)$$

If the scattering material consists of several types of various scattering compounds, say, j compounds, the total scattering material cross section is Σ_T and can be written as

$$\Sigma_T = \sum_1 + \sum_2 + \dots + \sum_j \quad (4)$$

Thus, the total scattering cross section for a mixture of bituminous material consisting of various types of aggregate and bitumen can be determined, although not easily.

As the asphalt content changes, the number of individual atoms N of asphalt changes or the term $N = \frac{\rho}{A} N_a$ changes. Thus, for an increase of N , the value of Σ_T for the entire mix would increase, resulting in more scattered or thermalized neutrons and a higher count for a counting period. In a typical bituminous mixture, it is the added hydrogen atoms present with an increase of asphalt that produce a higher count. Hydrogen has an elastic scattering cross section as much as 20 barns in the chemically unbounded state, whereas nearly all other elements lie in the range of 2 to 10 barns for neutrons of low or thermal energies (5). Therefore, any increase in the number of asphalt molecules means more hydrogen atoms and thus more scattered thermal neutrons, which results in a higher count rate on the gauge.

GAUGE CALIBRATION

The asphalt content gauge must be calibrated such that a curve of count rate versus asphalt content can be established. A sample pan containing only dry aggregate of the proper mix design (gradation) is first run to establish the zero asphalt content count rate. It was suggested by the Troxler gauge manufacturer that at least four times (24,000 g) the amount of aggregate required to fill a test pan ($\approx 6,000$ g) be mixed, that it be split with a sample splitter, and that one 6,000-g portion be used to establish the dry aggregate count rate. It is suggested that the remaining 12,000-g splitter portion be mixed with sufficient asphalt at about 300 F to produce a complete mix with a desired asphalt content in the range of the mix to be tested. This sample should be split, a test pan filled and packed, and a count rate obtained for the design bituminous mix. The two established count rates for the respective zero and design asphalt contents can be used to plot a curve that determines asphalt content values.

Calibration of the Nuclear-Chicago gauge leads basically to a similar curve, but here several sample pans of varying asphalt contents about the design mix value are carefully prepared and count ratios established versus the respective asphalt contents. Count ratios are obtained by dividing the average count rate for 10 counts taken on the sample pan by the average count rate similarly obtained on a standard supplied by the gauge manufacturer. No sample splitter is recommended for mix preparation although the manufacturer recommended extreme care in preparing accurate calibration mixes.

The calibration procedure used in this evaluation consisted of preparing a zero asphalt content pan of thoroughly mixed aggregate weighed to the nearest gram and reading it in both gauges. Asphalt was then added to the same aggregate in such an amount by

weight to produce the required design percentage of asphalt content. This mixture was thoroughly mixed at about 300 F, and an amount equal in weight to that of the dry aggregate was placed in the test pan and read in both gauges. All asphalt remaining in the mixing bowl and on all mixing utensils was accounted for, and a final, precise asphalt content for the mix was determined (usually a few tenths of a percent lower than the design value).

Similar mixing procedures were performed on other dry aggregate samples until four separate asphalt content count rates and a zero asphalt content count rate were determined with each nuclear gauge for the various mix designs required for the evaluation.

EXPERIMENTAL PROCEDURE

Phase one of the evaluation dealt only with carefully prepared laboratory samples of bituminous mixes.

Phase two of the study consisted of removing the Troxler nuclear gauge to several bituminous mix batch plants. Random samples of various bituminous mixes were tested. All calibration samples for the nuclear gauge were prepared at state facilities after obtaining hot-bin aggregate and asphalt samples from the plant. Extractions were run on the same samples tested in the nuclear gauge by use of laboratory extraction facilities.

Section 1

After nuclear-gauge calibration, two sample pans of each bituminous mix were prepared with the following mix design and percentages of asphalt content (asphalt used was all from the same supplier):

<u>Bituminous Mix Design</u>	<u>Design Percentage of Asphalt Content by Weight</u>
ID-2 wearing	5 to 10
ID-2 binder	4 to 8
FJ wearing	6 to 11

Gradation data for each mix design are given in Appendix A.

Each of the preceding duplicate sample pans was prepared using limestone, gravel, and slag. Each type was obtained from the same supply source for the entire test. Asphalt content determinations were made using the two calibrated nuclear gauges previously described for each sample mix. Immerex extractions (ASTM D 2172-65T, method C) were performed on each sample mix at the completion of nuclear determinations.

Section 2

After nuclear-gauge calibration, two sample pans each were prepared with the following bituminous mix designs and asphalt contents using only limestone aggregate (all limestone used was from the same supplier):

<u>Bituminous Mix Design</u>	<u>Design Percentage of Asphalt Content by Weight</u>
ID-2 wearing	5 to 7
ID-2 binder	3 to 6
FJ wearing	6 to 8

Each of the preceding duplicate samples was mixed with four manufactured brands of asphalt different from that used in the earlier test. The asphalt content determinations and Immerex extractions were the same as those used in the earlier test.

EXPERIMENTAL RESULTS AND COMMENTS

In the performance of the section 1 testing, the various representative aggregates and mix designs were accurately prepared in calibration pans of 0 percent asphalt and

Figure 1. Troxler asphalt content gauge, model 2226.



Figure 2. Diagram of Troxler gauge.

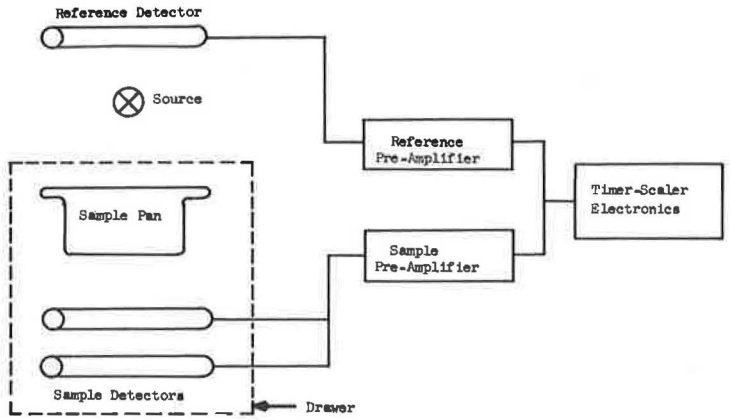


Figure 3. Calibration curves for Troxler gauge (various mix designs and aggregates).

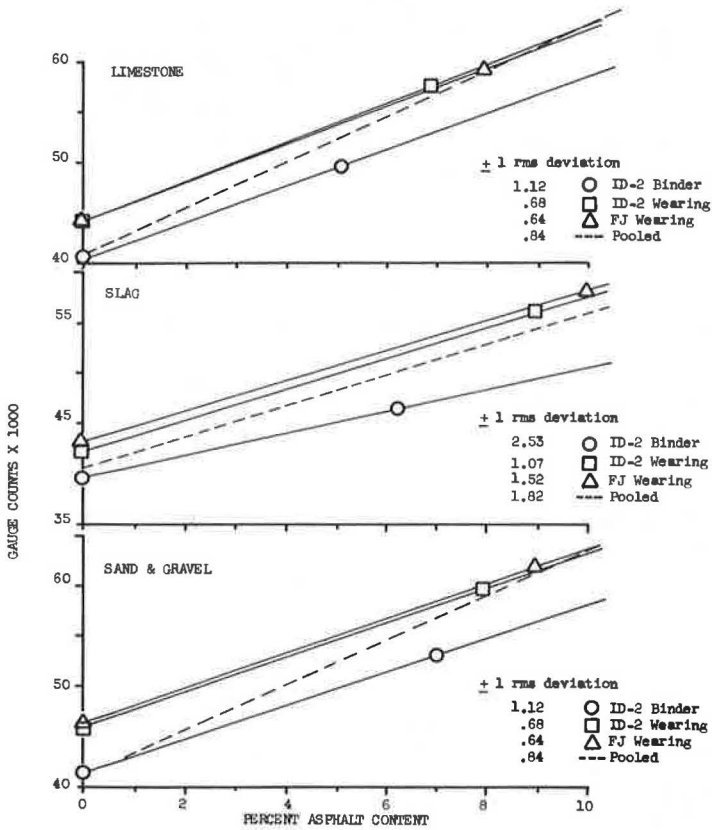


Figure 4. Calibration curves for Nuclear-Chicago gauge (various mix designs and aggregates).

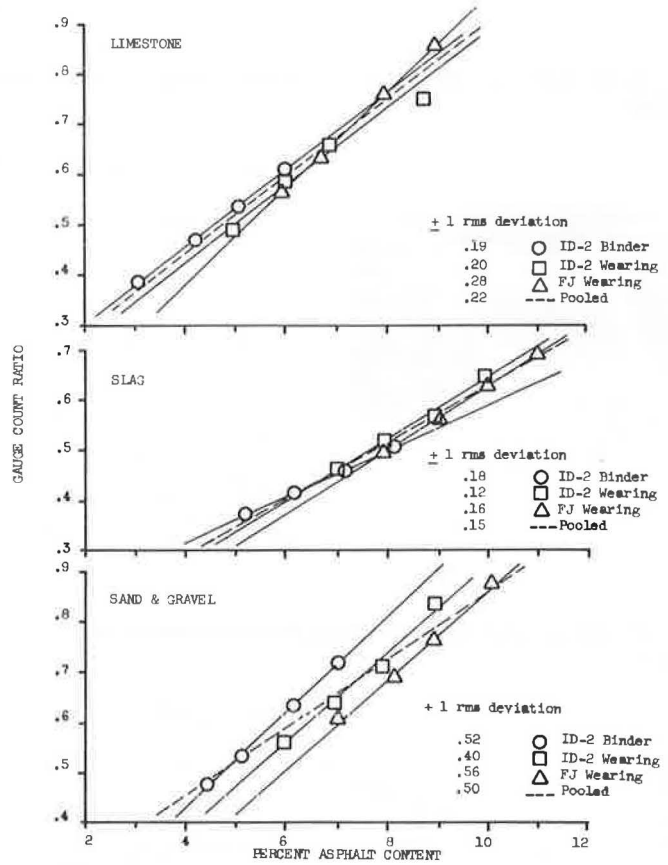


Table 1. One standard root mean square deviation (\pm) for design versus gauge-predicted asphalt contents by percent.

Aggregate	Mix Design			
	FJ Wearing	ID-2 Wearing	ID-2 Binder	Pooled
Limestone				
Troxler	0.37	0.30	0.43	0.37
Nuclear-Chicago	0.19	0.23	0.14	0.19
Slag				
Troxler	0.47	0.21	0.71	0.51
Nuclear-Chicago	0.20	0.15	0.19	0.18
Sand and gravel				
Troxler	0.37	0.57	0.33	0.44
Nuclear-Chicago	0.22	0.22	0.16	0.20
Pooled				
Troxler	0.38	0.35	0.48	0.41
Nuclear-Chicago	0.20	0.22	0.15	0.19

Table 2. One standard root mean square deviation (\pm) for extraction versus gauge-predicted asphalt contents by percent.

Aggregate	Mix Design			
	FJ Wearing	ID-2 Wearing	ID-2 Binder	Pooled
Limestone				
Troxler	0.48	0.40	0.54	0.47
Nuclear-Chicago	0.32	0.26	0.28	0.29
Slag				
Troxler	0.46	0.34	0.76	0.55
Nuclear-Chicago	0.33	0.24	0.20	0.26
Sand and gravel				
Troxler	0.24	0.78	0.32	0.51
Nuclear-Chicago	0.22	0.45	0.23	0.32
Pooled				
Troxler	0.44	0.48	0.55	0.49
Nuclear-Chicago	0.31	0.30	0.26	0.29

four additional pans containing design asphalt contents for the desired test range. Readings were taken with both nuclear gauges for each calibration pan. Regression-analysis techniques were used to establish equations for count versus asphalt content for the Troxler gauge and count ratio versus asphalt content for the Nuclear-Chicago unit. All counts on the Troxler gauge were taken in the calibrate position requiring about 11.5 min per test. The Nuclear-Chicago gauge took ten 1-min counts on each pan after establishing an average of 10 standard counts on a sealed Benelex standard provided with this gauge. A ratio of the average standard count divided into the averaged sample count establishes a ratio that is linearly related to asphalt content over successive testing.

Plots of the established calibration equations for each gauge showing the variations with aggregate and mix design are shown in Figures 3 and 4. The lines themselves are established from the regression calibration data.

It may be noted that, with the Troxler gauge, there is little effect of mix design for the ID-2 wearing and FJ wearing for respective types of aggregate, but the ID-2 binder mix curve gives from 2 to 5 percent higher asphalt content for the same gauge value. Definite variation with type of aggregate is apparent as noted on the dashed curve showing pooled data. Slopes of the pooled lines are quite different for each type of aggregate, and the intercept point varies for each type. Appendix B gives respective slope and intercept values for each gauge and test parameter.

Similar analysis of data for the Nuclear-Chicago gauge shows less variation with mix design. The sand and gravel mix have the widest variation, about 1.5 percent asphalt content among the three mix designs. Other aggregates show about 0.5 percent variation in asphalt content among the particular mixes. Again, the pooled data lines show a distinct variation in asphalt content for similar count ratios and different aggregates.

Also noted on each set of curves is the one standard deviation in asphalt content 1σ (assuming that there would be no calibration for mix design with particular aggregate types). As previously mentioned, the ID-2 binder mix in the Troxler gauge had the greatest deviation, about ± 1.77 percent asphalt content averaged for all three aggregates. The Nuclear-Chicago gauge has smaller deviations among mixes, about ± 0.7 percent, and yields a deviation between aggregates of about 0.2 percent for slag and limestone and 0.5 percent for sand and gravel. Better calibration and test results would be obtained if separate calibrations are made for each aggregate type and mix design.

The calibration curves established for each particular type of aggregate and mix design were used to determine the predicted asphalt contents of the design mixes of section 1 with each nuclear gauge. The same pans were then extracted to obtain an extraction asphalt content by percent. Again the one standard 1σ root mean square deviation was calculated for the various measurement techniques. The precisely designed pan values were used as a base in developing Table 1, which gives the standard deviation between design and gauge-predicted asphalt contents. Results obtained with the Nuclear-Chicago gauge were generally better than with the Troxler unit, which showed higher deviations with slag aggregates and an overall standard deviation of ± 0.41 percent asphalt content for the test. The Nuclear-Chicago gauge has an overall deviation of ± 0.19 percent. This was higher than that determined by similar investigations of the Troxler gauge (6) and may have been caused by the use of hand-mixed design pans instead of the mechanical splitter techniques.

Similar analysis was performed for extraction values as a base versus gauge-predicted asphalt contents (Table 2). When compared to the extracted values, both the gauges have a higher deviation about the extract value than does the pan design value. When a standard deviation of the extracted value about the base of designed asphalt content was determined, an overall value of ± 0.25 percent asphalt content was obtained. These data are given in Table 3. A curve of asphalt content by extraction and asphalt content by design is shown in Figure 5. The extracted value is uniformly lower than the design value with an average difference of 0.1 percent from design. This agreed well with similar tests performed earlier (7).

In section 2 of the study, the variation in gauge operation and calibration with dif-

Table 3. One standard root mean square deviation (\pm) for design versus extraction asphalt contents by percent.

Aggregate	Mix Design			
	FJ Wearing	ID-2 Wearing	ID-2 Binder	Pooled
Limestone	0.27	0.22	0.26	0.25
Slag	0.22	0.25	0.18	0.22
Sand and gravel	0.24	0.27	0.29	0.27
Pooled	0.26	0.23	0.26	0.25

Figure 5. Asphalt content by extraction and asphalt content by design.

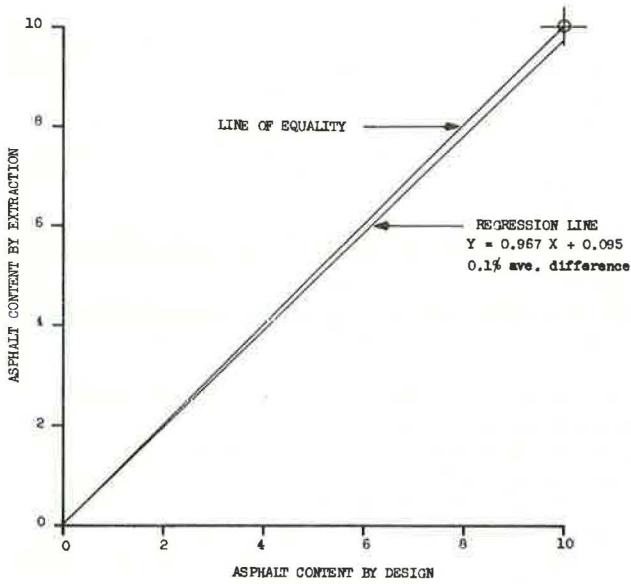


Figure 6. Asphalt-effect calibration curves for Troxler gauge (limestone aggregate), ID-2 binder mix.

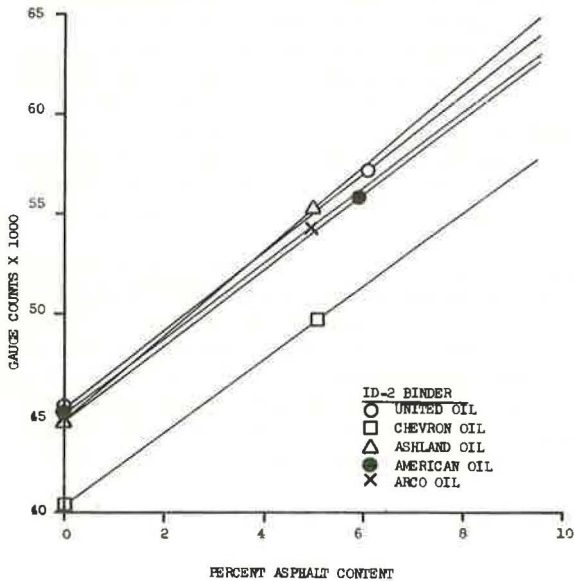


Figure 7. Asphalt-effect calibration curves for Troxler gauge (limestone aggregate), ID-2 wearing mix.

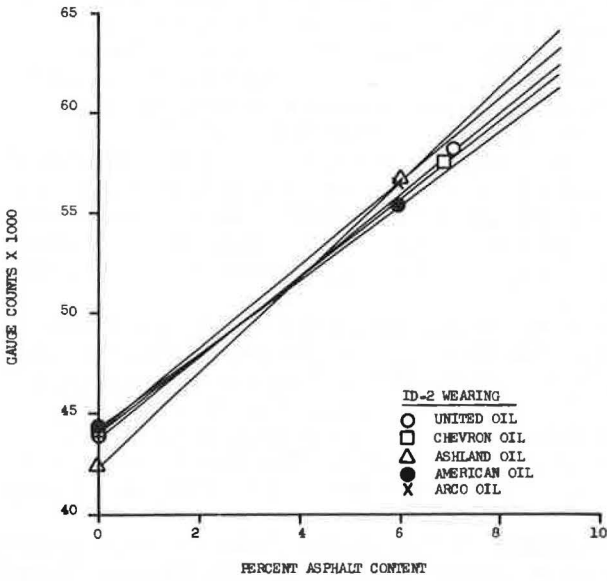
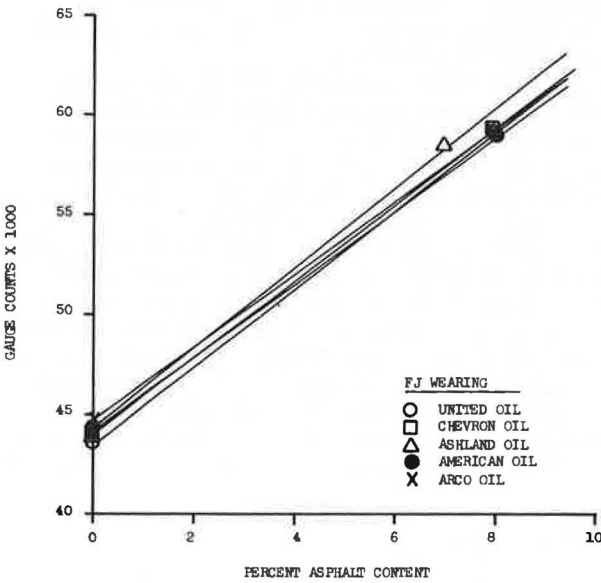


Figure 8. Asphalt-effect calibration curves for Troxler gauge (limestone aggregate), FJ wearing mix.



ferent asphalt manufacturers was examined. Calibration pans were prepared to accurately determined design values as described previously, but only limestone aggregate was used for the three mix designs. Figures 6, 7, and 8 show calibration curve variations for the three investigated mix designs for the Troxler unit. Similar calibration curves for the Nuclear-Chicago gauge are shown in Figures 9, 10, and 11. Neither gauge shows extreme sensitivity to variations in asphalt brand except for the Troxler gauge with ID-2 binder mix and Chevron asphalt. This is consistent with the data shown in Figure 3. Excluding this particular curve, the variation of which is not apparent with the other mix designs used, an average error of about ± 0.3 percent asphalt content could be expected without individual gauge calibration for each type of asphalt. This holds approximately true for the Troxler gauge with asphalt content values from 1 to 5 percent and the Nuclear-Chicago gauge with values of 3 to 7 percent. For values of asphalt content in the 8 to 9 percent region, errors in calibration of up to ± 0.75 percent asphalt content could be encountered.

After calibration, test pans of various design asphalt contents and types of asphalt were run, and the content was predicted using the previously described calibration curve equations. Table 4 gives the one standard deviation between design asphalt content as a base and the gauge-predicted values. No appreciable variation in gauge accuracy with either gradation or type of asphalt was apparent. Overall gauge deviation was slightly less for the Troxler unit than that found in section 1. This may have been the result of the absence of the aggregate variable and the relative insensitivity of the gauge to various types of asphalt.

During phase two of the testing, the Troxler gauge was used at several field locations to monitor the asphalt content of bituminous material from a typical batch plant. Samples of aggregate, asphalt, and the design gradation of the mix were acquired, and calibration pans were read with the gauge for 0 percent asphalt and an asphalt content slightly above the design value. All calibration pan preparation and readings were performed at state facilities. Samples of a field test mix were taken from various points in a loaded truck, mixed, placed in a sample pan, and run in the gauge. Insufficient time was available for extraction of all tested samples, so the tested material was placed in a sample box and returned to the laboratory for extraction.

Table 5 gives the 1σ for the gauge-predicted value compared with the extraction value as a base. The pooled data for all field studies yielded a 1σ of ± 0.72 percent asphalt content. It is not felt that this higher standard deviation can be attributed to inaccuracies in the nuclear gauge. The extraction samples were held up to several weeks prior to processing. Also all calibration readings with the gauge were performed in the state laboratory, whereas field test data were taken at the batch plant site, at times in open areas. Differences between standard counts taken with the Troxler gauge in the laboratory and similar counts taken at the field site gave a correction count that was added or subtracted from the field test count to allow for the different background conditions. Without such corrections, a 1σ for the field tests would have been nearly ± 1.0 percent. A higher overall accuracy and lower standard deviation, more comparable to that obtained in the laboratory phase, could undoubtedly have been obtained if all readings, including calibration tests, field sample tests, and extraction of the test samples, had been performed at the field plant. Such procedures will require services of a skilled technician and necessary equipment to produce accurately designed calibration mixes.

CONCLUSIONS

The following conclusions are supported by test results:

1. The overall results of the calibrated Troxler gauge, disregarding effects of gradation and type of aggregate, showed a standard deviation of about ± 0.40 percent asphalt content from design. It is felt that this value might possibly be reduced if the sample splitter technique is applied for calibration sample and test sample preparations, although it would require considerable cleaning and scraping when various mix designs are tested. It has also been suggested by the gauge manufacturer that light compaction with a small plate fitting within the test pan may improve accuracy. Vibration and striking of material in the pan were done manually in this study.

Figure 9. Asphalt-effect calibration curves for Nuclear-Chicago gauge (limestone aggregate), ID-2 binder mix.

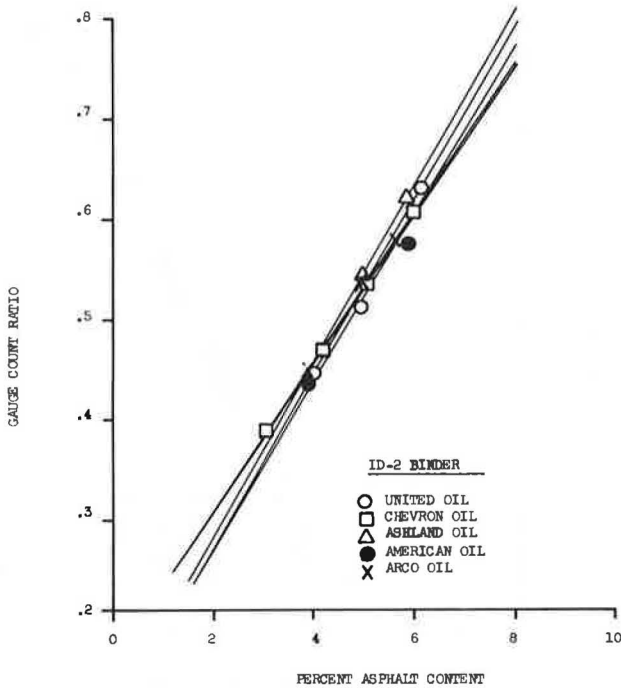


Figure 10. Asphalt-effect calibration curves for Nuclear-Chicago gauge (limestone aggregate), ID-2 wearing mix.

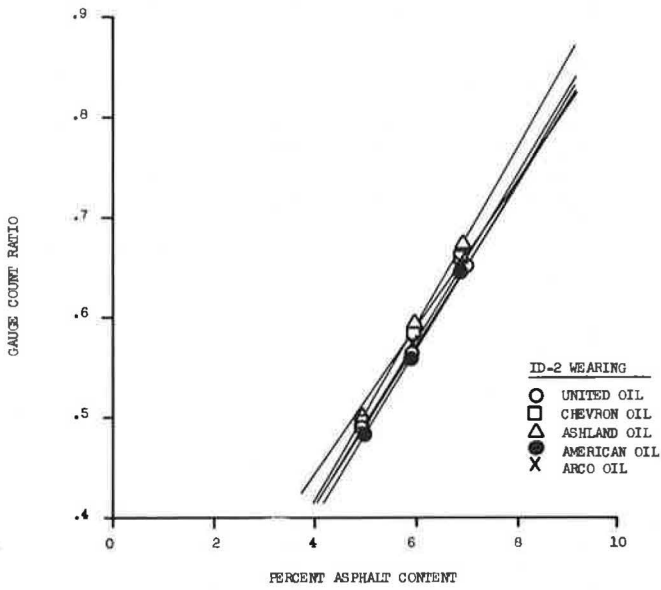


Figure 11. Asphalt-effect calibration curves for Nuclear-Chicago gauge (limestone aggregate), FJ wearing mix.

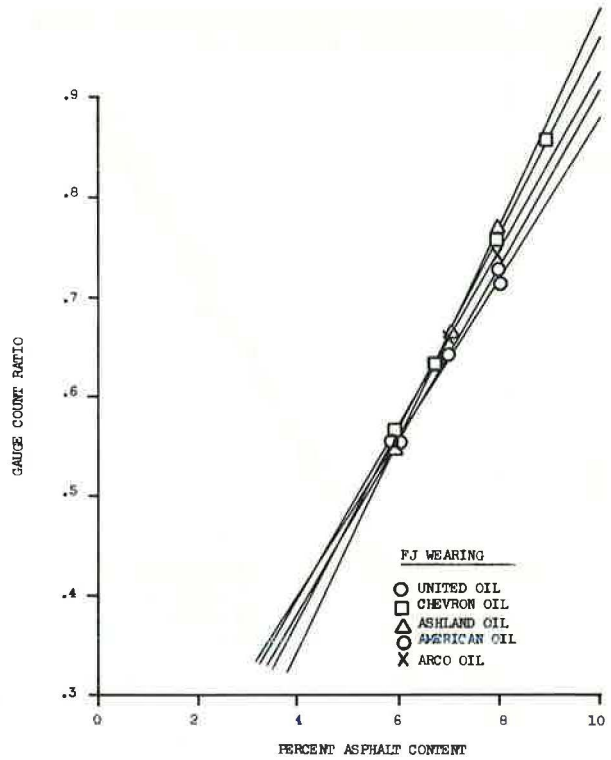


Table 4. One standard root mean square deviation (\pm) for design versus gauge-predicted asphalt contents by percent (various asphalts).

Asphalt	Mix Design			
	FJ Wearing	ID-2 Wearing	ID-2 Binder	Pooled
Chevron				
Troxler	0.39	0.18	0.62	0.43
Nuclear-Chicago	0.09	0.35	0.10	0.21
Ashland				
Troxler	0.25	0.48	0.17	0.33
Nuclear-Chicago	0.11	0.31	0.15	0.21
United				
Troxler	0.14	0.43	0.24	0.30
Nuclear-Chicago	0.10	0.27	0.14	0.18
American				
Troxler	0.40	0.32	0.34	0.35
Nuclear-Chicago	0.21	0.15	0.19	0.18
ARCO				
Troxler	0.32	0.37	0.52	0.41
Nuclear-Chicago	0.16	0.12	0.17	0.15
Pooled				
Troxler	0.32	0.32	0.30	0.37
Nuclear-Chicago	0.14	0.26	0.15	0.19

Table 5. One standard root mean square deviation (\pm) for extracted versus gauge-predicted asphalt contents by percent (field testing).

Aggregate	Mix Design			
	BCBC Binder	ID-2 Wearing	ID-2 Binder	Pooled
Limestone	0.63	0.78	0.79	0.74
Sandstone	—	0.47	—	0.47
Pooled	0.63	0.73	0.79	0.72

2. Recalibration of the gauge for each type of aggregate and mix design to be tested is recommended. A study of calibration procedures was made where a zero asphalt content pan and a pan containing asphalt by weight in the design percentage range were used to obtain the regression calibration curve. A similar regression curve was made using only three pans of various asphalt contents about the design percentage range. Better correlation with the sample test values was obtained when the two-point, 0 percent design calibration curve was applied.

3. This study included the application of slag aggregates to nuclear evaluation of asphalt content. These aggregates appeared to produce less reliable determinations of asphalt content. Studies with the Troxler gauge have shown that trace quantities of elements such as iron, boron, manganese, and cadmium in variable amounts between slag samples can vary the absorption microscopic cross section enough to affect the gauge calibration significantly. An increase of 0.05 to 0.60 percent in manganese content of two slag samples caused a decrease in count rate of as much as 5.3 percent. With even smaller content variations of cadmium (where the microscopic cross section is 185 times greater than manganese), serious count rate variations between slag samples could occur.

4. In general, there is only a slight variation in gauge readings between similar test specimens mixed with various brands of asphalt. All brands used in this test were of the viscosity known as AC-2000. For greatest accuracy, however, it is recommended that recalibration be performed for each change in asphalt brand and, if convenient, for each different truck load of similar asphalt brand.

5. Applications of this nuclear asphalt content gauge to field testing would appear to be more successful if the moisture content of the dry aggregate used in the batch mix is as small as possible. Any moisture left in the aggregate appears as added asphalt to the gauge and could account for the usually higher asphalt content than extraction for field samples. The requirements that recalibration be made with each mix parameter change should not be a problem with normal plant use, but the services of a skilled technician are an absolute necessity in calibration pan preparation.

6. In a final statistical analysis of the overall value of the Troxler gauge in providing a quicker determination of asphalt content, the following relation is applied to determine the number of tests required by the gauge to yield the actual asphalt content (plus or minus a desired standard deviation) with 95 percent confidence:

$$\pm t = 1.96 \sigma / n^{1/2} \text{ or } n = (1.96 \sigma / \pm t)^2$$

where

$\pm t$ = desired accuracy for overall content determinations,

σ = mean test method standard deviation, and

n = number of tests (where one test consists of an 11.5-min counting period).

For the data gathered in this study

$$\pm t = \pm 0.40$$

that is, 0.4 percent is the accepted accuracy required for 95 percent confidence of an extraction test of an asphalt sample;

$$\pm t = \pm 0.41$$

is the overall standard deviation for all pooled tests performed with the gauge; and

$$n = \left(\frac{1.96 \times 0.41}{0.40} \right)^2 = 4.0$$

Thus, a minimum of 4 tests must be performed with the Troxler gauge to obtain the required degree of accuracy.

Similar analysis of data for the Nuclear-Chicago gauge yielded a requirement of only one test for similar degrees of accuracy.

Thus, it would require a total of about 46 min to test a sample with the Troxler gauge operating in the calibrate test-mode position to obtain the required degree of accuracy. This is still only about one-half the time required to perform an extraction of a similar sample. Although not yielding the degree of accuracy specified by the manufacturer, use of the Troxler gauge can still provide a quick, accurate means of determining asphalt content in either field or laboratory locations.

ACKNOWLEDGMENTS

The author wishes to acknowledge the assistance of L. O. Lingle for his work in gathering experimental data, P. Kaiser for preparation of calibration and test samples, and Thomas Shrawder for data organization and analysis.

The project was carried out in cooperation with the U. S. Department of Transportation, Federal Highway Administration.

The opinions, findings, and conclusions expressed in this paper are those of the author and not necessarily those of the Pennsylvania Department of Transportation or the Federal Highway Administration.

REFERENCES

1. Grey, R. L. Determination of Asphalt Content in Hot Bituminous Mixes With a Portable Nuclear Asphalt Content Gage. Highway Research Record 248, 1968, pp. 77-81.
2. Lamb, D. R., and Zoller, J. H. Determination of Asphalt Content of Bituminous Mixture by Means of Radioactive Isotopes. HRB Proc., Vol. 35, 1956, pp. 322-326.
3. Walters, H. W. Nuclear Asphalt Content Determination at the Job Site. Highway Research Record 117, 1966, pp. 54-66.
4. Qureshi, T. H. Nuclear Asphalt Content Determination. North Carolina State Univ., Raleigh, 1964.
5. Glasstone, S., and Sesonske, A. Nuclear Reactor Engineering. D. Van Nostrand Co., Inc., Princeton, New Jersey, 1967, p. 82.
6. Hughes, C. S. Evaluation of a Nuclear Asphalt Content Gauge. Virginia Highway Research Council, 1971.
7. Grey, R. L. Asphalt Content Studies by the Nuclear Method. Pennsylvania Department of Highways, Research Project 64-15, Phase 2 Final Report, May 1970.

APPENDIX A

MIX GRADATION

PERCENT PASSING			
SIEVE SIZE	ID-2 BINDER	ID-2 WEARING	FJ WEARING
2-1/2			
2			
1-1/2	100.0		
1	99.1		
3/4			
1/2	63.4	100.0	
3/8		99.3	100.0
4	36.2	67.9	99.0
8	29.5	45.0	79.6
16	20.2	30.2	54.4
30	13.9	20.5	35.7
50	8.9	12.9	21.2
100	5.6	7.9	11.9
200	3.6	4.7	6.9

APPENDIX B

CALIBRATION CURVE SLOPE AND INTERCEPT VALUES

AGGREGATE	(TRUCKER GAUGE)			(NUCLEAR CHICAGO GAUGE)		
	MIX DESIGN	SLOPE	INTERCEPT	MIX DESIGN	SLOPE	INTERCEPT
LIMESTONE	ID-2 BINDER	2.155	38,925	ID-2 BINDER	.0763	0.1482
	ID-2 WEARING	1.949	44,014	ID-2 WEARING	.0780	0.1096
	FJ WEARING	1.903	44,143	FJ WEARING	.0972	-0.0156
	POOLED	2.216	41,297	POOLED	.0774	0.1287
SLAG	ID-2 BINDER	1.200	38,685	ID-2 BINDER	.0457	0.1334
	ID-2 WEARING	1.555	42,036	ID-2 WEARING	.0616	0.0261
	FJ WEARING	1.504	43,093	FJ WEARING	.0648	-0.0195
	POOLED	1.566	40,275	POOLED	.0576	0.0545
SAND & GRAVEL	ID-2 BINDER	1.688	41,364	ID-2 BINDER	.0865	0.1055
	ID-2 WEARING	1.703	46,212	ID-2 WEARING	.0910	0.0074
	FJ WEARING	1.760	46,016	FJ WEARING	.0987	-0.0264
	POOLED	1.907	43,484	POOLED	.0665	0.1893